Kinematic Analysis of Multi-Fingered, Anthropomorphic Robotic Hands

A THESIS SUBMITTED IN FULFILMENT OF

THE REQUIREMENT FOR THE AWARD OF THE DEGREE

OF

DOCTOR OF PHILOSOPHY

IN

MECHANICAL ENGINEERING

BY

PRAMOD KUMAR PARIDA

NATIONAL INSTITUTE OF TECHNOLOGY
ROURKELA, INDIA

July-2013

Dedicated to

My

Parents

NATIONAL INSTITUTE OF TECHNOLOGY
ROURKELA, INDIA

Dr. Bibhuti Bhusan Biswal
Professor and Head
Department of Industrial Design
NIT, Rourkela

CERTIFICATE

This is to certify that the thesis entitled "**Kinematic Analysis of Multi-Fingered, Anthropomorphic Robotic Hands**" being submitted by **Pramod Kumar Parida** for the award of the degree of Doctor of Philosophy (Mechanical Engineering) of NIT Rourkela, is a record of bonafide research work carried out by him under my supervision and guidance. He has worked for more than three years on the above problem at the Department of Mechanical Engineering, National Institute of Technology, Rourkela and this has reached the standard fulfilling the requirements and the regulation relating to the degree. The contents of this thesis, in full or part, have not been submitted to any other university or institution for the award of any degree or diploma.

(**Dr. B. B. Biswal**)

ACKNOWLEDGEMENT

This dissertation is a result of the research work that has been carried out at **National Institute of Technology, Rourkela**. During this period, the author came across with a great number of people whose contributions in various ways helped in the field of research and they deserve special thanks. It is a pleasure to convey the gratitude to all of them.

First of all the author expresses his heartiest gratitude to his supervisor and guide **Dr B. B. Biswal,** Professor and Head, Department of Industrial Design, NIT, Rourkela for his valuable guidance, support and encouragement in the course of the present work. The successful and timely completion of the work is due to his constant inspiration and constructive criticisms. The author cannot adequately express his appreciation to him. The author records his gratefulness to Madam **Mrs Meenati Biswal** for her constant support and inspiration during his work and stay at NIT, Rourkela.

The author take this opportunity to express his deepest gratitude to **Prof K.P. Maity,** Head of the Department and also faculty members, of the Department of Mechanical Engineering, NIT Rourkela for constant advice, useful discussions, encouragement and support in pursuing the research work.

The author is grateful to **Prof S.K. Sarangi**, Director, NIT, Rourkela, **Prof R.K. Sahoo**, former Head and **Prof R. K. Behera** of Mechanical Engineering Department, NIT, Rourkela, for their kind support and concern regarding his academic requirements.

The help and cooperation received from the **Principal** and **Head** of Mechanical Engineering Department, CET, Bhubaneswar are gratefully acknowledged.
The author also expresses his thankfulness to **Mr Anand Amrit,** Final year B.Tech. Department of Industrial Design and **Mr K. C. Bhuyan**, **Mr R. N. Behera**, **Mr R. N. Mahapatra, Mr Layatitdev Das, Mr B. Balabantaray, Mr B. Choudhury** and **Mr P. Jha**, researchers in NIT Rourkela for unhesitating cooperation extended during the tenure of the research programme.

The completion of this work came at the expense of author's long hours of absence from home. Words fail to express his indebtedness to his wife **Ranu** and loving son **Preet** for their understanding, patience, active cooperation and after all giving their times throughout the course of the doctoral dissertation. The author thanks them for being supportive and caring. His **parents** and **relatives** deserve special mention for their inseparable support and prayers.

Last, but not the least, the author thank the one above all, the omnipresent **God**, for giving him the strength during the course of this research work.

Pramod Kumar Parida

Abstract

The ability of stable grasping and fine manipulation with the multi-fingered robot hand with required precision and dexterity is playing an increasingly important role in the applications like service robots, rehabilitation, humanoid robots, entertainment robots, industries etc.. A number of multi-fingered robotic hands have been developed by various researchers in the past. The distinct advantages of a multi-fingered robot hand having structural similarity with human hand motivate the need for an anthropomorphic robot hand. Such a hand provides a promising base for supplanting human hand in execution of tedious, complicated and dangerous tasks, especially in situations such as manufacturing, space, undersea etc. These can also be used in orthopaedic rehabilitation of humans for improving the quality of the life of people having orthopedically and neurological disabilities. The developments so far are mostly driven by the application requirements. There are a number of bottlenecks with industrial grippers as regards to the stability of grasping objects of irregular geometries or complex manipulation operations. A multi-fingered robot hand can be made to mimic the movements of a human hand. The present piece of research work attempts to conceptualize and design a multi-fingered, anthropomorphic robot hand by structurally imitating the human hand.

In the beginning, a brief idea about the history, types of robotic hands and application of multi-fingered hands in various fields are presented. A review of literature based on different aspects of the multi-fingered hand like structure, control, optimization, gasping etc. is made. Some of the important and more relevant literatures are elaborately discussed and a brief analysis is made on the outcomes and shortfalls with respect to multi-fingered hands. Based on the analysis of the review of literature, the research work aims at developing an improved anthropomorphic robot hand model in which apart from the four fingers and a thumb, the palm arch effect of human hand is also considered to increase its dexterity.

A robotic hand with five anthropomorphic fingers including the thumb and palm arch effect having 25 degrees-of-freedom in all is investigated in the present work. Each individual finger is considered as an open loop kinematic chain and each finger segment is considered as a link of the manipulator. The wrist of the hand is considered as a fixed point.

The kinematic analyses of the model for both forward kinematics and inverse kinematic are carried out. The trajectories of the tip positions of the thumb and the fingers with respect to local coordinate system are determined and plotted. This gives the extreme position of the fingertips which is obtained from the forward kinematic solution with the help of MATLAB. Similarly, varying all the joint

angles of the thumb and fingers in their respective ranges, the reachable workspace of the hand model is obtained. Adaptive Neuro-Fuzzy Inference System (ANFIS) is used for solving the inverse kinematic problem of the fingers.

Since the multi-fingered hand grasps the object mainly through its fingertips and the manipulation of the object is facilitated by the fingers due to their dexterity, the grasp is considered to be force-closure grasp. The grasping theory and different types of contacts between the fingertip and object are presented and the conditions for stable and equilibrium grasp are elaborately discussed. The proposed hand model is simulated to grasp five different shaped objects with equal base dimension and height. The forces applied on the fingertip during grasping are calculated. The hand model is also analysed using ANSYS to evaluate the stresses being developed at various points in the thumb and fingers. This analysis was made for the hand considering two different hand materials i.e. aluminium alloy and structural steel.

The solution obtained from the forward kinematic analysis of the hand determines the maximum size for differently shaped objects while the solution to the inverse kinematic problem indicates the configurations of the thumb and the fingers inside the workspace of the hand. The solutions are predicted in which all joint angles are within their respective ranges.

The results of the stress analysis of the hand model show that the structure of the fingers and the hand as a whole is capable of handling the selected objects.

The robot hand under investigation can be realized and can be a very useful tool for many critical areas such as fine manipulation of objects, combating orthopaedic or neurological impediments, service robotics, entertainment robotics etc.

The dissertation concludes with a summary of the contribution and the scope of further work.

Table of Contents

List of Tables

List of Figures

List of Symbols

θ_I	Angle between index finger and normal to contact plane of object.
θ_L	Angle between little finger and normal to contact plane of object.
θ_M	Angle between middle finger and normal to contact plane of object.
θ_R	Angle between ring finger and normal to contact plane of object.
θ_T	Angle between thumb and normal to contact plane of object.
θ	Angle of inclination of thumb and finger to the normal at contact point.
$\beta_{1....5}$	Angles made by the line joining origins of global and local coordinate system and Y axis of hand.
μ	Coefficient of friction between fingertip and object surface.
γ	Co-efficient of torsional friction.
f_{ix}, f_{iy}, f_{iz}	Components of the grasp force in X, Y and Z axis in object coordinate frame respectively.
F	Force applied by thumb and finger.
F_f	Frictional force.
G	Grasp matrix
HB	Hand Breadth
HL	Hand Length
I	Index finger
θ	Joint angle
$q_{1....25}$	Joint angles of the hand model
d	Joint Distance
G_i	Linear transformation between the contact force f_i and the wrench produced on the object due to contact force
a	Link Length
L	Little finger
M	Middle finger
O	Origin Of Global coordinate system

$O_{1...5}$	Origins of Local coordinate systems of thumb and fingers
ζ	Positive constant
R	Ring finger
T	Thumb
F_n	Total normal force on the object.
F_t	Total tangential force of the object
${}^0H_{1.....5}$	Transfer matrices from local coordinate system to global coordinate system.
T	Transfer matrix
α	Twist angle
V	Volume of the object
σ_v	von Mises stress
W	Weight of the grasped object.
w_i	Wrench applied at contact point i
B_i	Wrench basis at contact point i
σ_y	Yield strength of the material
k	yield stress of the material in pure shear

Abbreviations

DOF	Degrees of freedom
D-H	Denavit- Hartenberg
CMC	Carpometacarpal
MCP	Mecapophalangeal
MC	Metacarpal
IP	Interphalangeal
PIP	Proximal interphalangeal
DIP	Distal interphalangeal
Ab/Ad	Abduction/ Adduction
F/E	Flexion/Extension
ANFIS	Adoptive Neuro-Fuzzy Inference System
LS	Least squares
BP	Back propagation
FIS	Fuzzy Interface System
MF	Membership function
GWS	Grasp wrench space
FC	Force closure
CATIA	Computer Aided Three-dimensional Interactive Application

Chapter 1

INTRODUCTION

1.1 Overview

A robotic hand is one that can mimic the movement of human hand in operation. Stable grasping and fine manipulation skills, for personal and service robots in unstructured environments are of fundamental importance in performing different tasks. In order to perform the tasks in human like ways and to realize a proper and safe co-operation between humans and robots, the robots of the future must be thought of having human excellence in terms of its structure as well as intelligence.

So far as manipulation of objects are concerned human hands have abundant potentiality for grasping objects of several shapes and dimensions, as well as for manipulating them in a dexterous manner. It is common experience that, by training the robot one can do flexible manipulation of stick-shaped objects, manipulate a pen by using rolling or sliding motions, and perform accurate operations requiring fine control of small tools or objects. It is also obvious that a simple gripper having open/close motion only cannot perform such type of dexterity. However, a multi-fingered robot hand can offer a great prospect for accomplishing such dexterous manipulation in a robotic system. Moreover, it is observed that in practice human beings do not use hands only for grasping or manipulating objects. Human beings are usually able to perform, by the hands more number of other important tasks such as exploration, touch, and perception of physical properties (roughness, temperature, weight, to mention just a few).Then it is natural that this type of capabilities are also expected from robotic end-effectors and therefore, by adding the required sensing equipment and proper control strategies, we may improve the interaction capabilities of the robot with the environment for achieving, active exploration, detection of sensing surface

properties (local friction, impedance, and so on), and such other tasks that are usually very hard or impossible for simple grippers. For these and other reasons the study of multi-fingered robot hands has greatly interested the research community since the early days of robotics.

Two of the major issues in the area are; design of more dexterous hand, and its grasp capability including quality of grasp. Robotic assembly and welding operations demand more dexterous and compliant devices to overcome the complicacies demanded by the desired motion and object manipulation. The mechanical design of an articulated robotic hand can be made according to many possible design concepts and options. One of the main issues is the design of a proper actuation and transmission system. This aspect is crucial because space and dimensions are usually limited in an anthropomorphic design.

1.2 Revisiting the Robot Hands

The hand has a major role in the advancement of human being. In fact, humans have empowered a relationship to the world different from that of animals, as being able to use tools. Relationship between hand and mind, the two most distinguished features of humans among animals, has been discussed by the great philosophers since ancient times [1]. It is because humans have more dexterous hands that they became intelligent, or the other way around?

Definitely, the exemplified characteristics of the human hand, like the motors, the sensors, the sensorimotor transformations and the constraints, influence learning process, behaviour, skills and perceptive functions, since human beings do not use hands only for grasping or manipulating objects but also for search, touch, sensitivity of physical properties.

Therefore, the hand has a major role in the improvement and evolution of intelligence. On the other side, intellectual ability distresses and decides the skill with which the hand is used.

There has been a revolution recently in neuroscience that concerns the synergies [2], which are a kind of alphabet with which our hands work and organize movements and that can be exploited to make a progress in technology. Based on those studies the promising future applications for research are prosthetic devices, the robot hands that come into our homes. Those hands may be more beneficial if they are proficient hands, and finally haptic interfaces, i.e. interfaces that allow our

hands to feel those feelings that the avatars feel in virtual reality in which they are engrossed.

Hence, if the robot is to be part of our world, working with people and substituting them, the robot manipulation capabilities need to be alike to those of human beings. In order to make robots able to enter in this world of complex functions, it must understand how the correlation between the hand and the development of the intelligence is expressed. This can be a big step forward in the study and development of intellectual robotics. This study is part of the "Evolutionary Robotics".

Trusting on more or less autonomous and intelligent robots offers safe improvement of human life and as a whole an improvement in society, both in terms of quality and efficiency. This is one of the most critical issues in the design of robotic systems, and involves highly intellectual level and the control modalities, as well as the mechanical structure, the kinematic configuration, the actuation and sensing system. The cognitive and control level and the development of new technologies are aspects that influence each other and will contribute to dexterous and autonomous manipulation capabilities of hand robotic systems.

The bio-mimetic approach is the preferred choice both for advanced actuation and sensing systems in order to make a robotic hand system approaching the human in functionality and aesthetics.

This perspective moves certainly a number of ethical issues. The presence of robots in homes and workplaces will inevitably lead to a change in habits and lifestyle.

Hence, there is the need for an ethic that inspires the design, production and use of robots, taking into account the cultural, historical, and customs of different people and cultures. These are things that scientists cannot and should not ignore. In this regard the "Roboethics", a new born discipline dealing with problems related to the acceptability of new robotics technologies, is a useful tool to sensitize robotics researchers towards their responsibilities to society [3, 4].

1.2.1 Classification of Robot Hands

Ordinarily robot grippers are employed in robotic manipulators that perform repetitive tasks. At an early stage the idea of offering complete unit construction systems and feeding technology, robots, and grippers, for automation technology was of major importance in order to be able to flexibly react to mechanical engineering demands. Consequently the first gripper module was developed as

standard products as early as approximately 30 years ego. Initially the major work of grippers was to pick and place, which requires holding the object as main objective. Accordingly, the grippers can be classified as “single finger”, “two fingered” and “multi fingered hands”. The single finger grippers consist of a single element for holding the object. Figure 1.1 (a) [5] shows a vacuum gripper which is an example of a single jaw gripper, the vacuum plate being used as a holding device of the object. Large flat objects are often difficult to grasp, for which vacuum gripper is the appropriate solution. These are used for picking up metal plates, pans of glass or large light weight boxes. Since the vacuum cups are made of elastic material, they are compliant.

Figure 1.1(b) [6] shows a magnetic gripper which is also a single finger gripper, mainly used for ferrous material objects. In this only one surface is required for gripping.

(a) SCHMALZ Vacuum Gripper

(b) SCHUNK Magnetic Grpper

(c) FIPA Adhesive Gripper

Figure 1.1: Examples of single fingered gripper.

An adhesive gripper, shown in Figure 1.1 (c) [7], is also a single jaw gripper, in which an adhesive substance can be used for grasping action in gripper design. The requirement on the items to be handled is that they must be gripped on one side only as shown in the figure. The reliability of this gripping device is diminished with each successive operation cycle as the adhesive substance loses its tackiness

on repeated use. Two finger grippers have two jaws, which are operated by some power source like hydraulic, pneumatic, electric etc. for closing and opening of jaws. These are generally used for pick and place operation of symmetrical and similar type objects made of hard material. This type jaws are used in mass production processes in industrial applications. A pneumatic gripper having two jaws is shown in Figure 1.2(a) [8], which is operated by the pneumatic pressure and basically used for holding hard, symmetrical and similar type objects. Figure 1.2 (b) [6] shows a hydraulic gripper having two jaws. Gripping force, speed, position, and acceleration of the gripper fingers can be adjusted and controlled by hydraulic pressure. The gripper can have high payloads and so it can be used for picking heavy components, but with similar constraint that the objects should be symmetric and of similar type. The electric gripper is shown in Figure 1.2(c) [9], which is operated by a servo motor. This one is also used for similar application for picking and placing of symmetric and similar objects.

(a) SCHUNK Pneumatic Gripper

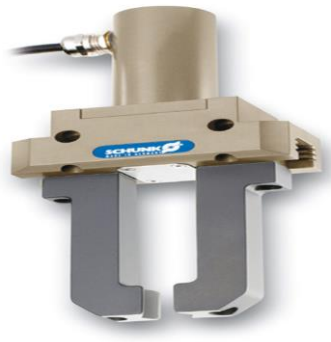

(b) SCHUNK Hydraulic Gripper

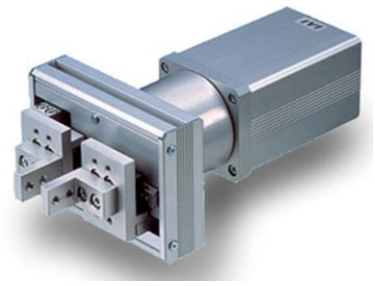

(c) ROBO CYLINDER Electric Gripper

Figure 1.2: Examples of two fingered gripper.

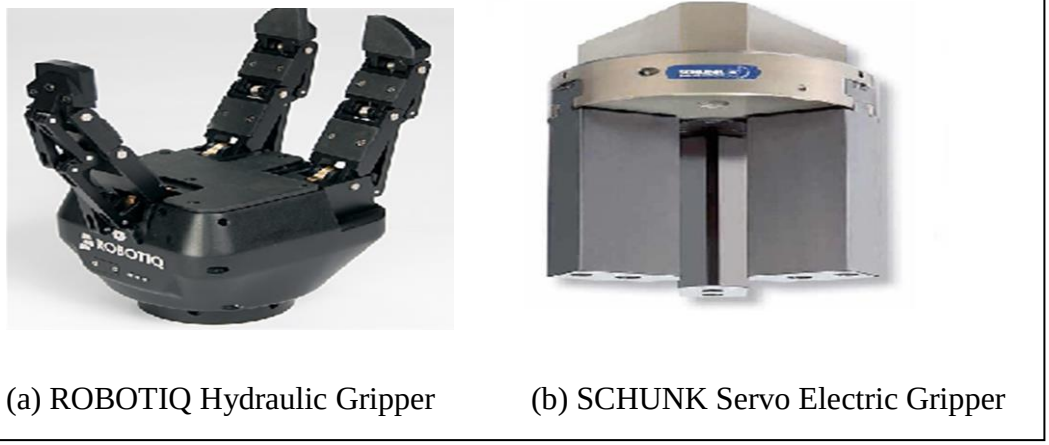

(a) ROBOTIQ Hydraulic Gripper (b) SCHUNK Servo Electric Gripper

Figure 1.3: Examples of three fingered gripper.

Figure 1.3 (a) [10] and Figure 1.3 (b) [6] show the hydraulic gripper and servo electric gripper having three jaws respectively. These grippers can only execute limited and specific manipulation tasks with objects that are very similar in shape, weight and manipulation requirement. The three finger grippers can handle some of the unsymmetrical objects. Such use of gripper is also limited to the grasping of object with regular geometries. The grippers with more than 3-jaws or fingers are called multi-fingered grippers and with a resemblance to human hands in behaviour, these are usually called multi- fingered hands.

According to structure of fingers used in hands, the robots hands can be classified as “hard finger”, “flexible finger” and “jointed finger” hands. Hard finger are those which are made of a single element with one end joined to the wrist directly or base of the hand and other end is free to contact with the object to be handled. Since the finger cannot bend and it is not flexible, these hands have very limited applications. Some single link fingers are made of tube like structure, which is filled in with air or liquid, so that it can bend to any shape. It can grasp any shape object as the contact along the finger not at tip only. But, the limitation is that the strength of the finger is less and hence it cannot handle heavier objects. Jointed fingers consist of number of segments joined at the ends like human hand fingers. They possess the advantage of both hard and flexible fingers with more strength and flexibility.

According to grasping ability of the hands they can be classified as “fixed hand” and “dexterous hand”. The fixed hand is generally with one and/ or two fingers, which have limited gasping capability of symmetric and similar geometric shape

objects. This type of hands cannot perform any precise manipulation during gasping or transporting from one place to another. A widely accepted definition states that the dexterity of a robotic end-effector is a measure of its capability of changing the configuration of the manipulated object from an initial configuration to a final one, arbitrarily chosen within the device workspace. Generally speaking, with the term dexterity we intend the capability of the end-effector, operated by a suitable robotic system, to perform tasks autonomously with a certain level of complexity. The multi-finger hands having jointed fingers like human hand do possess the properties of dexterity. Therefore, these hands are called as dexterous hands.

The hand becomes functional only when the different joints between segments of the fingers move with respect to each other. These motions to the joints are given by a device called actuator and the act of activating the joints is called actuation. The actuators are operated from certain source of energy, accordingly the hands are classified as "electrically actuated hand", "pneumatically actuated hand" and "hydraulically actuated hand" etc. depending on the source power they derive from. In electrically actuated hands generally DC motors are used to actuate the hand joints. In some cases very small motors are used, which are placed in the joint itself and the electric power is supplied to that and the motor gives necessary motion to the joint. In some other cases a large electric motor is used which placed at the base and the power is transmitted to different joints by means mechanical arrangement like gears, tendons, wires, rack and pinion etc. In case of pneumatically actuated hands pneumatic pressure is used as the motive power for giving motion to joints. Normally, compressed air used as working fluid in this type of hands. Similarly, hydraulic pressure is used as power source in hydraulically actuated hands.

Degrees of freedom (DOFs) refer to the independent motion produced at a joint either linear or rotational mode. Actuators are used to actuate or make the joints active. When the number of DOF is equal to number of actuators i.e. each joint actuated by an independent actuator then it is called a fully actuated mechanism, the hand in which this principle used is called a "fully actuated hand". The hands having number of actuators more than the number of DOFs or number of joints is termed as "redundantly actuated hands". The "under actuated hands" are those hands wherein under-actuation mechanism is used i.e. the number of actuators are less than the number of DOFs or joints. In case of under actuated hands some of the joints act as passive joints and these joints are actuated indirectly by the motion of the coupled joint.

Another way of classifying the robot hands with respect to its construction is “modular hand” and “integrated design hand”. In modular hands, one considers the hand as an independent device to be applied at the end of an arm; they include all components necessary for functioning such as actuators and sensors. The same hand can be applied to any kind of arm (i.e. the DLR Hands [21], the Barret Hand [14], the Salisbury's Hand [12]).In case of integrated design hands, the hand is considered as a non-separable part of the arm, intensely incorporated with it, mimicking the biological model, (i.e. the Robonaut Hand [19], the UB Hand [27]). Therefore, they do not need to have the actuators (driving system) integrated into their housing, those are mostly outsourced to the robot arm which allows the use of large actuators with relatively strong gripping force.

1.2.2 Chronology of Robot Hands

The kinematical configuration determines a potential dexterity essentially related to the hand structure. The potential dexterity of such an intricate structure can be wasted if proper actuation or sensory system is not implemented and suitable control procedures are not applied. A chronological order of the development various known robotics hands are presented in Table 1.1.

Table 1.1: Chronological order of the some robotic hands developed.

Name of Hand	Year of Development	Number of fingers	Number of joints	Number of actuations	View of the structure
Okada Hand [11]	1979	3	11	11	

Name of Hand	Year of Development	Number of fingers	Number of joints	Number of actuations	View of the structure
Stanford/JPL Hand [12]	1983	3	09	09	
Utah/MIT Hand [13]	1983	4	16	16	
Barret Hand [14], [15],	1988	3	08	04	
LMS Hand [16],	1998	4	16	16	

Name of Hand	Year of Development	Number of fingers	Number of joints	Number of actuations	View of the structure
DIST Hand [17], [18]	1998	4	16	16	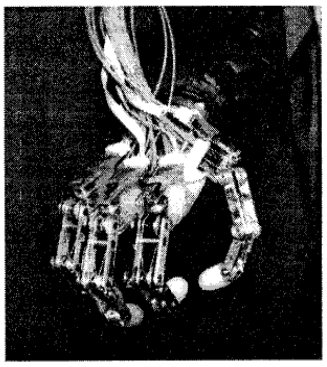
Robonaut Hand [19], [20],	1999	5	22	14	
DLR-Hand II[21]	2000	4	17	13	
Tuat/Karlsruhe Hand [22],	2000	5	20	20	

Name of Hand	Year of Development	Number of fingers	Number of joints	Number of actuations	View of the structure
Ultralight Hand [23]	2000	5	18	13	
Gifu Hand [24]	2001	5	20	16	
Shadow Hand [25]	2002	5	23	23	
High Speed Hand [26]	2003	3	8	8	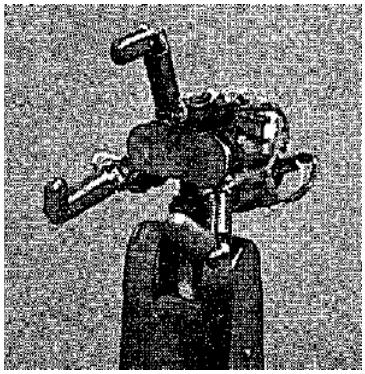

Name of Hand	Year of Development	Number of fingers	Number of joints	Number of actuations	View of the structure
Universal Hand [27]	2005	5	20	16	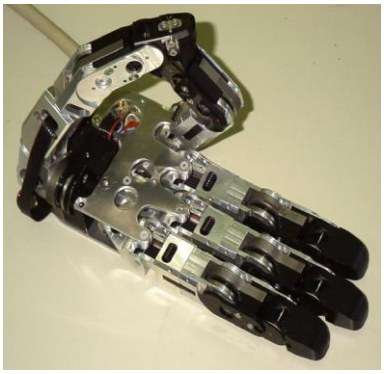
Multi fingered Hand [28]	2007	4	17	13	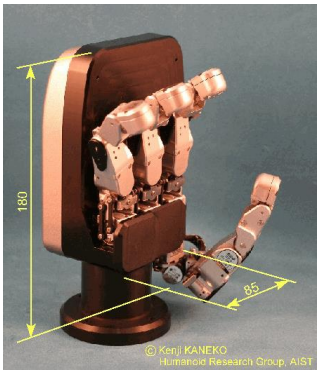
Anthropomorphic Hand [29]	2009	5	13	5	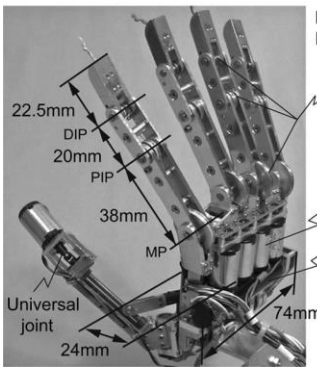
UB Hand III [30], [31]	2010	5	20	16	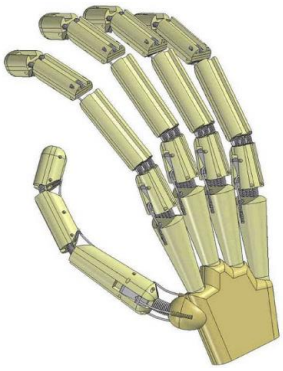

1.3 Multi-fingered, Anthropomorphic Robot Hands

Most of the commercial robots available in the market now-a-days are industrial robots which are mostly employed in industrial applications. An industrial robot is basically a robotic manipulator equipped with a tool, which can take different positions, and can perform different operations with a pre-programmed movement achieved through a computer and a series of motors. These manipulators, operating in a completely known environment, have a limited capability of alteration. In unstructured environments, which characterize the everyday life of human beings, it may be difficult for performing a task, where the robot replaces humans or works in cooperation with them. But the next generation of robots will interact with people directly, which needs to mimic the human activities, looks like human structure etc. Keeping a view on the future need, the interest on the implementation of artificial systems to replicate the manipulating ability of the human body parts like hand, leg etc. is growing among researchers. As far as handling of objects for precision manipulation, handling of object with different geometrical shapes, grasping of soft objects in unstructured environment is concerned the multi-fingered hand finds its best use. Dexterous manipulation is an area of robotics in which multiple manipulators or fingers co-operate to grasp and manipulate objects. In the application of robotic hand the following few aspects must be performed precisely for efficient handling of any type of objects in any environment. In the design and use of a robotic hand “dexterity” and “anthropomorphism” are two key issues:

Dexterity represents the capability of the end-effector to autonomously perform tasks with a certain level of complexity. The dexterity is a measure of hand capability of changing the configuration of the manipulated object from an initial configuration to a final one, arbitrarily chosen within the device workspace and divided in two main areas, i.e. grasping and internal manipulation.

Grasping is the capability of constraining objects in a fixed hand configuration such as the object is fixed with respect to the hand.

Internal manipulation is a controlled motion of the grasped object in the hand workspace, with the hand configuration changing with time.

Anthropomorphism represents the capability of a robotic end- effector to mimic the human hand in terms of shape, size, and aesthetic.

As the word itself suggests, anthropomorphism is related to external perceivable properties, and is not itself a measure of what the hand can do, while on the other

hand, dexterity is related to actual functionality and not to shape or aesthetic factors. It can find in the literature anthropomorphic end-effectors with very poor dexterity levels, (even if they are called hands), as the task they perform are limited to very rough grasping procedure. But in contrary it can find smart end-effectors, capable of sophisticated manipulation procedure, without any level of anthropomorphism [1]. Anthropomorphism itself is neither necessary nor sufficient to attain dexterity, even if it is rather obvious that the human hand achieves a very high level of dexterity and can be considered a valid model for dexterous robotic hands. Anthropomorphism is a desirable objective in the design of robotic end-effectors mainly for following reasons:

- the end-effector can operate on a man-oriented environment, where tasks may be executed by the robot or by man as well, acting on items, objects or tools that have been sized and shaped according to human manipulation requirements;
- the end-effector can be tele-operated by man, with the aid of special purpose interface devices (e.g. a data-glove), directly reproducing the operator's hand behaviour;
- it is specifically required that the robot has a human-like aspect and behaviour (humanoid robots for purposes of entertainment, assistance, and so on).
- anthropomorphism is an important design objective for prosthetic devices. The development of end-effectors for prosthetic purposes [32, 33] has recently produced such advanced devices that they can be fully considered robotic systems.

While it is hard to compute the effective degree of dexterity of a robotic hand, its anthropomorphism can be defined in an accurate and objective way. Especially, the major facets that contribute to determining the anthropomorphism level of a robotic hand are:

- *Kinematics*: the existence of the main morphological components (fingers, opposable thumb, and palm);
- *Contact surfaces*: the extension and smoothness of the contact surfaces, an aspect that reflects on the capability to locate contacts with objects all over the surface of the available links and on the presence of external compliant pads;
- *Size*: both referring to the average size of a human hand and the *correct* size ratio between the links.

From the study of the many robotic end-effectors, it can be concluded that the level of achieved resemblance with a human hand is significantly variable from case to case, even if all of them are defined as anthropomorphic hands. In the present circumstances of an increasing interest towards humanoid robots, and therefore anthropomorphic hands, new effort in developing mechanical design has been more inspired to the human hand model. Because the assimilation of the many technological subsystems (articulated work-frame, actuation, transmissions, sensors etc.) is one of the key-problems, the application of simultaneous engineering rules, with coordinated development of all the subsystems, must be developed for achieving the desired goal of making a better dexterous and anthropomorphic robot hands.

1.4 Application of Multi-fingered Robot Hands

Human body has always been the point of inspiration for researcher and developers during design of robotic system. From the first robotic systems appearing in movie theatres to modern motion pictures, the robotic system has always played the role of replacing and confronting the human being, often with a notable resemblance. The same holds true for industrial robotic systems as a whole. Earlier, the robots used for performing the repetitive tasks and so the grasping was the only prime importance for which mechanical grippers were sufficient to act as end-effectors. By the time, the ranges of applications of robots widen and along with grasping, manipulation also becomes importance for end effectors. Under such situation, multi-fingered hands are the best alternative end effector providing grasping and manipulation simultaneously. The ability of stable grasping and fine manipulation with the multi-fingered robot hand is playing an increasingly important role in manufacturing and other applications that requires precision and dexterity. The application area of multi-fingered hands has extended to different fields such as: industrial applications, rehabilitation of human hand, in service robots those are employed for different house hold work and also in modern humanoids.

1.4.1 Industrial Applications

The cost and simplicity have been the important factors in the design of end effectors for industrial robots. Therefore, the simple devices such as open/close grippers are mostly used as end effectors. With increase in automated working environment in industries like manufacturing, automobile etc. some special purpose robots with multi-fingered hands are being introduced and used for some specific

tasks. But, dexterous multi-fingered hands do not find much application in industrial environments. The reasons may be attributed to low payload, low reliability, high complexity and high cost. In spite of all these bottlenecks, robots with multi-fingered hands are also used for some tasks where grasping as well as manipulation is important from the application perspective as shown in Figure 1.4. A robotic hand developed by iRobot (of Roomba fame) is a three-fingered robotic hand that consists of a very closely resembling human thumb, two fingers and a palm (Figure 1.4 (a) [34]). Figure 1.4 (b) [35] shows a three fingered hand connected with a robot arm used for holding a cylindrical stud while welding is made on the surface of another part. The robot arm with multi-fingered Barret hand is used for material handling is shown in Figure 1.4(c) [36].

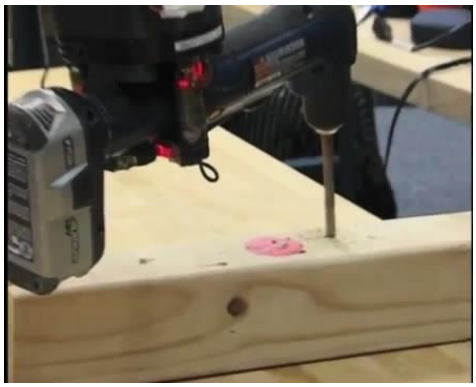

(a) iRobot hand

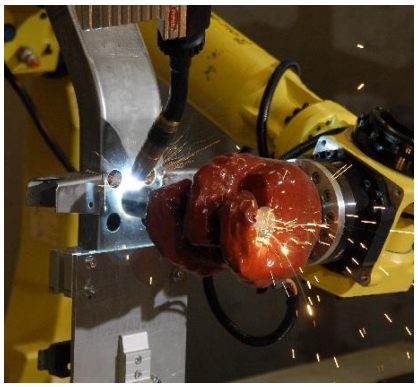

(b) Robotica

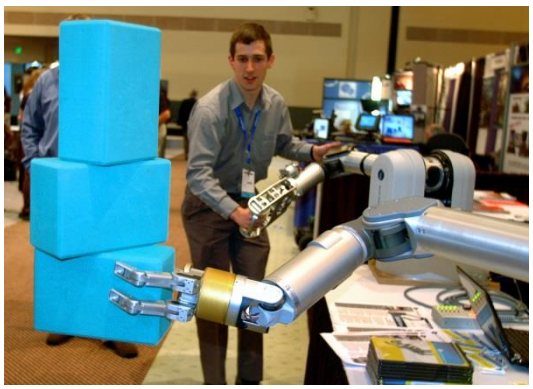

(c) Barret hand.

Figure 1.4: Multi-fingered hands used for different industrial applications.

1.4.2 Rehabilitation Applications

When human beings are unable to interact physically with the surrounding environment to perform the daily necessary activities due to injury or due to some disease in one or more physical parts of the human body, making him/her incapable of doing the physical work, they necessitate assistance for doing the same. These disabilities can be overcome by providing physical therapy or rehabilitating the particular part that has become disabled due to any reason. The hand of human beings is an essential part to interact with outer world. So it is very important to replace the damaged or injured or disabled hand, which can be possible only by the use of multi-fingered robotic hands.

(a) Liberating Tech. hand

(b) Michelangelo hand

Figure 1.5: Multi-fingered hands used in rehabilitation.

The multi-fingered robot hands are also helpful for the patients who are partially paralyzed due to neurological or orthopeadic damages. These are also used in medical rehabilitation for improving the quality of the life of people having orthopeadically and neurological disability. If the model of human hand is created with reasonable accuracy by respecting the type of motion provided by each articulation bone, it can function as the real organ providing the same motion. In Figure 1.5 (a) [37] and Figure 1.5(b) [38] examples of two robotic hands are shown which are used for rehabilitation purpose. The Liberating Technology introduces a new hand (shown in Figure 1.5 (a)) that consists of dexterous fingers and a thumb. The thumb and fingers have urethane over-molds to provide better grasping and

molded in finger nails for picking of small objects. These are also best suited for rehabilitating the human hand. The Michelangelo Hand (Figure 1.5(b)) has four movable fingers and a thumb like human hand. The thumb and fingers are positioned separately using muscle signals and offers innovative, never-before-seen gripping kinematics. In order to achieve a natural movement pattern, the hand is equipped with two electrical drive units.

1.4.3 Service Robots

Robots which are operated semi or fully autonomously and perform some useful services to the humans or equipment similarly as a human being are called service robots. Those are employed for different household work (Figure 1.6) [39] as well as in industry shop floors. The variety of work is abundant and uncertain. The multi-fingered hands are normally used as the end effector of these robots to facilitate the stable gasping and fine manipulation of objects. Figure 1.6 shows the robot ASIMO developed by Honda, at Honda's Wako Fundamental Technical Research Center in Japan, having multi-fingered hand being used for serving tea to the guests.

Figure 1.6: ASIMO a service robot performing human operation.

In recent years one of the incipient issues in the field of robotics is the development of the autonomous, anthropomorphic and multi fingered robots which are employed for variety of application. Service robots are now extending their applications to real human-robot coexistence environments, for which the anthropomorphic appearance along with multi-fingered hands are the important factors. Some service robots have been employed successfully for practical applications such as floor cleaning, visitor guidance and patrolling.

1.4.4 Humanoid Robot

A humanoid robot does not necessarily look like a real human being, but structurally it must be like a real human such as it must have two legs, two arms and a head. Ultimately, the objective of humanoid robot is to help people in their daily life, so the humanoid robots are also considered as service robots but vice versa is not true.

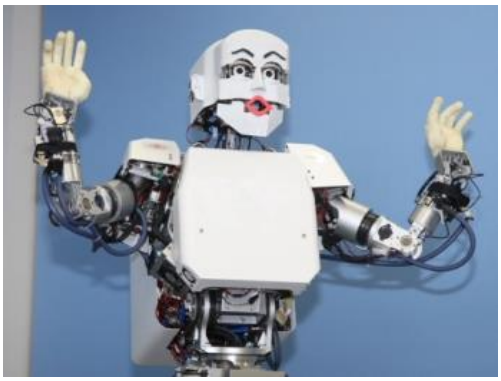

(a) KOBIAN

(b) Toyota's partner robot

(c) The atlas humanoid from Boston Dynamics

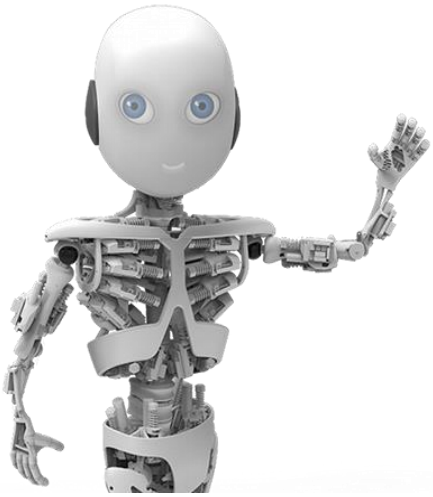

(d) Roboy

Figure 1.7: Humanoids having multi-fingered hands.

Since the humanoid robots are working along with human beings in human environment, the dexterity and manipulation issues are also as important as grasping. They do have multi-fingered hands as shown in Figure 1.7. Kobian is the latest technological invention humanoid robot developed by the Japanese company Tmsuk is shown in Figure 1.7 (a) [40]. It too has multi-fingered hand and it is able to express different emotions like delight, surprise, sadness and dislike. The Kobian incorporates a double jointed neck and the motors housed in its face allow it to move its lips, eyelids and eyebrows. Figure 1.7 (b) [41] shows a humanoid robot developed by Toyota in Japan. It also has multi fingered hands like human hand and mainly used for playing musical instruments. The Atlas humanoid developed by Boston Dynamics, USA, is a latest humanoid robot as shown in Figure 1.7 (c) [42]. It helps the human beings at the time of disasters. The main objective of developing this type of humanoids is that they do not have to be monitored and watched over by a human, rather they act automatically and respond to stimuli and think progressively in order to deliver humanitarian aid. Roboy (Figure 1.7(d) [43]) developed by Artificial intelligence laboratory of the University of Zurich, is one of the most advance humanoid robot having multi-fingered hands, which can execute service independently for the convenience of human beings. There are many humanoid robots in fictional stories, we imagined. Some real ones have been developed and commercialized. Almost in all cases the humanoid robots have multi-fingered hands at the end of its arm for the purpose of grasping and manipulating the objects in the course of theirs work.

1.5 Grasping and Manipulation using Robot Hand

In the history of robotic research the past decades has been marked with development work in multi-fingered, multi-DOFs, intelligent robots that can carry out tasks like human beings. Therefore dexterity and anthropomorphism have been given lots of emphasis and the quality of work has been in the fore. So far as robotic hands are concerned the design issues have been more oriented towards achieving stability, force-closure, task compatibility and other properties. Different approaches have been developed in the past to meet these goals and substantial improvements have been claimed.

The basic function of a multi-fingered gripper is to grasp objects and possibly manipulate them by means of its fingers. One of the essential properties looked for in the grasp configuration selection is the immobilization of the grasped object (its equilibrium) against the possible external disturbance. The set of fingers grasping

the object by fingertips can also be seen, from a mechanical point of view, as distributed impedance on the object surface.

Each finger of a multi-fingered hand may be considered as an independent manipulator with its base fixed to the wrist in a particular manner. While grasping the object by multiple fingers and manipulating it to carry out some specific task, the grasp must satisfy a number of conditions, such as static equilibrium, no slippage and the ability of resisting the disturbances in all directions including the external and reactive ones. This calls for a systematic determination of the contact locations and the related hand configuration so as to assure that all the conditions as mentioned beforehand are satisfied.

The important functions of the hand are: to explore or search, to grasp or restrain, and to alter or manipulate the arbitrary shaped objects in a number of ways. The first function is an independent vast research area which is not within the scope of this dissertation; whereas other two functions are co-related and depend on the kinematical structure and number of contact points between the object and hand. Researchers and designers have been trying to develop a robotic hand analogue of human hand. Most probably the first existence of mechanical hands was the prosthetic devices used to replace lost limbs [44], which have been designed to simply grasp the objects. Later on, variety of multi-fingered hands have been designed and developed (given in section1.2.2) as nearer as to the human hand in respect of appearance, functions and capabilities. Some of the major advantages of the multi-fingered hand in comparison to parallel jaw gripper with respect to grasping and manipulation are:

- Higher grip stability due to multi point contact between object and hand.
- Adaptability to varied shapes of objects.
- Ability to move the part during grasped condition.

Therefore, grasp planning is one of the key issues for robotic dexterous hands to accomplish the desire task. Nowadays, neuroscience, anthropology and philosophy converge in considering the activity of hand and touch as essential in the development of superior cognitive faculties like memory, imagination, and language [45].

The increasing interest in grasping is somewhat due to the evolution of industrial automation towards flexible automation. The transition from large batch size to medium and small batch size has led to the replacement of special purpose devices with more general purpose end effectors facilitating the manipulation of a wider

class objects. Simultaneously, more attention has been given to fine manipulation and assembly. This has prompted the necessities for appropriate tools to be able to increase the robot's manipulative capacity with fine position and force control. On the other hand, as end effector becomes more flexible, control becomes more multifaceted and a better indulgent of grasping turns out to be a thought-provoking issue [46]. Hence, grasp and manipulation are vital functions of robotic hands. In order to grasp and manipulate real world objects i.e. any arbitrary shape object in unstructured environment, automatic grasp planning systems are desirable. Therefore the good and effective grasps should have the following properties [47, 48]:

i) *disturbance resistance*: a grasp can stand disturbances in any direction if it is form-closure or force-closure.
ii) *dexterity*: a grasp is dexterous if the hand is able to move the object in task specified direction.
iii) *equilibrium*: a grasp is in equilibrium if the resultant of forces and torques applied on the object is null.
iv) *stability*: a grasp is stable if it can retrieve the equilibrium after disturbance vanishes by restitution forces.

Focusing on the first two properties disturbance resistance and dexterity, two groups of grasp quality measurements could be considered. One is related with the position of contact points and the other is associated with the hand configuration. The first group of quality measures includes those that only take into account the object properties, friction constraints, form-closure and force-closure conditions to quantify the grasp quality. The second group of quality measures includes those that consider the hand configuration to estimate the grasp quality, such as singularity avoidance or positions of finger joints. In the study of the first grasp of the first group of quality it is assumed that all the surfaces of the object could be reached by the hand. The selection of optimum contact points on the object surface measured this way ignoring the actual geometry of the hand can lead to contact locations unreachable for the real hand. So it is necessary to combine the grasp quality measurements in a serial or parallel way to accomplish common grasp tasks, besides the hand's internal degrees of freedom which set the finger positions. Grasp can be seen as a set of contacts on the surface of the objects. The force or torque that is applied on the object by the hand depends on the configuration and the contact model of the hand. Once the contact model is selected one can choose the closure properties of grasp that is required. Generally, the contact between the

fingertip and object is idealized as a point contact at some fixed locations. By assuming these conditions, the possibility of sliding or rolling of the fingers on the surface of the object can be considered. In other words, grasp planning requires sets of information which are to be collated and subsequently used to form a model. The necessary information and their relationship are shown in Figure 1.8.

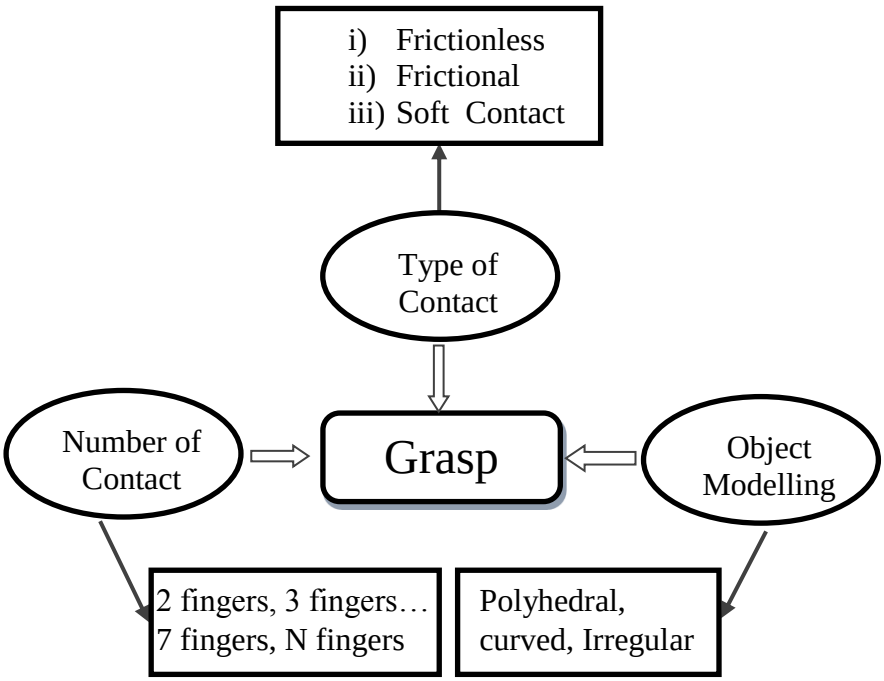

Figure 1.8: Information required for planning a grasp.

1.6 Motivation

The initial study of end effector for robot manipulators being employed in the recent times and to be employed in the future industries, especially, in the applications involving fine manipulation of small to medium size components towards the need of flexible and dexterous end-effector. The increasing application of intelligent robotics tools in service sectors, health sectors, entertainment sectors etc. also initiates thoughts to design and develop advanced end-effectors. Advancement of technology has given rise to many intelligent end-of-arm tooling which are smart enough to collect information about their environment, process them as per the need and act accordingly. However, actuating part has been constrained heavily due to lack of dexterity in the mechanism of the tool. It is

therefore, considered that if a structure very similar to that of human hand is developed, it can perform some specified tasks more effectively and efficiently.

Therefore, the research community since early days to till date are attracted towards the design and analysis of multi-fingered robot hands, not only as an exciting technical problem itself but perhaps also because of anthropomorphic motivations and the inherent interest in better knowledge of the human body. As presented in chronology of robot hands, it is observed that several important projects have been launched, and a number of robot hands have been developed. Still, the present situation is that reliable, flexible, dexterous hands are yet not available for real applications. It is also easy to foresee that in the future a consistent research activity is bound to happen in this fascinating field, with design, development and analysis of such tools at the technological (sensor, actuator, material, etc.), methodological (control, planning, etc.) and application (workspace, grasping, etc.) levels. Important connections with other scientific fields, such as cognitive science, are also expected.

The study of previous literatures and reports on achievements in developing multi-fingered anthropomorphic robot hands provides a moral boost to the fact that a more dexterous robot hand than even before can be designed and realized. Such a hand can find a wide range of use in industries as well as in many other applications.

1.7 Broad Objective

The initial study of the subject on multi-fingered robot hand, the pace of their development, the areas of their applications and the very potential of their applications in industries and other future use have led to formulate the following broad objective of the research work.

- Performing research study on a multi-fingered robot hand with more number of degrees-of-freedom than those studied by previous researchers in a view to recommend a flexible and dexterous hand in the light of a human hand.
- Analysing the system of structural arrangement of the robot hand for improved manipulability.
- Carrying out the kinematic modelling and simulation of the robot hand being conceptualized to check its feasibility.
- Carrying out the grasp analysis of the hand considering practical conditions.

1.8 Methodology

The hand consists of number of connected parts forming a number of open kinematic chains which consequently get constrained at a single wrist joint. At the same time, many motion constraints exist among fingers and joints that make the hand motion even harder to model. In order to develop a model for the anthropomorphic robot hand, the anatomy of the human hand is first studied to gain better understanding on the joint movements. Following that, the kinematic models are developed and necessary analyses are made. The major steps envisaged for accomplishing the research work and achieving the objectives are presented through the following lines:

- Review of literature
- Hand model
- Parameters and constraints
- Kinematic analysis
- Grasping analysis
- Discussion and recommendations

A complete chapter (Chapter 3) is devoted for explaining the research methodology.

1.9 Organization of the Thesis

The present *chapter 1* is the Introduction chapter gives brief idea about the history, types of robotic gripper and application of multi-fingered hand in various field. Apart from this introduction chapter, the thesis organized as follows:

Chapter 2 provides a review of literature based on different aspects of the multi-fingered hand like structure, control, optimization, gasping etc. Some of the important literatures are presented in a table and a brief analysis is made on the outcomes and shortfalls with respect to multi-fingered hands. The objective of the research work is also defined and presented based on the analysis of the review of literature.

Chapter 3 discusses about the research methodology. It provides a brief idea about the different steps should be taken care during the research work. Accordingly, the different activities, research methods and tools used for the present research work are presented briefly along with the scope of the present work.

Chapter 4 presents the anatomical structure of the human hand, which is the basis for the modelling of the anthropomorphic multi-fingered robot hand. A brief

discussion is made on the different bones of the fingers of the hand and the joints connecting those bones. Even if the human hand is highly dexterous in nature, it is also constrained as per the limit of the rotational angles of the different joints. Those angle limits are also presented in tabular form for different joints.

Chapter 5 proposes a 5 finger novel hand model with 25 DOFs. The each individual finger is considered as an open loop kinematic chain and each finger segment is considered as a link of the manipulator. The kinematic model and corresponding D-H parameters are also derived. The forward and inverse kinematic analyses are made for the proposed hand model. The workspace which contains all loci of fingertips is derived.

Chapter 6 discusses about the grasping theory and different types of contacts between the fingertip and object. The classification of grasp and the conditions for stable and equilibrium grasp are also elaborately discussed. The details about the force closure grasp is given which is applicable in case of multi-fingered hands as manipulation is the one of the important considerations in the present work.

In *Chapter 7* the analysis is made for the grasping capability of the proposed hand model with respect to different shaped objects. The forces applied on the fingertip during grasping are calculated. The hand model is also analysed to evaluate the stresses being developed at various points in the fingers. This is done using ANSYS.

Chapter 8 presents the results obtained during forward kinematics, inverse kinematics and grasping analysis. The results are summarised and are presented in the form of program outputs, tables and graphs.

Chapter 9 concludes the present dissertation with a summary of the contribution and the scope for future work.

1.10 Summary

In this chapter, the general overview of the robot hand is presented. The classification of robotic grippers and progressive development of robot end effector from single finger gripper to multi-fingered hands are presented, as per need and technological development. The chronological development of some of the multi-fingered robot hands from earlier time to till date are given in tabular form. The different design aspects to mimic the human hand are presented like anthropomorphism and dexterity. The grasping and manipulation requirement of robot hand is also discussed.

Chapter 2

REVIEW OF LITERATURE

2.1 Overview

With the growth of interest towards humanoid robots, anthropomorphism and dexterity of multi-fingered robotic hand becomes a key subject. The growth of anthropomorphic robotic hands with high level of dexterity and agility increases large number of technological concerns. At this moment hand research is a sizzling topic and there are number of researchers, who are into the research and development of dexterous robot hands. The design features of the robotic hands are: number and kinematic configuration of the fingers, anthropomorphism or non-anthropomorphism aspects, built-in remote actuation, transmission system, sensor assignment, integration with carrying devices (robot arm) and control [49]. In spite of, such a movement towards the development of human-like robotic hands, the results so far reached are not yet comparable with the performances of human hand. Still there is a gap between the current research hands and the dream robotic hand which is a multi-fingered, function like human hand and cost effective. Therefore, day by day more researchers are joining into this most challenging research area with a single aim that to develop a multi-fingered robotic hand which will mimic the human hand. In this chapter the current state of art on multi-finger robotic hand and its grasping capability analysis presented.

2.2 Literature Survey

Research on robotic hand is one of the complex topics in the field of humanoid robotics. A chronological development of some important multi fingered hands is

given in chapter-1[5-25]. Based on the extensive survey of previous literature, a list of some important work done in this area is presented in Table 2.1.

Table 2.1: List of some important literatures.

Sl.	Year	Author	Title	Contribution
1	1996	Lin and Huang[50]	Mechanism and Computer simulation of a new robot hand for potential use as an artificial hand	Developed a five fingered robotic hand consisting of 17 degrees of freedom. Each joint driven by independent motor through gear arrangement.
2	1997	Ponce et al. [51]	On computing four finger equilibrium and force closure grasp of polyhedral objects.	Proved the necessary and sufficient condition for equilibrium and force closure and also geometric characterization of all the types of four finger equilibrium grasp.
3	1998	Nagai et al.[52]	Development of a three fingered robotic hand wrist for compliant motion	Developed a three fingered robotic hand with wrist which having 15- DOFs.
4	1999	Ramos et al.[53]	Goldfinger: A Non-anthropomorphic, dexterous robot hand	Described a new four fingered dexterous robot hand having 12- DOFs and actuated by an independent motor placed at the base of the finger.
5	1999	Borst et al. [54]	A fast and robust grasp planner for arbitrary 3D object.	Showed that for the real robot average quality grasp is acceptable. They have also shown the statistical data that confirm their opinion that the randomized grasp generation algorithm is fast and suitable for robot grasping.
6	2001	Butterfa et al.[55]	DLR-Hand II: Next generation of a Dexterous Robot Hand	Proposed a 4 fingered robot hand with 13-DOFs along with fingertip force torque sensor and integrated electronics together with new communication architecture which enables a reduction of cabling to the hand.
7	2002	Massa et al.[56]	Design and Development of an under actuated prosthetic hand	Proposed a design approach based on under actuated mechanism, the model having three fingers i.e. thumb, index and middle finger (thumb having two phalanges and other two fingers have three phalanges). All the fingers actuated from two motors through wires.
8	2003	Haulin and Vinet[57]	Multi-objective optimization of hand prosthesis mechanisms	Considered a hand model having 5 fingers and 21- DOFs and optimized the five mechanisms with respect to seven positions.
9	2003	Zhu and Wang [58]	Synthesis of Force-Closure Grasps on 3-D Objects Based on the Q Distance	Presented a numerical test to quantify how far the grasp from losing force/form closure is. With the polyhedral approximation of the friction cone the proposed numerical test was formulated as a single linear program.
10	2003	Li et al. [59]	A New Algorithm for Three-finger Force-closure Grasp of polygonal object.	Developed a new necessary and sufficient condition for 2-D three finger equilibrium grasp. They implemented a geometrical algorithm for computing force closure grasp of polygonal object.

11	2006	Huang et al.[60]	The Mechanical Design and Experiments of HIT/DLR Prosthetic Hand	This hand having 5 fingers connected by 13 joints. All the fingers driven by three motors i.e. thumb and index finger by one motor each where as other three fingers by one motor.
12	2007	Zolla et al.[61]	Bio-mechatronic Design and Control of an Anthropomorphic Artificial Hand for Prosthetic and Robotic Applications.	The artificial hand consists of three fingers (i.e. thumb, index and middle). All fingers having 3 joints and thumb has another one joint for abduction and adduction. Driven by 4 DC motors.
13	2007	Dragulescu et al.[62]	The modeling process of a human hand prosthesis	Proposed a hand model having 22- DOFs in which 3-DOF are on the wrist, which enables the wrist rotate w.r.t. the forearm.
14	2007	Kargov et al.[63]	Development of a Multi-functional Cosmetic Prosthetic Hand	The fluidic hand consists of 5 fingers and 8 joints which are actuated by a hydraulic actuation system.
15	2007	Dragulescu et al.[64]	3D active work space of human hand anatomical model	Considered a model having 22-DOFs i.e. thumb having three, all other four fingers having 4 each and wrist having 3-DOFs. By conserving the wrist as the global reference plane they calculated the workspace for different range of motion of different joints.
16	2008	Yasuhisa and Takashi [65]	Under actuated Five-Finger Prosthetic Hand Inspired by Grasping Force Distribution of Humans	Described the under actuated hand which consists of 15-DOFs and 5 fingers. All the fingers are driven from a single actuator and controlled by myoelectric signals. The grasp force is distributed like human for stable and robust grasping.
17	2008	Controzzi et al.[66]	Mechatronic Design of a Transradial Cybernetic Hand	The smart hand has 5 fingers and 16 joints, driven by 4 actuators by a combination of differential and compliant transmission.
18	2008	Jung and moon[67]	Grip Force Modeling of a Tendon-driven Prosthetic Hand	This prosthetic hand incorporates 11 joints with 5 fingers, driven by 6 independent actuators.
19	2008	Peer et al. [68]	Multi- Fingered tele manipulation- mapping of a human hand to a three finger gripper	Presented the point to point mapping algorithm for a multi-finger tele-manipulation system, in which they mapped the fingertip motions of the human hand to a three finger robotic gripper i.e. barrett hand. This consists of three identical fingers, out of which one finger is fixed to carpus and the other two fingers are able to rotate about 180 degree around the base. Each finger consists of three links and two joints, driven by 4 independent motors.
20	2008	Bounab et al. [69]	Central Axis Approach for Computing *n*-Finger Force-closure Grasps	Developed a new necessary and sufficient condition to a achieve force closure grasp using central axis method.
21	2008	Niparnan et al. [70]	Positive Span of Force and Torque Components in Three Dimensional Four Finger Force Closure Grasps	Proposed a necessary condition for n-finger force closure grasp which considers true quadratic force cone without linearization. The condition finds its use as a heuristic for multiple queries force closure test.
22	2009	Lee et al. [71]	Development of Bio-mimetic Robot hand using Parallel Mechanism	Developed a four finger robot hand, which has parallel mechanism like human hand and actuated by coupled linear actuators and it can grasp various objects unknown and known that can be seen from environment.

23	2009	Wiste et al. [72]	Design of a Multifunctional Anthropomorphic Prosthetic Hand with Extrinsic Actuation.	Designed an anthropomorphic prosthetic hand to fully accommodate a set of grasp and gesture taxonomies with the minimum number of independent actuators.
24	2009	Parasuraman and Zhen[73]	Development of Robot assisted hand stroke rehabilitation system	Proposed the hand model similar to human hand. But for analysis purpose they considered three fingers and 13 They suggested it for rehabilitation purpose.
25	2009	Tarmizi et al.[74]	Kinematic and dynamic modeling of multi-fingered robot hand	Described the mathematical modeling of the fingers which enables the design of multi-fingered robot hand in future.
26	2010	Controzzi et al.[75]	Bio-Inspired Mechanical Design of a Tendon-Driven Dexterous prosthetic Hand	They proposed a 20-DOF and 11-DoAs hand able to manipulate and perform stable grasp .The hand will be connected to the forearm by means of a 2-DoAswrist.
27	2010	Wang et al. [76]	Bio-mechatronic Approach to a Multi-Fingered Hand Prosthesis	A bio-mechatronic approach to develop a human-like prosthesis. The proposed hand is composed of five active fingers with 15-DOF.
28	2011	Suhaib et al. [77]	Contact Force Optimization For Stable Grasp Of Multi-finger Robotic Grippers.	Presented the optimization method to obtain the most stable grasp for a nominated set of contact points on an object. The study concludes that the stable grasp for a nominated set of contact points and loading condition is obtained at maximum friction angles and minimum contact points.
29	2012	Zaid and Yaqub [78]	UTHM HAND: Performance of Complete System of Dexterous Anthropomorphic Robotic Hand	Describes a new robotic hand system working under master slave configuration. Bluetooth was used as the communication channel between master and slave. The UTHM robotic hand was a multi-fingered dexterous anthropomorphic hand comprises of five fingers (four fingers and one thumb), each having four degrees of freedom (DOF), which can perform flexion, extension, abduction, adduction and also circumduction.
30	2013	Lippiello et al. [79]	Multi-fingered grasp synthesis based on the object dynamic properties.	Proposed a new method for fast synthesis of multi-fingered grasp configuration. They evaluated all the regions of the object surface favoring the synthesis of minimal inertia grasps and then selected a reduced number of discrete grasping regions on the basis of the fingertip size, model uncertainty, and surface curvature. Finally, the performed an exhaustive search of the optimal grasp configurations with respect to the grasp.

It is evident from the study of large number or research publications that appeared in various journals, conference proceedings and technical articles that the various aspects of robotic hand research can be classified into following sub areas:

i) Structural analysis
ii) Optimization
iii) Control aspect
iv) Application and

v) Grasping analysis.

2.2.1 Structure of Multi-fingered Robot Hand

It is clear that the flexibility of the human hand can be thought of as the *Holy Grail* of robotic end-effectors. The first robot hand, as it is commonly referred to, was perhaps the end-effector of the *Handyman*, a robot developed by Ralph Mosher for General Electric in 1960 [80]. This hand included only two fingers similar to, the then usual grippers [81], but each finger had three degrees of freedom (DOF) and a wrist providing two additional DOF which is directly controlled by the operator. Around 1969, the first research projects on robotic hands with three fingers including a "thumb" in opposition were started. With start of those projects an anthropomorphic design of robotic hand began in the United States and in the Japan. Then only a robotic hand referred to a particular type end effector with an anthropomorphic inspiration. Robotic grippers have a simpler design and are much less versatile with respect to the variety of tasks that they can perform like robotic hands.

The multi-gingered prosthetic hand is essential to provide rehabilitation for individuals who lose hands due to accidents or some other reasons. A prosthetic hand serves two purposes; cosmetic and functionality for which that is most accepted for rehabilitation purpose. Lin and Huang [50] in 1997 explained the design and implementation of a dexterous artificial hand named as NTU- hand which was used as a prosthetic. They designed and fabricated in their laboratory the prototype of the said hand with an emphasis on functionality purpose of the prosthetic hand. The developed NTU- hand had 5 fingers and 17 degrees of freedom. The whole work was organized in two parts. The first part was the mechanical design of the NTU-Hand. This part presented the design concept of the NTU-Hand and shows the detailed scheme of the mechanism. The hand mechanism specially designed in such a way that the hand had an uncoupled configuration in which each finger and joint were all individually driven. The size of the hand was almost same as the human hand. The specification and some issues of the mechanical considerations were also stated. All actuators, mechanical parts and sensors are on the hand. The modular design was developed to limit the hand size so that the hand could be useful for both prosthetic and industrial applications. The compact design made that feasible to adopt the hand to the injured wrist. The second part was the computer simulation. It was built to evaluate the manipulable range of the artificial hand with three-dimensional graphics. From the results of the simulation, the posture of the artificial hand and the relationship between the hand

and the grasped object in a specific viewpoint could be obtained. The control and grasping analysis of the NTU-Hand were not addressed in this paper. In their proposed design they considered 2 DOF at MCP joint of thumb and index finger whereas only 1 DOF at MCP joint of other three fingers, which limits the flexibility of those three fingers as well as the flexibility of hand. In the proposed hand used gear trains as diver mechanism. Due to backlash problem of gear drives the accuracy of joint position not so high. Since the hands are mostly used for grasping propose, the backlash problem not as serious as that was not happen during grasping. Because of high gear ration the force on the hand was large. The limitation of the force is determined by the capacity of motor and strength of gears. The modulus and thickness of the final stage of the gear train should be larger than previous one to stand against large torque. The torque of motors was decreases while the heat accumulates in the chamber of finger segment. The seat of the motor was used to transfer the heat to outside of finger segment.

The research of humanoid hand is mainly divided into two categories: one consists of multi-sensor, multi-degree of freedom, high intelligent and multi-fingered dexterous hands. Most of them were developed for space operation and complicated with large weight. The other consists of lightweight anthropomorphic hands with simple structure and multiple fingers. They are mainly used as prosthetic hands for rehabilitation purpose. However, surveys revealed that more than 30 to 50% of handicapped persons only used their prosthetic hands once in a while. The main factors for the rejections were [60]:

- The appearance of hands is far from human hand.
- The unnatural movements caused by the limited DOF.
- The low functionality of hands resulted in single grasp and unstable grasp caused by few finger's DOF.
- The heavy weight of hands.

Huang et al. [60] in 2006 designed and developed a multi-sensory, five-fingered bio-prosthetic hand named as HIT/DLR hand based on the mechanism of under-actuation. An under-actuated mechanism is the one which has fewer actuators than DOF, which reduces the complexity of control strategy and overall weight of hand. They claimed that their hand was very similar to adult hand, simple in construction and encompassed of 13 joints. Modularization idea was adopted during the development of the hand: the index finger, middle finger and ring finger were designed in the same structure having three phalanges. The thumb and little finger have two phalanges each. The thumb and index finger were actuated by a motor

each and the other three fingers were actuated by only one motor. They stated that the thumb of the developed hand can move along cone surface like human thumb and superior in appearance. They were verified by experiment that the hand has strong capability of self-adoption, cam accomplish precise and power grasp for objects with complex shapes. The authors have taken more importance on the appearance of the hand than functionality and capacity. They had not given much attention on the control part of the hand. Due to decreased under-actuation, the control complexity decreases and at the same time the power supply to each finger also decreases. Hence the grasping forces are also less due to less power supply. Structurally the little finger has two phalanges whereas in actual human hand there are three phalanges. Due to this the flexibility of little finger decreases. The DOFs are also very less in comparison to human hand, which lead to decrease in degree of dexterity and manipulability.

If the hand model is designed and developed with accuracy by respecting the type of motion provided by each articulation and the dimensions of articulated bones of human hand, it can function as the real organ providing the same motions. Keeping this fact in mind all researchers has been trying to design and develop their own hand model. Unfortunately, the human hand is hard to model due to its kinematical chains submitted to motion constraints. On the other hand, if an application does not impose a fine manipulation it is not necessary to create a model as complex as the human hand is. Dragulescu et al. [64] proposed a hand model that represents a new solution compared to the existing ones. That model was capable to make special movements like power grip and dexterous manipulations. During those operations, the fingertips did not exceed the active workspace encapsulated by determined surfaces. The proposed kinematical model consists of 5 fingers including thumb and has 22 DOFs in all. The thumb had 3 DOFs, all the four fingers had 4 DOFs each, and the wrist had 3 DOFs. They used the Denavit-Hartenberg rules for kinematical analysis of the model and derived the forward kinematic equation of each fingertip and ultimately the fingertip position. Using MATLAB they generated the work space for the proposed hand model. The proposed model is very close to the human hand as far as number of fingers and joints are concerned. They have not discussed about the grasping capability and control of the hand model. Although, the 3 DOF in the wrist will help the hand model for positioning with respect to object, they will not much influence the grasping and manipulating capability of hand. They considered the palm as rigid body unlike the human palm.

Rehabilitation robotics is a potential area of multi-fingered robotic hand research. It includes many areas such as electrical, mechanical and biomedical engineering, artificial intelligence and sensor technology. A robot assisted hand stroke rehabilitation system has become a boon to severe disabilities in the world. Parasuram and Zhen [73] in 2009 focused the human's upper limb rehabilitation. They proposed an arm and hand combination model for the said purpose. They stated that due to simplifications, the upper limb analysis was divided into two parts; the human arm consisted of seven degrees-of freedom and the human hand with the thumb was modelled with five degrees-of-freedom and the other fingers were modelled with four degrees-of freedom. They considered the hand with 13 DOF that comprised of thumb, middle finger and ring finger for the purpose of analysis. The index finger and little finger were ignored from analysis with reason that index finger and middle finger are similar in structure and function and same in case of ring and little finger. The joint limits and segmental length of finger segments considered exactly same as human hand. They also made the dynamic and control analysis for the same hand model. Similar to other's work they had not considered the palm arch effect of the human hand. The authors did not consider the workspace generation and grasping capability of hand. They concentrated only the structure of the hand.

Tarmizi et al. [74] stated that a robot hand can mimic the movements of a human hand in operation. Stable grasping and fine manipulation with the multi fingered robot hands (MFRH) are playing an increasingly important role in manufacturing and other applications that require precision and dexterity. Various types of MFRH have already been developed with advantage that the hand can be used with different types of robot arms because the robot hand has independent structure. On other hand, there were number of disadvantages with such hands. The most serious one was the limitation on size. Most of this type of robot hand had equal to or less than four fingers. Even, those with five fingers were not very similar to human hand as they had less number of joints or Degrees of Freedom (DOFs). The need for improving the MFRH arises from the desire for handling objects and shapes more effectively. Therefore, mechanical design plays an important role in the development of a MFRH. Simulation eases the design process. Mathematical modeling is an asset to establish simulation. They proposed a MFRH model based on the biological equivalent of human hand where each links interconnected at the metacarpophalangeal (MCP), proximal interphalangeal (PIP) and distal interphalangeal (DIP) joints respectively. The first step in realising a fully functional MFRH was mathematical modeling. They considered a model which

had 4 fingers and a thumb. All four fingers had similar structure consisting of 4 DOFs and the thumb had 5 DOFs including 3 DOFs at CMC joint. The kinematic and dynamic modelings were carried out using Denavit-Hartenburg (DH) algorithm and Euler Langrange formula for the proposed MFRH model. Although they considered the hand model having 5 fingers like human hand, the selection joints particularly in case of thumb are very different. They only developed the mathematical model for forward kinematics, inverse kinematics and dynamic cases but did not consider the fingertip position which result the workspace. Also they have not discussed about grasping capability of the hand model which was the main function of the developed hand.

Kriegman et al. [82] described the computational architecture for the Utah-MIT hand (jointly developed by The Center for Engineering Design at the University of Utah and the Artificial Intelligence Laboratory at the Massachusetts Institute of Technology in 1983). They discussed the design issues encountered in the hardware and software development. The developed hand had been made of approximate anthropomorphic size, consists of three fingers with an opposing thumb and designed for grasping an arbitrary object.

Bergamasco and Marchese [83] described the mechanical design for the development of a new three-fingered poly-articulated myoelectric prosthesis. The prosthetic hand was equipped with position, force, and slip sensors while a sensor based control allows maintaining a stable grasping of the object without affecting the user attention. They gave a general description of the whole system by emphasizing the mechanical solutions utilized for the three fingers. They also integrated the force sensors at the level of fingertip and palm. The control strategy allows the automatically increment the force on the grasped object if slippage condition occurs.

Vinet et al. [84] proposed the design of a hand prosthesis based on a new plane of action for the thumb, proposed design specifications and functional characteristics. The design methodology divided into two steps: the morphology design of the hand prosthesis and the 4-bar mechanism design for each finger. It was noted that identical flexion angles of the finger joints were obtained for these two prehension patterns, the difference being in the inclination angle of the thumb's plane of flexion. This finding greatly simplified the design of the internal mechanisms of the fingers.

Yasumuro et al. [85] described the modeling of human hand considering the dynamics and natural constraints of the motion and the shape of the hands. The

hand model they proposed consists of a dynamic model and a surface model. Even using few hand parameters like some key angles of the joints, the desired natural posture of the hand could be generated by them. The surface model was built up based on the digitized 3D shape information of a real hand and used it to synthesize photo-realistic images. They showed experimentally that the hand animation could be designed easily and the generated hand animation is natural and smooth.

Lalibert and Gosselin [86] proposed the design of under actuated mechanical hands. It was shown that under actuation is a very promising avenue when only grasping is required (no manipulation). They proposed the architectures of two degrees of freedom under actuated fingers and designed a simulation tool to analyze their behavior. Simulation results were given and discussed in order to illustrate the usefulness of the simulator and general design guidelines were proposed. Based on simulation results, an under actuated finger was selected and that finger was used in the design of a three fingered hand.

Lane et al. [87] described the mechanical design, finger modeling, and sensor signal processing for a dexterous subsea robot hand incorporating force and slip contact sensing. The hand used a fluid-filled tentacle for each finger, which had inherent passive compliance, and no moving parts. Force sensing used strain gauges mounted in the fingertip, potted within a silicon elastomer. The design of a stochastic estimator was also described, for sensor fusion of contact force magnitude and direction data, obtained using redundant strain gauges in the fingertip. Finally, linear dynamic models of the finger dynamics in contact with a rigid surface were obtained using least squares and recursive least squares parameter estimation, as a precursor to closed-loop force control during grasping.

Visser and Herder [88] presented the design of a body-powered voluntary closing prosthetic hand. They argued that the movement of the fingers before establishing a grip is much less relevant for good control of the object held than the distribution of forces once the object has been contacted. Based on this notion, the configurations of forces on the fingers and the force transmission through the whole mechanism were taken as a point of departure for the design, rather than movement characteristics. For a good distribution of pinching forces on the object and a natural behaviour, the prosthesis was made adaptive and flexible. To achieve good force feedback, the disturbing influences of the cosmetic glove were strongly reduced by a compensation mechanism. To further improve the transmission of forces, friction was reduced by furnishing the whole mechanism with rolling links.

This force-directed design approach has led to a simple mechanism with low operating force and good feedback of the pinching force.

Griffin et al. [89] suggested a calibration scheme and kinematic mapping to support dexterous tele-manipulation. The calibration scheme was intended for use with an instrumented glove and permits an accurate determination of the intended motions of a virtual object grasped between a human operator's thumb and index finger. The motions of the virtual object were then mapped to analogous motions of a scaled virtual object held in a two fingered robot hand. A non-linear mapping scheme allows better utilization of the human and robot hand workspaces.

Bicchi [1] in 2000 made an attempt to summarizing the evolution and the state of the art in the field of robot hands. In such exposition, a critical evaluation of what in the author's view were the leading ideas and emerging trends was privileged with respect to exhaustiveness of citations. The survey was focused mainly on three types of functional requirements a machine hand can be assigned in an artificial system, namely, manipulative dexterity, grasp robustness, and human operability. A basic distinction was made between hands designed for mimicking the human anatomy and physiology, and hands designed to meet restricted, practical requirements. In the latter domain, arguments were presented in favour of a "minimalistic" attitude in the design of hands for practical applications, i.e., use the least number of actuators, the simplest set of sensors, etc., for a given task. To achieve this rather obvious engineering goal was a challenge to our community.

A very lightweight artificial hand was presented by Schulz et al. [90], which approximated the manipulation abilities of a human hand very well. A large variety of different objects could be grasped reliably and the movements of the hand appeared to be very natural. That five finger hand had 13 independent degrees of freedom driven by a new type of power full small size flexible fluidic actuator. The actuators were completely integrated in the fingers which made possible the design of a very compact and lightweight hand that can either be used as a prosthetic hand or as a humanoid robot hand. A mathematical model for the expansion of a flexible fluidic actuator was given and the mechanical construction and features of the new anthropomorphic hand were illustrated.

Dechev et al. [91] described the mechanical features of an experimental, multi-fingered, prosthetic hand which had been designed for children in the age group of 7-11. Conventional prosthetic hand existed for this age group, but they had limited mechanical functions. The experimental hand presented was able to perform passive adaptive grasp, which was ability of the fingers to conform to the shape of

an object held within the hand. During grasping, the four fingers and thumb were able to flex inward independently, to conform to the shape of the object. This passive design was simple and effective, not require sensors or electronic processing. The adaptive grasp system developed, results in a hand with reduced size and weight compared to other experimental hands, and had increased mechanical function and cosmetic appearance to conventional prosthetic hands.

Chappell et al. [92] suggested that the design of a three fingered end effector for use in an unstructured environment. The design had three driven inputs per finger to move the tip to the desired position in order to make contact with an object. A theoretical analysis of the three-dimensional workspace of the three-fingered gripper had been used to form a Jacobian matrix based on two inputs per finger, to provide a numerical inverse kinematics solution. Simulation of the theoretical model had shown that this approach was capable of highly accurate predictions of tip position.

Renault and Ouezdou [93] presented an anthropomorphic model of a human hand which structural and functional properties permits the simulation of grasping tasks. The proposed model had 27 degrees of freedom (DOF) which were split into 23 DOF for the hand, 2 DOF for the flexion–extension and the abduction -adduction of the wrist and 2 DOF for the pronation-supination and the flexion-extension of the forearm. Their model allowed simulating the grasp of an object multi hand adapting to its shape by including the movements of fourth and fifth metacarpals. The model, designed with ADAMS', was based on bio-mimetic approach which attempted to simulate the most realistic behaviour during grasping tasks. In order to achieved dynamic simulations, different link masses and inertia parameters were chosen according to the human hand forearm properties. The simulation of model was taken into account the joint motion coupling laws and the contact distribution.

Carrozza et al. [94] described the development of a novel prosthetic hand based on a “bio mechatronic” design. They designed and fabricated a bio mechatronic hand prototype with three fingers and a total of six independent DOF. The proposed hand was designed to supplement the dexterity of customary prosthetic hands while maintaining nearly the same dimension and weight. The approach was aimed at providing enhanced grasping capabilities and “natural” sensory-motor coordination to the amputee, by integrating miniature mechanisms, sensors, actuators, and embedded control.

Wilkinson et al. [95] suggested that the human finger possesses a Structure called the extensor mechanism, a web-like collection of tendinous material that lies on the

dorsal side of each finger and connects the controlling muscles to the bones of the finger. They claimed that, earlier robotic hand designs, this extensor mechanisms had generally not been employed due in part to their complexity and a lack of understanding of their utility, where as they done the first design and analysis effort of an artificial extensor mechanism. Their analysis was to provide an understanding of the extensor mechanism's functionality so that it can extract the crucial features that need to be mimicked to construct an anatomical robotic hand. They identified that this extensor mechanism gives independent control of the metacarpo-phalangeal (MCP) joint and acts not only as an extensor but also as a flexor, abductor, adductor, or rotator depending on the finger's posture.

Yamano et al. [96] developed a robot finger for five-fingered robot hand having equal number of DOF to human hand. The robot hand was driven by a new method proposed by authors using ultrasonic motors and elastic elements. The method utilized restoring force of elastic element as driving power for grasping an object, so that the hand can perform the soft and stable grasping motion with no power supply. In addition, all the components were placed inside the hand thanks to the ultrasonic motors with compact size and high torque at low speed. Applying the driving method to multi-DOF mechanism, a robot index finger was designed and implemented. That had equal number of joints and DOF to human index finger and that was also equal in size to the finger of average adult male.

Borst et al. [97] (2003) stated that at Institute for Robotics and Mechatronics, Germany, two generations of anthropomorphic hands had been designed. In quite a few experiments and demonstrations they could show the abilities of these hands and gain a lot of experience in what artificial hands can do**,** what abilities they need and where their limitations lie. In their paper, they would like to given an overview over the experiments performed with the DLR hands, the hands abilities and the things that need to be done in the near future.

Haidacher et al. [98] developed a newly designed manipulators greatly out perform their ancestors in term of available sensor signals, applicable grasping force, mechanical stability, reliability, kinematic design and more. That development extended the possible range and level of complexity of applications of robotic grippers to areas outside of well-structured laboratories and simple tasks. That also called for more flexible control structures to provide a framework for implementing and executing those newly arising tasks without having to start from scratch for each new task. During the last few years, they developed a control system

architecture fur DLR Hand II that proved to be useful for a great variety of different applications.

Yang [99] proposed the design and analysis of a multi-finger hand prosthesis. The proposed hand had multi-actuated fingers in which the thumb consists of three joints and other four fingers consists of two joints. Each joint was designed using a novel flexible mechanism based on the loading of a compression spring in both transverse and axial directions and using cable-canal systems. The rotational motion was transformed to tendon-like behaviour, which allows the location of the actuators far from the arm (i.e. on belt around the waist). They presented the forward kinematics of the mechanism and shown that the solution of the transverse deflection of each finger segment was obtained in a general form through a haring model followed by an element stiffness model. The hand prosthetics was built up after testing experimentally a prototype finger and verifying the result. They claimed that new design was a low cost alternative, enables the actuation and control of a multi-fingered hand with relatively high degree of freedom.

Kargov et al. [100] discussed about the mechanism, design, and control system of a new humanoid-type hand with human-like manipulation abilities. The hand was designed for the humanoid robot, which had to work autonomously or interactively in cooperation with humans. The idyllic end effector for such a humanoid would be able to use the tools and objects that a person uses when working in the same environment. Hence, a new hand was designed for anatomical consistency with the human hand. That includes the number of fingers and the placement and motion of the thumb, the proportions of the link lengths, and the shape of the palm. The hand could perform most of human grasping types. In this paper, particular attention was dedicated to measurement analysis, technical characteristics, and functionality of the hand prototype.

Based on the under actuated mechanism and coupling principle, a five-fingered prosthetic hand was presented by Zhao et al. [101]. The design of the finger was based on two types of four bar linkage mechanisms. One was the under actuated linkage mechanism, which implements self-adapt grasp with wide variety of objects placed between base joint and middle joint. The other was the coupling linkage which employs between the middle and distal joints. A motor respectively actuated the thumb, the index finger and other three fingers. The multi-DOF hand was comprised of 13 joints and driven by three motors. Torque and position sensors were integrated into the fingers. All actuators, sensors and electronic

boards were implanted into the hand, which presented a highly integrated mechatronics system

Moon [102] proposed a finger mechanism that mimics human finger motion with contact aided compliant mechanisms. The motion mimicking was done through well-known linkage synthesis theories, and was converted to a compliant mechanism to reduce the number of actuators and to achieve compactness. To achieve these goals, the design procedures, modeling methods and design criteria of the contact aided compliant mechanism were presented.

Onno et al. [103] presented a skeletal linked model of the human hand that had natural motion. They showed how that can be achieved by introducing a new biology-based joint axis that simulated natural joint motion and a set of constraints that reduced an estimated 150 possible motions to twelve. The model was based on observation and literature. To facilitate testing and evaluation, they presented a simple low polygon count skin that can bounce and swell. To evaluate they first introduced hand-motion taxonomy in a two dimensional parameter space based on tasks that were evolutionary linked to the environment. Second, they discussed and tested the model.

Carbone and Ceccarelli [104] addressed the main design issues for developing a low-cost easy-operation robotic hand named as LARM Hand. Design evolution of LARM Hand was reported by describing peculiarities and differences among LARM Hand from version I to version IV. Special attention had been addressed to the design characteristics of a 1 degree-of-freedom (DOF) driving mechanism that can be embedded into the finger body and can actuate the three phalanxes of a human-like robotic finger. Attention had been also focused to selection, location, and use of proper force sensors together with easy operation force control architecture.

Shi et al. [105] proposed a structural model of skeletal muscle based on the bone–muscle lever system to describe the relationship between wrist angle and thickness of the extensor carpi radialis muscle during the process of wrist flexion–extension. That model applied the cosine theorem to the expression for muscle length, in order to relate wrist angle to muscle thickness by the invariance of muscle volume, which was used to calculate the length of the extensor carpi radialis muscle from the muscle thickness. To validate the proposed model, wrist angles were also computed by other models based on regression, such as linear regressions, an artificial neural network, and a support vector machine. More importantly, that model could be clearly related to physiology. Thus, it can potentially be used to investigate the

relationship between internal structural changes of skeletal muscle and external limb behaviours, and to develop prosthetic hands and functional electrical stimulation systems.

Montana [106] stated that in past, general models of the kinematics of multi-fingered manipulation had only treated instantaneous motion (i.e., velocities). However, such models, which ignore the underlying configuration (or state) space, were inherently incapable of capturing certain properties of the fingers-plus-object system important to manipulation. They derived a configuration-space description of the kinematics of the fingers-plus-object system. For that, they first formulated contact kinematics as a "virtual" kinematic chain and then the system could be viewed as one large closed kinematic chain composed of smaller chains, one for each finger and one for each contact point. They examined the underlying configuration space and two ways of moving through that space. The first, kinematics-based velocity control was a generalization of some previous velocity-based approaches. The second, hyperspace jumps, was a purely configuration-space concept.

Kurita et al. [107] proposed a human-sized multi-fingered robot hand with detachable mechanism at the wrist. The actuators are entrenched in the arm and the finger joints are connected to the actuators through tendon-driven wires. The driving forces from the arm part are transmitted to the hand part by a gear mechanism at the wrist. The gear mechanism makes the hand part and the arm part detachable, which enables separate maintenance of the hand and arm. The developed robot hand has the size of 200[mm](length)×78[mm](width)×24.6[mm] (thickness) and can exert 10[N] at the fingertip. The performance of the developed robot hand was shown by a motion control experiment.

2.2.2 Design Optimization of Robot Hand

Sancho-Bru et al. [108] proposed a three dimensional scalable biomechanical model of the four fingers of the hand to evaluate the forces involved during grasping and to predict maximal achievable grip forces. The model had been validated by means of reproducing an experiment in which the fingers exerted the maximal grasping force over cylinders of different diameters, as well as the contribution of each finger to the total grasping force. A significant reduction of the muscle force was predicted when the diameter that optimizes the maximal grip force was used as handle diameter, reducing the risk of developing cumulative hand trauma disorders. It is suggested that the model can be applied to the design

and evaluation of handles for power grip and to the study of power grasp for normal and abnormal hands.

Natsuki et al. [109] proposed that the total protocol to determine the link structure of a human hand using optical motion rapture data. The difficulty in capturing hand motion came from the hand's relatively high degree of freedom located in very small space. To deal with the problem caused by closeness between markers, the number of markers was reduced. The effect of reduced markers was compensated by simplifying the problem. The adverse effect of skin movement and the limited range of movement were avoided by regulating the calibration motion appropriately. A link estimation experiment was performed to show the effectiveness of the proposed method.

Barkera et al. [110] stated that implant loosening and mechanical failure of components are frequently reported following metacarpophalangeal (MCP) joint replacement, whereas, the studies of the mechanical environment of the MCP implant-bone construct were occasional. They studied thoroughly to evaluate the prophetic ability of a finite element model of the intact second human metacarpal to provide a validated baseline for further mechanical studies. A right index human metacarpal was subjected to torsion and combined axial/bending loading using strain gauge (SG) and 3D finite element (FE) analysis. Four different representations of bone material properties were considered. The validated FE model provided a tool for future investigations of current and novel MCP joint prostheses

A realistic skeletal musculo-tendon model of the human hand and forearm were presented by Tsang et al [111] . There were 16 joints in their hand model. Joints were modelled as hinges that were capable of rotation about their principal axes. There were 23 degrees of freedom in the joint system. Each finger has four, with two DOFs for the MCP joint for flexion/extension and adduction/abduction, and one DOF each for the PIP and DIP of joints for flexion/extension. The thumb has five: one for the MCP joint, one for the IP joint, and three for the CMC joint. Finally there are two DOFs for the rotation of the wrist. They introduced an extra degree of freedom for the CMC joint of the thumb because the two axes of rotations are not orthogonal. The flexion/extension of the CMC joint occurs in the trapezium, and its abduction/adduction occurred in the first metacarpal bone. The model permitted direct forward dynamics simulation, which accurately predicted hand and finger position given a set of muscle activations. They also presented a solution to the inverse problem of determining an optimal set of muscle activations

to achieve a given pose or motion; muscle fatigue, injury or atrophy can also be specified, yielding different control solutions that favour healthy muscle. As there can be many (or no) solutions to this inverse problem, they demonstrated how the space of possible solutions that can be filtered to an optimal representative. Of particular note is the ability of their model to take a wide array of joint interdependence into account for both forward and inverse problems. Finally, they suggested the visualization and understanding of the dynamically changing and spatially compact musculature using various interaction techniques. They mostly concentrated on the anatomical modelling of the hand, not much attention was given on the work space and grasping analysis of the model. In their work they discussed more about the dynamic behaviour of hand than kinematic analysis and structure. Similar to the work of Binti et al. [58] they considered CMC joint of thumb with 3 DOFs and the MCP with 2 DOFs.

The optimization and design process of a two-fingered micro hand that used a hybrid motion mechanism was presented by Ahmed et al. [112] in 2008. Their proposed hybrid hand consists of two 3-PRS parallel modules upper and lower connected serially back to back in a mirror image style. Those were driven by piezo-electric actuators and had two long glass petites. The most important part in the development process was the optimization of the design parameters. That was carried out using discretization method and genetic and Evolutionary algorithm (GEAs) for the theoretical models. The GEAs had superior behaviour than discretization method but the genetically optimized deign parameters are difficult to be practically implemented with high accuracy. Then a complementary optimization for the web thickness of the pin flexure hinge was done to build the final CAD model.

One of the most important parts of gesture interfaces is hand motion capturing, for which, many current approaches are involved a formidable nonlinear optimization problem in a large search space. Motion capturing can be achieved more cost-efficiently when considering the motion constraints of a hand. Although some constraints can be represented as equalities or inequalities, there exist many constraints, which cannot be explicitly represented. Lin et al. [113] proposed a learning approach to model the hand configuration space directly. The redundancy of the configuration space could be eliminated by finding a lower-dimensional subspace of the original space. Finger motion was modelled in this subspace based on the linear behaviour observed in the real motion data collected by a Cyber

Glove. Employing the constrained motion model, they were able to efficiently capture finger motion from video inputs.

An adaptive particle swarm optimization (APSO) approach was used to solve the grasp planning problem by Walha et al. [114]. They represented each particle as a configuration set to describe the posture of the robotic hand. The aim of the algorithm developed by them is to search for the optimum configuration that satisfies a good stable grasp. In their approach they used a Guided Random Generation (GRG) to guide the particles in the generating process. According to the number of contacts between the fingertips and the object, the algorithm can take off the inactive particles. The kinematic of the modelled hand was described and incorporated in the fitness function in order to compute the contact positions. They tested APSO in the Hand Grasp simulator with four different objects and the experimental results demonstrate that this approach outperforms the compared simple PSO in terms of solution accuracy, convergence speed and algorithm reliability.

2.2.3 Control of Multi-fingered Hand

Tomovic et al. [115] presented an approach to synthesizing the control required by a dexterous multi fingered robot hand to reach and safely grasp an arbitrary target object. The synthesis was based on analysis of the grasping task as performed by human beings. They divided the task into a target approach phase (including target identification, hand structure and grasp mode selection, selection of approach trajectory, hand pre-shaping and orientation) and **a** grasp execution phase (including shape and force adaptation). Each aspect of the required control was discussed. Particular attention was paid to the role of geometric modeling in target identification, to pre-shaping during the approach trajectory and to the requirements for autonomy in completion of the grasping task. The underlying philosophy was that of reflex control; each aspect of the grasping task was initiated and terminated using sensory data and rules of behaviour derived from human expertise in such tasks. The contents and organization of the knowledge base, which codifies this expertise, were discussed.

Kyberd et al. [116] proposed that an important factor in the acceptance of prosthesis is the ease with which the wearer can operate the device. Multiple degrees of freedom of prosthesis were difficult to control independently and require a high level of concentration. They stated that, if the control arranged in a hierarchical manner and the lower levels' detailed control is performed by a

microprocessor, it is possible to control a number of degrees with little direct intervention by the operator. Accordingly, they developed a two degree of freedom hand to demonstrate this concept and have been made sufficiently compact to allow users to gain experience with it.

Shields et al. [117] presented a prototype of a powered hand exoskeleton model that was designed to fit over the gloved hand of an astronaut and offset the stiffness of the pressurized space suit. The model had a three-finger design, the third and fourth fingers being combined to lighten and simplify the assembly. The motions of the hand were monitored by an array of pressure sensors mounted between the exoskeleton and the hand. Controller commands were determined by a state-of-the-art programmable microcontroller using pressure sensor input. Those commands were applied to a dc motor array which provides the motive power to move the exoskeleton fingers. The resultant motion of the exoskeleton allows the astronaut to perform both precision grasping tasks with the thumb and forefinger, as well as a power grasp with the entire hand.

Baek et al. [118] considered design and control of a robotic finger for prosthetic hands. A linkage driven robotic finger actuated by single motor was developed such that the motion of the robotic finger is very close to the motion of human finger. Signal measured from strain gauges attached on the tendon of the hand was used as a position command to control the motion of the robotic finger. They presented the result of the simulation and experiment to show that the proposed robotic finger is fit for a prosthetic hand.

Zecca et al. [119] suggested that the human hand is a complex system, with a large number of degrees of freedom (DOF), sensors embedded in its structure, actuators and tendons, and a complex hierarchical control. Despite this complexity, the effort required to the user to carry out the different movements is quite small (albeit after an appropriate and lengthy training). On the other hand, prosthetic hands were just a light replication of the natural hand, with significantly reduced grasping capabilities and no sensory information delivered back to the user. Several attempts had been carried out to develop multifunctional prosthetic devices controlled by electromyographic (EMG) signals (myoelectric hands), harness (kinematic hands), dimensional changes in residual muscles, and so forth, but none of these methods permits the “natural” control of more than two DOF. This article is presented a review of the traditional methods used to control artificial hands by means of EMG signal, in both the clinical and research contexts, and is introduced what could be the future developments in the control strategy of these devices.

Secco and Magenes [120] described the dynamic control of a 3 degree of freedom finger imitating a human finger for reaching a required fingertip position in space. They focused the attention to the basic motor unit for the artificial grasp and haptic perception the finger. The minimum jerk theory was used by them to eliminate the redundancy due to third joint and described the mathematical equation for natural movement. The classic Lagrange equations were applied to compute the three-motor torques. They also introduced the neural network control which provides the three motor torques necessary for the phalanges granting a smooth and natural speed profile for finger tips. The result suggested that, the approach should pursue for multi finger hand in order to achieve a natural Neural Network prosthetic or robotic dynamic control system.

Ferguson and Dunlop [121] discussed the development of a system that will allow complex grasp shapes to be identified based on natural muscle movement. The application of this system can be extended a general device controller where input is obtained from forearm muscles, measured using unobtrusive surface electrodes. That system provided the advantage of being less fatiguing than traditional input devices. The instrumentation hardware, computer software and algorithms developed to achieve this task were described by them.

Koura and Singh [122] suggested that the human hand is a complex organ capable of both gross grasp and fine motor skills. Despite many successful high-level skeletal control techniques, animating realistic hand motion remains tedious and challenging. Their research based on the complex finger positioning required playing musical instruments, such as the guitar. They first described a data driven algorithm to add sympathetic finger motion to arbitrarily animated hands. They presented a procedural algorithm to generate the motion of the fretting hand playing a given musical passage on a guitar. The work was aimed as a tool for music education and analysis.

Ueda et al. [123] introduced a multi-fingered robotic hand NAIST-Hand and a grip force control by slip margin feedback. The developed prototype finger of the NAIST-hand had a new mechanism by which all 3 motors can be placed inside the palm without using wire-driven mechanisms. A method of grip force control was proposed using incipient slip estimation. A new tactile sensor was designed to activate the proposed control method by the NAIST-Hand. The sensor consists of a transparent hemispherical gel, an embedded small camera, and a force sensor in order to implement the direct slip margin estimation. The structure and the principle of sensing were described in details.

Carrozza et al. [124] developed a new prosthetic hand device in order to improve functionality and controllability in addition to. They presented the design of the Cyber Hand, a cybernetic anthropomorphic hand to provide amputees with functional hand replacement. Their design was bio-inspired in terms of its modular architecture, its physical appearance, kinematics, sensorization, and actuation, and its multilevel control system. The Cyber Hand was designed as a prototype for testing and evaluating neural interfaces, control algorithms, and sensory feedback protocols. That had 16 DoFs and 6 motors (that is, 6 Degrees of Mobility, DoM): each finger of the Cyber Hand has 3 DOFs and 1 DoM (flexion/extension) and the thumb has, in addition 1 DoM for positioning. The size of the Cyber Hand was comparable to that of human hands and can generate many different grasps. However, the control was limited to a subset of functional grasps: lateral pinch, cylindrical and spherical grasps, and the tripod grasp. They adopted under-actuated mechanisms which allow separate control of each digit as well as thumb–finger opposition and, accordingly, can generate a multitude of grasps. The Cyber- Hand control system presumed just a few efferent and afferent channels and was divided in two main layers: a high-level control that interprets the user's intention (grasp selection and required force level) and could provide pertinent sensory feedback and a low-level control responsible for actuating specific grasps and applying the desired total force by taking advantage of the intelligent mechanics. The grasps made available by the high-level controller include those fundamental for activities of daily living: cylindrical, spherical, tridigital (tripod), and lateral grasps. They concentrated more on control issues in comparison to flexibility of the hand. The hand performance could be improved by increasing DOF to some optimum value of at least 20: 15 flexion of the phalanges, 1 thumb opposition, 3 ad/abduction (for little finger, ring finger and index) and 1 hollowing of the palm (flexing little and ring finger toward the thumb) for manipulating purpose. Under- actuation principle could reduce the control complexity but at same time decreased the grasping capacity of hand.

Yang et al. [125] proposed that when developing a humanoid myo-control hand, not only the mechanical structure should be considered to afford a high dexterity, but also the myoelectric (electromyography, EMG) control capability should be taken into account to fully accomplish the actuation tasks. They presented a novel humanoid robotic myocontrol hand (AR hand III) which adopted an under actuated mechanism and a forearm myocontrol EMG method. The AR hand III has five fingers and 15 joints, and actuated by three embedded motors. Under actuation can be found within each finger and between the rest three fingers (the middle finger,

the ring finger and the little finger) when the hand was grasping objects. For the EMG control, two specific methods were proposed: the three-fingered hand gesture configuration of the AR hand III and a pattern classification method of EMG signals based on a statistical learning algorithm – Support Vector Machine (SVM). Eighteen active hand gestures of a testee were recognized effectively, which could be directly mapped into the motions of AR hand III. An on-line EMG control scheme was established based on two different decision functions: one is for the discrimination between the idle and active modes; the other is for the recognition of the active modes. As a result, the AR hand III could swiftly follow the gesture instructions of the testee with a time delay less than 100ms.

Biomedical signal means a set of electrical signals acquired from any organ that represents a physical variable of interest. These signals are normally a function of time and can be analyzed in its amplitudes, frequency and phase. Wojtczak et al. [126] in 2009 used biomedical signal electro myo-graphic (EMG) to control the movement of prostheses. Prosthesis systems for upper limb were mainly based on myoelectric control, recognizing EMG signals that occur during muscle contraction on the skin surface. Myoelectric control takes advantage of the fact that, after a hand amputation great majority of the muscles that generate finger motion was left in the stump. The activity of these muscles still depends on the patient's will, so bio signals that occur during it, can be used to control prosthesis motion. The control strategy of prostheses was based on to generate set of repeatable muscle contraction that is different from ordinary arm function. Contrary to conventional prosthesis control methods, it was possible to extract some feature from the myoelectric signals which may provide information about muscle activity below the skin. In the proposed approach, an identification system was tried to recognize a certain group of hand movements based on electrical signals (EMG signals) recorded on a patients forearm. The features used were based on time and energy histograms combined with a neural network based classification. The measurements were done on a specialized stand designed for such research.

Dario et al. [127] suggested that in a broad sense, the research on humanoids can be seen as efforts aiming at replicating the human being in his integrity or some of her/his main components. Thus, the development of a cybernetic prosthesis, replicating as much as possible the sensory-motor capabilities of the natural hand, can be seen as an important goal in this field. They presented the current research efforts towards the development of this cybernetic hand prosthesis which will overcome some of the drawbacks of current prosthetic systems. This new

prosthesis will be felt by an amputee as the lost natural limb delivering her/him a natural sensory feedback by means of the stimulation of some specific afferent nerves. Moreover, that should be controlled in a very natural way by processing the different neural signals coming from the central nervous system (thus reducing the discomfort of the current EMG-based control prostheses). In particular, they discussed three main issues: the design optimization of the existing developed mechatronic prostheses, the sensorization of the prosthetic hand, and its control.

Carrozza et al. [128] proposed that Current prosthetic hands are basically simple grippers with one or two degrees of freedom, which barely restore the capability of the thumb-index pinch. They developed a novel prosthetic hand featured by multiple degrees of freedom, tactile sensing capabilities, and distributed control. The main goal was to pursue an integrated design approach in order to fulfil critical requirements such as cosmetics, controllability, low weight, low energy consumption and noiselessness. This approach could be synthesized by the term "bio-mechatronic design", which means developing mechatronic systems inspired by biological world. They described the first implementation of one single finger of a future bio-mechatronic hand. The finger had a modular design, which allows obtaining hands with different degrees of freedom and grasping capabilities. Current developments include the implementation of a hand comprising three fingers (opposing thumb, index and middle) and an embedded controller.

A multi-fingered tele-manipulation system was presented by Peer et al. [129], where the human hand controlled a three finger robotic gripper and force feedback was provided by using an exoskeleton. Since the human hand and robotic grippers had different kinematic structures, appropriate mappings for forces and positions were applied. A point-to-point position mapping algorithm as well as a simple force mapping algorithm were presented and evaluated in a real experimental setup.

Jaffar et al. [130] are designed and developed a multi-fingered anthropomorphic robotic hand with fourteen Degrees of Freedom (DOF) which is able to mimic the functional motions of a biological hand especially in handling complex objects. They used micro- servomotors as actuation mechanisms, that connected with the finger joints by pulleys and belts which promote bending and extending of the fingers. Two kinds of sensors, i.e. force sensor and light dependent resistor, are integrated into the system. The said robotic hand can be controlled via a graphical user interface embedded with control codes or a joy stick integrated to a control board. Furthermore, the robotic hand is able to operate autonomously with the aid

of sensory elements and embedded control software. Workability tests showed the capability of the system to move every finger individually and to perform grasping tasks on objects with varying sizes and geometries such as a tennis ball and a screw driver.

Boughdiri et al. [131] considered the problem of model-based control for a multi-fingered robot hand grasping an object with known geometrical characteristics. They mainly worked on two topics one is to derive a mathematical model of the dynamics of a designed multi-fingered robot hand with five fingers with twenty DOF (three for each finger, two for the thumb and six for the wrist) which grasps a rigid object. Their methodology based on the Lagrange formulation, to identify the parameters of dynamic models of hand-object system. In second part they presented that these models are instrumental for the design problems of control for dynamic stable grasping. Finally, several simulation results demonstrated the controller performance based on the derived model.

Chen and Naidu [132] proposed a hybrid controller of soft control techniques, adaptive neuro-fuzzy inference system (ANFIS) and fuzzy logic (FL), and hard control technique, proportional-derivative (PD), for a five-finger robotic hand with 14-degrees-of-freedom (DoF). The ANFIS was used for inverse kinematics of three-link fingers and FL is used for tuning the PD parameters with 2 input layers (error and error rate) using 7 triangular membership functions and 49 fuzzy logic rules. Simulation results with the hybrid of FL-tuned PD controller exhibit superior performance compared to PD, PID and FL controllers alone.

2.2.4 Application of Multi-fingered Hands

Kuch and Huang [133] presented a new method for building lifelike hand models which articulate in a realistic manner. That method had distinct benefits over previous methods, since the fitting to a particular person's hand was quick, simple and very accurate. Following the calibration process which fitted it to a particular person's hand, this hand model could be used in numerous human computer interactions (HCI) scenarios. Calibration was based on anatomical studies of the human hand and on the specific method of recognition to be employed in the HCI scenarios; the calibration method was done visually and requires only three views of the hand to be modeled. The calibration system was designed to be accurate, to be easy to use and to allow for a short calibration time. These characteristics were all desirable when one was working in the realm of a human computer interfacing.

Lin and Huang [50] suggested that a prosthetic hand is essential to provide rehabilitation for individual who lose a hand. A prosthetic hand serves two purposes: cosmetic and functional. In this paper, a prototype of the artificial hand with an emphasis on the functionality purpose was presented. A new mechanism, the NTU-Hand (NTU-Hand. patent number 1071 15, Taiwan, R.O.C.), which had *5* fingers with 17 degrees of freedom, had been designed and fabricated in their laboratory. Due to the special design of the mechanism, the hand had an uncoupled configuration in which each finger and joint were all individually driven. The size of the hand was almost the same as a human hand. All actuators, mechanical parts, and sensors were inside the hand. The compact design made it feasible to adapt the hand to the injured wrist. A computer simulation with three-dimensional graphics was also built to evaluate the manipulability range of the artificial hand. From the results of this simulation, the relationship between the hand and the grasped object in a specific viewpoint could be obtained.

Doshi et al. [134] suggested that prosthetic hands, although functional, had the potential of being improved significantly. They proposed the design and development of a novel prosthetic hand that is lighter in weight, less expensive, and more functional than existing hands. The new prosthesis features an endoskeleton embedded in self-skinning foam that provided a realistic look and feel and obviates the need for a separate cosmetic glove. The voluntary-closing mechanism offered variable grip strength. Placement of joints at three locations (metacarpophalangeal and proximal and distal interphalangeal) within each of four fingers afforded realistic finger movement. High-strength synthetic cable attached to the distal phalanx of each finger was used to make flexion. A multi-position passive thumb provided both precision and power grips. The new prosthesis can securely grasp objects with various shapes and sizes. Compared to current hands, weight had been reduced by approximately 50%, and cable excursion required for full finger flexion by more than 50%. The new endoskeletal prosthesis required approximately 12-24% less force input to grasp a variety of everyday objects, largely due to its adaptive grip. Despite the initially promising results, there was still room for improvement. First, force transmission could be improved. If the DIP joints were stationary, force transmission would increase, resulting in greater pinch forces available at the fingertips. This change would add function without dramatically detracting from finger movement realism. Cable actuation could also be improved. Since harness cable excursion required to effect full flexion is only 1.3 cm, it is possible to use mechanical advantage to double the force available at the fingertips while also doubling the required input cable excursion. This increased cable

excursion would offer the user more fine control over finger flexion. Cosmetic improvements in the foam are also required. Several seams are apparent along the sides of the fingers where the two halves of the mold meet. Improving the mold in which the foam is cast would correct these flaws.

Lovchik and Diftler [135] presented the design of a highly anthropomorphic human scale robot hand for space based operations. That five finger hand combined with integrated wrist and forearm had fourteen independent degrees of freedom. The device approximated very well the kinematics and required strength of an astronaut's hand when operating through a pressurized space suit glove. The mechanisms used to meet these requirements were described in detail along with the design philosophy behind them. Integration experiences reveal the challenges associated with obtaining the required capabilities within the desired size.

Cuevas [136] stated that as per given biomechanical complexity of the human hand, it was not surprising that the grasping ability of individuals after treatment for severe paralysis or injury could seldom be restored to the level of the "normal" hand. To improve clinical outcomes will require i) developing experimental paradigms to evaluate hand function objectively, ii) understanding how the nervous system controls the redundant musculature of the digits, and iii) increasing the clinical impact of computer biomechanical models by validating their anatomical assumptions. Recognizing that the human hand was also a mechanical system, the principles of robotics developed for the analysis of manipulators could be applied to each of these three clinical challenges. They discussed an overview of experimental and theoretical work aimed at understanding individual human digits as serial manipulators.

Eriksson et al. [137] described an autonomous assistive mobile robot that aids stroke patient rehabilitation by providing monitoring, encouragement, and reminders. The robot navigates autonomously, monitors the patient's arm activity, and helped the patient remember to follow a rehabilitation program. Their experiments showed that patients post-stroke were positive about this approach and that increasingly active and animated robot behaviour was positively received by stroke survivors.

2.2.5 Grasping Analysis

In analyzing the human hand grasp, not only motion of fingers but also contact force acting on the fingertips should be calculated. Nagata et al. [138] suggested that analysis of human hand grasp provides information that can be used to develop

a grasping algorithm of robot hands that takes advantage of human knowledge and experience. They presented a new master hand which can be attached to a human hand and measures motion of the human fingertips and contact forces acting on the fingertips. The purpose of developing the master hand is to clarify the strategy of a human hand grasp, which is subjected to the same physical constraint as those of a robot hand, and use the obtained information to develop a grasping algorithm of robot hands.

Van-duc Nguyen [139] presented the fast and simple algorithm for directly constructing the stable force closure grasp based on the shape of the grasped object and proved that a grasp is in force closure if and only if it can exert, through a set of contacts, arbitrary forces and moments on the object in such a way that the net force and moment acting on object is zero which implies the equilibrium of the object. Further, he also proved that not only the equilibrium grasp is a force closure grasp but also the non-marginal equilibrium grasp is a force closure grasp, if it has at least two soft finger point contacts with friction in 2D or three hard finger contacts in 3D and all force closure grasp can be made stable by using either active or passive springs at the contacts. A geometrical relation between the stiffness of the grasp and the spatial configuration of the virtual spring at the contacts was developed by him in his further work [140] in 1987. He synthesized the grasps considering the virtual springs at the contact points by which the grasped object is stable and has a desired stiffness matrix about its stable equilibrium. For directly constructing the stable grasps in 3D a fast and simple algorithm was developed by him and presented in the same paper. He that stable equilibrium grasps is feasible with reference to contact points only. Nothing was suggested about the hand structure and kinematics of the hand model for stable grasp. He also did not discuss about the amount of forces exerted on the finger tips during the grasping of an object.

Haidacher and Hirzinger [141] presented a way of estimating the position of contact and the normal of the contact surface, using only joint position and velocity measurements, applying hand kinematics and exploiting constraints on motion between finger and object when having a stable contact. This method additionally requires only a geometric description of the finger tips in contact, which usually is available. That method was valid for any type of contact providing enough constraints and any convex finger geometry. Based on the kinematics of contact, a method had been proposed, to determine the error in an estimate of the contact joint parameters. With these estimates, the position of the contact point between finger

and object on the finger surface and the normal direction on the object surface could be computed. Second, an observer structure dual to a Kalman filter has been proposed, which allows computation of this exteroceptive information on the fly during grasping and thus observed the rolling motion of the fingers on the object. This information was applied to methods used for synthesizing grasps, grasp control and grasp force optimization. The validity of the taken approach has been verified in simulations. Further work should be done, examining the observer with respect to sensitivity to noise, developing optimal object motions for detection, applying the proposed algorithms to an experimental setup and examine the applicability for enhanced object controllers used for manipulation.

Bounab et al. [69] proposed a new approach for computing force closure grasps of two-dimensional and three-dimensional objects. They developed a new necessary and sufficient condition for n-finger with Coulomb friction at contact point of grasps to achieve force closure. They suggested that a grasp is force closure if and only if its wrench can generate any arbitrary central axis. Accordingly, the problem was reformulated as linear programing problem without computing the convex hull of the primitive contact wrenches, which reduced the overall computing time. An efficient algorithm for computing n-finger force closure grasp was proposed. They extended their work in 2010 [142] by developing a modified force closure algorithm and were by giving rigorous theoretical demonstrations. They claimed that the advantages of the proposed approach is its capability to give a good quality measure of the force closure grasp without computing the sphere in six-dimensional wrench space, which efficiently reduced the computation time. They proposed the algorithm for testing a set of contact points satisfying the condition of force closure or not. Only the analysis of grasp made without much involving the hand shape and force exerted at fingertip contact points. The inclination of finger with respect to object surface also influence the positioning of contact point for stable and equilibrium grasp, which was not taken into consideration in their work.

Mishra et al. [143] stated that the grasp is called positive grip if there is no static friction between the object and the fingertip at the point of contact. Assuming the grasp as positive grip they studied about the equilibrium condition of the body, when the body is under some constant external force or torque and when the body is under varying external force or torque. Finally they developed an efficient algorithm to synthesize such positive grips for bounded polyhedral/polygonal objects. Also they presented in the same paper the number of fingers employed in the grips.

Jeffrey C. Trinkle [144] suggested that the planning for grasp and manipulation of slippery objects depends on the form closure grasp, which can be managed regardless of the external force applied to the object. He formulated a test in form of a linear program, which gave the optimal objective value measure of how far a grasp is from losing the form closure grasp. Despite of its importance, no quantitative test for form closure grasp for any number of contact points was available they introduced that solution. The test was formulated for frictionless grasps but they discussed how it can be modified to identify grasps with frictional force closure.

Two quality criteria, for planning optimal grasp were suggested by Ferrari & Canny [145] . The two criteria are the total finger force and the maximum finger force. The formalization was done using various matrices on space of generalized forces. The geometric interpretation of the two criteria leads to an efficient planning algorithm. They also had shown the example of its use in different type grippers.

Omata [146] had shown that in a planar grasp the moment equilibrium equation can be made linear by replacing each real finger by a pair of virtual fingers fixed at vertices of the region. Using such virtual fingers in 3D grasps, nonlinear constraints still remain, but they exhibit the same properties as the integer requirement in an integer programming problem. He also discussed about the finger position computation for 3- dimensional equilibrium grasps. He proposed an algorithm based on the branch and bound method and had discussed the case where two fingers push the same region and the case where the finger contact used is a soft finger contact.

Ponce et al. [147] dealt with the problem of characterizing the Force closure grasps of a three-dimensional object by a hand equipped with three or four hard fingers. They proved the necessary and sufficient conditions for force-closure grasp of polyhedral objects are linear in the unknown parameters. This reduces the problem of computing force-closure grasps of polyhedral objects to the problem of projecting a polytope onto some linear subspace. They also presented an efficient, output-sensitive algorithm for computing the projection and an algorithm using linear programming for computing maximal grasp regions.

Mirtich and Canny [148] considered the problem of finding the optimum force closure grasp of two and three dimensional object. They had developed an optimal criterion based on the notion of decoupled wrenches, and used that criterion to derive optimum two and three finger grasps of 2-D objects, and optimum three

finger grasps for 3-D objects. They also presented a simple and efficient algorithm for grasping convex and non-convex polygons, as well as polyhedral.

Varma and Tasch [149] had introduced a graphical representation of the finger force values and the objective function that, enable one in selecting and comparing various grasping configurations. Compared to earlier grasp measures that had been suggested by other researchers the measure described by him shown the influence of the external force on the grasp.

The concept of partial Form closure and Force closure properties were introduced and discussed by Bicchi [150]. He had also proposed an algorithm to obtain artificial geometric description of partial form closure constraints. His study also proved the equivalence of force closure analysis with the study of equilibrium of an ordinary differential equation, to which Lyapunov's direct method was applied. These all lead to an efficient algorithm for the force closure grasp.

Jia [151] proposed a numerical algorithm to compute the optimal grasp on a simple polygon, given contact forces of unit total magnitude. Forces were compared with torques over the radius of gyration of the polygon. He assumed non-frictional contacts and addressed a grasp optimality criterion for resisting an adversary finger located possibly anywhere on the polygon boundary. The difference between these two grasp optimality criteria were demonstrated by simulation with results advocating that grasps should be measured task-dependently.

Buss et al. [152] presented algorithm that satisfied the nonlinear friction force limit constraints which was equivalent to positive definiteness of a suitable matrix containing contact wrenches and friction coefficients, and the remaining constraints were linear constraints. The method for grasp force optimization for dexterous robotic hands was developed by them. The algorithms allow to easily accommodating the various friction models of point contact with Coulomb friction or soft-finger contacts. They considered a linear and elliptical friction force limit approximation for the soft-finger contact friction model.

Howard and Kumar [153] suggested the categories of equilibrium grasps and establish a general framework for the determination of the stability of a grasp. For the analysis of the stability of the multi-fingered grasp, they claimed that, they had first modeled the compliance at each finger. They had also shown that the stability of a grasp is depends on the local curvature of the contacting bodies, as well as the magnitude and arrangement of the contact forces.

Liu and Wang [154] presented the qualitative test of 3D frictional form-closure grasps of n robotic fingers as a problem of linear programming. Since, one of the most necessary and sufficient condition of force closure grasp is that the origin of the wrench space should lie inside the convex hull of primitive contact wrenches. So as to find the condition whether origin lies within convex hull, they had suggested a new method called Ray Shooting Method which is dual to the linear programming problem. Finally they had experimentally confirmed that real time efficiencies of the proposed algorithm.

Zitar and Nuseirat [155] using inequality theory the new neural network architecture to solve the arisen linear complementarity problems was developed. They converted the problem into a heuristic search problem utilizing the architecture and the learning capabilities of a single layer two-neuron network. The approach allows them to reach some acceptable solutions for external force values that do not have an exact solution, and therefore, exact solution techniques usually fail to solve. Their proposed neural network technique found almost exact solutions in solvable positions, and very good solutions for positions that Lemke fails to find solutions where Lemke is a direct deterministic method that finds exact solutions under some constraints.

Miller and Allen [156] reported a unique grasp analysis system for a given 3D objects. The analysis accurately determine the hand, its pose, also the types of contacts that will occur between the links of the hand and the object, and finally computes the two measures of quality for the grasp. These measures compare the stability of a grasp only. The research was done on the simple grippers and analysed on polyhedral objects. They use a novel technique to visualize the 6D space used in these computations.

Xionga et al. [157] proposed the problem of grasp capability analysis of multi-fingered robotic hands. In this study they presented the systematic method of grasp capability analysis which was a constrained optimization algorithm. In this optimization algorithm the optimality criterion is the maximum external wrench and the constraints used is equality constraint to balance the external wrench and the inequality constraint to prevent the slippage of the fingertips, the excessive force over physical limits of the object. They formulated the problem as non-linear programming which maximized the external wrench in any direction. The main advantage of that method was, that can be used in more diverse field for example Multiple robot arms, Intelligent fixtures etc. They had shown the effectiveness of proposed algorithm with a numerical example of a tri-fingered grasp.

Bicchi and Kumar [158] surveyed the work done in the field of robotic grasping for past two decades and summarized in the given paper. Basically, they focused on the issues that are central to the mechanics of the grasping and the finger-object contact interaction. In addition, the review mainly addressed research that has established the theoretical framework for grasp analysis, simulation and synthesis.

Ding et.al. [159] presented a simple and efficient algorithm for computing a form-closure grasp on a 3D polyhedral object. The algorithm searches for a form-closure grasp from a "good" initial grasp in a promising search direction that pulls the convex hull of the primitive contact wrenches towards the origin of the wrench space. The local promising searches direction at every step is determined by the ray-shooting based qualitative test algorithm developed in in their previous work. As the algorithm adopts a local search strategy, its computational cost is less dependent on the complexity of the object surface. Finally, the algorithm had been implemented and its efficiency has been confirmed by three examples.

A new necessary and sufficient condition for 2-D three finger equilibrium grasp was developed by Li et al. [160]. They implemented a geometrical algorithm for computing force closure grasp of polygonal object. The algorithm was simple and needs only algebraic calculation. They have also shown the computable measure for how far a grasp is from losing force closure.

Borst et al. [161] proposed statistical data that confirmed their opinion that a randomized grasp generation algorithm is fast and suitable for the planning of robot grasping tasks. They showed that it is not necessary to generate optimal grasps, due to a certain quality measure, for real robot grasping tasks; an average quality grasp should be acceptable. They generated many grasp and filtered them with simple heuristics calculation of force-closure grasps. The method could be done very fast with easy implementation.

Sudsang [162] proposed the approach that searches the force-closure grasps from a collection of sampled points on the object's surface. The proposed approach could be implemented to large class of shapes of the object. The efficiency of the approach arises from a heuristic search space pruning which is based on ability to efficiently locate regions in three dimensional space where friction cones intersects and a randomized test for checking force closure condition were done. They implemented the proposed approach and shown the results.

Zhu, and Ding [163] presented a numerical test to quantify how far is the grasp from losing force/form closure. With the polyhedral approximation of the friction

cone the proposed numerical test was formulated as a single linear program. They also developed an iterative algorithm for computing optimal force closure grasp by minimizing the proposed numerical test in the grasp configuration space. The proposed approach can be used for computing force/form closure grasps in 3D objects with curved surface and with any number of contact points.

Zheng and Quin [164] worked on the handling the uncertainties in force-closure analysis. The uncertainties like friction uncertainty and the contact point uncertainty have disastrous effect on the closure properties of grasp. The former uncertainty is quantified by the possible reduction rate k of friction coefficients, while the latter is measured by the radius ρ of contact regions. The first problem was solved by searching for a non-zero consistent infinitesimal motion using nonlinear programming technique. The second problem was transformed to an algebraic equation of one variable, to which the bisection method is applied. Using the two algorithms, the last problem was readily settled and its result evaluates the overall tolerance of a grasp to both uncertainties. In order to solve the above problems efficiently, they generalized the infinitesimal motion approach from form-closure to force-closure analysis. This approach covers the three contact types and does not use linearization, and does not need to compute the rank and the null space of the grasp matrix. In the force-closure analysis, the sets of feasible contact forces, feasible resultant wrenches, consistent infinitesimal motions, and consistent functional movements are formulated. They are convex cones and were discussed systemically.

Cornella et al. [165] proposed a new mathematical approach to efficiently obtain the optimal solution of finding the suitable grasping force for grasping the object. They used the dual theorem of non-linear programming for finding the solution. The basic requirements in grasping and manipulation of objects is the determination of a suitable set of grasping forces such that the external forces and torques applied on the object are balanced and the object remains in equilibrium. The examples had been solved to show the efficiency and accuracy of the proposed method.

Wang et al. [166] used powerful 3D model reconstruction of unknown objects with the help of a laser scanner, simulation environment, a robot arm and the HIT/DLR multi-fingered robot hand. The object to be grasped were scanned by a 3D laser scanner and reconstructed in simulation scene. After different grasping was evaluated within the simulation scenes, an accurate arm and hand configuration were calculated to command the robot arm and multi-fingered hand. The

experimental results strongly authenticate the effectiveness of the proposed strategy.

Zheng and Qian [167] presented an advanced ray-shooting approach to force closure test as that was presented by Liu in 1998. This paper enhances the above approach in three aspects. Firstly the exactness was completed in order to avoid trouble or mistakes, the dimension of the convex hull of primitive wrenches were taken into account, which was always ignored. Secondly the efficiency was increased as the shortcut which skips some steps of the original force closure test was found. Lastly the scope was extended yielding a grasp stability index suitable for grasp planning. The superiority was shown with numerical examples in fixturing and grasping.

Roa and Suarez [168] presented geometrical approach to compute force closure (FC) grasps, with or without friction and with any number of fingers. They discretized the objects surface in a cloud of points. Hence the algorithm is applicable to objects of any arbitrary shape. With this geometrical approach one or more force closure grasps could be obtained, which embeds the FC test in the algorithm to simplify achieving the force-closure property. This initially force closure grasp obtained were improved with a complementary optimization algorithm. The grasp quality was measured considering the largest disturbed wrench that the grasp can resist with independence of the disturbed direction. The both algorithms efficiency was illustrated through numerical examples.

Ohol and Kajale [169] presented enhanced grasp ability with better sensors backup, which enable the robot to deal with real life situations. As the required task for the robots has become very much complicated because of handling the objects with various properties e.g. material, size, shapes, mass etc. and the physical interaction between the finger and an object is also one of the complications in grasping. e.g. grasping of object with slippage. They discussed about the Design procedure, solid modelling, Force analysis and simulation for confirmation of the viability.

Khoury and Sahbani [170] dealt with the demonstration that wrenches associated to any three non-aligned contact points of 3D objects form a basis of their corresponding wrench space. The result obtained permits the formulation of a new sufficient force-closure test. Considering the number of contacts greater than four any general kind of object could be dealt with this method. They developed the corresponding algorithm for computing robust force-closure grasps and the efficiency was confirmed by comparing it to the classical convex hull method.

Bounab et al. [171] developed a new necessary and sufficient condition for n-finger grasps to achieve force-closure property with stability. They reformulated the proposed force-closure test as a new linear programming problem, which were solved using an Interior Point Method. Simulated Annealing technique was used for synthesizing suboptimal grasps of 3D objects.

Krug et al. [172] paper introduced a parallelizable algorithm for the efficient computation of independent contact regions, under the assumption that a user input in the form of initial guess for the grasping points. The proposed approach works on discretized 3D-objects with any number of contacts and can be used with any of the following models: frictionless point contact, point contact with friction and soft finger contact. An example of the computation of independent contact regions comprising a non-trivial task wrench space was given.

Sahbani et al. [173] presented a computational algorithm for generating 3D object grasps with autonomous multi-fingered robotic hands. They focused on analytical as well as empirical grasp synthesis approaches. They stated that during grasping fingers must be controlled so that the grasp processes dexterity, equilibrium, stability and dynamic behaviour. In their algorithm such control schemes they adopted by computing the finger parameters like positions and forces of fingertips and joints. They name the algorithms as robotic grasp synthesis algorithms.

Saut and Sidobre [174] presented a simple grasp planning method for a multi-fingered hand. The main purpose of the proposed grasp planning was to compute a context-independent and dense set or list of grasps, instead of just a small set of grasps regarded as optimal with respect to a given criterion. Initially they were considered the robot hand and the object to grasp only. Thereafter, the environment and the position of the robot base with respect to the object were considered. Such a dense set can be computed offline and then used to let the robot quickly choose a grasp adapted to a specific situation. They claim that this can be useful for manipulation planning of pick-and-place tasks. Another application is human–robot interaction when the human and robot have to hand over objects to each other. If human and robot have to work together with a predefined set of objects, grasp lists can be employed to allow a fast interaction.

Lberall [175] shown that the two key issues of the grasping an object i.e. affixing the object in the hand and gathering the information about the state of the object during the task are balanced through combination of three basic methods of applying oppositions around object. Also he has shown how these relate to the posture of standard prehensile classifications.

Laberall [176] presented that the human hand in prehensile movements can offer insights into the design of robot grasp planners. He proposed the design for a two level llierarchical grasp planner. The first phase maps an object and task representation into a grasp oriented description of the task and the second phase maps this description into an opposition space, which captures the available foices and degrees of freedom of the hand. He also discussed about the constraints acting on the hand/object/task interaction.

2.3 Review Analysis and Outcome

An exhaustive survey presented in the above section on multi-finger robot hands (MFRH) considering different aspects like: structure of the hand, optimum motion of the fingers and the workspace generation, control, application and grasping ability. It is observed that many researchers tried to develop a multi-finger robot hand from late 70's to till date with resemblance to the human hand. Initially robots used for industrial applications for performing repetitive work like pick and place same type objects, so the prime requirement was to grasp the object firmly for which parallel jaw grippers are best alternative. Now a days, also parallel jaw grippers used for same purpose as earlier for transporting the heavy objects on shop floor. But, with the widening of the area of application of robots along with industrial application to human environment for performing human like operation then along with grasping the function of dexterity and manipulation becomes indeed. From the literature it is concluded that, to accomplish the property of dexterity and manipulability along with grasping, the need of MFRH arises. Almost all the research articles stated that human hand is the main point of inspiration and design follow up to develop a MFRH. Many were tried to design and develop the hand which structurally similar to human hand such as consists of three to five fingers and joints varying from 9 to 27. The multi-fingered hands are used as the end effector in robotic system, where each individual finger considered as an open loop kinematic chain or independent robot manipulator. The main properties of the human hand which researchers tried to mimic are: dexterity, anthropomorphic appearance, manipulability and control. It is observed that depending on the use of the particular robot hand the specific properties are given priority. The dexterity and manipulability capability of the hand is more when the number of fingers and joints are more, which lead to more complex control system of the hand as a result the load carrying capacity decreases. Many hands are

developed and commercialized already, which are used as part of service robots, humanoids and rehabilitation prosthetics.

Even many different types of multi finger hands are developed, but still it consider as the MFRH at its infancy. The main objective of the MFRH research is to mimic the hand as close as possible to human hand. But from literature it is observed that none of the MFRH possessing all the properties of human hand simultaneously, as it is very hard to design all at time. Dexterity and manipulability are the two important properties of the human hand, which increases the control complexity of MFRH. To reduce the complexity in some MFRH the number of fingers and number of joint angles reduced which ultimately reduces the dexterity and manipulability capability of the hand. Not much attention given to the anthropomorphic appearance of the developed hands, which is also an important factor when the hand is used for rehabilitation purpose. Most of MFRH designs the palm is considered as a non-flexible part, but in actual practice the palm of human hand is flexible and it is more important when grasp a very small object. Most of the work done on grasping planning strategy for different type grasps considering the number of contact points only. Not much work has done in the area of grasping analysis of a five fingered robot hand, maximum work has done with respect to three and four finger hands. Also not much work are found in the area of force exerted by the fingers at the contact points on the object for grasping and the stress distribution over the fingers due to these forces.

2.4 Problem Statement

After going through the several research work carried out in the related areas under investigation and considering the trend as well as outcomes vis-a-vis the objectives of the present work, the following problem statement and hypotheses are made:

Problem statement:

"*This piece of research work investigates the feasibility of a 5-fingered, anthropomorphic robot hand model having 25- degrees of freedom that enables the palm arch effect of the hand.*"

Hypotheses:

Hypothesis 1: The hand with more degrees of freedom (25 numbers in the present case) would describe more complicated trajectories with its fingertips than those with lower degrees of freedom.

Hypothesis 2: The hand with palm arch motion would yield improved reachability of the finger tips than those without this motion.

Hypothesis 3: The palm arch effect of the hand improves its capability to deal with wider range of the object size than the ones without this effect.

Hypothesis 4: The opposing motion of the fingers and the thumb follow larger trajectories with the palm arch effect and makes the hand more capable of dealing with irregular shaped objects.

2.5 Summary

An extensive study of the literatures from all available sources and related directly or indirectly with the present piece of work has been made. Some of the more relevant work has been elaborately reviewed in order to understand the extent and direction of research in the area of the present work. Literature of the past dating back to 1983 [82] till the present time were explored and studied to understand the existence of scope for abetting the current work. A comprehensive presentation has been attempted through the present work for the benefit of the readers.

Chapter 3

RESEARCH METHODOLOGY

3.1 Overview

This chapter presents a detailed chronological steps planned for completing this piece of work. It describes the methodology adapted right from the concept of the multi-fingered anthropomorphic robot hand to the final recommendations after appropriate modelling and analysis.

3.2 Selection of Methodology

There are many models of the research process, most of them devised according to a series of stages. Cohen and Manion [177] identify eight stages of action research, which appeared rather too scientific in approach. Other representations of the research process, including one with five stages of research viz. design, sampling, data collection, data analysis and the report are presented by Blaxter et. al. [178]. This seems to be a rather over-simplification of a long and complex process.

Johnson identifies the following stages of activity which must be worked through in carrying out and completing an investigation (Johnson, [179]).

1. Establishing the focus of the study
2. Identifying the specific objectives of the study
3. Selecting the research method
4. Arranging research access
5. Developing the research instrument
6. Collecting the data
7. Pulling out of the investigative phase
8. Ordering the data

9. Analysing the data
10. Writing up
11. Enabling dissemination

These and other representations of the research process such as those presented in diagrammatic format by Blaxter et. al. are simplifications and idealizations of the research process [178]. They acknowledge that the work of researchers is anything but linear. The representation of research process is given in Figure 3.1 as suggested by Blaxter et.al.

However, Johnson's stages have guided the present research as the preferred approach through clearly defined small steps and which fits well with the model of the present research. Therefore, the steps followed in abetting the research work are planned to be the following.

i) Establishing the focus of the study
ii) Identifying the specific objectives of the study
iii) Selecting the research components
iv) Detailing the units of research
v) Collecting and generating the data
vi) Analysing the data
vii) Writing up
viii) Enabling dissemination

Using the above models the remainder of this chapter describes and explains the methods that are undertaken during the period of the research.

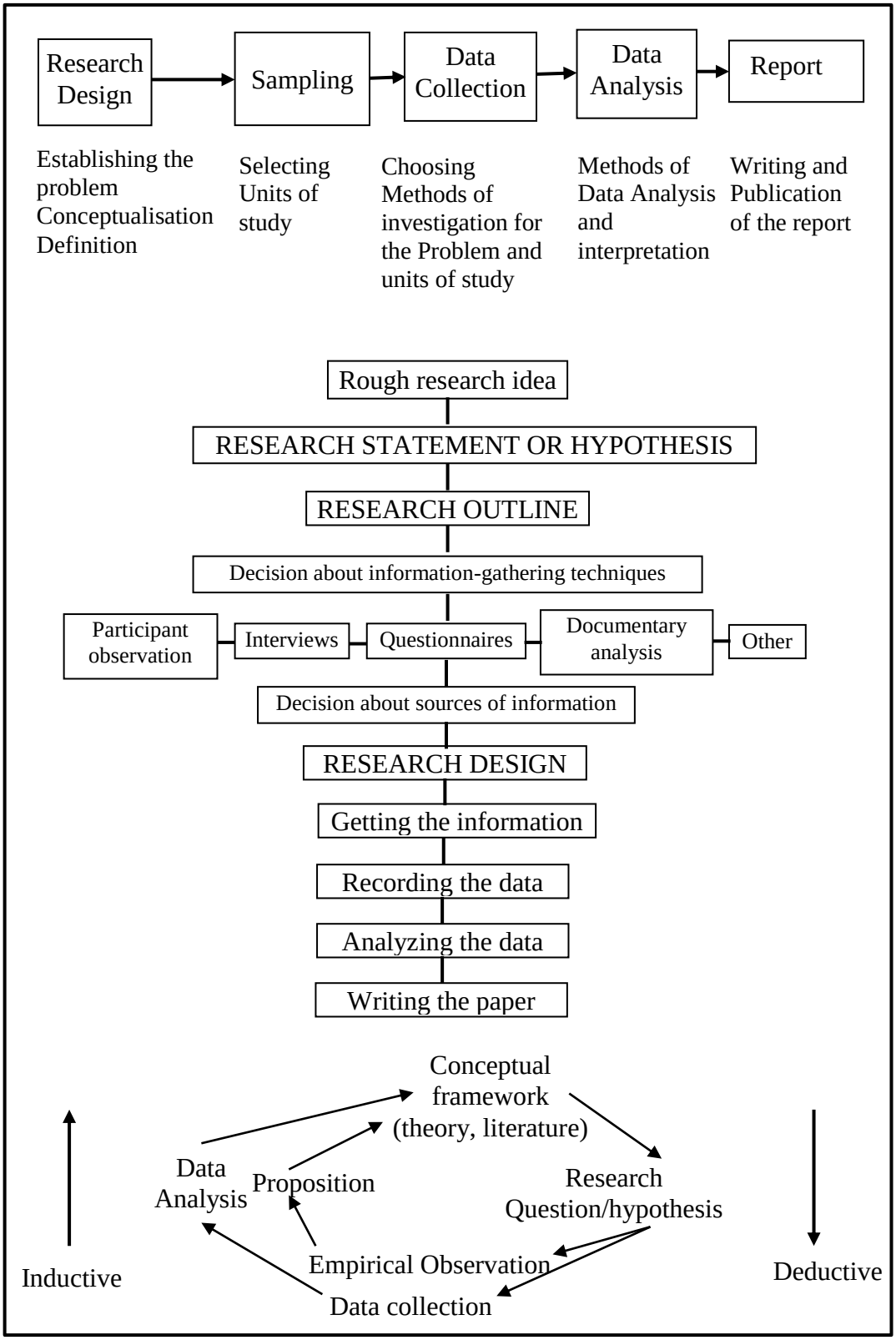

Figure 3.1: Representation of the research process.

3.3 Establishing the Focus of the Study

The first chapter (Chapter-1) introduced the subject of this dissertation wherein the evolution of robot hands, its types and applications are studied and presented elaborately. The focus of the study is on kinematic analysis of a multi-fingered and anthropomorphic robotic hand which can be advantageously used for orthopedic rehabilitation of humans and for certain specialized applications in manufacturing industries requiring complex manipulation of small objects. Therefore, an explicit study on the various multi-fingered grippers, developed so far, became a necessity. A chronological study along with their structures is also briefly presented in the thesis. A thread of study could then be made to move from only multi-fingered hands to the anthropomorphic hands and their desired properties are enumerated. Some of the applications of the hands are also studied in order to understand their usefulness in various sectors such as in industries, service, rehabilitation and entertainment.

In line with the motive, the research study also includes an initial study on grasping and manipulating capabilities of the hand which is the primary goal of the hand under investigation.

A broad objective for the work is formulated after a preliminary study of the broad subject matter and considering the developments that had already taken place. Accordingly an elaborate search for previous work in the related subject is carried out and the same is presented in Chapter-2 of the thesis. The literatures that were looked for could be categorised under the following:

i) Structural analysis: to understand the structure that has been used in developing the multi-fingered hands.
ii) Optimization: to learn the parameters that could be optimized with respect to their purpose.
iii) Control aspects: to assess the complexity that is involved with various structures as well as applications.
iv) Applications: to collect information on which domain have been covered so far.
v) Grasping capability analysis: to learn the approaches that have been followed and their outcomes.

3.4 Identifying the Specific Objectives of the Study

At the end of the literature study a summary of the review is made in order to locate the gaps that exist even after decades of work towards developing robotic hands with respect to their structure, application and capability. This leads to prepare a comprehensive problem for the present research work. Every problem for a research work has many facets which need thorough investigation. These investigations may lead the research to certain points which may be very different from the desired goals. At the same time it is possible that a problem has certain components which may be either redundant or unexplorable from the view point of the objective of the research work. Therefore it is necessary to mention the scope of the present research work (Section 3.10). On finalizing the problem statement for the research work, the line of work is decided to move towards achieving the objectives of the research work.

3.5 Selecting the Research Components

The chronology of activities for the same is presented through the following steps:

a) Structure of the multi-fingered Hands: This is essentially derived from the physiology of the human hand.
b) Kinematics of the multi-fingered Hands: Some of the useful data are taken from the previous work carried out by other researchers.
c) Multi-fingered Grasping and Object Manipulation: The motive is to look for using simple joint type which is typically used in robotics.
d) Grasp Analysis: The attention has been on two major areas; i) orthopaedic rehabilitation and ii) assembly of parts in industry.

3.6 Detailing the Units of Research

3.6.1 Structure of the Multi-fingered Hands

As the research work involved anthropomorphic robot hands, it becomes necessary to have a detailed study of the human hand. This part of work is majorly devoted towards understanding the structure of the human hand, the types of joints therein, the types of motion at each of the joints and their range of motion. The inclusion of palm arch of the human hand in developing a robot hand has not been reported by any other previous researchers. This is also investigated in order to incorporate the same in the proposed hand.

In order to get some in-depth knowledge on multi-fingered hands some of the already developed multi-fingered hands such as three fingered (Barret hand [180]), four fingered hand (DLR Hand II [181]) and five-fingered hand (Rutger hand [182]) are investigated. On the basis of the investigation, a robotic hand with five fingers (including thumb) with twenty one degrees-of –freedom and the palm arch having another four degrees of freedom with a total of twenty five degrees of freedom could be visualized. In order to design a hand having all these structural characteristics, a line model of this is prepared for kinematic analysis. The details of the structure along with the joint types, motion types and motion ranges are prepared and presented in Chapter-4.

Data Collection

Since the objective is to prepare a five-fingered, anthropomorphic hand, it was conceived that emulating a human hand will be the best option. Therefore, a study of the physiology [183] of the human hand is done to understand the structure and the kinematic relationship between the various finger segments of the human hand.

However, the kinematic modelling of the hand which needs to be taken up next requires certain other additional parameters to be known. These parameters include i) length of each segment, ii) the type of joints between two segments in the links of the fingers and iii) the range of motions. The study of literatures on ergonomics mentioning anthropometric data [184] and on biomechanics using physical parameters of human on [185, 186] are used to get the necessary data for modelling.

3.6.2 Kinematic Modeling and Analysis

Although, the present work attempted to emulate the human hand, there ought to happen some deviations between the physiological structure of the human hand and the mechanical structure of the hand. The deviations are envisaged in the following form:

i) Characteristics of biological joint vis-a-vis mechanical joint.
ii) Parametric data used in the proposed robotic hand are chosen on the basis of the breadth and length of the human hand [184, 185, 187].

Therefore, in order to ensure the functional behaviour of the proposed hand it becomes essential for carrying out the kinematic modelling and analysis of the hand. The kinematic modelling is done using the classical method of homogeneous transformation following the Denavit-Hertenberg (D-H) algorithms.

The forward kinematics is used locate the loci of the finger tips, whereas the inverse kinematics is used to check the joint angles and the angular limits of the various joints. Another good reason for doing the forward kinematic simulation is to obtain the workspace of the hand, which otherwise could not be determined to assess the grasping space of the hand.

Since the inverse kinematic problem yields multiple solutions (innumerable), ANFIS (Adaptive Neuro-Fuzzy Inference System) [188] is used to carry out the inverse kinematic analysis. ANFIS is chosen because of its simplicity in structure and easy-to-use characteristic. It takes care of the desired range of angles and makes the interpretation easier. The details about the forward and inverse kinematics are presented in Chapter-4.

3.6.3 Multi-fingered Grasping and Object Manipulation

Grasping theory is considered to be one of the important part in object securing and consequent manipulation. Since the robotic hand is intended to grasp objects and manipulate, it is important to orient the readers towards the specific applications in a fashion as is done by a human being The application areas are considered to be i) artificial hand for orthopaedic rehabilitation and ii) multi-fingered robotic hand in case of complex manipulation of objects in product assembly in the industries. Therefore, it is necessary to present the theories of grasping precisely.

In order to visualize the motion aspects of the hand, the hand is modeled using CATIA, V-5, a general Computer Aided Design tool, available in the place of research. It may be mentioned that CATIA offers good transportability to other analysis platform such as ANSYS where in further design related analysis of the hand can be done. Using the data from the CAD model using CATIA a mathematical model is derived to test the motion behaviour of the thumb with respect to other fingers. These motions are opposing in nature and are important from the grasping view point. (An object can be grasped securely by a multi-fingered hand if and only if some fingers can describe opposing motions). A program using MATLAB-8 is written to use the kinematic equations and plot the loci of the finger tips.

The data from the CAD model and simulation are used to construct the convex hull of the moving fingers which in turn determines the maximum size of the object that can be handled by them.

3.6.4 Grasp Analysis

In order to recommend the structure for detailed design and to determine the forces and torques being exerted on the various fingers while grasping the object under force closure grasp condition the mathematical models are developed.

Data generation for the model

The mathematical models need the following data:

i) Size and shape of the object
ii) Angle of incidence of the applied force
iii) Value of the co-efficient of friction and
iv) Weight of the object to be handled.

Therefore, objects of various shapes within the maximum size as decided by the convex hull are considered. The coefficient of friction between the fingers and the object is taken from the standard design data book with an assumption that for the combination of finger object materials. The weight of the object could be calculated from the size and its material..

However, as obtained from the inverse kinematic analysis, there might be a number of possible values for the incident angles. This number gets multiplied by the position of the hand with respect to the object. Further the value of the exerted force is dependent on the angle of incident. As a result the mathematical equation becomes indeterminate.

Therefore, ANFIS is used to determine a set of possible values of the exerted force after properly training its structure with a set of values for incident angles. The maximum values of the forces are recorded.

Thereafter, the hand model is modeled using finite element analysis tool (ANSYS) to check the stress being developed at various critical points of the hand while applying the maximum force for grasping and manipulating the object under force-closure conditions.

3.7 Results and Analysis

The results obtained through various analysis carried out during the work are further checked and analysed from the complete hand prospective to come out with proper recommendations. The results are obtained from the following exercises conducted during the research process:

i) Forward kinematics modelling

ii) Inverse kinematic modelling
iii) Multi-fingered grasp analysis
iv) Stress analysis of the fingers

The results of forward kinematics and inverse kinematics are checked with real human hand motion and those obtained by other researchers to validate the hand design.

The data collected from the previous literatures on structures and the data picked up through the simulation of the hand in virtual environment are also checked with other available literature.

3.8 Writing up

The aim of this stage was to draw the overall conclusions and to summarize in an adaptable form.

3.9 Enabling Dissemination

It is important to carry out research in an interesting aspect of design that is topical and relevant to the present day as well as future researchers and product developers. It is an important part of the research process that the findings and the recommendations be made available to wider audience and help influence the future developments and strategies.

3.10 Scope of Work

The present thesis aims to propose an anthropomorphic robot hand model which is structurally similar to human hand so that the robot can perform more dexterous tasks. However, there are certain limitations to the extent of increased dexterity in terms of the structural as well as control complexities. Considering these issues, the scope of the present work is stated as follows:

- Increase the total degrees-of-freedom to 25. This includes 4-DoFs in the palm arch. The work considers only the palm and fingers with the wrist as a fixed point.
- The joints of the finger segments to be made of standard mechanical joints. The exact physiology and anatomy of the human hand is difficult to reproduce in a mechanical hand. The proposed hand considers standard revolute type joints with their motion limits.

- Mathematical equations and necessary algorithm to be developed only for virtually simulating the hand in order to make the feasibility study of the hand.
- During the grasp analysis only force-closure condition is considered as it is desired to have grasping and manipulating the orientations simultaneously.
- Only standard tools/platforms are used to make the readers understand easily and make the algorithm generic and user friendly.

3.11 Summary

A brief description on the research methodology is presented in this chapter. The steps followed in performing the research work are also presented. The different activities are planned to perform during this research work along with the methods used for achieving the objective also discussed. The scope of the present research work to achieve the objective is also presented.

Chapter 4

STRUCTURE OF THE MULTI-FINGERED HANDS

4.1 Overview

Human hand is the prime inspiration for robotic hand designers and researchers. Hence, the objective of this chapter is to describe briefly the structure of the hand; which is taken as the basis for designing the proposed hand model. As mentioned under the objective of the present work, the robot hand, being designed, need to be dexterous and anthropomorphic. Therefore, it is essential to discuss on the anatomy, especially the skeleton structure of the human hand. A hand is a prehensile, multi fingered extremity located at the end of an arm or forelimb of primates and humans. Hands are the main structures for physically manipulating the environment, used for both gross motor skill (such as grasping a large object) and fine motor skills (such as picking up a small pebble). The fingertips contain some of the densest areas of nerve endings on the body, are the richest source of tactile feedback, and have the greatest positioning capability of the body; thus the sense of touch is intimately associated with hands. It is not attempted here to provide a comprehensive depiction for the hand as it is made by the physicians, but only it tries to present the knowledge required for designing the proposed hand model. The hand is an exceptionally complex mechanism. This introduction to anatomy (what parts make up the hand) will add to the knowledge as well as understanding the conditions affecting the hands. The main structures of the hand can be divided into several categories. These include: bones and joints, ligaments and tendons, muscles, nerves, circulatory system, and skin. This dissertation more concentrates on the bones and joint structure of the hand, the other categories like muscles, nerves, skin etc. are beyond the scope of this dissertation. Tables and

short descriptions are used to make the presentation precise and clear. The range of motion for the wrist and the joints of the hand are also presented. Some important connections among muscles and bones are also briefly discussed in this chapter for better understanding of the structural and functional view of the hand.

4.2 Structure of the Human Hand

The study of human hand is interesting and has been studied for many years by the different group of people like medicine practitioners for the purpose of treatment of the different parts when infected. The researchers and designers of artificial prosthetic hand also studied it for the purpose of rehabilitation. In the present dissertation the physiology of the hand is not the major topic of discussion, but a thorough knowledge about the structure of the hand is needed in order to understand and design the hand model. This topic has been well studied by researchers viz. Kapandji [189], and Tubiana et al. [190, 191].

4.2.1 Bones

The major parts of the human hand are wrist, palm, four fingers, and thumb as shown in Figure 4.1.

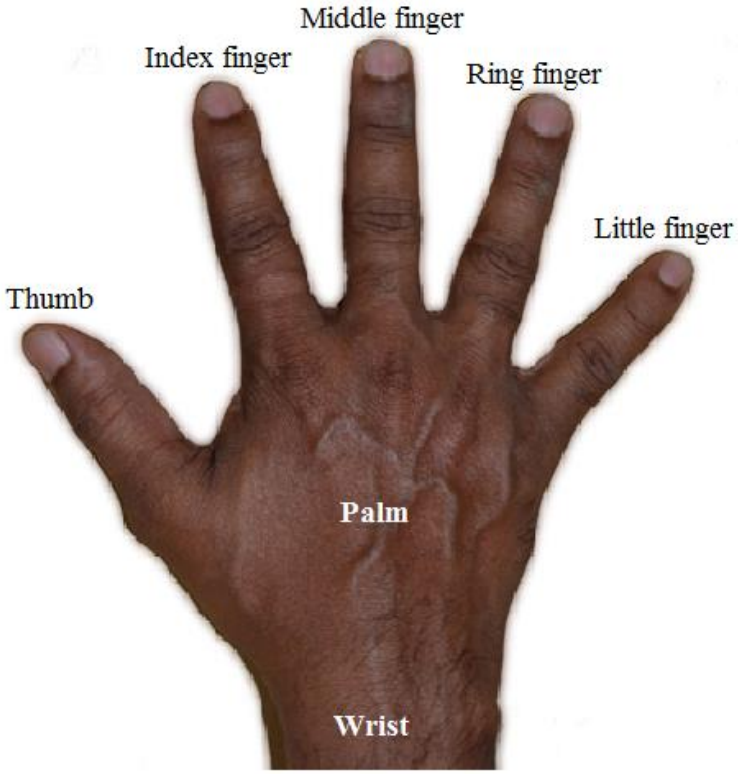

Figure 4.1: The human hand.

The special property of the thumb in the hands of the humans and other primates is that, it is opposable, i.e., it can be moved in a direction opposite to the other four digits always. Only this opposable movement of thumb makes it possible to make precise movements for grasping small objects. In vertebrates other than humans, the primary function of the hand is locomotion; the human hand, due to the evolutionary development of bipedalism, is freed for manipulative tasks. There are 27 bones within the wrist and hand. The wrist is the part that joins the hand to the forearm and it contains eight cubes like bones arranged in two rows of four bones each. The carpals join with the two forearm bones, the radius and ulna, forming the wrist joint. The metacarpus, or palm, is composed of five long metacarpal bones. One metacarpal connects to each finger and thumb. Fourteen phalangeal bones constitute the four fingers and thumb (three in each finger, two in the thumb).The details of the arrangement of bones in wrist and hand shown in Figure 4.2.

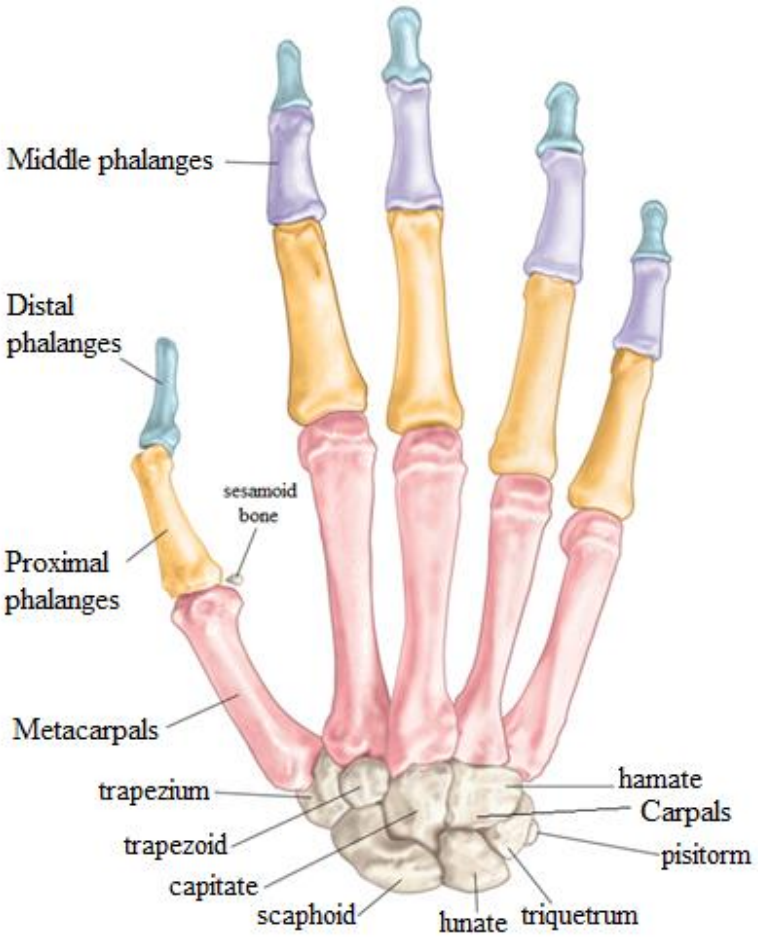

Figure 4.2: The bones of the hand and wrist.

4.2.2 Ligaments and tendons

Ligaments interconnect the bones of the hand. These are tough bands of tissue that connect bones together. Two important structures, called collateral ligaments, are found on either side of each finger and thumb joint. The function of the collateral ligaments is to prevent abnormal sideways bending of each joint.

Tendon is a tough band of fibrous connective tissue that usually connects muscle to bone and is capable of withstanding tension. The tendons that allow each finger joint to straighten are called the extensor tendons. The extensor tendons of the fingers begin as muscles that arise from the backside of the forearm bones. These muscles travel towards the hand, where they eventually connect to the extensor tendons before crossing over the back of the wrist joint. As they travel into the fingers, the extensor tendons become the extensor hood. The extensor hood flattens out to cover the top of the finger and sends out branches on each side that connect to the bones in the middle and end of the finger.

4.2.3 Muscles

Muscle is a kind of soft tissue of animals. Muscle cells contain protein filaments that slide past one another, producing a contraction that changes both the length and the shape of the cell. Muscles function to produce force and cause motion. They are primarily responsible for maintenance of and changes in posture, locomotion of the organism itself, as well as movement of internal organs. Many of the muscles that control the hand start at the elbow or forearm. They run down the forearm and cross the wrist and hand. Some control only the bending or straightening of the wrist. Others influence motion of the fingers or thumb. Many of these muscles help position and hold the wrist and hand while the thumb and fingers grip or perform fine motor actions. Most of the small muscles that work the thumb and little finger start on the carpal bones. These muscles connect in ways that allow the hand to grip and hold. Two muscles allow the thumb to move across the palm of the hand, an important function called thumb opposition. The smallest muscles that originate in the wrist and hand are called the intrinsic muscles. The intrinsic muscles guide the fine motions of the fingers by getting the fingers positioned and holding them steady during hand activities.

4.3 The Articular System

In the context of designing the proposed robot hand, it is useful to gain knowledge about the articular system of the human hand. The joints are the places of union

between skeletal elements that are more or less moveable. Joints are commonly defined as being between bones, but joints also occur between bones and cartilages, between cartilages, and between bones and teeth. In the present dissertation, only the joints between bones are considered. The articular system joins the skeleton together and allows and/or restrains movement [193]. It also allows growth of the skeleton until the end of puberty. While designing the robot hand these properties of the joints are maintained.

4.3.1 Joints of the Hand

The joints of the human hand can be studied with reference to section 4.2.1 and the Figure 4.2. The wrist consists of 8 bones and hand consists of 19 bones. The wrist part consisting of 8 bones are arranged in two rows and each row has four bones. The connections among bones are as follows:

The scaphoid has articulations with the scapholunate, lunotriquetal, capitolunate, and radiolunate bones, and are attached to the abductor pollicis brevis muscle. The lunate has articulations with the scapholunate, lunotriquetal, and capitolunate bones and the radiolunate joint. The triquetum has articulations with the lunotriquetral, pisotriquetral, and triquetriohamate bones. The trapezoid has articulations with the scaphotrapezoidal, trapeziotrapezoidal, and index carpometacarpal bones, and is attached to the abductor pollicis muscle. The trapezium has articulations with the scaphotrapezoidal, trapeziotrapezoidal, and thumb basal bones, and is attached to a five muscles. The capitate has articulations with the middle carpometacarpal, and midcarpal bones, and is attached to the abductor pollicis muscle. The hamate has articulations with the capitohamate, triquetriohamate, ring carpometacarpal, and small carpometacarpal, and is attached to the opponens digiti minimi and flexor carpi ulnaris muscles. The pisiform has articulations with the pisotriquetral bones and is attached to the opponens carpi ulnaris, and abductor digiti minimi muscles.

The relative movements among the wrist bones have been studied by Neu et al. [193] and Sonenbluma et al. [194], and they considered the motion of the scaphotrapezio-trapezoidal (STT) joint. However, for the purpose of simplicity in design this movement has been considered as shared in common with the different bones in each finger.

The hand consists of two layers of bones one set is metacarpals and another set is phalanges. Figure 4.3 shows the skeleton of the hand with all the joints. In the figure ‘T’ represents the thumb, ‘I’ represents the index finger, ‘M’ represents the middle finger, ‘R’ represents the ring finger and ‘L’ represents the little finger. The

different joints are represented as the carpometacarpal (CMC) joint is the joint between the carpal bones and metacarpal bones; mecapophalangeal (MCP) joint is the joint between metacarpal bones and phalange of the thumb and metacarpal (MC) joint is the joint between metacarpal bones and phalanges of the fingers. The metacarpal bones of the hand and their articulations are described in Table 4.1.

Table 4.1: Metacarpal bones articulation.

Thumb and Finger	Articulation
Thumb	Thumb CMC joint and Thumb MCP joint
Index	Index CMC joint and Index MCP joint
Middle	Middle CMC joint and Middle MCP joint
Ring	Ring CMC joint and Ring MCP joint
Little	Little CMC joint and Little MCP joint

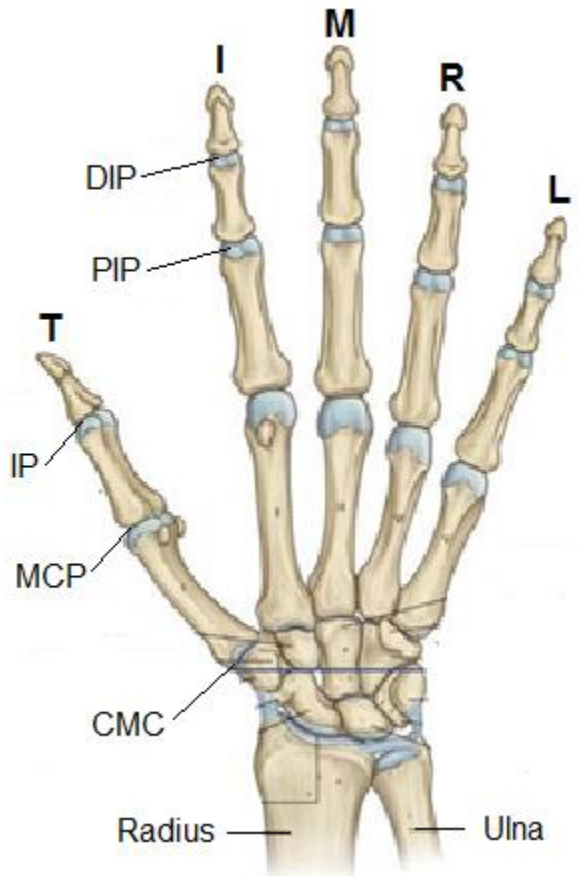

Figure 4.3: Joints of the hand.

In case of thumb, there are two phalangeals as proximal and distal phalangeal and in all four fingers there are three phalangeals as proximal, middle and distal phangeal. The different joints between phalangeals and between metacarpal and phalangeals are described in Table 4.2, where interphalangeal (IP) joint is the joint between proximal and distal phalangeal of the thumb, the proximal interphalangeal (PIP) joint is the joint between proximal and middle phalangeal of the fingers and distal interphalangeal (DIP) joint is the joint between middle and distal phalangeals of the fingers.

Table 4.2: Joints of metacarpal bones and phalangeals.

Phalanx	Articulation
Thumb Proximal	Thumb MCP joint and Thumb IP joint
Index Proximal	Index MCP joint and Index PIP joint
Middle Proximal	Middle MCP joint and Middle PIP joint
Ring Proximal	Ring MCP joint and Ring PIP joint
Little Proximal	Little MCP joint and Little PIP joint
Index Middle	Index PIP joint and Index DIP joint
Middle Middle	Middle PIP joint and Middle DIP joint
Ring Middle	Ring PIP joint and Ring DIP joint
Little Middle	Little PIP joint and Little DIP joint
Thumb Distal	Thumb DIP joint
Index Distal	Index DIP joint
Middle Distal	Middle DIP joint
Ring Distal	Ring DIP joint
Little Distal	Little DIP joint

4.3.2 Motion at the Joints

The joints of the wrist and hand can move in two planes, one parallel to the plane of the palm and other perpendicular to the plane of palm. The motion parallel to the pane of palm is called radial and ulnar deviations in case of wrist as shown in Figure 4.4.

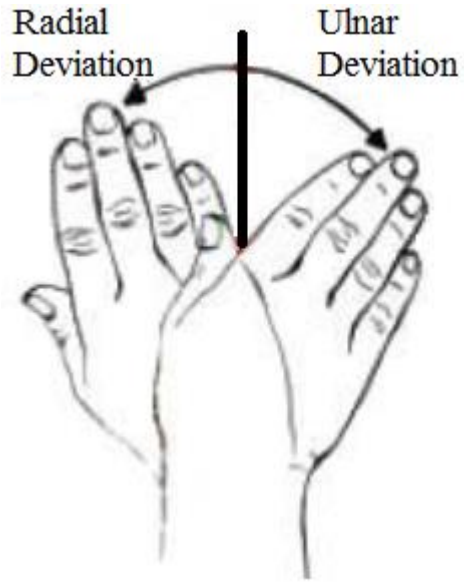

Figure 4.4: Radial/ulnar motion of the wrist.

The movement of the wrist perpendicular to the palm plane is called extension and flexion as shown in Figure 4.5.

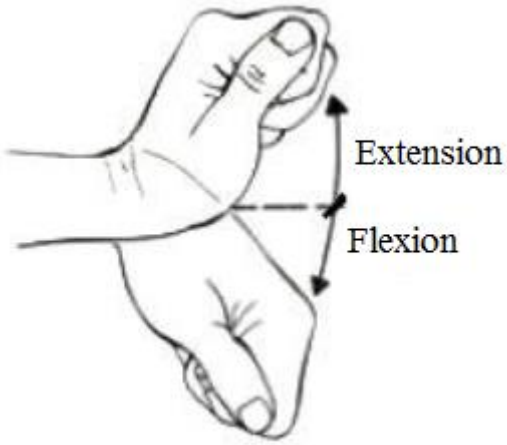

Figure 4.5: Flexion/extension motion of the wrist.

The range of joint motions of the wrist is given in Table 4.3[184,185].

Table 4.3: Range of joint motion for the wrist (in degrees).

Joint	Motion	Range
Wrist	Extension/Flexion	70-75
Wrist	Radial/Ulnar	20-35

The CMC and MCP joints of the hand as shown in Figure 4.3 are having two types of motions one is abduction/ adduction (Ab/Ad), which is on the plane parallel to the plane of the palm and another is flexion/extension (F/E), which is on the plane perpendicular to the plane of the palm as shown in Figure 4.6(a). Hyper extension is referring to the motion of any finger segment above the palm plane as shown in Figure 4.6(b).

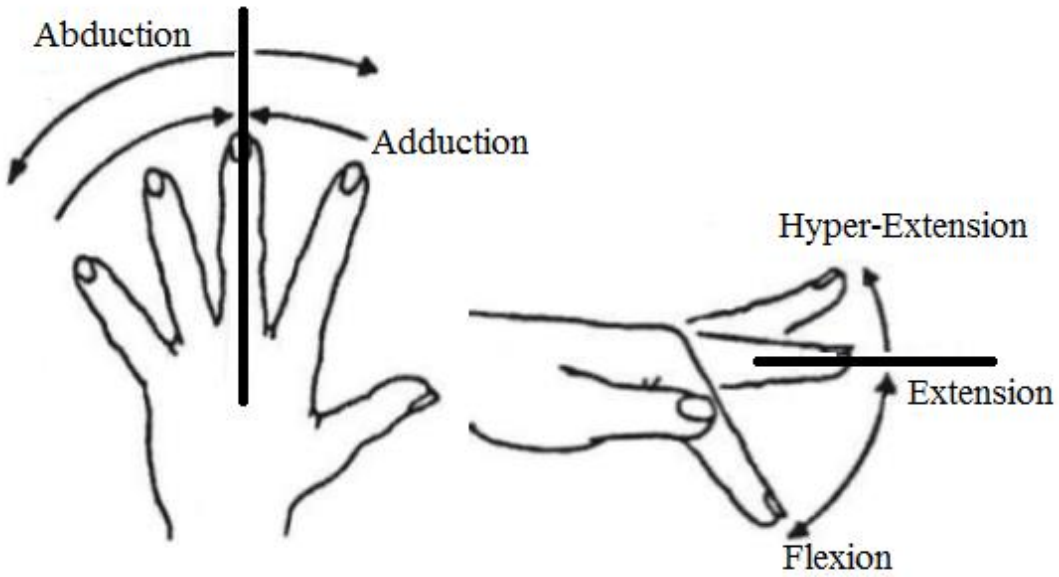

(a) (b)

Figure 4.6: Abduction/Adduction and Flexion/Extension motion of the hand.

The range of motion for all the joints of thumb and fingers are given in the tables from Table 4.4 through Table 4.8. The values of these joint limits are chosen in the light of the previous work by Jang and Pitarch [184,185,186].

Table 4.4: Range of joint motion for thumb (in degrees).

Joint	Motion	Range
CMC	Abduction/Adduction	0 to 60
CMC	Extension/Flexion	-25 to 35
MCP	Abduction/Adduction	0 to 60
MCP	Extension/Flexion	-10 to 55
IP	Extension/Flexion	-15 to 80

Table 4.5: Range of joint motion for index finger (in degrees).

Joint	Motion	Range
MCP	Abduction/Adduction	-30 to 30
MCP	Extension/Flexion	-10 to 90
PIP	Extension/Flexion	0 to 90
DIP	Extension/Flexion	0 to 60

Table 4.6: Range of joint motion for middle finger (in degrees).

Joint	Motion	Range
MCP	Abduction/Adduction	-8 to 35
MCP	Extension/Flexion	0 to 80
PIP	Extension/Flexion	0 to 100
DIP	Extension/Flexion	-10 to 90

Table 4.7: Range of joint motion for ring finger (in degrees).

Joint	Motion	Range
MCP	Abduction/Adduction	-14 to 20
MCP	Extension/Flexion	0 to 80
PIP	Extension/Flexion	0 to 100
DIP	Extension/Flexion	-20 to 90

Table 4.8: Range of joint motion for little finger (in degrees).

Joint	Motion	Range
MCP	Abduction/Adduction	-19 to 33
MCP	Extension/Flexion	0 to 80
PIP	Extension/Flexion	0 to 100
DIP	Extension/Flexion	-30 to 90

4.4 Palm Arch

When the palm hollows for the purpose of grasping a small object, the movement of the metacarpal bones occur with respect to wrist [183]. When the hand is flat the heads of the last four metacarpal bones lie on a straight line AB as shown in Figure 4.7. But, the heads of the last three metacarpal bones move anteriorly and lie on a curve line A^1B. These movements occur at the carpometacarpal joints.

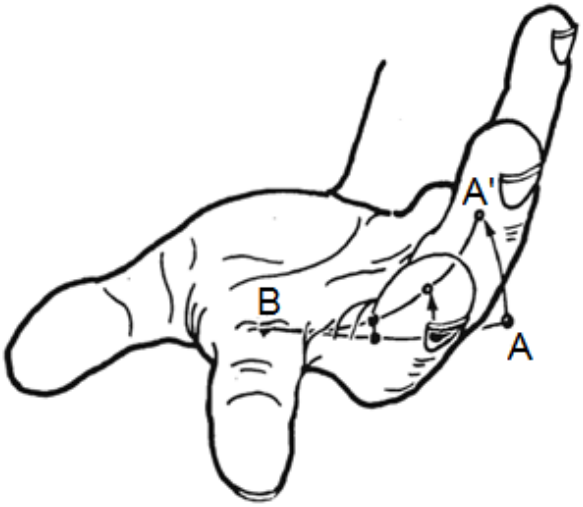

Figure 4.7: Position of the metacarpal bones.

The range of these movements increases from the second to the fifth metacarpal. It is observed that the second and third metacarpal heads do not move appreciably, so the movement at CMC joint of these two fingers is negligible and is not considered during the design process. The fourth and fifth metacarpal head, which are the most mobile, are move not only anteriorly but also slightly laterally. This movement of the metacarpal head is termed as hand arches at the palm, which is called palm arch as shown in Figure 4.8. This movement decomposes into two, one in the direction of flexion/extension (F/E) and the other in the direction of abduction/adduction (Ab/Ad) [183].

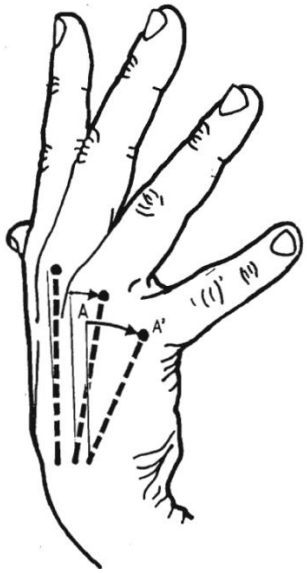

Figure 4.8: Palm arch of the hand.

4.5 Structure of Some Three and Four-fingered Hands

As described earlier, the hand or end effector is the link between the manipulator (arm) and the operational environment. When the objective of the manipulator is to only perform some simple operations with stable and regular shaped objects then the traditional two or three jaw non-jointed grippers are best suited as they offer low initial cost, less maintenance and high grasping forces. However, when the objects are unstable, have non-uniform cross sections, and need complex manipulation, then the dexterity becomes important for robot hands. In order to increase the dexterity of robot hands the concept of multi-fingered hands comes into picture. As discussed earlier in Chapter 1, mostly the first multi-fingered hand prototype was produced in the name of Okada hand which was built at the Electromechanical Laboratory in Japan in 1979 [11]. This is a three fingered robot hand consisting of two fingers and an opposable thumb as resemblance to the human hand. The hand has eleven joints and all are controlled and actuated from electrical revolute motors and the cables. In 1988 one of the sophisticated three fingered hand was developed by Barrett Technology at the University of Pennsylvania [180] as shown in Figure 4.9. This is a three finger mechanical hand having 8 joints, out of which 4 are actuated. Therefore, it is an under-actuated hand. The novelty of this hand is that each finger has two joints for closing and opening with respect to palm as like as flexion/extension movement of the human hand.

Figure 4.9: The Barrett hand model.

Out of its three multi-jointed fingers two have an extra degree of freedom with 180 degrees of lateral mobility as like as abduction/ adduction movement of human hand for grasping large variety of objects. Later on, many three-fingered hands were designed, developed and were made commercially available. Some of the important hands are given in Table 1.1.

The three-fingered hands are similar to three jaw grippers which have the advantage of better grasping of an arbitrary shaped object. It is observed from the functioning of the human hand that the manipulating capability is more when number of contacts between hand and object is more. In 1983 at Utah university one multi fingered hand was developed unlike earlier hands. This hand has three fingers along with an opposable thumb. The three fingers and thumb have four degrees of freedom (DOF) each; as a result the hand has 16 DOF. All the 16 joints of the Utah hand were actuated by pneumatic actuation system through cables. In 1998 at German Aerospace Centre, a four fingered articulated robotic hand was developed named as DLR hand [181]. Unlike Barrett hand the placement of fingers in the DLR hand resembles the human hand structure as shown in Figure 4.10.

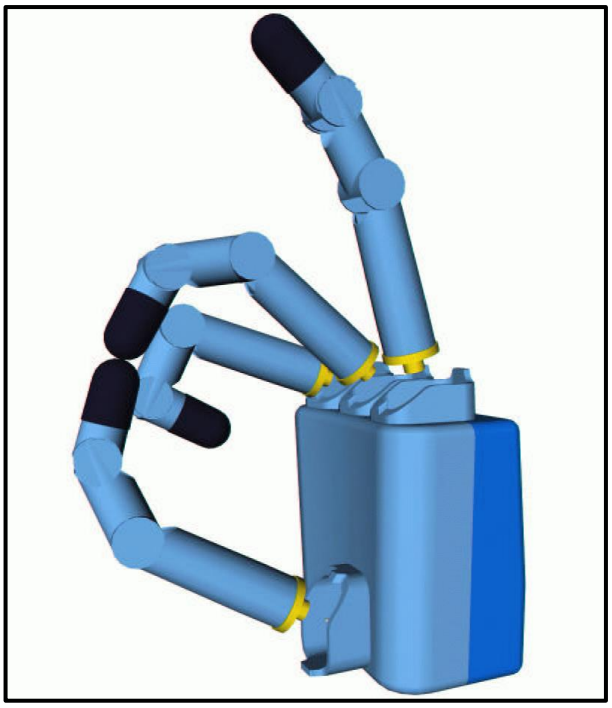

Figure 4.10: DLR hand II.

The DLR hand has four identical fingers consisting of three links each. It is also an under-actuated hand as out of 17 joints only 13 are actuated and the rest are

coupled with other joints. Since all the actuating motors are placed internally, the hand is almost 1.5 times the size of an average human hand. By the time many more type of four fingered robot hands were developed along with different actuation and control strategies including under actuation principle. Although the dexterity and manipulating capability of four fingered hands are obviously more in comparison to three fingered hands as the numbers of contact points are more, they still lack the capability of human hand in the same terms.

4.6 Dexterous Five-fingered Hand

Robotic hands are categorized mostly based on the purpose that they are used for, such as grasping or manipulating or both simultaneously. Human hand is the best example which performs both the function precisely and successfully. Certainly, some devices can mostly outperform the human hand in dedicated applications of either grasping or manipulating. However the performance of these hands has not been very successful in comparison to the human hand due to high complexity. The main lesson that has been learned from biology and actual prototypes can be summarized in two words; versatility and simplicity. The idea is to approach the versatility of the human hand i.e. ability to achieve multiple tasks with a device as simple as possible.

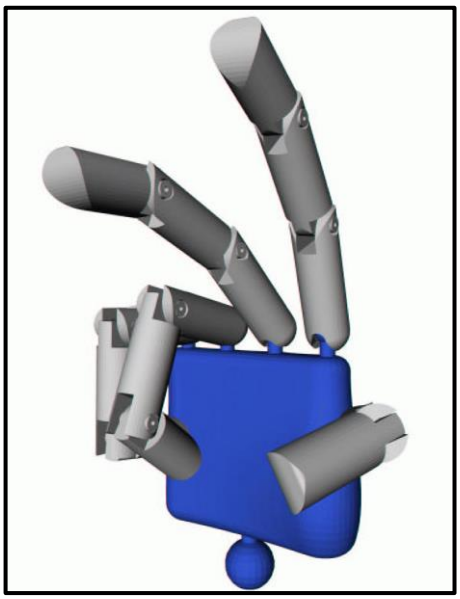

Figure 4.11: The Rutger hand model.

The simplicity refers to the appearance of the human hand which looks very general. The Mechanical and Aerospace Engineering Department at Rutgers

University added a new hand to the robotic hand family by developing a new robotic hand named as Rutger Hand [182] which is shown in Figure 4.11. This hand is also a 5-fingered anthropomorphic hand. The most novel aspect was the use of shape memory alloys to actuate the joints. Shape memory alloys are very compact and lightweight and provide a method of actuation similar to human muscle fibers which contract when excited. Each of the four fingers has 3 links and the thumb has 2, and the base of each finger is connected to the palm with a ball and socket joint that has 2 independently controllable degrees of freedom. This gives a total of 19 degrees of freedom: 4 for each of the 4 fingers and 3 for the thumb.

4.7 Proposed Hand Model

The study of human hand in the context of its structure details, motion capabilities and object manipulation mechanism vis-a-vis that of some of the multi-fingered robot hand is very clear on the fact that, there has been an attempt to mimic the human hand to certain extent while designing the robot hand. The status of development in this particular field is also quite encouraging. Therefore, it is proposed that, the multi-fingered, anthropomorphic robot hand should be close to the human hand with respect to its arrangement of structure and functions. Therefore, the size of the various individual components of the robot hand should be proportional to those of its counter part of the human hand and the motion characteristics ought to be replicated.

In order to, achieve the aforementioned features in the robot hand and to make it more dexterous with additional DoFs, the palm arch effect of the hand is included. The palm arch effect of the human hand is considered in the proposed hand model by introducing 2 DOFs each at CMC joint of ring and little finger.

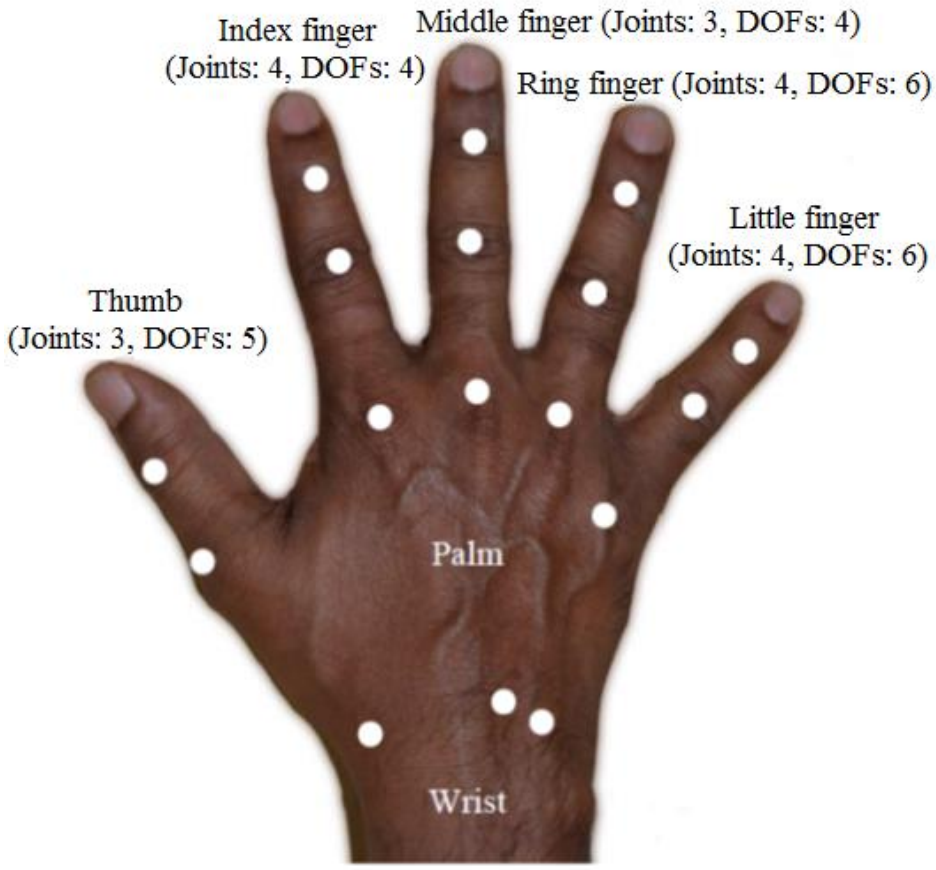

Figure 4.12: Human hand with joints.

A human hand with joints at CMC, MCP, IP, PIP and DIP including joints at CMC of ring and little finger to facilitate palm is shown in Figure 4.12. Keeping the position of joints as shown in Figure 4.12 in view, and considering the number of joints and DOFs for thumb and the fingers as mentioned a hand model is proposed for the present work. Therefore, a conscious effort has been made to make in the proposed hand model more like a human hand by adding more DOFs. Since in the present work more concentration is given on the grasping and manipulating function of the hand, it is assumed that the wrist is a fixed point, and it is considered as the origin of global co-ordinate system for the purposes of kinematic analysis.

The line diagram of the proposed hand model with 5-fingered and a total of 25-DOFs showing the links and joints is presented in Figure 4.13. This model considers all the thumb and finger segment lengths as the proportionate lengths in terms of hand length and hand breadth, which enables the proposed model to get an anthropomorphic appearance. The details about the location of the joints and

provision of DOFs of the proposed hand model are presented in next Chapter under section 5.2.

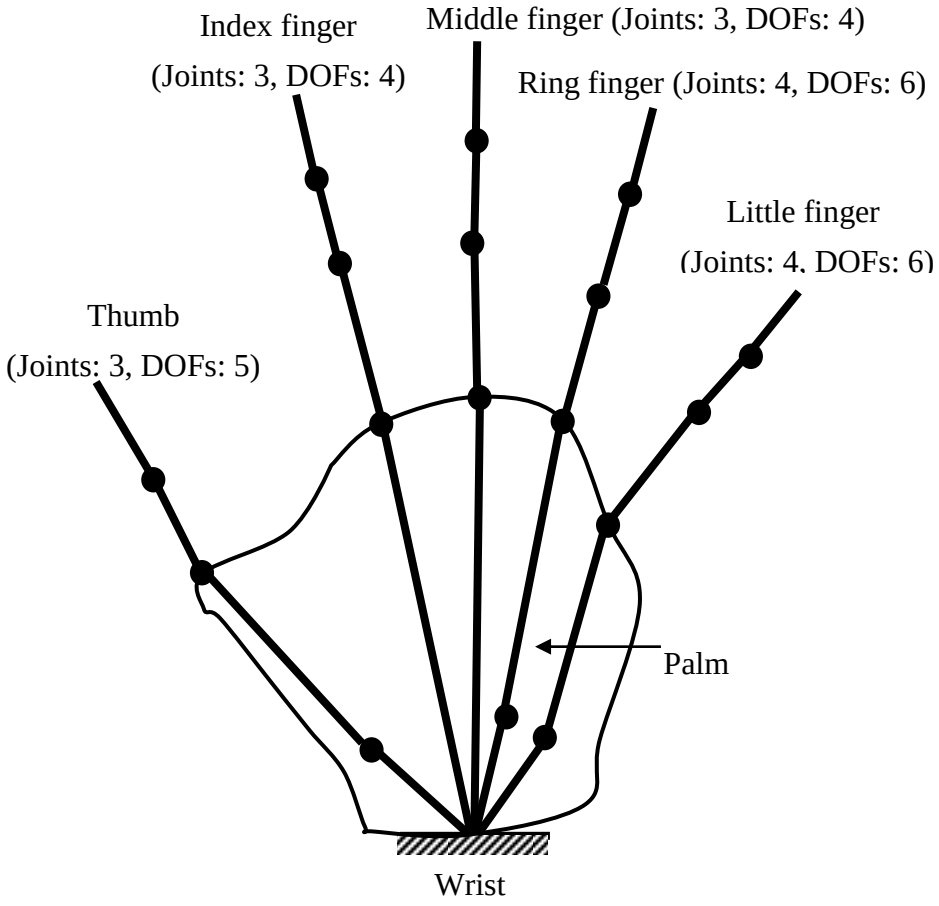

Figure 4.13: Concept of proposed hand model.

4.8 Summary

This chapter provides the basis for modelling the proposed hand. The purpose of this chapter is to provide a brief idea about the hand anatomy. The hand anatomy is presented through the tables, considering only about the bones, joints, muscles, connections and movements. This Chapter also presents the structure of various types of already developed multi-fingered hands and discusses briefly about their functions as well as their limitations. Based on some of the relevant past work, the concept of palm arch is introduced and discussed. For the purpose of this work the palm arch is decomposed in to two movements as flexion/extension (F/E), abduction/adduction (Ab/Ad) at the CMC joints of the ring and little finger. Hence, a hand model is proposed which consists of five fingers with 25- DOFs in all including 4- DOFs for palm arch.

Chapter 5

KINEMATICS OF THE MULTI-FINGERED HAND

5.1 Overview

The kinematic model of the proposed hand is presented in this chapter. The multi-fingered robot hand acts as a multipurpose gripping device for various tasks. Since it is designed to mimic the human hands, most anthropomorphic robot hands duplicate the shape and functions of human hands. The structure of the proposed anthropomorphic hand is almost the same as that of a human hand. The finger segments in human hand give the inspiration to design an independently driven finger segment to construct a whole finger. Hence, each finger of the hand is considered as an open loop kinematic chain or otherwise an independent manipulator with base at wrist and tip is the end effector. The whole hand consists of five independent manipulators or open loop kinematic structures, so the Denvit-Hartenberg (D-H) convention [194] which is a well-known procedure, becomes necessary to represents the parameters of the hand. A novel hand model with 25 DOFs and the wrist as fixed point is proposed here, the justification of 25 DOFs is already discussed in Chapter 4. The parametric model, D-H model and D-H parameters of thumb and each finger are also presented in this chapter. The transformations from local to global coordinates are explained and the kinematic formulation for manipulating the proposed model is presented.

5.2 Kinematic Model of the Hand

The 25 DOFs hand model is shown in Figure 5.1 with associated movements such as Abduction/Adduction (Ab/Ad) and Flexion/ Extension (F/E). The point O is

considered as the fixed point which is on the wrist of the hand, and is considered as the base for the analysis of D-H parameters. Analogous to human hand, the pairs of movements are in the same planes for the four fingers, but for the thumb the planes of movement are just reverse as in case of fingers and these are shown in Figure 5.1.

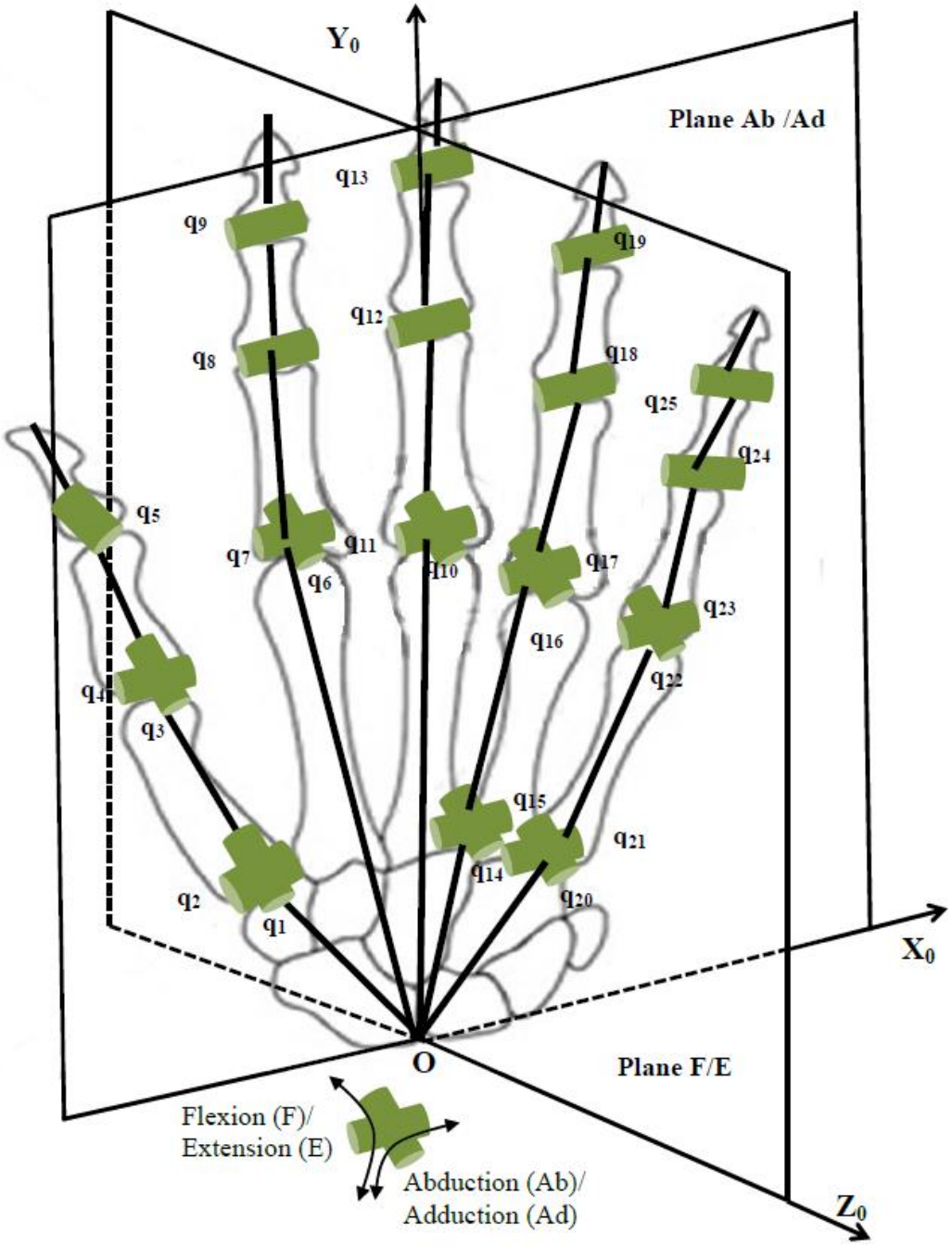

Figure 5.1: The 25 DOF hand (Posterior view of right hand).

In the figure the DOFs for each joint are located at the respective joints. The thumb is modeled with 5 DOFs. The index and middle fingers are modeled with 4 DOFs each. The ring and little fingers are modeled with 6 DOFs each considering two degrees of freedom each at Carpometacarpel (CMC) joint for palm arch. All five Mecapophalangeal (MCP) joints and three CMC joints are considered with two rotational axes each for both abduction-adduction (Ab/Ad) and flexion-extension (F/E). The Interphalangeal (IP) joint on the thumb, the Proximal-Interphalangeal (PIP) and Distal- Interphalangeal (DIP) joints on the other four fingers possess 1 DOF each for the flexion-extension rotational axes.

5.3 Hand Anthropometry

Anthropometry is a branch of anthropology dealing with measurement of the human body to determine the differences in individuals, groups, etc. The hand joints under design are similar to those of the human hand. However the joints considered for the dexterous hand consist of the metacarpal joints present in the palm connecting to the fingers and the joints right on the fingers. In order to make the dexterous hand similar in construction and in function to that of a human being, the links between the joints are taken proportional to their respective bones in a human hand. The parameters shown in Figure 5.2 are used to know the bones' lengths are hand length (HL) and hand breadth (HB) which are different from person to person.

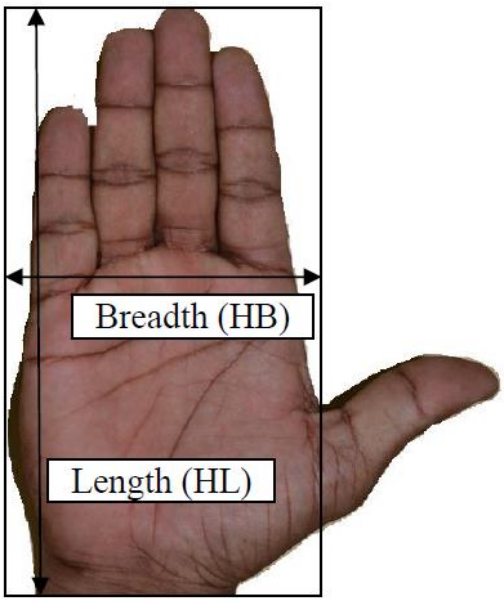

Figure 5.2: Parametric length for a hand.

5.3.1 Parametric Model for Each Segment

The individual fingers are considered as an open link manipulators; hence each segment of the finger is considered as a link. The length of segments is important to finding the fingertip position and subsequently the work envelope of a particular hand model. The segment lengths are also different for different hands. It is required to generalize the proportion of each segment with the hand parameters, so that for a particular hand the individual segment lengths can be calculated. The parametric lengths for four fingers i = I, M, R, L, where the notations I, M, R and L stand for the index finger, middle finger, ring finger and little finger respectively. Figure 5.3 shows the parametric lengths of the finger segments [184,185]. The subscript -0 is the length from global coordinate system, which is located at the wrist. Subscript -1 is the length of the metacarpal bones, subscript -2 is the length of proximal phalanx bones, subscript -3 is the length of medial phalanx bones and subscript -4 is the length of distal phalanx bones.

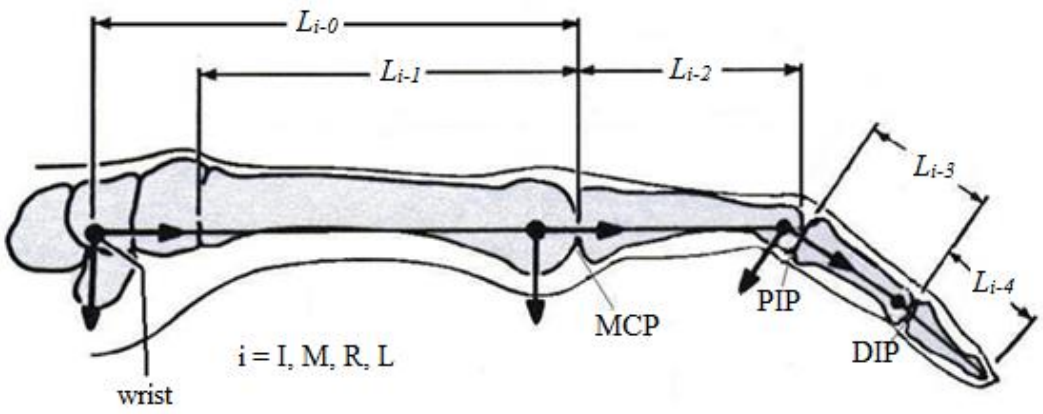

Figure 5.3: Parametric length for a finger.

The parametric lengths for thumb is shown in Figure 5.4 [184,185], where, *i*=T is the notation for thumb and the subscripts -1, -2, -3 are the lengths of metacarpal, proximal phalanx and distal phalanx bones of the thumb respectively.

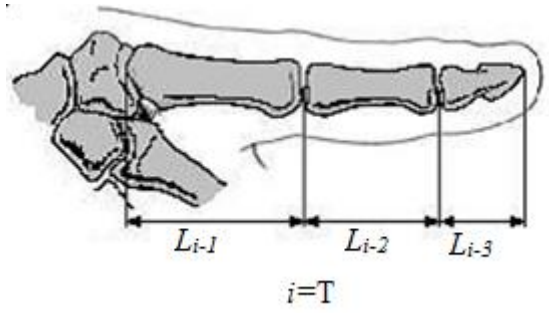

Figure 5.4: Parametric length for thumb

The anthropometric data of a typical male human hand has been considered for the purpose of building the model. Similarly the degrees of freedom and angle limits for motion have been emulated in the hand model to make it dexterous. The anthropometric data for the palm (metacarpal region) are presented in Table 5.1, where as that of fingers (phalangeal region) are presented in Table 5.2, where HL and HB are the length and breadth of the hand respectively [184, 185,187].

Table 5.1: Lengths of the Metacarpal Bones.

	Metacarpal Bones	
Thumb	0.251*HL	L_{T-1}
Index	$\sqrt{(0.374 * HL)^2 + (0.126 * HB)^2}$	L_{I-1}
Middle	0.373*HL	L_{M-1}
Ring	$\sqrt{(0.336 * HL)^2 + (0.077 * HB)^2}$	L_{R-1}
Little	$\sqrt{(0.295 * HL)^2 + (0.179 * HB)^2}$	L_{L-1}

Table 5.2: Lengths of the Phalangeal Bones.

	Proximal		Middle		Distal	
Thumb	0.196*HL	L_{T-2}	-	-	0.158*HL	L_{T-3}
Index	0.265*HL	L_{I-2}	0.143*HL	L_{I-2}	0.097*HL	L_{I-4}
Middle	0.277*HL	L_{M-2}	0.170*HL	L_{M-2}	0.108*HL	L_{M-4}
Ring	0.259*HL	L_{R-2}	0.165*HL	L_{R-2}	0.107*HL	L_{R-4}
Little	0.206*HL	L_{L-2}	0.117*HL	L_{L-2}	0.093*HL	L_{L-4}

The parametric lengths are used for two purposes: one is for lengths applied in the D-H method (i.e. a_i, α_i, d_i and θ_i) and the other is to transform local coordinates to global coordinates.

5.4 D-H Representation

Any robot can be described kinematically by giving the values of four quantities for each link. The link length (a) and the twist angle (α) describe the link while the joint distance (d) and the joint angle (θ) describe the connection and configuration. In the present hand model the joint angle 'θ' is the angle of different joints of the fingers i.e. from q_1 to q_{25}. Once all the parametric lengths for thumb and each finger are known, then following the algorithm for D-H representation, the open loop chain and D-H table are built for thumb and each finger. The algorithm proposed in literature [195, 196] to compute the D-H parameter is adopted for the hand model and can be explained as follows:

Step 1. Identify and number the joints from 1 to n starting with base and ending with fingertip.

Step 2. Assign a right handed orthogonal coordinated frame {0} to the finger base, making sure that Z_0 aligns with the axis of joint 1 (Set $i = 1$).

Step 3. Align axis Z_i with the axis of joint (i+1) for $i = 1, 2 \ldots n$.

Step 4. Locate the origin of frame {i} at the intersection point of the Z_i and Z_{i-1}. If they do not intersect, use the intersection of Z_i with a common normal between Z_i and Z_{i-1}.

Step 5. Select X_i to be orthogonal to both Z_i and Z_{i-1}. If Z_i and Z_{i-1} are parallel, point X_i away from Z_{i-1}.

Step 6. The Y_i axis has no choice and is fixed to complete the right handed orthogonal coordinate frame {i}. This axis normally is not shown to avoid encumbering the drawing.

Step 7. Set $i = i + 1$. If $i <$ n, go to step 3; otherwise, continue.

Step 8. The origin of frame {n} is chosen at the tip of the finger which is a convenient point on the last link. Align Z_n with the approach vector Y_n with the sliding vector, and X_n with the normal vector of the phalanx (Set $i = 1$).

Step 9. Locate point b_i at the intersection of the X_i and Z_{i-1} axes. If they do not intersect use the intersection of X_i with a common normal between X_i and Z_{i-1}. Once the frames are assigned to each link, the joint link parameters (θ_i, d_i, α_i, a_i) can be easily computed for each link, using which the direct kinematic model is developed for each finger.

Step 10. Compute θ_i as the angle of rotation from X_{i-1} to X_i measured about Z_{i-1}.

Step 11. Compute d_i as the distance from the origin of frame $\{i\text{-}1\}$ to point b_i measured along Z_{i-1}.

Step 12. Compute a_i as the distance from point b_i to the origin of frame $\{i\}$ measured along X_i.

Step 13. Compute α_i as the angle of rotation from Z_{i-1} to Z_i measured about X_i.

Step 14. Set $k = k + 1$. If $k \leq n$, go to step 9; otherwise, stop.

Considering each segment as a link and using the parametric lengths of each finger segments as presented in Table 5.1 and Table 5.2 the open loop chain and D-H table for each finger can be prepared.

5.4.1 D-H Model and Parameters of the Thumb

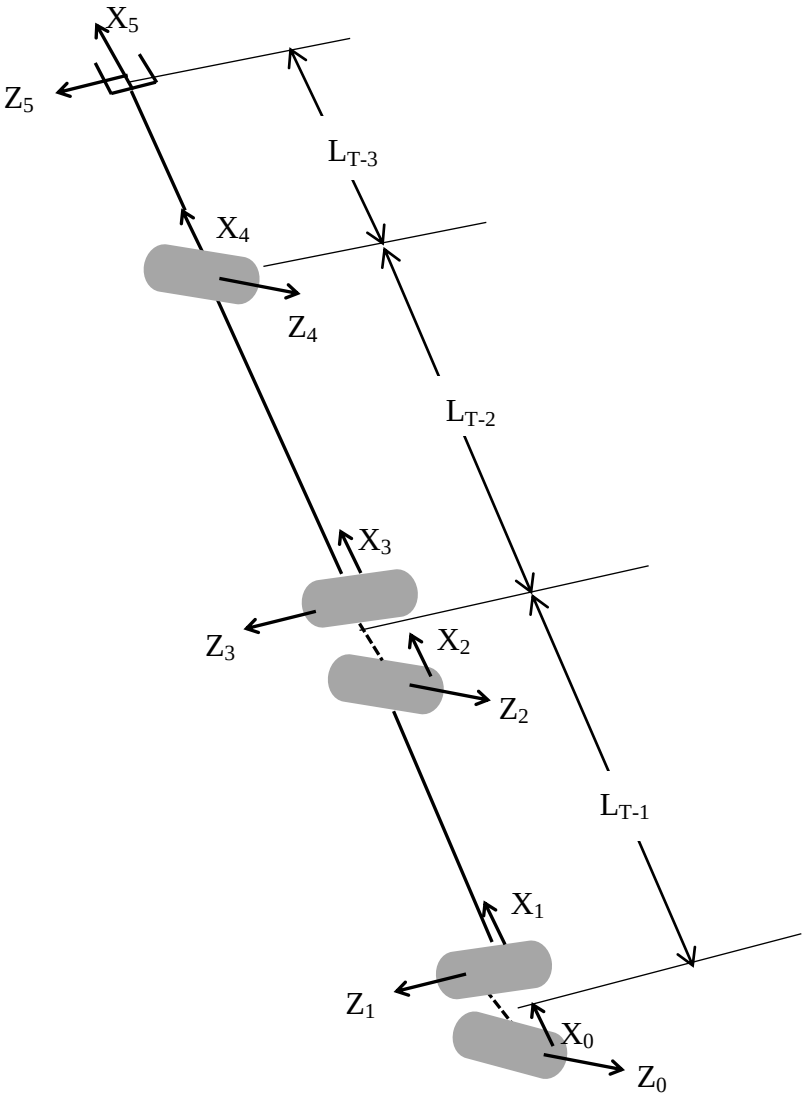

Figure 5.5: D-H model of the thumb.

Table 5.3: D-H parameters of the thumb.

Joint	θ_i	d_i	a_i	α_i
1	q_1	0	0	-90
2	q_2	0	L_{T-1}	90
3	q_3	0	0	-90
4	q_4	0	L_{T-2}	90
5	q_5	0	L_{T-3}	-90

5.4.2 D-H Model and Parameters of the Index Finger

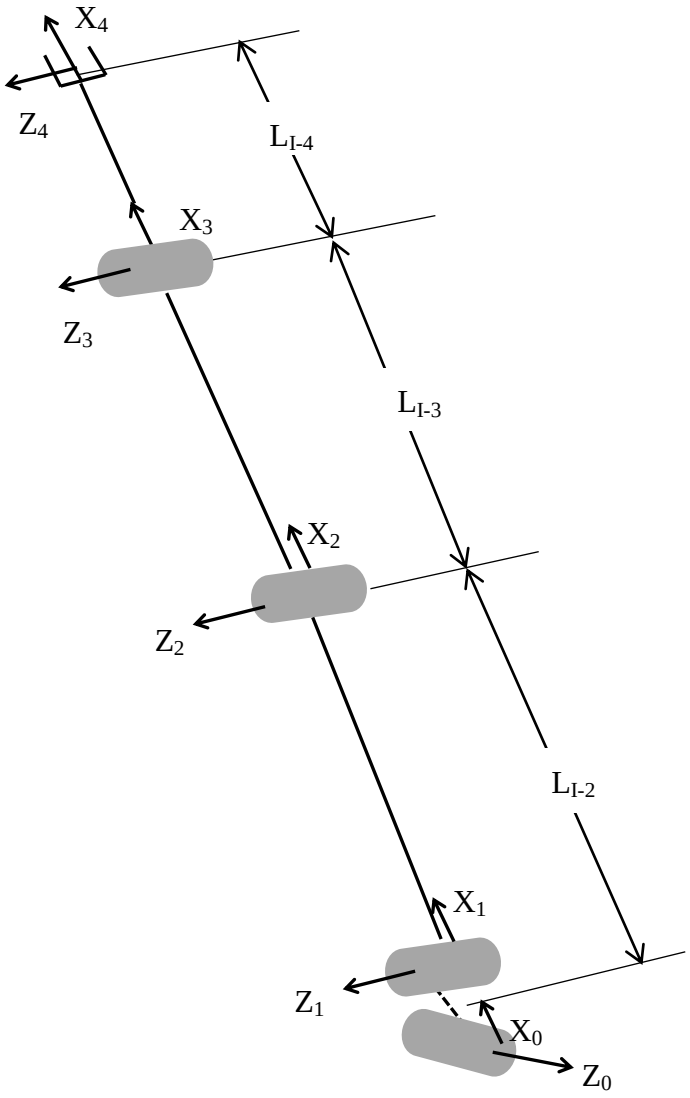

Figure 5.6: D-H model of index finger.

Table 5.4: D-H parameters of index finger

Joint	θ_i	d_i	a_i	α_i
1	q_6	0	0	-90
2	q_7	0	L_{I-2}	0
3	q_8	0	L_{I-3}	0
4	q_9	0	L_{I-4}	0

5.4.3 D-H Model and Parameters of the Middle Finger

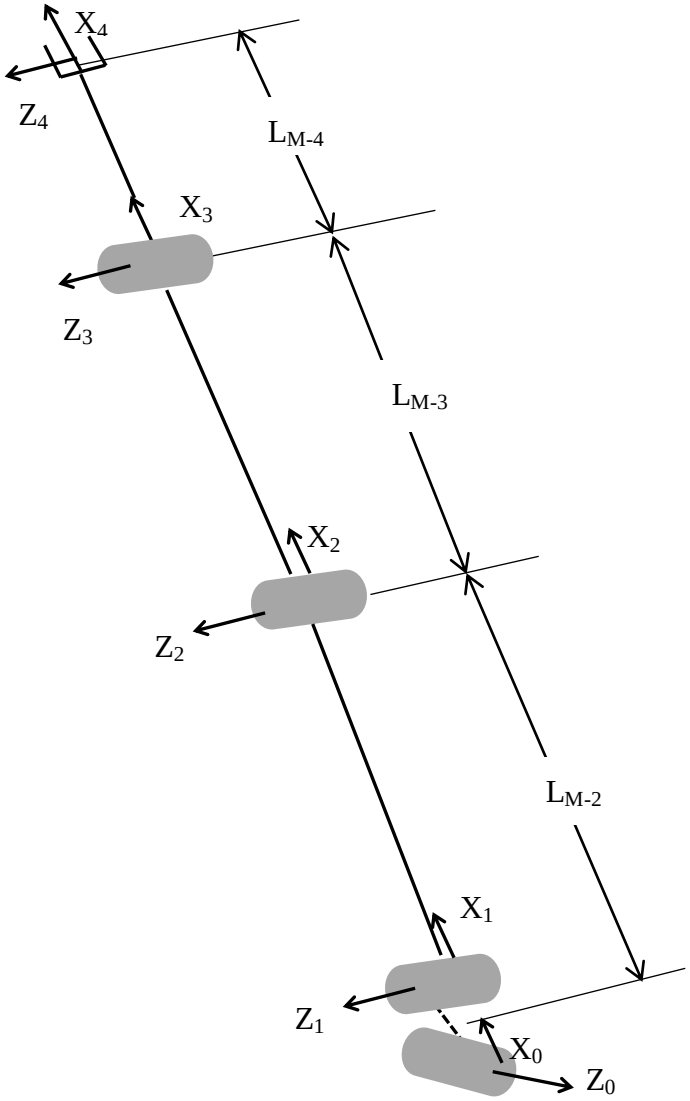

Figure 5.7: D-H model of middle finger.

Table 5.5: D-H parameters of middle finger

Joint	θ_i	d_i	a_i	α_i
1	q_{10}	0	0	-90
2	q_{11}	0	L_{M-2}	0
3	q_{12}	0	L_{M-3}	0
4	q_{13}	0	L_{M-4}	0

5.4.4 D-H Model and Parameters of the Ring Finger

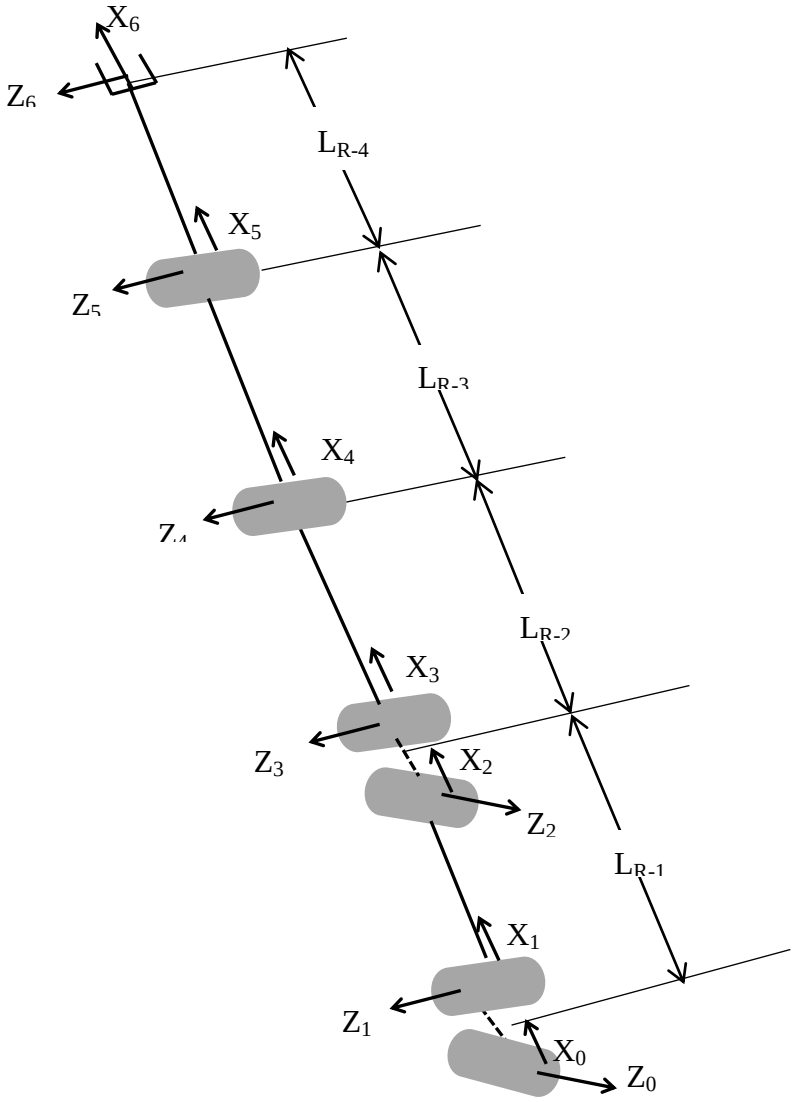

Figure 5.8: D-H model of ring finger.

Table 5.6: D-H parameters of ring finger.

Joint	θ_i	d_i	a_i	α_i
1	q_{14}	0	0	-90
2	q_{15}	0	L_{R-1}	90
3	q_{16}	0	0	-90
4	q_{17}	0	L_{R-2}	0
5	q_{18}	0	L_{R-3}	0
6	q_{19}	0	L_{R-4}	0

5.4.5 D-H Model and Parameters of Little Finger

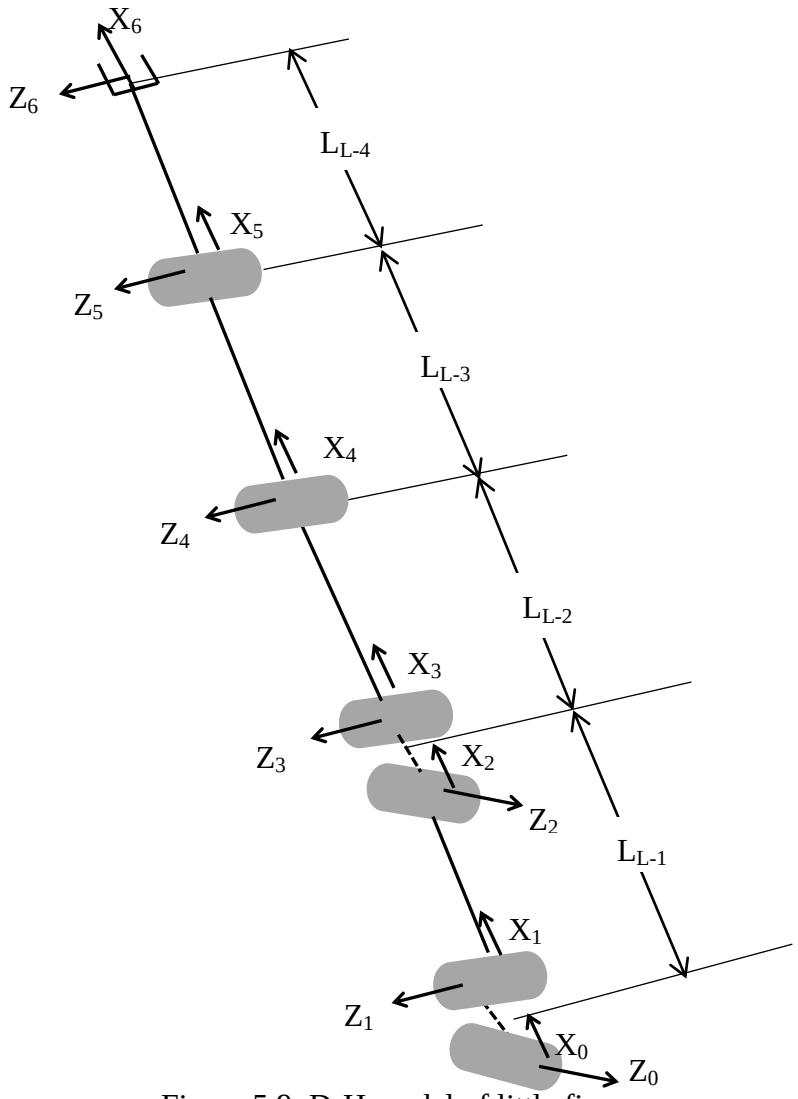

Figure 5.9: D-H model of little finger.

Table 5.7: D-H parameters of little finger.

Joint	θ_i	d_i	a_i	α_i
1	q_{20}	0	0	-90
2	q_{21}	0	L_{L-1}	90
3	q_{22}	0	0	-90
4	q_{23}	0	L_{L-2}	0
5	q_{24}	0	L_{L-3}	0
6	q_{25}	0	L_{L-4}	0

Once the D-H parameters for each finger are known, then the transfer matrix (used for transferring the coordinate system from one joint frame to the adjacent joint frame) ${}^{i-1}T_i$, is given as:

$$ {}^{i-1}T_i = \begin{bmatrix} \cos\theta_i & -\sin\theta_i \cos\alpha_i & \sin\theta_i \sin\alpha_i & a_i \cos\theta_i \\ \sin\theta_i & \cos\theta_i \cos\alpha_i & -\cos\theta_i \sin\alpha_i & a_i \sin\theta_i \\ 0 & \sin\alpha_i & \cos\alpha_i & d_i \\ 0 & 0 & 0 & 1 \end{bmatrix} \quad (5.1) $$

Where, i= Joint Number varying from 1 to 25.

T= Transfer matrix at a particular joint.

θ= Joint angle (q).

α= Link twist angle.

a=Link or finger segment length (L).

d= Joint distance

5.5 Transformation of Local Coordinates to Global Coordinates

The D-H models shown for thumb and all the fingers of the hand in the section 4.4 as open kinematic chains, considering the base or origin at CMC joints of thumb, ring finger and little finger and at MCP joint of Index and middle finger. The origins are located at the respective joints marked as O_1, O_2, O_3, O_4 and O_5 as shown in Figure 5.10; these are considered as local coordinate systems. But, it needs to express the fingertip positions of all the fingers with respect to same coordinate system which is called as global coordinate system. In the present case the wrist of the hand which is a fixed point is considered as the origin of the global coordinate system. So, it is required to transfer the origins from local coordinate system to global coordinate system, which is explained in this section.

In order to change the coordinate system from local to global one the palm of the right hand put in the position of pronation in Figure 5.10 (dorsal view of right hand). The Point O considered as origin of global coordinate system placed at the wrist, (X_0, Y_0, Z_0) are the global coordinate axis drawn at point O as shown in Figure 5.10. The axis Y_0 located in the radius bone and positive towards metacarpal bone. The axis X_0 is drawn positive to the direction of the ulnar bone and

perpendicular to the axis Y_0. The axis Z_0 is drawn with the right-hand rule and perpendicular to hand.

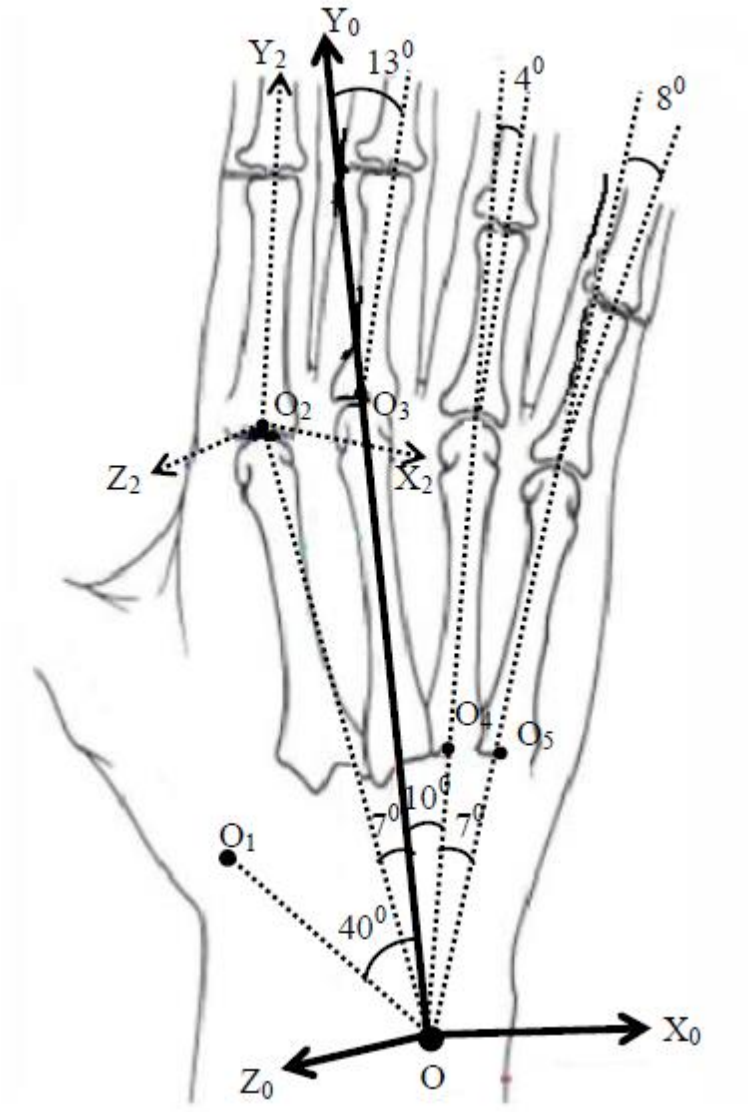

Figure 5.10: Global coordinate system of the hand.

Now for the purpose of transformation, the distance between the origin of local and global coordinate system and the deviation of the local origin with respect to global origin must be measured. The following steps are followed for the purpose:

Step 1. The local origin O_1 (Figure 5.10) of the thumb is in the carpometacarpal joint at a distance between O and O_1 (Loo_1) and angle $\beta_1 = 40^o$, where, β_1 is the angle between O-O_1 and axis Y_0 and which is measured for an adult male hand.

Step 2. Locate in the metacarpophalangeal joint for the index finger the point O_2 as local origin. The distance between O and O_2 (Loo_2) and one angle $\beta_2 = 7^o$, where, β_2 is the angle between O-O_2 and axis Y_0 and which is measured for an adult male hand.

Step 3. The point O_3 which is the local origin of middle finger, located in the top of the metacarpophalangeal joint at a distance between O and O_3 (Loo_3) and one angle $\beta_3 = 13^o$, where, β_3 is the angle between O-O_3 and axis Y_0 and which is measured for an adult male hand.

Step 4. Locate in the carpometacarpal joint for the ring finger the point O_4 at a distance between O and O_4 (Loo_4) and one angle $\beta_4 = 14^o$, where, β_4 is the angle between O-O_4 and axis Y_0 and which is measured for an adult male hand.

Step 5. The local origin O_5, located in the carpometacarpal joint of the little finger at a distance between O and O_5 (Loo_5) and one angle $\beta_5 = 25^o$, where, β_5 is the angle between O-O_5 and axis Y_0 and which is measured for an adult male hand.

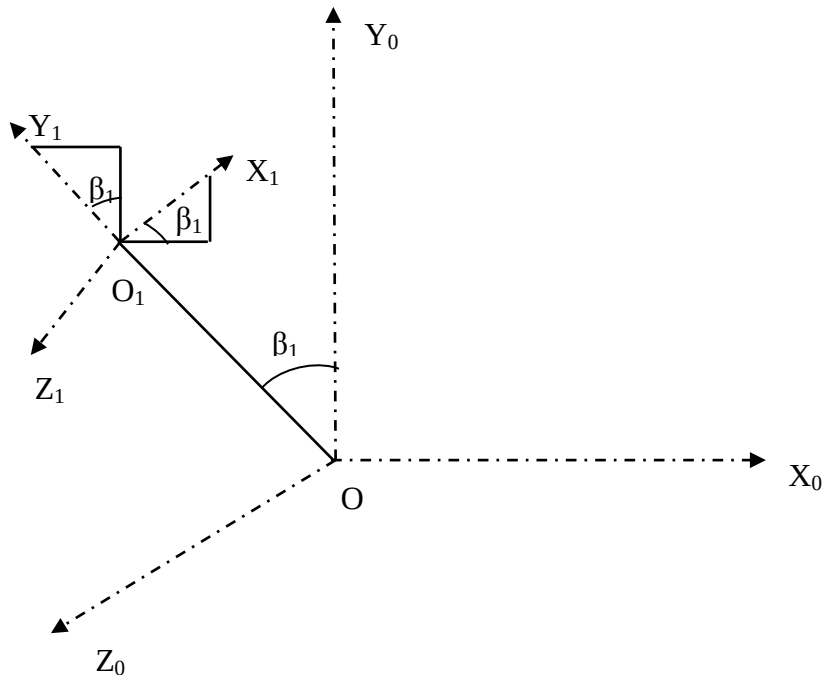

Figure 5.11: Transfer of local coordinates to global coordinates of thumb.

The local coordinate (X_1, Y_1, Z_1) having origin at O_1considered at the CMC joint of the thumb. The distance between the two origins O and O_1, $L_{oo1} = L_{T\text{-}0} = 0.118HL$

from the literature [164, 165], where the subscript T represents thumb. From the Figure 5.11, the rotational matrix due to rotation of the axes by an angle β_1 [195] is given by:

$$ {}^{0}R_1 = \begin{bmatrix} \cos\beta_1 & \cos(90+\beta_1) & \cos 90^0 \\ \cos(90-\beta_1) & \cos\beta_1 & \cos 90^0 \\ \cos 90^0 & \cos 90^0 & \cos 0^0 \end{bmatrix} = \begin{bmatrix} \cos\beta_1 & -\sin\beta_1 & 0 \\ \sin\beta_1 & \cos\beta_1 & 0 \\ 0 & 0 & 1 \end{bmatrix} \quad (5.2) $$

The translation matrix D due to displacement of the origin from O to O_1 by distance $L_{T\text{-}0}$ [173] is given by:

$$ {}^{0}D_1 = \begin{bmatrix} L_{T-0}\cos(90+\beta_1) \\ L_{T-0}\cos\beta_1 \\ L_{T-0}\cos 90^0 \end{bmatrix} = \begin{bmatrix} -L_{T-0}\sin\beta_1 \\ L_{T-0}\cos\beta_1 \\ 0 \end{bmatrix} \quad (5.3) $$

Combining the Eq. 5.2 and Eq. 5.3, the transformation matrix for transformation of global to local coordinate of thumb is given by:

$$ {}^{0}H_1 = \begin{bmatrix} \cos\beta_1 & -\sin\beta_1 & 0 & -L_{T-0}\sin\beta_1 \\ \sin\beta_1 & \cos\beta_1 & 0 & L_{T-0}\cos\beta_1 \\ 0 & 0 & 1 & 0 \\ 0 & 0 & 0 & 1 \end{bmatrix} \quad (5.4) $$

Similarly, the transformation matrix for the other fingers can be derived and given below.

For Index finger:

$$ {}^{0}H_2 = \begin{bmatrix} \cos\beta_2 & -\sin\beta_2 & 0 & -L_{I-0}\sin\beta_2 \\ \sin\beta_2 & \cos\beta_2 & 0 & L_{I-0}\cos\beta_2 \\ 0 & 0 & 1 & 0 \\ 0 & 0 & 0 & 1 \end{bmatrix} \quad (5.5) $$

For Middle finger:

$$ {}^{0}H_{3} = \begin{bmatrix} \cos\beta_3 & -\sin\beta_3 & 0 & -L_{M-0}\sin\beta_3 \\ \sin\beta_3 & \cos\beta_3 & 0 & L_{M-0}\cos\beta_3 \\ 0 & 0 & 1 & 0 \\ 0 & 0 & 0 & 1 \end{bmatrix} \tag{5.6} $$

For Ring finger:

$$ {}^{0}H_{4} = \begin{bmatrix} \cos\beta_4 & -\sin\beta_4 & 0 & -L_{R-0}\sin\beta_4 \\ \sin\beta_4 & \cos\beta_4 & 0 & L_{R-0}\cos\beta_4 \\ 0 & 0 & 1 & 0 \\ 0 & 0 & 0 & 1 \end{bmatrix} \tag{5.7} $$

For Little finger:

$$ {}^{0}H_{5} = \begin{bmatrix} \cos\beta_5 & -\sin\beta_5 & 0 & -L_{L-0}\sin\beta_5 \\ \sin\beta_5 & \cos\beta_5 & 0 & L_{L-0}\cos\beta_5 \\ 0 & 0 & 1 & 0 \\ 0 & 0 & 0 & 1 \end{bmatrix} \tag{5.8} $$

5.6 Kinematics of the Hand Model

Kinematics referred to the analysis of motion without regard to the forces cause it. So the study of kinematics involves all the geometrical and time based properties of motion. For hand kinematics, there are two aspects one is forward kinematics and the other one is inverse kinematics. When all joint angles (q_1 to q_{25}) of the hand are known and the fingertip position is to be calculated with reference to global coordinate system, is called forward kinematics. But, in inverse kinematics the fingertip positions are known and the joint angles (q_1 to q_{25}) need to be found out. In inverse kinematics case the solutions are not direct, it need to solve several non-linear equations.

5.6.1 Forward Kinematics of the Hand Model

The mathematical formulation for forward kinematics problem of n-DOF manipulator is given in literature [196,197], which describes position and orientation of the end effector with reference to the base frame as a function of joint angles. An n-DOF manipulator consists of (*n*+1) links from base to end effector. That we applied to our model considering each finger as independent manipulator. Eq. (5.1 is the transformation matrix between two consecutive joints. Multiplying the individual transformation matrix for each joint, the transformation matrix from local coordinate system to fingertip can be found out, which is given in Eq. 5.9.

$$^{0}T_{n} = {}^{0}T_{1}\,{}^{1}T_{2}\,{}^{2}T_{3}\,{}^{3}T_{4}\,\ldots\ldots\ldots{}^{n-1}T_{n} \tag{5.9}$$

In order to represent the position vector with reference to the global coordinate system (wrist), the transformation matrix for each finger given in Eq. 5.4, Eq.5.5, Eq. 5.6, Eq. 5.7 and Eq. 5.8 need to be multiplied with the transformation matrix given in Eq. 5.9.

$$^{0}T_{n} = [{}^{0}H_{i}][{}^{0}T_{1}\,{}^{1}T_{2}\,{}^{2}T_{3}\,{}^{3}T_{4}\,\ldots\ldots\ldots{}^{n-1}T_{n}] \tag{5.10}$$

Where: *i*=1 for thumb, *i*=2 for Index finger, *i*=3 for middle finger, *i* =4 for ring finger and *i*= 5 for little finger. The Eq. 5.10 is known as the kinematic model of any finger.

With the application of homogeneous transformation matrix, it can write as:

$$^{0}T_{n} = [{}^{0}H_{i}][{}^{0}T_{1}\,{}^{1}T_{2}\,{}^{2}T_{3}\,{}^{3}T_{4}\,\ldots\ldots\ldots{}^{n-1}T_{n}] = \begin{bmatrix} n_x & o_x & p_x & d_x \\ n_y & o_y & p_y & d_y \\ n_z & o_z & p_z & d_z \\ 0 & 0 & 0 & 1 \end{bmatrix} \tag{5.11}$$

Where the vector; $d = [d_x \quad d_y \quad d_z]^T$ is the position vector of the fingertip and the matrix; $\begin{bmatrix} n_x & o_x & p_x \\ n_y & o_y & p_y \\ n_z & o_z & p_z \end{bmatrix}$ is the orientation of the fingertip with respect to the global coordinate system.

With the application of Eq. 5.11 for thumb and each finger, the fingertip position can be found out, with a given set of joint angles and parametric length of finger segments. The results are presented in chapter-8.

5.6.2 Inverse Kinematics of the Hand Model

The inverse kinematics determines the joint variables i.e. joint angles that would result in a desired position of the end-effector of the manipulator with respect to a reference coordinate system. The inverse kinematics solution is difficult since the mapping between the joint space and Cartesian space is non-linear and involves transcendental equations having multiple solutions. A unique solution may be obtained in such cases if a performance criterion, like total joint displacement minimization, is incorporated in the solution scheme. Using the theory of robotics [196,197], the inverse kinematics of the proposed hand model is solved. Inverse kinematics of middle finger, which consists of 4-DOF is considered as example problem. The forward kinematics model for middle finger is given by:

$$T = [{}^{0}H_{3}][{}^{0}T_{1}\,{}^{1}T_{2}\,{}^{2}T_{3}\cdots\cdots{}^{n-1}T_{n}] \tag{5.12}$$

When, *n* (Number of DOFs) = 4, the transformation matrix can express as:

$$T = [{}^{0}H_{3}][{}^{0}T_{1}\,{}^{1}T_{2}\,{}^{2}T_{3}\,{}^{3}T_{4}] = \begin{bmatrix} n_x & o_x & p_x & d_x \\ n_y & o_y & p_y & d_y \\ n_z & o_z & p_z & d_z \\ 0 & 0 & 0 & 1 \end{bmatrix} \tag{5.13}$$

Where, the vector $d = [d_x \quad d_y \quad d_z]^T$ is known as position vector of fingertip.

Using the D-H parameters for middle finger from Table 5.5 in general transformation equation, Eq. 5.1, the transformation matrices derived as:

$${}^{0}T_{1} = \begin{bmatrix} \cos(q_{10}) & -\sin(q_{10})\cos(-90) & \sin(q_{10})\sin(-90) & 0 \\ \sin(q_{10}) & \cos(q_{10})\cos(-90) & -\cos(q_{10})\sin(-90) & 0 \\ 0 & \sin(-90) & \cos(-90) & 0 \\ 0 & 0 & 0 & 1 \end{bmatrix}$$

$$= \begin{bmatrix} \cos(q_{10}) & 0 & -\sin(q_{10}) & 0 \\ \sin(q_{10}) & 0 & \cos(q_{10}) & 0 \\ 0 & -1 & 0 & 0 \\ 0 & 0 & 0 & 1 \end{bmatrix} \tag{5.14}$$

$${}^{1}T_{2} = \begin{bmatrix} \cos(q_{11}) & -\sin(q_{11})\cos(0) & \sin(q_{11})\sin(0) & L_{M-2}\cos(q_{11}) \\ \sin(q_{11}) & \cos(q_{11})\cos(0) & -\cos(q_{11})\sin(0) & L_{M-2}\sin(q_{11}) \\ 0 & \sin(0) & \cos(0) & 0 \\ 0 & 0 & 0 & 1 \end{bmatrix}$$

$$= \begin{bmatrix} \cos(q_{11}) & -\sin(q_{11}) & 0 & L_{M-2}\cos(q_{11}) \\ \sin(q_{11}) & \cos(q_{11}) & 0 & L_{M-2}\sin(q_{11}) \\ 0 & 0 & 1 & 0 \\ 0 & 0 & 0 & 1 \end{bmatrix} \tag{5.15}$$

$${}^{2}T_{3} = \begin{bmatrix} \cos(q_{12}) & -\sin(q_{12})\cos(0) & \sin(q_{12})\sin(0) & L_{M-3}\cos(q_{12}) \\ \sin(q_{12}) & \cos(q_{12})\cos(0) & -\cos(q_{12})\sin(0) & L_{M-3}\sin(q_{12}) \\ 0 & \sin(0) & \cos(0) & 0 \\ 0 & 0 & 0 & 1 \end{bmatrix}$$

$$= \begin{bmatrix} \cos(q_{12}) & -\sin(q_{12}) & 0 & L_{M-3}\cos(q_{12}) \\ \sin(q_{12}) & \cos(q_{12}) & 0 & L_{M-3}\sin(q_{12}) \\ 0 & 0 & 1 & 0 \\ 0 & 0 & 0 & 1 \end{bmatrix} \tag{5.16}$$

$${}^{3}T_{4} = \begin{bmatrix} \cos(q_{13}) & -\sin(q_{13})\cos(0) & \sin(q_{13})\sin(0) & L_{M-4}\cos(q_{13}) \\ \sin(q_{13}) & \cos(q_{13})\cos(0) & -\cos(q_{13})\sin(0) & L_{M-4}\sin(q_{13}) \\ 0 & \sin(0) & \cos(0) & 0 \\ 0 & 0 & 0 & 1 \end{bmatrix}$$

$$= \begin{bmatrix} \cos(q_{13}) & -\sin(q_{13}) & 0 & L_{M-4}\cos(q_{13}) \\ \sin(q_{13}) & \cos(q_{13}) & 0 & L_{M-4}\sin(q_{13}) \\ 0 & 0 & 1 & 0 \\ 0 & 0 & 0 & 1 \end{bmatrix} \tag{5.17}$$

The overall transfer matrix for the middle finger is given by

$$ {}^{0}T_{4} = {}^{0}T_{1}\,{}^{1}T_{2}\,{}^{2}T_{3}\,{}^{3}T_{4} \tag{5.18} $$

$$ {}^{0}T_{1}\,{}^{1}T_{2} = \begin{bmatrix} \cos(q_{10}) & 0 & -\sin(q_{10}) & 0 \\ \sin(q_{10}) & 0 & \cos(q_{10}) & 0 \\ 0 & -1 & 0 & 0 \\ 0 & 0 & 0 & 1 \end{bmatrix} \begin{bmatrix} \cos(q_{11}) & -\sin(q_{11}) & 0 & L_{M-2}\cos(q_{11}) \\ \sin(q_{11}) & \cos(q_{11}) & 0 & L_{M-2}\sin(q_{11}) \\ 0 & 0 & 1 & 0 \\ 0 & 0 & 0 & 1 \end{bmatrix} $$

$$ = \begin{bmatrix} \cos(q_{10})\cos(q_{11}) & -\cos(q_{10})\sin(q_{11}) & -\sin(q_{10}) & L_{M-2}\cos(q_{10})\cos(q_{11}) \\ \sin(q_{10})\cos(q_{11}) & -\sin(q_{10})\sin(q_{11}) & \cos(q_{10}) & L_{M-2}\sin(q_{10})\cos(q_{11}) \\ -\sin(q_{11}) & -\cos(q_{11}) & 0 & -L_{M-2}\sin(q_{11}) \\ 0 & 0 & 0 & 1 \end{bmatrix} \tag{5.19} $$

$$ {}^{0}T_{1}\,{}^{1}T_{2}\,{}^{2}T_{3} = $$

$$ \begin{bmatrix} \cos(q_{10})\cos(q_{11}+q_{12}) & -\cos(q_{10})\sin(q_{11}+q_{12}) & -\sin(q_{10}) & L_{M-3}\cos(q_{10})\cos(q_{11}+q_{12}) + L_{M-2}\cos(q_{10})\cos(q_{11}) \\ \sin(q_{10})\cos(q_{11}+q_{12}) & -\sin(q_{10})\sin(q_{11}+q_{12}) & \cos(q_{10}) & L_{M-3}\sin(q_{10})\cos(q_{11}+q_{12}) + L_{M-2}\sin(q_{10})\cos(q_{11}) \\ -\sin(q_{11}+q_{12}) & -\cos(q_{11}+q_{12}) & 0 & -L_{M-2}\sin(q_{11}) - L_{M-3}\sin(q_{11}+q_{12}) \\ 0 & 0 & 0 & 1 \end{bmatrix} \tag{5.20} $$

$$
{}^{0}T_{4} = {}^{0}T_{1}\,{}^{1}T_{2}\,{}^{2}T_{3}\,{}^{3}T_{4} =
$$

$$
\begin{bmatrix}
\cos(q_{10})*\cos(q_{11}+q_{12}+q_{13}) & -\cos(q_{10})*\sin(q_{11}+q_{12}+q_{13}) & -\sin(q_{10}) & \begin{matrix} L_{M-4}\cos(q_{10})* \\ \cos(q_{11}+q_{12}+q_{13}) \\ +L_{M-3}\cos(q_{10})\cos(q_{11}+q_{12}) \\ +L_{M-2}\cos(q_{10})\cos(q_{11}) \end{matrix} \\
\sin(q_{10})*\cos(q_{11}+q_{12}+q_{13}) & -\sin(q_{10})*\sin(q_{11}+q_{12}+q_{13}) & \cos(q_{10}) & \begin{matrix} L_{M-4}\sin(q_{10})* \\ \cos(q_{11}+q_{12}+q_{13}) \\ +L_{M-3}\sin(q_{10})* \\ \cos(q_{11}+q_{12}) \\ +L_{M-2}\sin(q_{10})\cos(q_{11}) \end{matrix} \\
-\sin(q_{11}+q_{12}+q_{13}) & -\cos(q_{11}+q_{12}+q_{13}) & 0 & \begin{matrix} -L_{M-4}\sin(q_{11}+q_{12}+q_{13}) \\ -L_{M-2}\sin(q_{11}) \\ -L_{M-3}\sin(q_{11}+q_{12}) \end{matrix} \\
0 & 0 & 0 & \begin{matrix} -L_{M-3}\sin(q_{11}+q_{12}) \\ 1 \end{matrix}
\end{bmatrix}
\tag{5.21}
$$

The position vector of the middle fingertip with respect MCP joint (origin of local system 'O_3') is given $[d_x\ d_y\ d_z]^T = {}^{0}T_{4}(3{:},4)$

$$
\Rightarrow \begin{bmatrix} d_x \\ d_y \\ d_z \end{bmatrix} = \begin{bmatrix} L_{M-4}\cos(q_{10})\cos(q_{11}+q_{12}+q_{13}) + L_{M-3}\cos(q_{10})\cos(q_{11}+q_{12}) + L_{M-2}\cos(q_{10})\cos(q_{11}) \\ L_{M-4}\sin(q_{10})\cos(q_{11}+q_{12}+q_{13}) + L_{M-3}\sin(q_{10})\cos(q_{11}+q_{12}) + L_{M-2}\sin(q_{10})\cos(q_{11}) \\ -L_{M-2}\sin(q_{11}) - L_{M-3}\sin(q_{11}+q_{12}) - L_{M-4}\sin(q_{11}+q_{12}+q_{13}) \end{bmatrix}
$$

So,

$$
d_x = L_{M-4}\cos(q_{10})\cos(q_{11}+q_{12}+q_{13}) + L_{M-3}\cos(q_{10})\cos(q_{11}+q_{12}) + L_{M-2}\cos(q_{10})\cos(q_{11}) \tag{5.22}
$$

$$
d_y = L_{M-4}\sin(q_{10})\cos(q_{11}+q_{12}+q_{13}) + L_{M-3}\sin(q_{10})\cos(q_{11}+q_{12}) + L_{M-2}\sin(q_{10})\cos(q_{11}) \tag{5.23}
$$

$$
d_z = -L_{M-2}\sin(q_{11}) - L_{M-3}\sin(q_{11}+q_{12}) - L_{M-4}\sin(q_{11}+q_{12}+q_{13}) \tag{5.24}
$$

By solving Eq. 5.22, Eq. 5.23 and Eq. 5.24 for a given position of the middle fingertip, the values of joint angles q_{10}, q_{11}, q_{12} and q_{13} can be found out. But, it is observed that there are three equations having four unknowns, similarly for other fingers also the number unknowns number of DOFs but number of equation always remains same as three, which results a non-linear set of equations. To solve this

system of non-linear equations some iteration method or optimization method is required.

Using inverse matrix approach [195] the problem can be solved as follows:

From Eq. 5.18, we get that

$$T={}^{0}T_{4}={}^{0}T_{1}\,{}^{1}T_{2}\,{}^{2}T_{3}\,{}^{3}T_{4}=\begin{bmatrix} n_x & o_x & p_x & d_x \\ n_y & o_y & p_y & d_y \\ n_z & o_z & p_z & d_z \\ 0 & 0 & 0 & 1 \end{bmatrix} \tag{5.25}$$

In order to solve for first joint variable θ_{10}, both matrices of Eq. 5.21 and Eq. 5.25 multiplied by ${}^{0}T_{1}^{-1}$ (inverse of ${}^{0}T_{1}$). Then the equation is

$${}^{0}T_{1}^{-1}.T={}^{1}T_{2}\,{}^{2}T_{3}\,{}^{3}T_{4} \tag{5.26}$$

With multiplying the respective matrices, it can be seen that the element (3, 4) of left hand matrix is $-d_x\cos(q_{10})-d_y\sin(q_{10})$ and the element (3, 4) of right hand matrix is 0. Assuming both elements are equal, we get that

$$\begin{aligned} &-d_x\cos(q_{10})-d_y\sin(q_{10})=0 \\ &\Rightarrow \tan(q_{10})=-\frac{d_y}{d_x} \end{aligned} \tag{5.27}$$

The solution of Eq. 5.27 for given values of fingertip position will give two values of 'θ_{10}' which is in the range of the angle 'θ_{10}' that value can consider as solution. Note that this equation is only for this 4-DOFs system. For solution of other three unknowns the same inverse matrix approach can apply. Now multiplying ${}^{1}T_{2}^{-1}$ (inverse of ${}^{1}T_{2}$) to both sides of the Eq. 5.26, we get

$${}^{1}T_{2}^{-1}\,{}^{0}T_{1}^{-1}.T={}^{2}T_{3}\,{}^{3}T_{4} \tag{5.28}$$

Now, comparing matrices of both the sides and equating element (1,4) and (2,4) of both side matrix, two equations with three unknowns will get,

$$\begin{aligned} &d_y\cos(q_{10})\cos(q_{11})-d_x\cos(q_{11})\sin(q_{10})-d_z\sin(q_{11})-L_{M-2} \\ &=L_{M-3}\cos(q_{12})+L_{M-4}\cos(q_{12}+q_{13}) \end{aligned} \tag{5.29}$$

$$\begin{aligned} &-d_y\cos(q_{10})\sin(q_{11})+d_x\sin(q_{11})\sin(q_{10})-d_z\cos(q_{11})-L_{M-2} \\ &=L_{M-3}\sin(q_{12})+L_{M-3}\sin(q_{12}+q_{13}) \end{aligned} \tag{5.30}$$

Similarly, multiplying ${}^{2}T_{3}^{-1}$ (inverse of ${}^{2}T_{3}$) to both sides of the Eq. 5.28, we get

$${}^{2}T_{3}^{-1}\,{}^{1}T_{2}^{-1}\,{}^{0}T_{1}^{-1}.T={}^{3}T_{4} \tag{5.31}$$

Again comparing both sides of the matrices and equating element (1, 4) of both sides, we get that,

$$\begin{aligned}&-L_{M-2}\cos(q_{12})-L_{M-3}-d_z\sin(q_{11}+q_{12})+d_y\cos(q_{10})\cos(q_{11}+q_{12})-\\&d_x\sin(q_{10})\cos(q_{11}+q_{12})=L_{M-4}\cos(q_{13})\end{aligned} \tag{5.32}$$

5.6.3 Solution to the Inverse Kinematic Problem

The three equations viz. Eq. 5.29, Eq. 5.30 and Eq. 5.32 need to be solved for the solution of inverse kinematics problem of the mechanism. However, these three equations are non-linear in nature shall give rise to multiple solutions. In order to obtain an appropriate and optimal solution an iterative technique with capability to handle undesirable solutions need to be applied. It is essential that fingers may be trained in a correct manner and then be allowed to move using the inverse kinematics logic for its proper functioning. As an obvious option neural network techniques may be gainfully utilized for getting such results. From the study of previous literature it is imperative that the neural network alone does not give the correct results due to restrictions of the results such as; only selected inverse kinematics solutions are acceptable and 100% training of the data is not possible. There have to be quite a large number of interpolation and extrapolation. Hence hybridizing this with fuzzy- inference should yield better result under the set conditions. Therefore the adaptive network-based fuzzy inference system developed by Jang [188] that can handle non-linear functions in even online mode is selected and the same has been employed here to do away with complicated mathematical equations and to obtain acceptable values for the desired tasks. The structure and the processes of use of Adoptive Neuro-Fuzzy Inference System (ANFIS) are described briefly in the following sub-sections. The results of the inverse kinematics problem of the proposed hand model solved by ANFIS are presented in chapter 7.

5.6.4 The ANFIS Structure

ANFIS uses a hybrid Neuro-fuzzy technique that brings learning capabilities of neural networks to fuzzy inference system using the training input output data. The

learning algorithm tunes the membership functions of a Sugeno-type Fuzzy Inference System using the training input-output data. In the present case, the input-output data refers to the coordinate- angle data base. The coordinates act as input to the ANFIS and the angles act as the output. The learning algorithm teaches the ANFIS to map the coordinates to the angles through a process called training. At the end of training, the trained ANFIS network would have learned the input-output map and get ready to be deployed into the larger control system solutions. The architecture of ANFIS structure selected for the problem is shown in Figure 5.12, in which a circle indicates a fixed node, whereas a square indicates an adaptive node. The end-effecter position (*X*, *Y*, *Z*) are the inputs and the outputs are the joint variables angles. Among FIS models, the Sugeno fuzzy model is applied because it's high interpretability and computational efficiency. The learning algorithm tunes the membership functions using the training input-output data. The fuzzy if then rules are expressed as:

If *x* is *A* and *y* is *B* and *z* is *C* then $K = px + qy + sz + r$

Where *A*, *B* and *C* are the fuzzy sets in the antecedent, and *p*, *q*, *s* and *r* are the design parameters that are determined during the training process.

The ANFIS architecture comprises of five layers. The role of each layer is briefly presented as follows:

Let o_i^l denote the output of node *i* in layer *l*, and x_i is the i^{th} input of the ANFIS,

$i = 1; 2; \ldots\ldots; p$ [198].

Layer1:

Every node '*i*' is employing a node function *R* given by:

$$O_i^1 = R_i(x_i) \tag{5.33}$$

Where R_i can adopt any fuzzy membership function (MF).

Layer 2:

Every node calculates the firing strength of a rule via multiplication:

$$O_i^2 = w_i = \min(R_i) \tag{5.34}$$

Where w_i represent the activation level of a rule.

Layer 3:

Fixed node i in this layer calculate the ratio of the i^{th} rules activation level to the total of all activation level:

$$O_i^3 = \bar{w}_l = \frac{w_i}{\sum_i w_i} \tag{5.35}$$

Where $\bar{w}_l$ is referred to as the normalized firing strengths.

Layer 4:

Every node i has the following function:

$$O_i^4 = \bar{w}_l k_i = \bar{w}_i(p_i x + q_i y + s_i z + r_i) \tag{5.36}$$

Where $\bar{w}_l$ is the output of layer 3, and (p_i, q_i, s_i, r_i) are the parameter set. The parameters in this layer are referred to as the consequence parameters.

Layer 5:

The single node in this layer computes the overall output as the summation of all incoming signals, which is expressed as:

$$O_i^5 = \bar{w}_l k_i = \frac{\sum_i \bar{w}_l k_i}{\sum_i w_i} \tag{5.37}$$

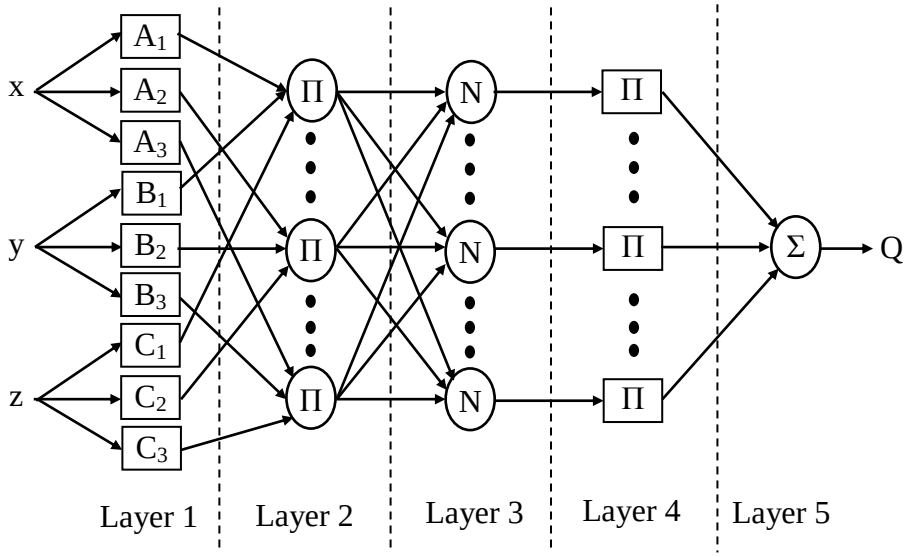

Figure 5.12: Neuro-Fuzzy (ANFIS) Architecture.

ANFIS distinguishes itself from normal fuzzy logic systems by the adaptive parameters, i.e., in the way that both the premise and consequent parameters are adjustable. The most remarkable feature of the ANFIS is its hybrid learning algorithm. The process is carried out using the ANFIS toolbox of MATLAB and is presented by a flowchart in Figure 5.13.

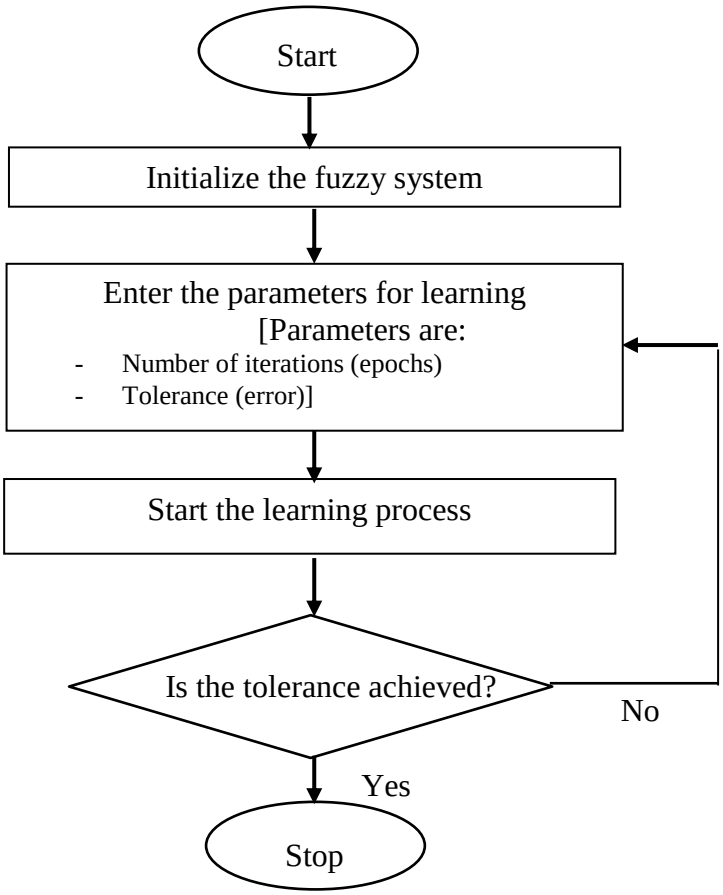

Figure 5.13: Flow chart for computations in ANFIS.

The adaptation process of the parameters of the ANFIS is divided into two steps. For the first step of the consequent parameters training, the Least Squares method (LS) is used, because the output of the ANFIS is a linear combination of the consequent parameters. The premise parameters are fixed at this step. After the consequent parameters have been adjusted, the approximation error is back-propagated through every layer to update the premise parameters as the second step. This part of the adaptation procedure is based on the gradient descent principle, which is the same as in the training of the back propagation (BP) neural network. The consequence parameters identified by the LS method are optimal in the sense of least squares under the condition that the premise parameters are fixed. Therefore, this hybrid learning algorithm is more effective than the pure gradient decent approach, because it reduces the search space dimensions of the original back propagation method. The pure BP learning process could easily be trapped into local minima. When compared with employing either one of the above two methods individually, the ANFIS converges with a smaller number of iteration steps with this hybrid learning algorithm.

5.6.5 Formulation of ANFIS Structure for Inverse Kinematics

The ANFIS structure as described in previous section was use to simulate and to obtain solutions to the inverse kinematics of the 25-DOFs anthropomorphic hand structure. The ANFIS structures were used in MATLAB-8 platform. In order to cover all the joints 25 different ANFIS structures were designed for the simulating the structure with the specified ranges of values of the joint angles and for obtaining the inverse kinematic solution accordingly. Each structure was designed with seven Gaussian membership function in each input and 43 rules in second layer. The ANFIS editor display is shown in Figure 5.14, which consists of 4 main sub displays as: Load data, Generate FIS, Train FIS and test FIS. The displays can be described as follows:

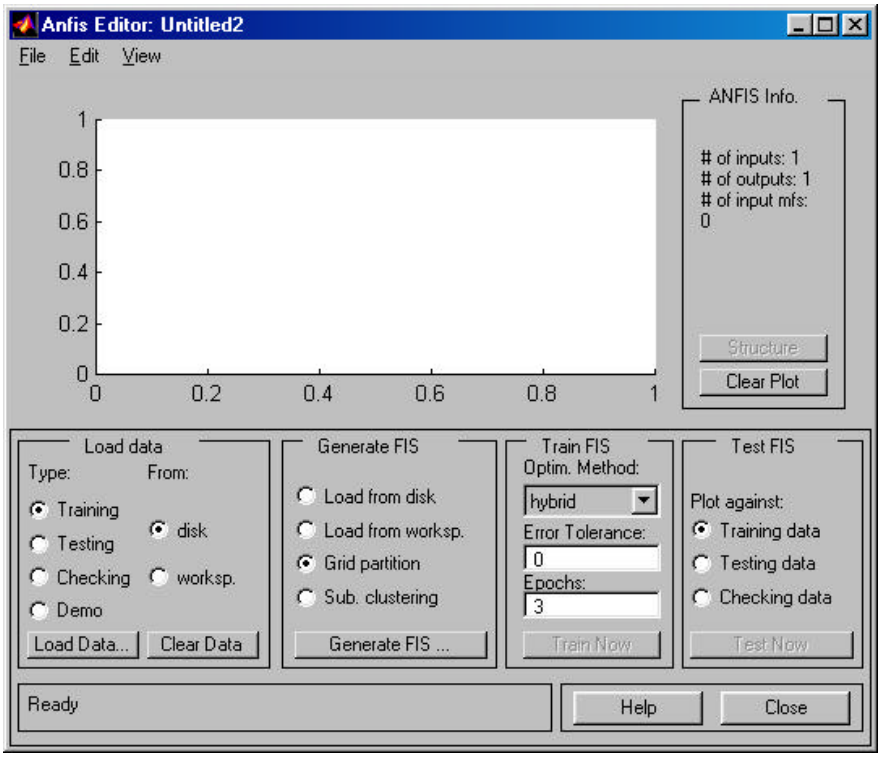

Figure 5.14: ANFIS editor display in MATLAB.

Load data: Here the different type data such as training data, testing data and checking data are loaded into the system for the purpose of training, testing and checking the proposed structure. In the present case the data sets are generated using the forward kinematic and loaded input as coordinate of fingertip position and output as joint angle.

Generate FIS: Once data have been loaded, an initial fuzzy interface system (FIS) can be generated using generate FIS. In this stage the number and type of membership function (MF) will vary to get the better FIS structure. In the present case seven number of MF, Gaussian type input MF and linear output MFs are chosen.

Train FIS: The main computing occurs in the Training block. Here the hybrid algorithm is used. The tolerance (Error) is at 0 by default. In practice, a complete fit is not achieved, hence it changed to 0.01. In the present case the epoch value is chosen to be 100. Now the system is ready for training. By clicking "Train now" option the FIS structure is trained as per the given training data set.

Test FIS: Here the performance of FIS can be tested against the testing data set. It will give the testing error. In this case 300 to 700 data are taken for training the FIS for thumb and fingers depending on the number of joints and 1000 to 1800 data are taken for testing.

After completion of the above four steps with very minimum acceptable testing error the FIS structure is ready for use. This procedure is repeated for all 25 joint angles and 25 FIS structures are finalized, which are used for predicting the value of all 25 joint angles for a given position coordinate. Finally, the checking data set is used for predicting the value of all joint angles for given position as inverse kinematic problem. Using the FIS structures for all 25 angles of the hand, through MATLAB, for any position of the fingertip the angles of the joints are determined.

5.7 Workspace Analysis

In general, the workspace represents the portion of space around the base of the manipulator that can be accessed by the end point of the arm [195]. Each of the fingers of the hand is assumed as individual manipulator, so the workspace of each finger is the space around the wrist of the hand at which the fingertip can reach. The shape and size of the workspace depends on the finger configuration, structure, degrees of freedom, size of finger segments (links) and the range of the joint angles. The workspace gets specified by the existence and non-existence of solution to the inverse problem. The region that can be reached by the fingertip at least in one configuration is called reachable workspace. The space where the fingertip can reach every point for all configurations is called dexterous workspace. The dexterous workspace is smaller than and is a subset of reachable workspace. The reachable workspace is the geometrical locus of the points that can be achieved

by the fingertip as determined by the position vector of direct kinematic model. The factors that decide the dexterous workspace of a hand apart from degrees of freedom are configuration of fingers, their arrangement over the palm, and the type of joints.

The workspace of hand therefore, is the conjugate of those of the fingers. This can be determined by the space covered by the loci of fingertips of all the fingers with respect to a common coordinate system. By multiplying the corresponding transfer matrices written for every finger as in Eq. 5.10, the kinematical equations describing the fingertip motion with respect to the global coordinate system (located at the wrist) can be determined. It is now possible to develop a model using Eq.5.1 and Eq.5.10. A computer program using these equations in MATLAB is developed to capture the motion of the fingertips. The range of joint angles for every finger (Table 4.4 to Table 4.8), is divided to a finite number of intervals in order to have enough fingertip positions to give confident images about the spatial trajectories of these points. By connecting these positions and by the complex surface bordering the active hand model workspace is obtained. The complex surface could be used to verify the model correctness from the motion point of view, and to plan the hand motion by avoiding the collisions between its active workspace and obstacles in the neighborhood. The results obtained out of this exercise are presented in Chapter-8.

5.8 Summary

The kinematic model of the robot hand having five human like fingers and 25-DOFs is presented in this chapter. The DH model and DH table for thumb and each finger of the hand are developed considering each finger as an individual manipulator and with respect to local coordinate system having the origin at CMC joint of thumb, ring and little fingers and MCP joints of index and middle fingers respectively. Detail procedure for the solution of this problem is presented and explained. The parametric model for thumb and each finger are also presented. The forward and inverse kinematic models are developed for the proposed anthropomorphic hand model. The 25- DOFs anthropomorphic hand model is modelled in such manner that, it resemblance a realistic hand model. The workspace of the hand has been determined considering the combined trajectory of the fingers and the thumb.

Chapter 6

MULTI FINGERED GRASPING AND OBJECT MANIPULATION

6.1 Overview

Robot end effectors have developed from simple parallel gripper to multi-fingered hands to provide greater flexibility and dexterity in manipulation and assembly operations. Robot hands come in many shapes, but they all have a common objective of grasping and manipulating an object. In order to achieve proper grasping and do subsequent manipulation, it should be ensured that the object is grasped correctly and securely with sufficient amount of force being applied at predesigned points/surfaces. The character of grasp changes with change in shape of the object and the requirement of manipulation thereafter. In other words, when there is an increase in the number of faces or a larger gradient on a single face (i.e. change in shape), there has to be multiple contacts for a secured grasping. In the similar manner, if the manipulation requirement is such that the grasped object needs several types of motion in the workspace or very fine manipulation, there has to be sufficient scope for achieving the same; meaning there should be more degrees of freedom (DOFs) available in the hand to permit such actions. The determination of such grasps with multiple fingers needs correct analytical models that may use good amount of input data depending upon the type of grasping, type of objects to be grasped, the requirement of manipulation, the materials in contact etc. As a whole, determination of correct grasping or the determination of the capability of a grasping mechanism (here the multi-fingered hand) is a complex study. So, before analysing the grasping of an object, a thorough and clear idea about the theory and the condition of grasping is required. The present chapter begins with basic concepts of the grasping, definitions, contact models etc. along

with various mathematical background related to contact models, wrench, wrench space, friction cone etc. so as to help in the determination of correct grasp of a given object for a given task. A description of the different types of grasps such as form and force closure is also presented and discussed along with the conditions required to achieve the same.

6.2 Basic Concepts of Grasping Process

The system in which the desired object is gripped by the fingers of a hand is called grasp. For the purpose of grasping an object the hand as well as individual fingers of the hand must be moved. Such motion of the hand can be classified as free motion and resisted motion [189,190,191].

6.2.1 Free Motion

When the hand and fingers move freely in space without any objective is called free motion. The different free motions of hand are:

- Opening: Fully extended the fingers and the thumb until the hand is fully open as in case of anatomical position of hand.
- Closing: Fully arching until the hand is closed in a bunch with the thumb overlapping the other fingers.
- Clawing: The motion that reaches the terminal position of metacarpophalangeal (MCP) extension and interphalanreal (IP) flexion.
- Reciprocal: The motion that reaches the terminal position of MP flexion and IP extension.

6.2.2 Resisted Motion

When motion is performed by the hand and fingers against an external resistance i.e. exerting force on an external object for the purpose of grasping and manipulating the object, then the motion is called resisted motion. The different resisted motions of the hand are:

- Power grip: Gripping an object against the palm
- Precision grip: Gripping and manipulating the object by the thumb and fingers without touching palm.
- Pinch: Gripping and compressing the object between thumb and fingers.

Based on these resisted motions, the grasping process can be categorized as: (i) power grasp, (ii) precision grasp and (iii) partial grasp.

a) Power Grasp

In case of power grasp the hand performs power grip motion. The fingers and the palm enclose the object with multiple numbers of contacts with each finger and palm. The object is firmly held in between fingers and palm. Figure 6.1 shows the examples of power grasp of different type. The hand grasps the object so securely that there is no relative motion between the hand and the object. In other words, the force applied by the hand on the object is so high that it resists all possible external force that may act on the object.

b) Precision Grasp

In precision grasp the object is grasped by the finger tips only. There is neither more number of contact points at the fingers nor there is palm contact with the object. Figure 6.2 shows some examples of precision grasp of different type objects. In this type of grasp fine motion can be admitted on the object simply by moving the fingers on it. Although precision grasp has a high degree of manipulability, it does not have a large capability to resist loads. So the firm grasp is not achieved in this type of grasp. There are many more situations, where more force is required to do the desired task but due to some physical constraints between the hand and the object the required amount of force cannot be applied. One of the examples of this kind is removal of work piece from a die. In this case the fingers cannot encircle the work piece since it is mounted on a die; a precision grasp is used to extract it out.

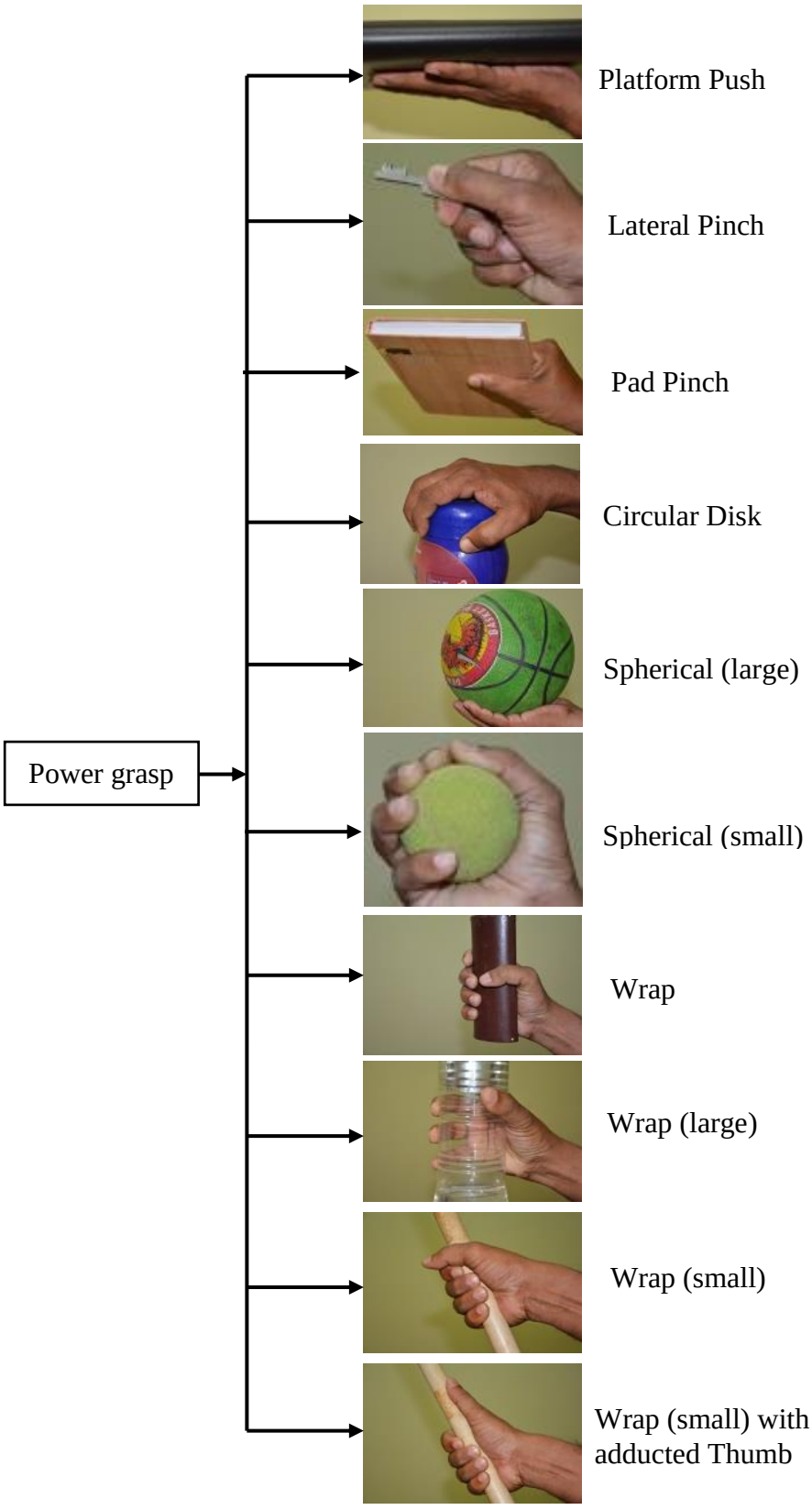

Figure 6.1: Examples of power grasp.

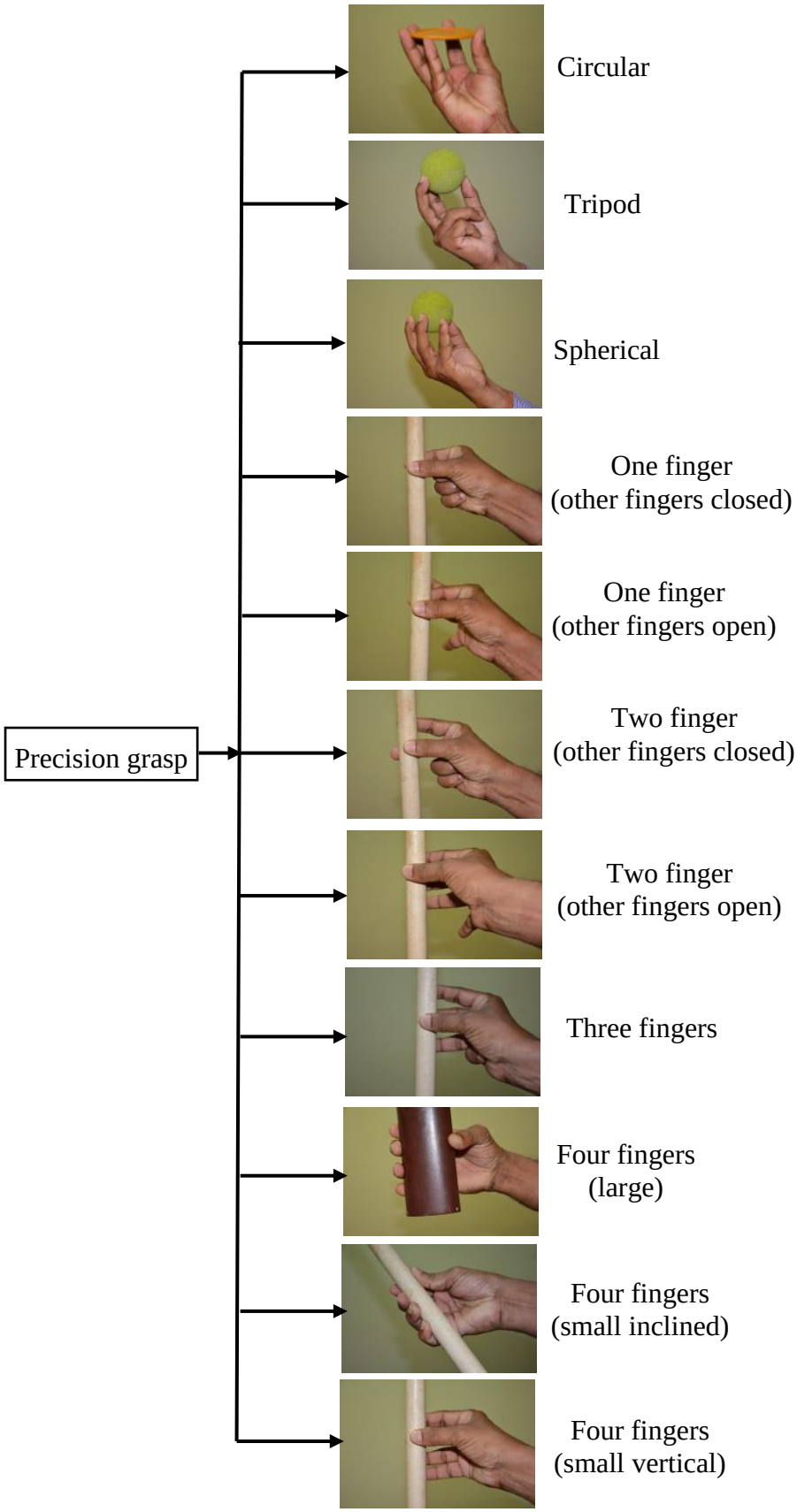

Figure 6.2: Examples of precision grasp.

c) Partial Grasp

This type of grasp does not totally constrain the movement of the grasped object. The objects whose motions are limited, on that type of object the task of partial grasp can be performed. One example of a partial grasp is the hooked fingers, used to open the door with curved handles. In this grasp the hand performs the pinch motion only and one or two fingers are used for grasping the object and performing the task. Some of the examples are shown in Figure 6.3.

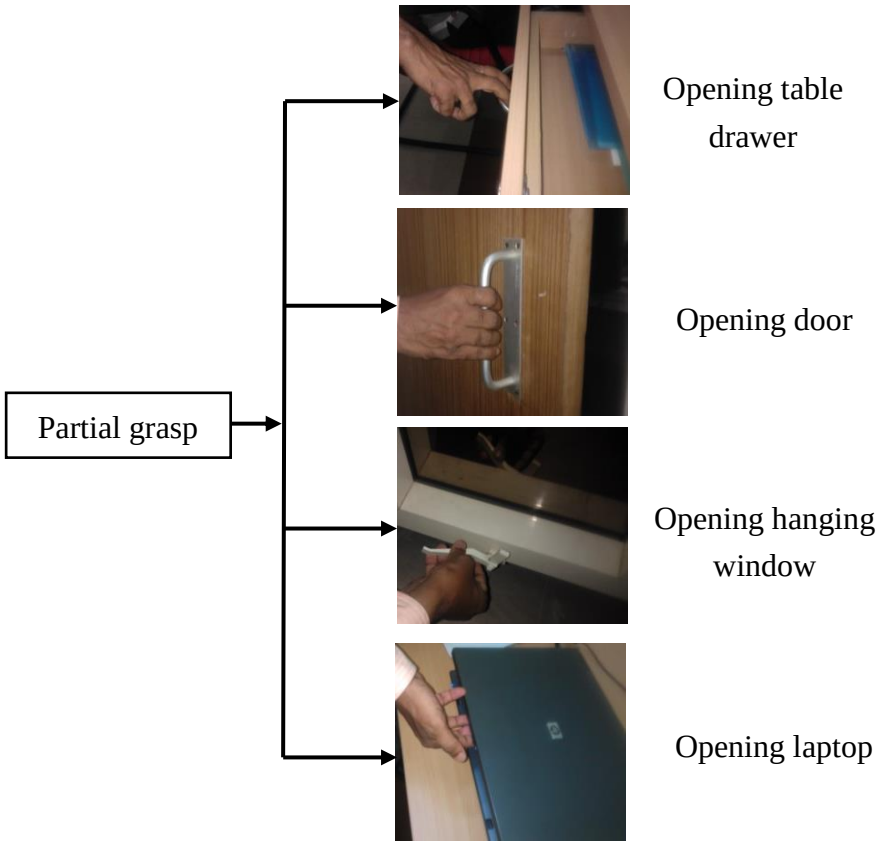

Figure 6.3: Examples of partial grasp.

6.3 Grasp Properties

The grasp properties decide about the type of grasp. i.e., good grasp or bad grasp. The decision is taken upon before the grasp is synthesized. A number of researchers proposed different properties which may be categorized into five basic types as given in Table 6.1[47].

Table 6.1: Categorization of different properties in to five basic properties.

Sl. No.	Five basic properties	Grasp properties studied by researchers
1	Force/Form closure	Connectivity
2		Force closure
3		Form closure
4	Dexterity	Dexterity
5		Force applicability
6		Isotropy
7		Manipulability
8	Equilibrium	Equilibrium
9		Internal forces
10		Slip Resistances
11	Stability	Stability
12		Disturbance resistance
13		Robustness
14	Compliance	Compliance
15		Dynamic behavior

- Force/Form closure – If a grasp can resist any applied force through its contact points only, such a grasp is a force-closure grasp. But, when the object is firmly grasped by many number of contact points in such a way that the motion of the object is totally constrained that type grasp is called form closure grasp.
- Equilibrium - A grasp is in equilibrium if and only if the sum of forces and moments acting on the grasped object is zero.
- Stability - A grasp is said to be stable if and only if grasped object is always pulled back to its equilibrium configuration, whenever it is displace from that configuration.
- Dexterity - It is the ability of grasp to impart motion to the grasped object.

- Compliance- A grasp is compliant if the grasped object behaves as a generalized spring, damper, or impedance, in complying with external constraints such as hard surface, velocity or force. E.g., generalized springs and dampers.

6.3.1 Force-closure / Form-closure

These properties concern the capability of the grasp to completely or partially constrain the motion of the grasped object and to apply arbitrary contact forces on the object itself, without violating friction constraints at the contact points. The basic difference between these two is that in Force closure grasp there is movement of fingers over the object for fulfilling the condition of resisting external force so that the object should remain at the desired position. In case of form closure there is no relative movement between the fingers and the object, the object is totally constrained by the set of contacts, irrespective of the magnitude of the contact forces.

a) **Force-closure**: Force-closure implies that motion of the grasped object are completely or partially restrained despite of whatever external disturbance, by virtue of suitable large contact forces that the constraining device is actually able to exert on the object. The study of force-closure is of obvious importance in the choice of grasping mechanism, with particular regard to positioning the fingers of a robot hand on the grasped object so as to guarantee robustness against slippage. Figure 6.4 (a) shows the force-closure grasp of an object by three point contacts, the friction cone is shown at the contact points.

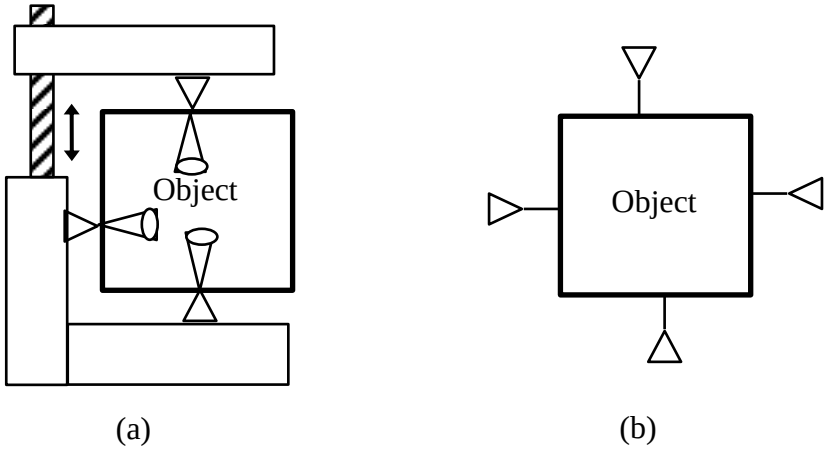

Figure 6.4: Example of grasp (a) force-closure (b) form-closure.

b) **Form-closure**: Form-closure is related to the ability of constraining devices to prevent motions of grasped object. Relying only on unilateral, frictionless contact constraints. In a form closure grasp the constraints on the object comes only from geometry of the contacts. An example of a form-closure-grasp of a square object by means of four contacts is shown in Figure 6.4 (b). The contacts are represented by fixed pins at the contact points of the object indicating that only motions of the object that cause penetration of the pin in the object are prevented by that constraint.

6.3.2 Equilibrium

A grasp is said to be in equilibrium when the resultant of forces and torques applied on the object both by the fingers and by external disturbances is zero. An associated problem is the optimization of the finger forces making them as low as possible in order to avoid damages on the object and unnecessary wastage of energy, provided that the object is properly restrained. The force components at each contact force are represented by individual wrenches (which are a combination of both force and moment), on the object and the equilibrium equations are represented as the linear sum of the individual wrenches and improved by adding internal grasping forces between pairs of fingers.

6.3.3 Stability

It is one of the equilibrium states of the object. Due to application of the external forces or torques on an object, some disturbance produced in the position of the object, if the object returns back to its original position after removal of external force or toque the object said to be in stable equilibrium. Thus grasp should produce compensative force when the object is moved from the desired position. A simple and fast algorithm for constructing a stable force-closure grasp based on the shape of the grasped-object was proposed by Nuygen [139]. He used virtual springs at the contacts, such that the grasped object is stable, and has a desired stiffness matrix about its stable equilibrium. A simple geometric relation between the stiffness of the grasp and the spatial configuration of the virtual springs at the contacts is developed in his work.

6.3.4 Dexterity

Grasp dexterity is defined as the ability of a grasp to achieve one or more useful secondary objective while satisfying the kinematic relationship (between joint and Cartesian space) as the primary objective [63]. So, the grasp is a kinematically

redundant system which includes not just manipulability but ability to achieve a certain condition. In general, without task specifications, a grasp is considered dexterous if the manipulator device is able to move the object in any direction i.e. if the manipulator can arbitrarily change the position and orientation of the object.

6.3.5 Compliance

Compliance is the displacement of a manipulator in response to a force or torque. A high compliance means the manipulator moves a good bit when it is stressed. This type of compliance is called spongy or springy compliance. Low compliance is the stiff system when stressed an algorithm for constructing 2^{nd} order stable grasps by Nugen [140]. The grasp compliance is modelled by virtual springs at the contacts points. The grasp is stable if the resulting grasp stiffness matrix is positive definite. Algorithms for achieving a desired grasp stiffness matrix are presented in the study. The number and type of contacts are also being considered. He also proved that all 3D force closure grasps can be made stable, assuming that the hand system must include a form of compliance control system in it. This is important for grasp synthesis because the synthesis algorithm does not need to include stability analysis if the selected grasp configuration satisfies force closure.

All the properties discussed above like Force closure, equilibrium, stability, dexterity, compliance are the required component for attaining a good grasp. The first three components are required for the successful grasp. And the remaining two properties are used to measure the grasp capability to do some specific task.

6.4 Grasping with Multi-fingered Hands

As mentioned earlier, the designed multi-fingered hand is anthropomorphic in nature and is designed to grasp and manipulate various types of objects in human like manner. Hence the hand must be capable of carrying out both form-closure as well as force-closure grasping. Typically robot hands with two fingers or three fingers are designed for form-closure grasping while that with more fingers are designed mostly for force-closure grasping. Although, both of these aspects have been considered in the present work, more attention has been given to the capability of the hand under force-closure conditions. The following sections, therefore, present the modelling and analysis of the force-closure grasping by the multi-fingered hand.

6.5 Grasping Preliminaries

Grasp is a set of contacts which enables to hold some object.

Contact is the position of a finger placed on the object. Hence, information regarding the contact type, number of contact, size and shape of contact, the object surface properties and the finger surface properties are required to determine the grasp quality.

Grasp force is the force applied by each finger on the object at the contact point. If the contact is frictionless contact between object and fingertip, the grasp force is normal to the object surface at contact point. But, in case of contact with friction the grasp force must satisfy the Coulomb's law of friction [199], to ensure there is no slipping at the contact point. If *fi* is the grasp force at contact points i then;

$$\sqrt{f_{ix}^2 + f_{iy}^2} \leq \mu f_{iz} \tag{6.1}$$

Here, f_{ix}, f_{iy}, f_{iz} are the components of the grasp force in *X*, *Y* and *Z* axis in object coordinate frame respectively and μ is the coefficient of friction between fingertip and object surface.

Friction cone is the geometrical representation of the friction force at the contact point. For simplicity the friction cone is linearized by a polyhedral convex cone having 'm' number of sides as shown in Figure 6.5.

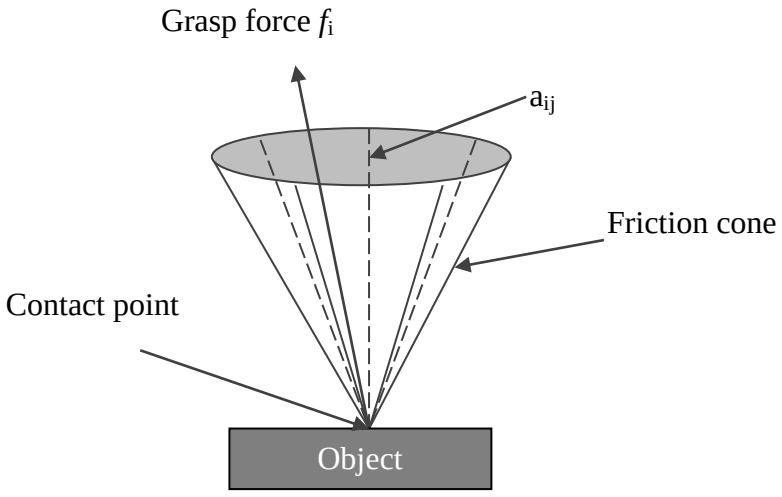

Figure 6.5: Grasp force in form of friction cone.

Now, considering approximately the friction cone as friction pyramid the grasp force can be represented as:

$$f_i = \sum_{i=1}^{n} \alpha_{ij} a_{ij}, a_{ij} \geq 0 \tag{6.2}$$

Where a_{ij} represents the j^{th} edge vector of the polyhedral convex cone and coefficients α_{ij} are non-negative constants.

Wrench is the combination of both, the force and the torque or moment, corresponding to the grasp force f_i. If w_i is the wrench applied at contact point i then,

$$w_i = \begin{pmatrix} f_i \\ \tau_i \end{pmatrix} = \begin{pmatrix} f_i \\ r_i \times f_i \end{pmatrix} \tag{6.3}$$

Where r_i denotes the position vector of the i^{th} grasp point in the object coordinate frame which is at the center of mass of the object.

Wrench matrix is a 6 × *nm* matrix called wrench matrix (for 3D objects) where its column vectors are the primitive contact wrenches. Where *nm* is the total number of primitive contact wrenches applied at the object by *n* fingers.

$$W = \begin{pmatrix} l_{11}.....l_{16}.....l_{nm} \\ r_1 \times l_{11}.....r_1 \times l_{16}.....r_n \times l_{nm} \end{pmatrix} \tag{6.4}$$

6.6 Contact Models

The force applied by the finger at the point of contact on the surface of the object generates a wrench on the object at some other point in the object. A contact between a finger and an object can be described as mapping between forces exerted by the finger at the point of contact and the resultant wrenches at some reference point on the object i.e. the center of mass of the object which is termed as contact model. The reference point of the object is considered as the origin of the object reference frame O. For convenience the z-axis of contact coordinate frame is always chosen in the direction of inward surface normal of the contact point and origin at the contact point. So the force applied is always in the z-direction inwards to the object. So, the applied force *'f_i'* at the contact point by the fingertip during

grasp is modeled as a wrench 'w_i' applied at the origin of the contact frame is given by [200];

$$w_i = B_i f_1 \tag{6.5}$$

Here: B_i is the wrench basis that characterizes the contact model, which is a (6xr_i) matrix and r_i is the number of independent components of the applied force at contact point 'i'.

There are many types of contact models are possible for grasping the object but the main two aspects taken in to account are the friction between the finger and object and the finger is hard or soft. On basis of these two main aspects contact models can be classified as: *frictionless point contact*, the *frictional point contact* and the *soft finger contact* as shown in Figure 6.6. All these models fulfil the positive constraint i.e. the fingers can only push but cannot pull the object.

6.6.1 Frictionless Point Contact

A contact between fingertip and object surface is considered as frictionless point contact when the contact takes place at one point only and there is no friction between the two. This type of contact occurs between a hard finger and object as shown in Figure 6.6(a). In this case the force applied in the direction normal to the surface of the object only. So the applied wrench for this type of contact is given by the Eq. 6.6.

$$w_i = [0 \quad 0 \quad 1 \quad 0 \quad 0 \quad 0]^T f_i = B_i f_i \tag{6.6}$$

Here, r_i =1 and wrench basis for this model is $B_i = [0 \quad 0 \quad 1 \quad 0 \quad 0 \quad 0]^T$

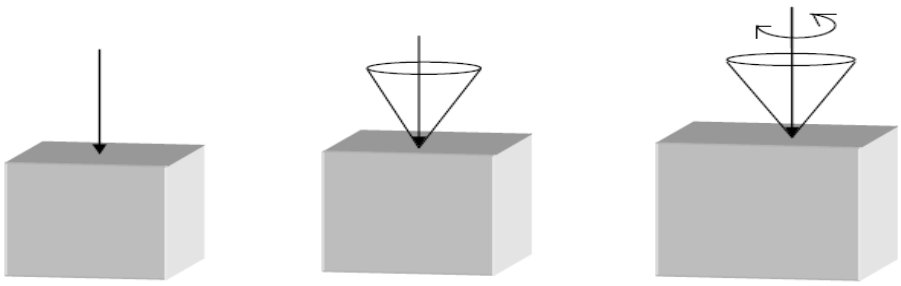

(a) (b) (c)

Figure 6.6: Contact Models: (a) Hard finger frictionless point contact, (b) Hard finger frictional point contact and (c) Soft finger contact.

These type contacts are for the grasps where at the contact points there have a negligible friction. The frictionless assumption is convincing in those type grasps where a total kinematic restriction on the object like fixtures. Furthermore, the frictionless point contact enhances the robustness of the grasping as it does not trust on friction forces to grasp or manipulate the object.

6.6.2 Frictional Point Contact

In this type of contact model there exist friction between the finger and the object as shown in Figure 6.6(b), this happens in case of hard finger also. So the applied force at contact point has two components one normal to the contact surface and another tangential to the surface. The equivalent wrench at the contact point is given by the Eq. 6.7.

$$W_i = \begin{bmatrix} 1 & 0 & 0 \\ 0 & 1 & 0 \\ 0 & 0 & 1 \\ 0 & 0 & 0 \\ 0 & 0 & 0 \\ 0 & 0 & 0 \end{bmatrix} \begin{bmatrix} f_{ix} \\ f_{iy} \\ f_{iz} \end{bmatrix} = B_i f_i \tag{6.7}$$

Here, r_i = 3 and wrench basis for this type model is $B_i = \begin{bmatrix} 1 & 0 & 0 \\ 0 & 1 & 0 \\ 0 & 0 & 1 \\ 0 & 0 & 0 \\ 0 & 0 & 0 \\ 0 & 0 & 0 \end{bmatrix}$

By using the most common Coulomb friction model it can show that how much force a contact can apply in the tangent directions to a surface as a function of the applied normal force. The range of tangential forces which can be applied at a contact is given by the eqn.

$$\left| f^{t} \right| \leq \mu f^{n}$$

Here,

f^{t} = Tangential force

f^{n} = Normal force

μ = Coefficient of friction

Therefore, the set of allowable contact force is

$$F_i = \{ f_i \in \mathrm{R}^3 : \sqrt{f_{ix}^2 + f_{iy}^2} \leq \mu f_{iz}, f_{iz} \geq 0 \}$$

With friction all forces lie within the friction cone around the surface normal, can be exerted. The cone angle with respect to normal is defined as $\alpha = \tan^{-1} \mu$.

6.6.3 Soft Finger Contact

This type of contact is like PCWF one additional thing that is added is a torque around the normal applied in the contact point as shown in Figure 6.6(c). The wrench that is applied is given by the equation as follows

$$W_i = \begin{bmatrix} 1 & 0 & 0 & 0 \\ 0 & 1 & 0 & 0 \\ 0 & 0 & 1 & 0 \\ 0 & 0 & 0 & 0 \\ 0 & 0 & 0 & 0 \\ 0 & 0 & 0 & 1 \end{bmatrix} \begin{bmatrix} f_{ix} \\ f_{iy} \\ f_{iz} \\ \tau_{iz} \end{bmatrix} = B_i f_i \qquad (6.8)$$

When, $r_i = 4$ and the wrench basis is $B_i = \begin{bmatrix} 1 & 0 & 0 & 0 \\ 0 & 1 & 0 & 0 \\ 0 & 0 & 1 & 0 \\ 0 & 0 & 0 & 0 \\ 0 & 0 & 0 & 0 \\ 0 & 0 & 0 & 1 \end{bmatrix}$

In this case for friction model it is assumed that friction limits due to torsion and shear forces are independent to each other. Then the set of allowable forces is

$$F_i = \{ f_i \in R^4 : \sqrt{f_{ix}^2 + f_{iy}^2} \leq \mu f_{iz},\ f_{iz} \geq 0, |\tau_{iz}| \leq \gamma f_{iz} \}$$

Where $\gamma > 0$ is the coefficient of torsional friction.

6.7 Grasp Wrench

Any force acting at a contact point on the object, creates a torque relative to reference point i.e. centre of mass of the object as discussed in section 6.4. These force and torque vectors are concatenated to a wrench. The net wrench acting on an object is obtained by summing the wrenches due to each finger. To determine the contribution of each contact force on the object, the corresponding wrenches are transferred to the object coordinate frame. Then adding all the individual wrenches, the net wrench calculated due to all contact points on the object during grasping. The wrench exerted by a single finger contact on the object is given by

$$w_{o_i} = W_{oc_i} w_i = W_{oc_i} B_i f_1 \tag{6.9}$$

Here

w_{o_i} is the wrench at the origin of the object coordinate frame O due to force at contact point i.

W_{oc_i} is the wrench transformation matrix from contact point to O.

w_i is the wrench due to applied force at contact point i as given in Eq. 6.7, Eq. 6.8 and Eq. 6.9.

The *contact map* G_i is defined as the linear transformation between the contact force f_i and the wrench produced on the object due to contact force, w_{oi} is given as [201]

$$G_i = W_{oc_i} B_i \tag{6.10}$$

Therefore, the wrench for a single contact is

$$W_{o_i} = G_i f_i \tag{6.11}$$

The total wrench on the object is the sum of the wrenches due to forces at contact points of all fingers is

$$W_o = G_1 f_1 + G_2 f_2 + \cdots + G_n f_n = [G_1 \ldots G_n] \begin{bmatrix} f_1 \\ \vdots \\ f_n \end{bmatrix} \tag{6.12}$$

The *grasp map* or *grasp matrix G* is the linear transformation between the contact force vector and the net wrench [201] as given in Eq. 6.12. So *G* is given by

$$G = [G_1 \ldots G_n] = \left[w_{oc_1} B_1 \ldots w_{oc_n} B_n \right] \tag{6.13}$$

The resultant or net wrench exerted by all the fingers on the object is given by

$$w_o = G f_c \tag{6.14}$$

Here,

$f_c = \begin{bmatrix} f_1 \\ \vdots \\ f_n \end{bmatrix}$, be the contact force vector, obtained by adding all the finger contact forces.

A *grasp wrench space (GWS)* is characterized by the set of wrenches that can be applied to the target object from the contacts of a grasp, given certain limitations on applied forces. The grasp wrench space is bounded by the convex hull of the contact wrenches formed from unit applied forces at the contact of the grasp [143]. Note that only the contact model and contact locations on the object are factors in determining the grasp wrench space.

6.8 Friction

Contacts without friction are purely theoretical concept but in which the friction between the finger and the object is low or unknown, that is considered as frictionless contact. In frictionless contact the forces exerted in the normal direction only, so modelling a contact as frictionless contact insures that frictional forces do

not relied when manipulating the object. But in practice at the contact point of any two surfaces there must have some amount of friction, which oppose the force components within the tangent plane. Any contact with greater than zero area uses friction to resist moments about the normal to plane at contact point.

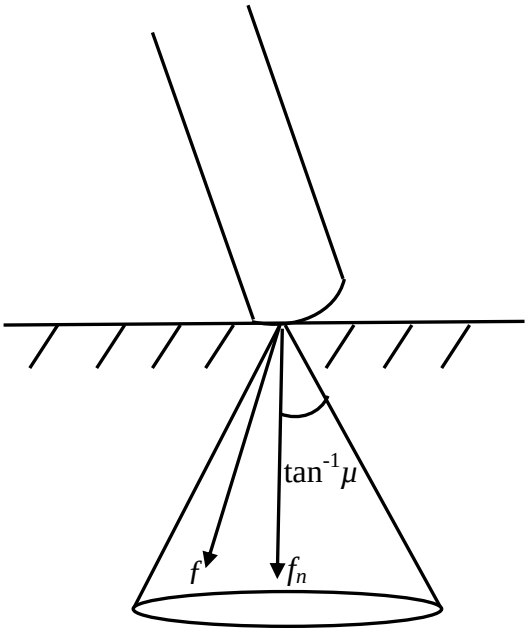

Figure 6.7: Friction at a contact point.

Frictional forces that can arise at a point contact are most commonly determined using Coulomb's model, which states:

$$f_t \leq \mu f_n \tag{6.15}$$

Where, f_t is the tangential force component,

f_n is the normal force component,

and μ is the empirically determined coefficient of friction.

If the condition is not satisfied then slipping occurs. When working in 3 dimensions, this can also be written as:

$$f_x^2 + f_y^2 \leq \mu^2 f_n^2 \tag{6.16}$$

Where, f_x and f_y are perpendicular force components within the tangent plane.

From this equation, it is apparent that the forces that may be applied at the contact lie within a cone aligned with the contact normal, commonly known as a friction cone. The half angle of this cone is $\tan^{-1}\mu$ as shown in Figure 6.7.

6.9 Analysis of Grasp

The physical representation of interaction between the object and the hand is termed as grasp. For the purpose of analysing the grasp analytically this physical action of the hand must be expressed in forms of mathematical models. In the process of analysis the different properties of a given grasp are determined using the laws of physics, kinematics and dynamics. From the literature, it is concluded that different variety of multi-fingered hands are available for grasping an object. The complication of the analysis increases due to the versatile structure of the multi-fingered hand and the various numbers of conditions that has to be satisfied for a good grasp. As there are large numbers of range, for the exploration of feasible grasp, the grasp has to be synthesized in order to find a grasp that satisfies the required properties. One of the more additional complexities in this process is the number of feasible solution. Most of the literature that has been reviewed concentrates on the analysis of grasps. In most cases, the scope of the analysis is restricted to a particular grasp property but this can be extended to much more.

6.9.1 Grasping Strategy

Grasp strategy is the systematic planning for a multi-finger hand to perform a good grasp for versatile objects and environment. The important objectives of any grasping strategy are, it should be task compatibility, adaptable to new objects and provide a stable grasping as shown in Figure 6.8.

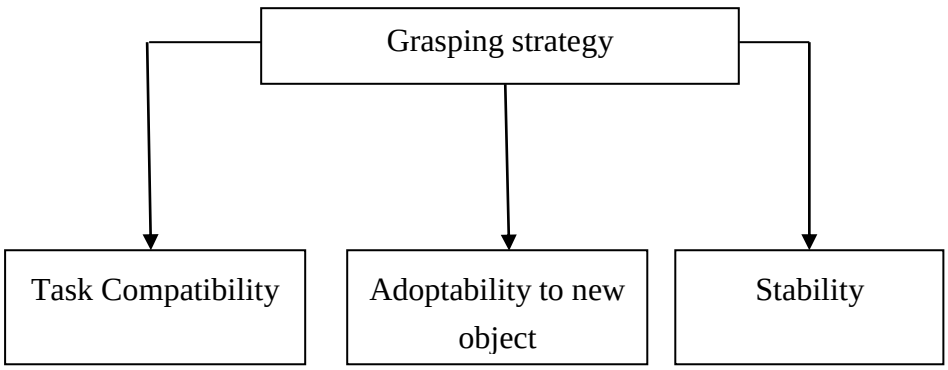

Figure 6.8: Grasping Strategy.

When any object is grasped, that must be performed in a particular fashion to achieve the task accomplish with that, depending on the type of object and propose of use. Hence, for ensuring that the task will perform successfully, the hand and grasp strategy should be compatible with the task requirements. For a grasping strategy, the adaptable to new object is very crucial, because of the variety in the shapes and sizes of the objects to be grasped. A grasping strategy must be flexible enough, so can able to grasp new objects, then only the multi-finger hand used as general purpose grasping tool. One more goal of the grasp strategy is stability of the grasp. A grasp is stable if any disturbance on the object position or finger force generates a restoring wrench that tends to bring the system back to its original configuration. Nguyen [139] proposed an algorithm for constructing stable grasps and also proved that all 3D force closure grasps can be made stable. A grasp is force-closure when the fingers can apply appropriate forces on the object to produce wrenches in any direction to resist some external disturbing wrench. This condition may be confused with form-closure. The form closure induces complete kinematical restraint of the object and is obtained when there is no relative motion between the palm and the object which ensure the complete immobility of the object. Bicchi [158] described in detail about these conditions. Thus, a grasping strategy should ensure stability, task compatibility and adaptability to novel objects.

6.9.2 Minimum Number of Contacts for Grasp

The number of contacts or number of fingers required to grasp an object is a very important and first decision in the grasping process. According to the contact between hand and object the grasp classified as two types one is form closure grasp and other is force-closure grasp, the details about this discussed in section 6.3.1. The number of fingers required for getting a form or force closure grasp depends on the type of contact considered between the finger and the object. In the study it was concluded that minimum 4 to 7 numbers of fingers are required for frictionless grasp to get Force Closure grasp in 2D and 3D objects, respectively, for objects without rotational symmetry i.e. planar objects [141]. For objects with rotational symmetry like sphere, it is not possible to obtain Force Closure grasps using only frictionless point contacts. Frictionless and frictional grasps were also studied from the geometrical point of view, concluding that for frictional contacts -frictional point contact and soft finger contact - 3 and 4 fingers are sufficient to get Force Closure(FC) grasps on any 2D or 3D objects, respectively, which are independent of the friction coefficient [201]. However, in many cases and depending on the

particular object and the value of the friction coefficient, it is possible to get FC grasps with a lower number of fingers even with 2 fingers for both 2D and 3D objects [139]. These frictional bounds were lowered by one contact each by Mirtich and Canny [148] who predicated the rounded finger tips to provide continuity to the contact normal around the boundary of the object. Table 6.2 summarizes the lower bounds on the number of fingers required to get FC grasps in any 2D or 3D object [44].

Table 6.2: Number of contacts required to grasp an object.

Space	Object type	Lower	Upper	Frictionless Point Contact	Point Contact With Friction	Soft Finger
Planar (p = 3)	Exceptional	4	6	n/a	3	3
	Non-exceptional			4	3	3
Spatial (p = 6)	Exceptional	7	12	n/a	4	4
	Non-exceptional			12	4	4
	Polyhedral			7	4	4

6.10 Force Closure Grasp

The major requirement of a grasp planning problem is the grasp ensures that there is no mobility of the object due to any external wrench applied on the object. Hence, the grasp planning for multi- fingered hands looks for a set of contact locations of fingers on the object surface that satisfy some desired properties, mainly the resistance to external disturbances. Grasps with this property will satisfy one out of two conditions form closure and force closure. The details about this are discussed in section 6.3.1. The form closure condition is a stronger condition than force closure condition, so it is called completely kinematical restraint. A grasp fulfils the form closure condition if it is force closure with frictionless contact. Form closure is used when the task requires a robust grasp without any manipulation, whereas force closure is used in both grasping and manipulating the object. In the present work the hand model is a multi-fingered anthropomorphic

hand model proposed for dexterous assignment including both grasping and manipulation. Hence the force closure grasp condition is considered for analysis of the grasp planning for the proposed hand model. Some examples of force-closure grasp found from the work of Nguyen [202] are depicted in Figure 6.9. The independent regions of contact are high-lighted with bold segments and circles in case of 2D and 3D objects respectively. The grasp is force-closure no matter where the fingertips are placed in these regions.

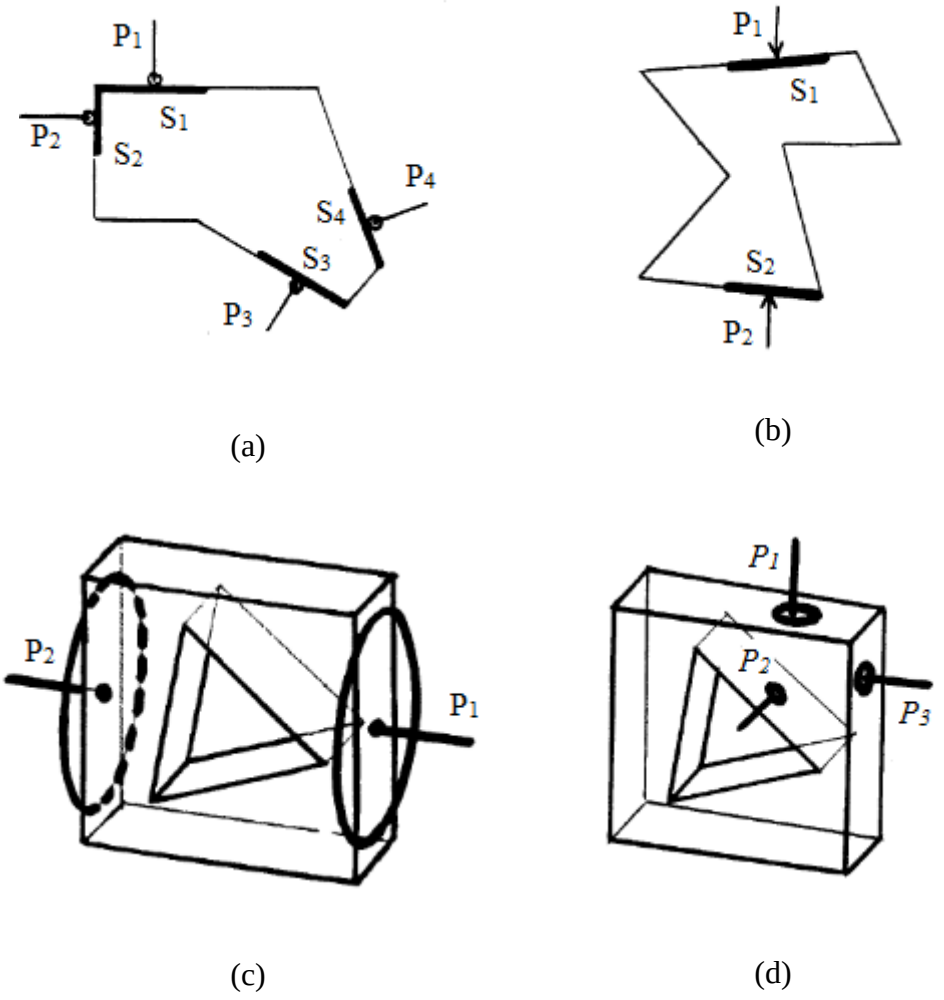

(a) (b)

(c) (d)

Figure 6.9: Examples of force-closure grasps.

The first two figures i.e. Figure 6.9 (a) and Figure 6.9 (b) are 2D grasps first one with four frictionless points contacts and second one with two point contacts with friction. Figure 6.9 (c) is a 3D grasp with two soft finger contacts and Figure 6.9 (d) represents a 3D grasp with three hard fingers. However, the present research work analyses the problem of synthesizing the grasps of different shaped objects by

the proposed multi-fingered hand are force-closure. Synthesizing the force-closure grasp is equivalent to finding places to put the contacts, such that the contacts totally constrain the motion of the grasped object. Constructing an equilibrium grasp is synthesizing the force and moments at the contact, such that the object is in equilibrium. In 1993 Ponce [147] characterized the force closure grasps of 3D, polyhedral objects for hard finger contacts. The necessary linear conditions for three and four-finger force closure grasps were formulated and implemented as a set of linear inequalities in the contact positions. Analyses were limited to polyhedral objects and concentrated on producing independent regions of contact for each finger. From these discussions it is clear that, one of the most important properties of hand during grasping is the ability to balance any disturbing external object wrenches by applying suitable finger wrenches at the contact points. For example, if an object moves from one place to other with a multi-fingered hand, it must be able to exert forces on the object which should hold the object until the task is over. For this force applied should be in opposite direction to gravity and also depending on the task, it resists wrenches in other directions. This is complicated because it ensures that the applied finger forces remain in its position all the times so as to avoid slippage of the fingers on the surface of the object. One of the important features of a force-closure grasp is the existence of internal forces. An internal force is a set of contact forces which result in no net force on the object. It can be used to insure that contact forces satisfy friction cone constraints.

6.10.1 Purpose of Solving the Grasping Problem with Force-closure Condition

This work presents a formal framework for analysing and synthesizing grasps. The scope of this work is limited to force-closure grasps, stable grasps, and grasps with possible slip at the contacts.

The work is marked with the following characteristics:

- Fast and simple algorithms for direct constructing force closure grasps. The aim is to find not only single grasps but the complete set of all force-closure grasps on a set of edges in 2D or respective faces in 3D.
- A representational frame work for describing contacts and grasps is prepared. A grasp is described as the combination of individual contacts, which in turn are modelled as the combination of a few primitive contacts: point contacts with friction in 2D and in 3D.
- A proof that non-marginal (an equilibrium grasp is non-marginal if the forces of contact point strictly within their respective friction cone)

equilibrium grasps are also force-closure grasps, if each grasp has at least two points with friction in 2D, or two soft finger contacts or three hard finger contacts in 3D. This proof supports a very simple heuristic for grasping: “Increase friction at the contacts by covering the finger tips with soft rubber. Then grasp the object on two opposite sides.”

6.10.2 Formulation of the Force-closure Problem

Force-closure grasp is one of the interesting research topics in the field of grasping and manipulation. Although a good amount of work has been done in this direction in the distance past it received a lot of attention during the last two decades. Many necessary and sufficient conditions of the force-closure grasp are proposed by many researchers, but only few are considered for 3D objects grasping due to their complicated geometry and high dimension of the grasp space. Some of the researcher considered polyhedral 3D objects [139, 202], while others considered smooth curved surfaces [59] or objects modeled with a set of points [70]. Nugyen [139] studied force-closure grasps of polyhedral objects and proposed the following necessary and sufficient condition:

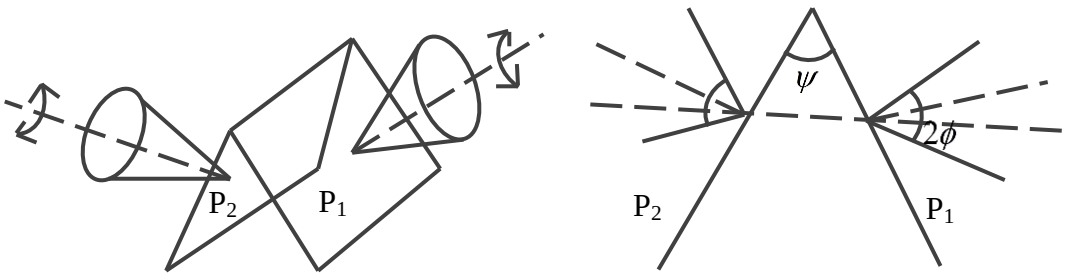

Figure 6.10: Grasp with two soft finger contact points.

Proposition 1: A grasp having two soft-finger contacts is force-closure if and only if the segment P_1P_2, or P_2P_1, joining the two points of contact P_1 and P_2, points lies strictly into and out of the friction cones respectively at P_1, P_2 (Figure 6.10). Another important result proposed by Nguyen is:

Proposition 2: If a grasp achieves non-marginal equilibrium with at least two distinct soft-finger contacts, then that grasp is force-closure.

One of the closest related properties of force closure is equilibrium. Equilibrium indicates that the net resultant wrench of the system should be a zero vector. A

grasp is in equilibrium condition when it is possible for the contacts of the grasp to exert wrench '*w*' such that the net resultant wrench is zero vectors.

$$\sum_{i=1}^{n} \zeta_i w_i = 0 \text{, where } \zeta \text{ is a positive constant} \qquad (6.17)$$

Formally, a grasp is said to be an equilibrium grasp when Eq. 6.17 has a non-trivial and non-negative solution. A grasp that achieves force closure is also an equilibrium grasp. However, the inverse may not be true always. In the case of frictional contact a special class of equilibrium grasp is present called non-marginal equilibrium. A grasp achieves non-marginal equilibrium when the wrenches achieved equilibrium, are not the wrenches associated with the boundary of the friction cone. Hence it means that any equilibrium grasp is also a force closure grasp having greater frictional coefficient. It seems that non-marginal equilibrium implies force closure but it is not always true for any number of fingers. For example a 3D two finger non-marginal equilibrium grasp does not achieve force closure grasp.

The force closure condition in terms of wrench space was suggested by Nattee Niparnan in 2007 [70]. They described that grasp achieves force closure when its grasp wrench set covers the entire wrench space. The concept of positively span is introduced by them, which described that the positive span of a vector set covers the entire space. The following definitions amply clarify this fact.

Definition 1: (Positively Span) A set of n wrenches $\{w_1, w_2 \ldots w_n\}$ positively spans R^n if and only if, for any vector V in R^n there exists non-negative constants $\zeta_1 \ldots\ldots \zeta_n$ such that $V = \zeta_1 w_1 + \cdots\cdots + \zeta_n w_n$.

Therefore, the force closure property can be defined using the notion of positively spanning, particularly, a grasp achieves force closure when wrenches are related to it, i.e., the primitive contact wrenches generates the polyhedral convex cone which positively span their particular wrench space (For planar grasp 3D wrench and 6D wrench space in case of 3D grasp).

Definition 2: (Force Closure) A wrench set $W=\{w_1 \ldots\ldots w_n\}$ achieves force closure property when they positively span R^6.

Force closure property is defined over a set of vector *i.e.* wrenches, associated with a grasp, it is more appropriate to say that a set of vector achieves force closure, even though a set of vector cannot achieve force closure exactly. Hence it can be

said that a set of wrenches achieves force closure if a grasp whose associated set of wrenches positively span R^n.

6.10.3 Force Closure Conditions

The force closure property is defined using the positively spanning of wrench space notion. Still, it is indefinite to declare whether a set of vectors positively span a space. Some of the well-known conditions that assert on positively spanning of a set of vectors and some conditions of Force closure are shown in this division. Mishra et al. in 1987[143] related the positively spanning set of vectors with a convex hull of the vectors. A set of vectors W positively span a space when the origin of the space lies strictly inside the convex hull of W. Hence the following proposition can be put forth.

Proposition 3: A set of wrenches W in R^n achieve force closure when the origin lies in the interior of the convex hull.

The above proposition converts the force closure testing problem into a computational geometry problem. A direct way of solving the problem is to compute the convex hull of the primitive contact wrenches and directly show that whether the origin lies inside the interior of the convex hull. From this approach it is identified that if a half space is through the origin that contains all primitive contact wrenches, the primitive contact wrenches cannot positively span the space and it may further be proposed that:

Proposition 4: A set of wrenches W do not positively span R^3 if there exists a vector V such that the closed half space H(v) contains every wrench in W.

The above proposition 4 provides a general method for force closure declaration. This method given by the above proposition is applicable in any dimension for any number of contact wrenches. In some case where few contacts are required in small dimensions, there exist conditions that need no specific calculation of the convex hull which allows more efficient implementation.

Proposition 5: Necessary and Sufficient condition for three 2D vectors w_1, w_2 and w_3 positively span the plane when the negative of any of these vectors lies in the interior of the polyhedral convex cone formed by the other two vectors.

This proposition can be easily extended to cover 3D cases as follows. The proposition 5 represented as example in Figure 6.11, in which the dashed lines representing the negative of the vector. The example shown in Figure 6.11 (a) is satisfying the proposition 5, so the vectors are positively span, whereas in example

shown in Figure 6.11(b) the vectors are not positively span as they not satisfying the proposition 5.

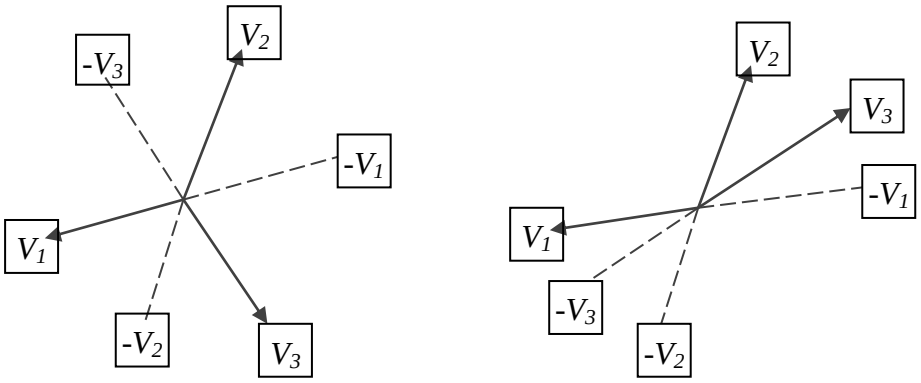

(a) (b)

Figure 6.11: Representation of proposition 5.

The necessary and sufficient conditions for 3 fingered force closure grasp of a 2D and 3D polygonal object proposed by Li et al. [160] which is stated in proposition 6 and 7 respectively.

Proposition 6: A necessary and sufficient condition for the existence of three nonzero contact forces which achieve equilibrium for 2D objects, not all being parallel, is that there exist three forces in the friction cones at contact points which positively span the plane and whose lines of action intersect at some point.

Proposition 7: A three-finger 3-D grasp achieves force closure if and only if there exist contact plane S and contact unit vectors n_{11}, n_{12}, n_{21}, n_{22}, n_{31} and n_{32} and the contact unit vectors construct a 2-D force-closure grasp in S (Figure 6.12).

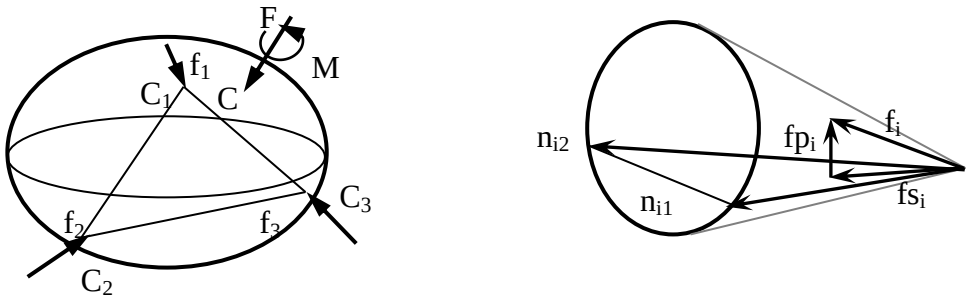

(a) (b)

Figure 6.12: (a) Three finger 3d-grasp (b) Decomposition of force into components.

The 3D grasps considered as combination of number of 2D grasps in the contact plane as done in a planar grasp problem and that in the direction perpendicular to the plane. Thus the 3D problem is reduced to 2D problem. The different cases are presented in Figure 6.13.

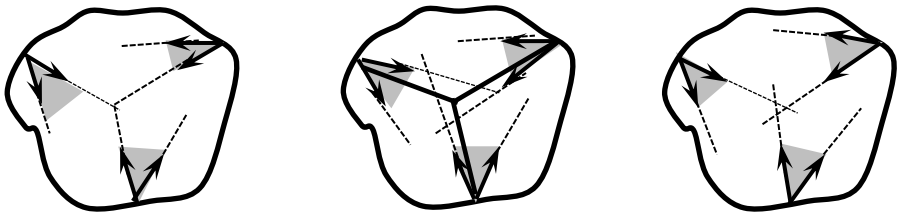

(a) (b) (c)

Figure 6.13: Three-finger grasps, (a) Equilibrium but not force-closure grasp, (b) Non-marginal equilibrium but force-closure grasp, (c) Non-equilibrium grasps.

A new geometric characterization to force-closure grasp of objects with three fingers and four fingers can be analysed assuming hard-finger contact and Coulomb friction [160]. The following paragraphs are devoted to present the theories behind grasping in a precise manner for various grasping conditions.

(a) Grasping with three fingers.

Proposition 8: A grasp in the presence of friction, a sufficient condition for three-dimensional n-finger force-closure with $n \geq 3$ is non-marginal equilibrium.

Proposition 9: For three points necessary condition to form a force-closure grasp is that there exists a point in the intersection of the plane formed by the three contact points with the double-sided friction cones at these points (Figure 6.14).

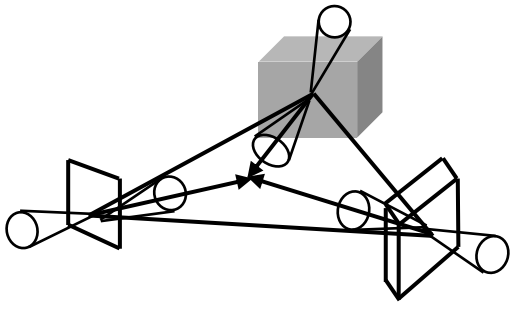

Figure 6.14: Grasping a polyhedron with three frictional fingers.

Proposition 10: A sufficient condition for three points to form a force-closure grasp is that there exists a point in the intersection of the three open internal friction cones with the triangle formed by these contact points as shown in Figure 6.14.

(b) Grasping with four fingers.

Proposition 11: A necessary condition for four points to form a force-closure grasp is that there exist four lines in the corresponding double-sided friction cones which should intersect in a single point, form two flat pencils having a line in common but lying in different planes, or form a regulus (Figure 6.15).

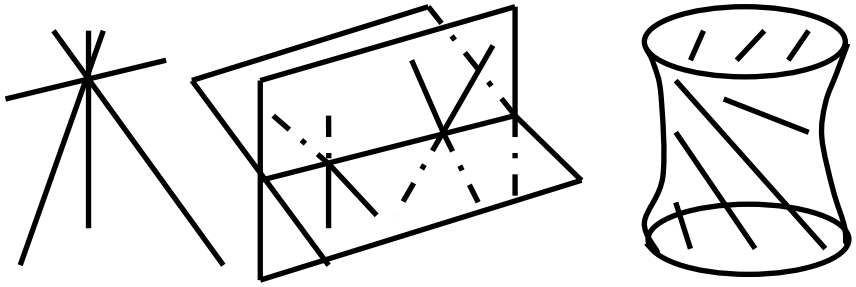

Figure 6.15: Four-finger grasps. (a) Four intersecting lines. (b) Two flat pencils of lines having a line in common. (c) A regulus.

Proposition 12: A sufficient condition for four contact points to form a force-closure grasp is that there exists a point in the intersection of the four open internal friction cones with the tetrahedron formed by these points (Figure 6.16).

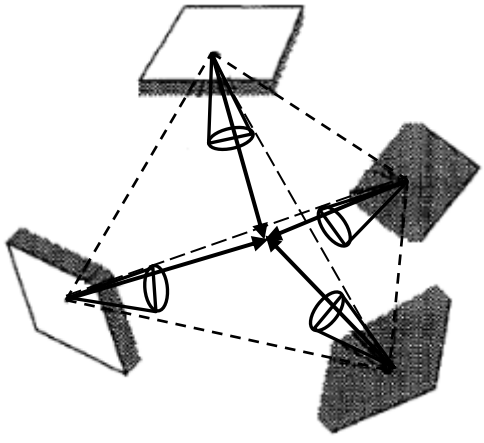

Figure 6.16: Grasping a polyhedron with four frictional fingers.

The present work has been done with five fingers in the light of these established theories.

6.11 Simulation of the Grasping of Different Shaped Objects using CATIA

The three dimensional model of the proposed multi-fingered anthropomorphic robotic hand is prepared using Computer Aided Three-dimensional Interactive Application (CATIA) version 0.5 solid modeling software. The segmental lengths of the thumb and different finger segments are taken exactly same as the proposed hand model. The normal view of the hand is shown in Figure 6.17 in which all the fingers are straight. All the joints of the thumb and fingers are assigned the range of the joint angles from Table 4.4 through Table 4.8.

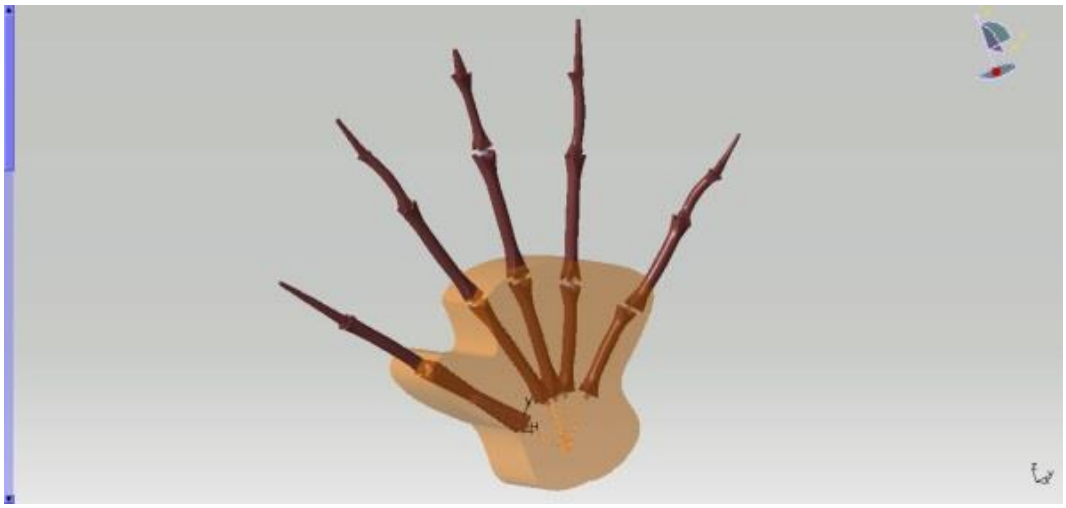

Figure 6.17: CATIA model of the hand.

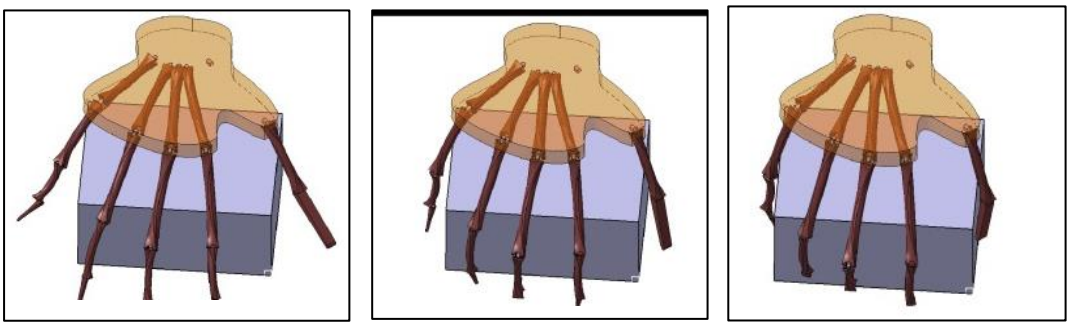

(a) (b) (c)

Figure 6.18: Grasping of cubical object (a) open (b) half closed (c) closed.

As discussed earlier in section 5.10 different shaped objects can be grasped by the multi-fingered hand if the object within the convex hull as shown in Figure 6.29.

The simulation is done using the CATIA model of the proposed multi-fingered, anthropomorphic hand and grasping of a cubical object is shown in Figure 6.18. The opening condition of hand and the object is within the convex hull is shown in Figure 6.18 (a), half closing of hand to grasp the object is shown in Figure 6.18 (b) and fully grasping of the cubical object is shown in Figure 6.18(c).

The simulation for grasping a cylindrical object by the proposed hand model is shown in Figure 6.19. The Figure 6.19(a), Figure 6.19(b) and Figure 6.19(c) are shown the three different stages during grasping i.e. opening of hand, half closed and fully grasping the object respectively.

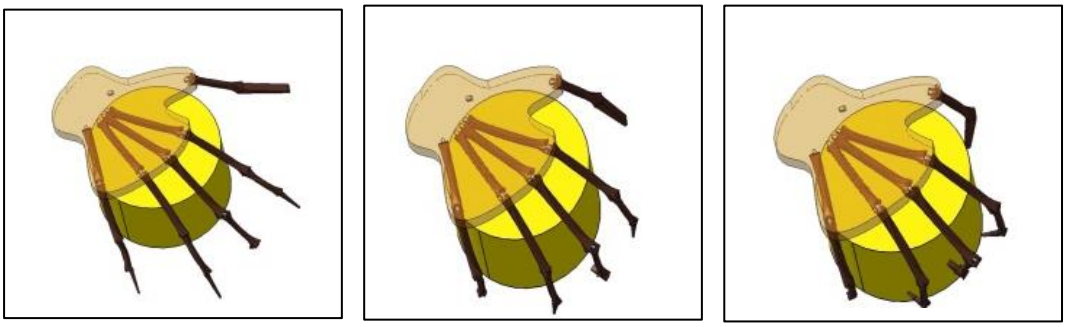

(a) (b) (c)

Figure 6.19: Grasping of cylindrical object (a) open (b) half closed (c) closed.

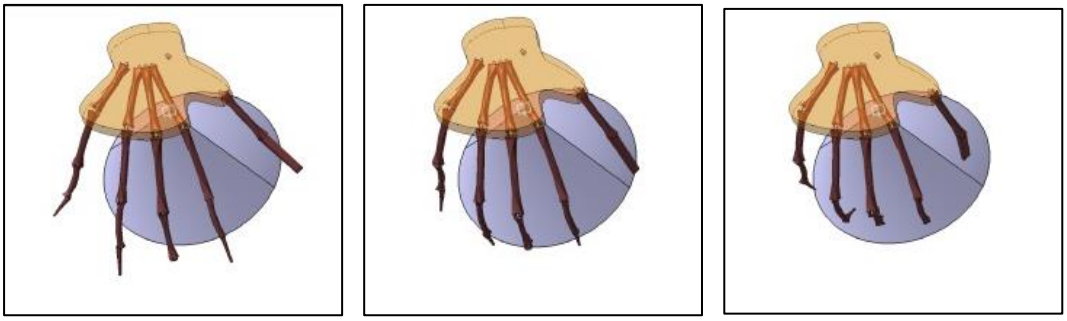

(a) (b) (c)

Figure 6.20: Grasping of conical object (a) open (b) half closed (c) closed.

Figure 6.20(a), Figure 6.20(b) and Figure 6.20 (c) are shown the three stages during simulation of grasping process of a conical object as fully opened hand, half closed hand and grasped object respectively.

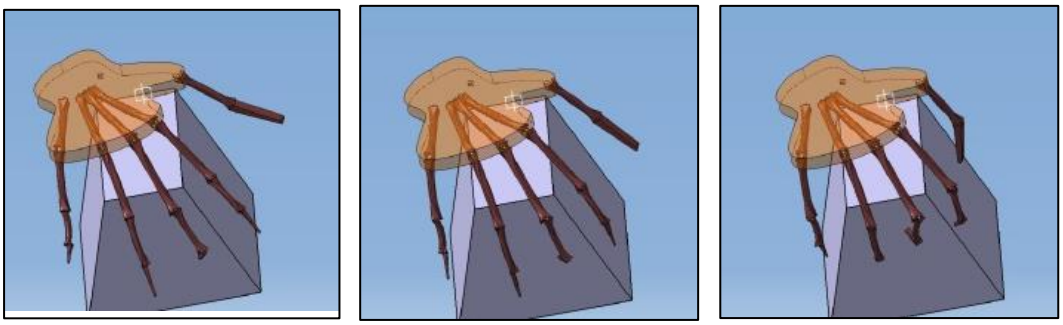

(a) (b) (c)

Figure 6.21: Grasping of trapezoidal object (a) open (b) half closed (c) closed.

Using CATIA software the simulation for grasping a trapezoidal object is done which is shown in Figure 6.21. The three different figures Figure 6.21 (a), Figure 6.21(b) and Figure 6.21(c) are shown as the opened condition of hand placed over the object just preparing for grasping, half closing of hand when the grasping process continue and fully grasped the object respectively.

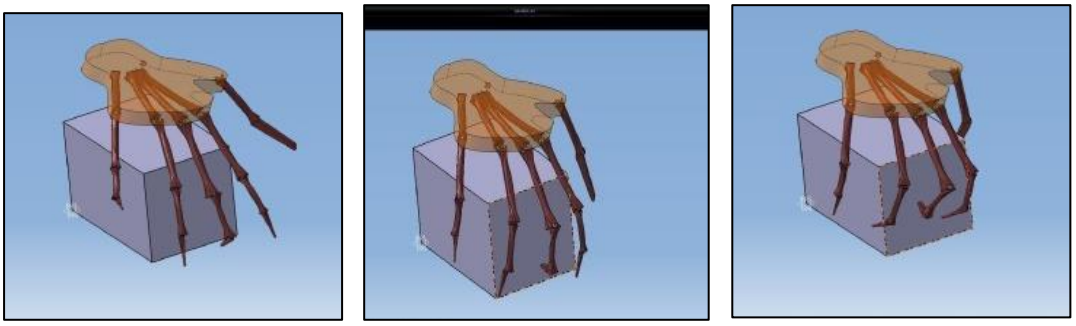

(a) (b) (c)

Figure 6.22: Grasping of parallelepiped object (a) open (b) half closed (c) closed.

Similarly, as in other cases Figure 6.22 shows the grasping simulation of a parallelepiped object. This also consists of the figures as Figure 6.22(a). Figure 6.22(b) and Figure 6.22(c) for opening of hand preparing to grasp the object, half closed hand trying to grasp the object and grasped the object respectively.

6.12 Grasping of the Object with the Multi-fingered Hand

It is of great importance to know which kind of object the hand can grasp. The type includes the size, weight etc. of the object. In general it is observed from the human hand grasping that thumb and at least one finger is required to grasp an object as shown in Figure 6.23. The number of fingers may vary along with thumb to grasp

the object depending on the shape, size and weight of the object. Thumb is always used for any grasping operation along with any number of fingers, as thumb and finger movement is opposite to each other. The trajectory of the tip of the thumb and number of finger combination is shown in following sections, from which it is concluded that thumb and finger movement are opposite to each other. Since the grasping analysis concentrated on the force-closure grasp in the present dissertation, the distance between the tip of the thumb and finger will limit the size of the object to be grasped. A program has been written to find the size of the object that can be grasped. The trajectory motion of the thumb and finger could also be known with the help of this program. The program is being written in MATLAB-08.

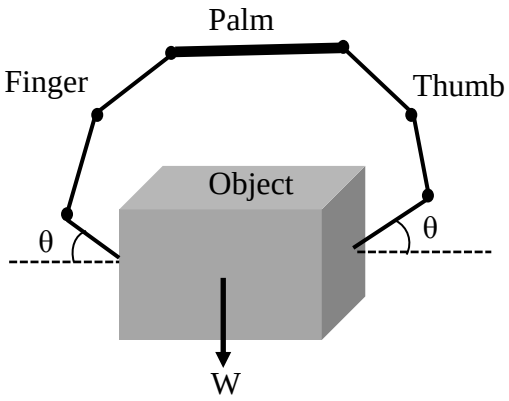

Figure 6.23: Grasping an object by thumb and a finger.

6.12.1 Trajectory of Thumb and Fingertips

The joints of the fingers of the hand are perform two types of motion i.e. extension/flexion and abduction/adduction (discussed in section3.3.2 in details). The extension/flexion motion is performing the opening and closing of the hand whereas the abduction/adduction motion responsible for rotating or manipulating the object. So, as far as grasping of object is concerned, the extension/flexion motions of the joints are only considered. A simplest kinematic model of thumb and one finger considering extension/flexion motions of joints only is shown in Figure 6.24 (a) and Figure 6.24 (b) respectively. On considering the segmental lengths from Table 5.1 and Table 5.2, and considering the values of range of angles of extension/flexion motion of joints from the Table 4.4, Table 4.5, Table 4.6, Table 4.7 and Table 4.8 the trajectory of thumb and fingertips are found out.

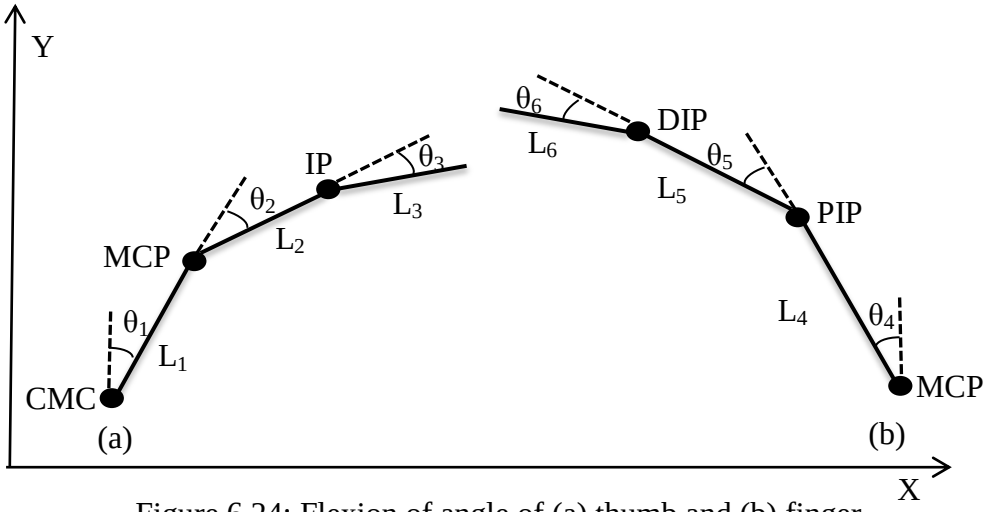

Figure 6.24: Flexion of angle of (a) thumb and (b) finger.

Using the principle of basic trigonometry, the expression for the position of the tip of thumb and finger can be written in terms of the joint coordinates and segmental lengths as:

$$y = L_1 \cos\theta_1 + L_2 \cos(\theta_1 + \theta_2) + L_3 \cos(\theta_1 + \theta_2 + \theta_3) \tag{6.18}$$

$$x = L_1 \sin\theta_1 + L_2 \sin(\theta_1 + \theta_2) + L_3 \sin(\theta_1 + \theta_2 + \theta_3) \tag{6.19}$$

It may be noted that all the angles have been measured counter clockwise and the link lengths are assumed to be positive going from one joint axis to the immediately distal joint axis. Equation is a set of two equations that describe the relationship between finger coordinates and joint coordinates. The trajectories are drawn by varying the values of all the joint angle values in their respective ranges. The trajectories are shown in Figure 6.25, Figure 6.26, Figure 6.27, and Figure 6.28 for thumb with index finger, thumb with index and middle finger, thumb with index, middle and ring fingers and thumb with all four fingers respectively. The segmental lengths of the thumb and fingers are found out from measurement for a normal human hand of Hand length (HL) is equal to 18.5cm and hand breadth (HB) is equal to 9cm. The simulation is made for a robotic hand having dimension of normal human hand, but not for any specific purpose. The Eq. 6.18 and Eq. 6.19 are used find the fingertip position and the angles are varied in their respective ranges to h show the movement of the thumb and finger tips.

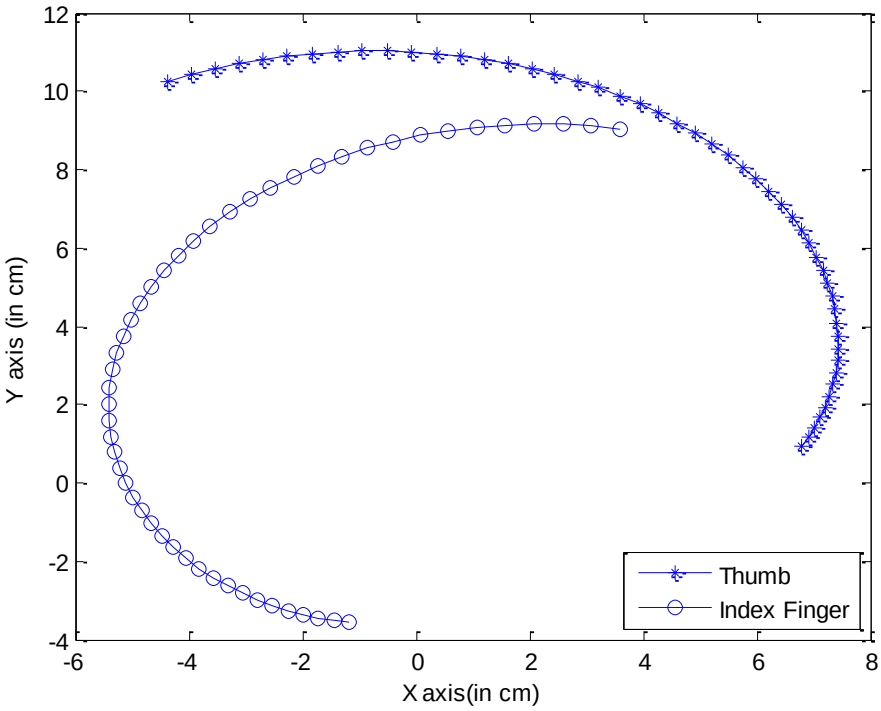

Figure 6.25: Trajectory of motion of the tip of thumb and index finger

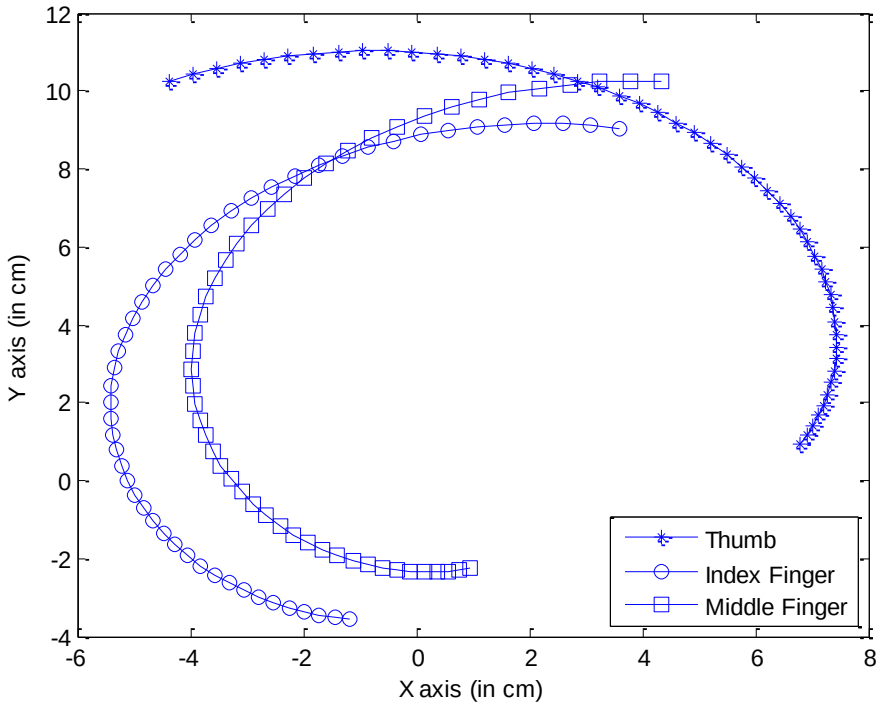

Figure 6.26: Trajectory of motion of the tip of thumb, index and middle finger.

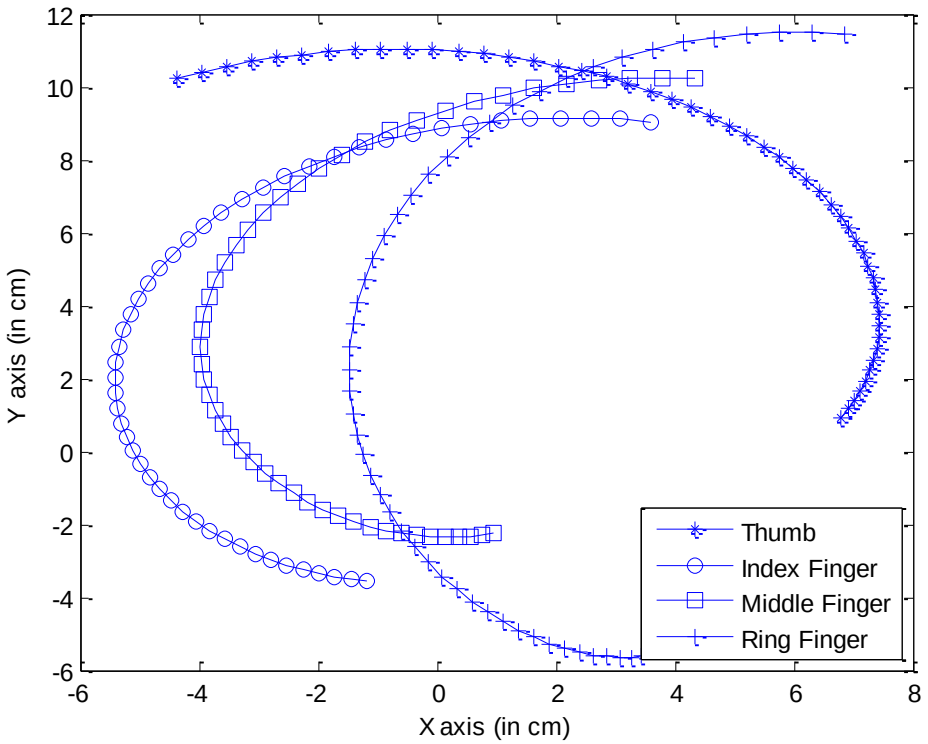

Figure 6.27: Trajectory of motion of the tip of thumb and other three fingers.

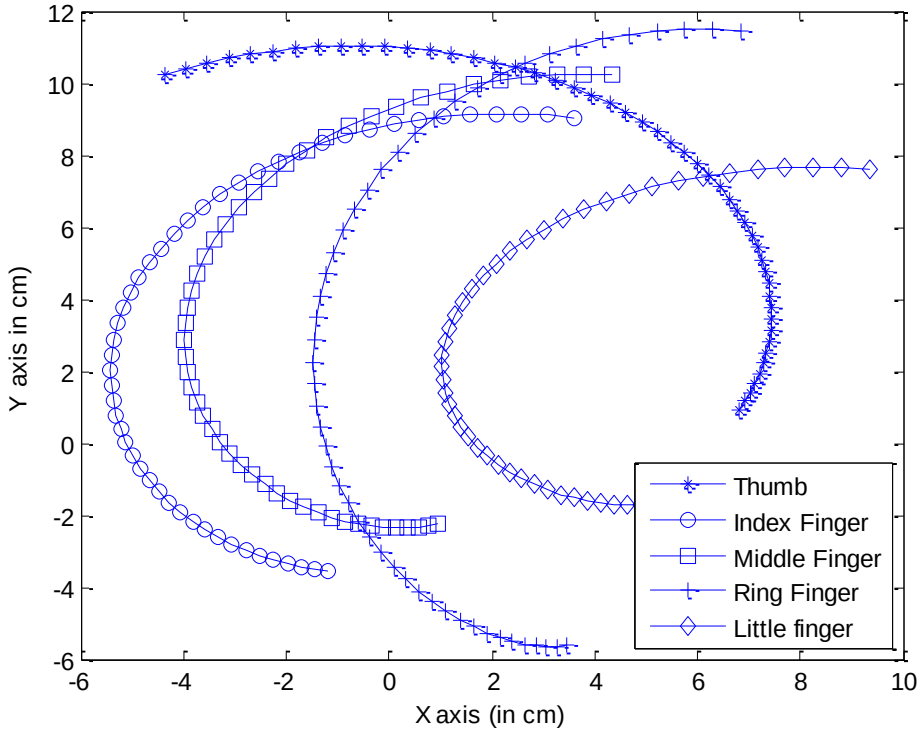

Figure 6.28: Trajectory of motion of the tip of thumb and all four fingers.

The figures show the movement pattern of the tips of thumb and fingers which are in opposite direction to each other. With increase of the values of x-coordinate, that of the y-coordinate is decreasing in case of thumb and with decrease in the values of x-coordinate, that of y coordinate is decreasing in case of fingers. For both the cases the reference point is considered at the same point. Hence the graph shows the reverse trajectories for the fingers and thumb. The motion for the thumb is in clockwise direction whereas that for the fingers is in counter-clock wise direction.

6.13 Force-Closure Space and Convex Hull of Hand

The contact space is the space defined by N parameters that represent the grasping contact points on some given edges of an object. The force-closure (FC) space is the subset of the contact space where FC grasps can be obtained. A methodology to obtain the FC space as the union of a set of convex subspaces is presented in this section. Besides, the approach developed here determines additional information on the finger forces that is quite useful in the determination of the independent regions. Figure 6.29 shows the space (convex hull) of the hand which decides the size of the object that can be grasped. The outermost circle shown in dotted line in the figure is the convex hull of the hand. The other figure inside the circle are the objects that can be grasped within the given size range. The parameters used to define the contact space are the torques produced by unitary normal forces when frictionless contacts are considered and the torques produced by the unitary primitive forces when friction contacts are considered. If the object is able to resist that pull force or some external force then it can define that object is in force closure condition.

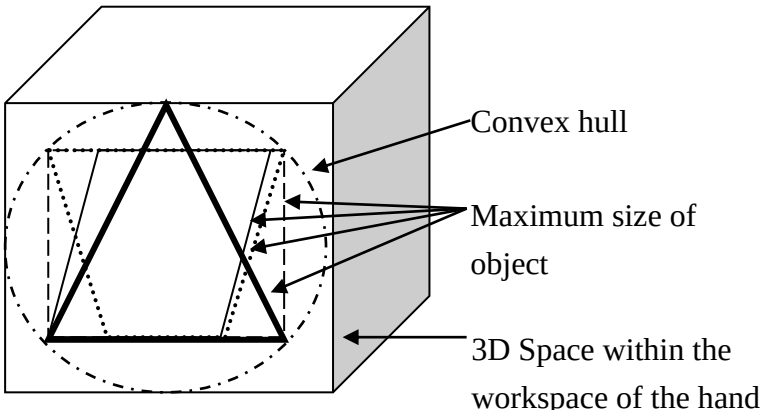

Figure 6.29: Convex hull of the hand.

6.13.1 Computation of Maximum Size of the Object

Given the two points (x_1, y_1) and (x_2, y_2) the distance between these points is given by the formula:

$$d = \sqrt{(x_2 - x_1)^2 + (y_2 - y_1)^2} \tag{6.20}$$

In order to determine the maximum size of the object, one needs to determine the distance between the tips of the thumb and one of the fingers in a plane with their maximum opening configuration. Let $P_1(x_1, y_1)$ be the position of the tip of the thumb and $P_2(x_2, y_2)$ be the position of tip of a finger in the same plane, then the distance between the two tips can be determined by using equation Eq. 6.20. The first two joints of the thumb and finger have been kept at maximum opening by keeping the extension/flexion angle of CMC and MCP joint of thumb, and MCP and PIP joint of finger at minimum value. The last joint has minimum opening by keeping the value of the extension/flexion angle of IP joint of thumb and DIP joint of finger set at maximum value, so that the force applied by the tip of the thumb and finger should be maximum. The maximum distance between the end points of the proposed hand which decides about the size of the object was found to be 11.8468cm. Thus an object with dimension of this size or less in any direction can be grasped by the hand.

6.14 Summary

In this chapter all the preliminaries that is used in grasping are discussed, which enables to know about the various terms used in grasping. The types of grasp and their properties are presented precisely for the benefit of readers. The conditions of force-closure grasp are also explained based on past work of different researchers. Further it contains information about the requirement of friction, the number of points of contact, wrench etc. The grasping of an object by multi-fingered hands is also discussed and the trajectories of the motion of tips of thumb and fingers are determined and are shown by means of graphs that the motions of the thumb and that of the fingers are opposable to each other. Finally the maximum size of the object can be grasped by the hand is determined.

Chapter 7

GRASP ANALYSIS OF THE HAND

7.1 Overview

The analysis of the grasping capability of the proposed hand model is mainly discussed in this chapter. The mathematical models for different shaped objects under force closure condition of the grasp have been developed. From those mathematical equations the force exerted on each fingertip and possible position/orientation of the fingertips on the surface of the objects is determined using Adaptive Neuro-Fuzzy Inference (ANFIS). The stress concentration on each finger of the proposed hand model under the reactive force exerted on the fingertip for stable and equilibrium grasping of an object are analysed using ANSYS.

7.2 Forces on the Fingertips at Contact Points

When an object is grasped by frictionless point contact there is a provision that the contact force should always act in normal direction, otherwise grasping is not possible. Hence this type of contact has got limited application like pushing. In case of the object being grasped and manipulated as in Force-closure conditions, there is always some friction between the grasped object and the hand. It is important to analyse the effect of friction on the grasping of the object. It is a fact that the force of friction depends on the amount of applied force, the direction of the applied force with respect to the surface of the object and the interface materials. It is obvious that the maximum force that the finger can exert on the object is at normal direction. In order to estimate the effect of friction during grasping of the object, a set of codes is developed using MATLAB platform. The coding is done in MATLAB for analysing the effect of incident angle on the

applied force. A simplest case of grasping of an object is considered by thumb and another finger (i.e. with minimum number of fingers) as an example. It is assumed that equal amount of forces applied by thumb and finger and both inclined equally to the normal of the surface at point of contact and the frictional force acting on the surface of the object in upward direction as shown in Figure 7.1.

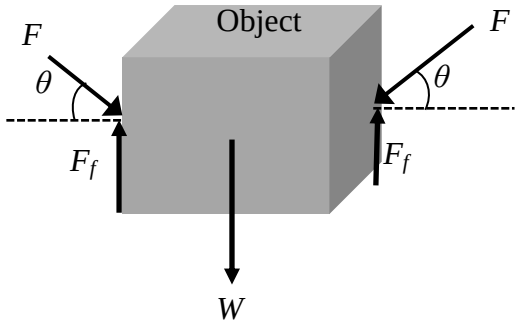

Figure 7.1: Force acting on object during grasping with friction.

The general expression for equilibrium of the grasped object is given as:

$$W = 2F_f = 2\mu F \cos\theta \tag{7.1}$$

where,

W= weight of the grasped object.

F_f = Frictional force.

μ = co-efficient of friction between object surface and tip of fingers.

F= Force applied by thumb and finger.

θ= Angle of inclination of thumb and finger to the normal at contact point.

The effect of incident angle on the contact force is shown in Figure 7.2. The trend of the graph shows that as the incident angle i.e. the angle of inclination of the finger to normal of the contact surface at point of contact (shown in Figure 7.2), is increased the force required to grasp the object is increased. So the best condition is that the force should be applied normally to the object so that the force required by the fingers to grasp the object will be minimum.

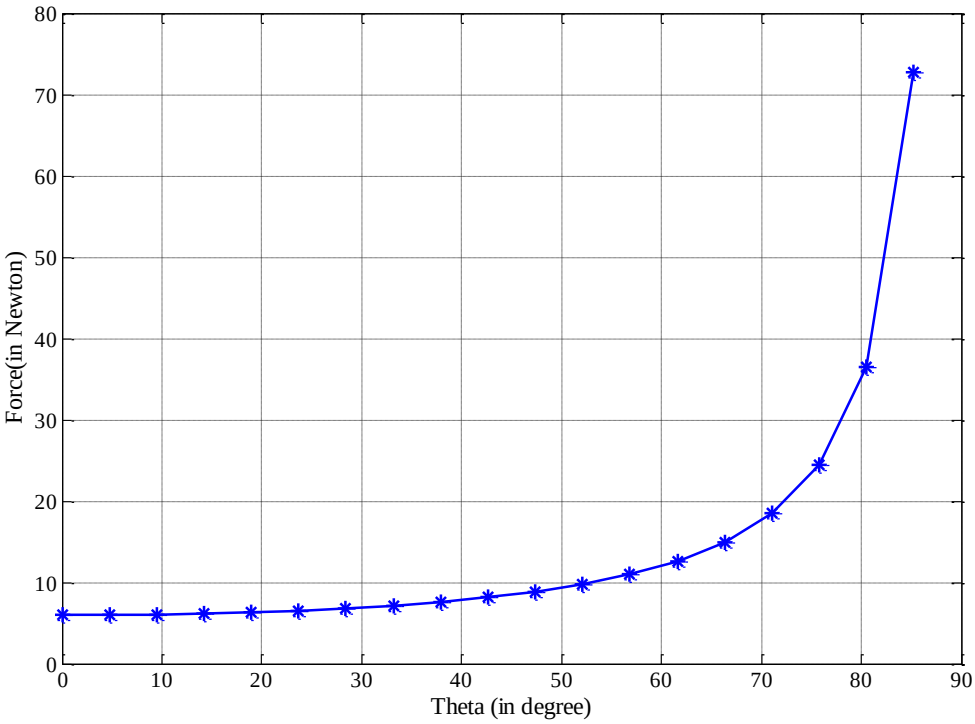

Figure 7.2: Effect of angle on the applied force by finger.

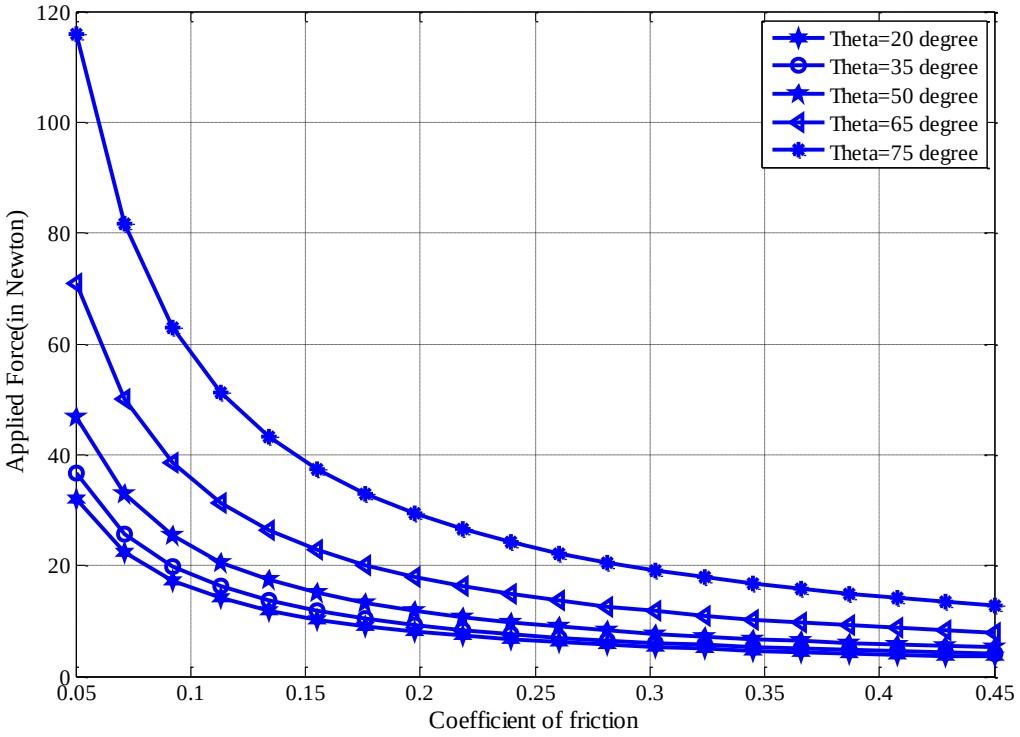

Figure 7.3: Effect of angle and co-efficient of friction on the applied force by finger.

Figure 7.3 shows the variation of the force value with change in values of coefficient of friction at different incident angles. There are five different values of incident angles are considered i.e. 20^0, 35^0, 50^0, 65^0 and 75^0. It is observed from the above figure that as the coefficient of friction is increased the force required by the finger to grasp the object is decreased. So the coefficient of friction (the finger-object interface) should be chosen according to the necessity of work and weight of the object.

7.3 Grasp Synthesis by Five fingered, Anthropomorphic Hand

The force closure grasp is desirable in case of multi-fingered hands (as discussed in previous chapter), which facilitates the manipulation of the object during grasping and transportation. So, the grasp synthesis of the proposed multi- fingered hand is restricted to force closure grasp of different shaped objects having proportionate weights, with point contacts between hard finger of the hand and object as shown in Figure 7.4. Coulomb friction is considered at the contact points of the fingertips and object. The wrench associated with a hard finger located at a point and exerting a force '*f*' is '*w*'. Wrench is basically a single force applied along a line combined with torque. Any system of forces on rigid body can be described with wrench. Force and moment are encoded in wrench as:

$$w = \begin{pmatrix} F \\ F \times d \end{pmatrix} \tag{7.2}$$

In order to achieving force closure grasp the net wrench on the object must be equal to zero. Hence, the net force and net moment acting on the object must be equal to zero for stable and equilibrium grasp.

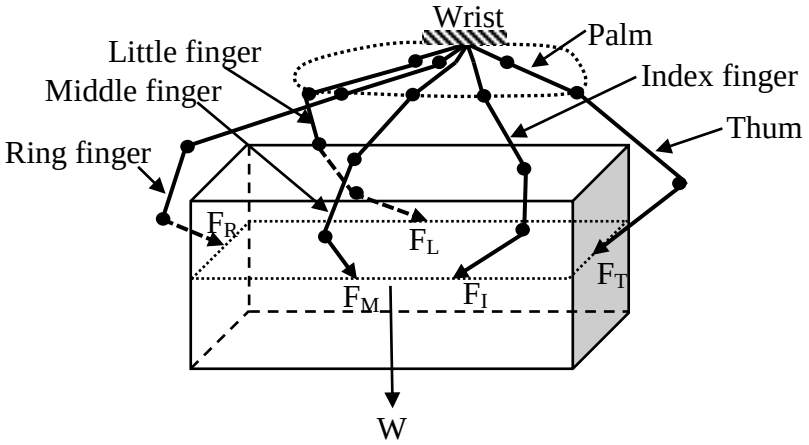

Figure 7.4: Grasping of an object by a five-fingered hand.

Considering the equilibrium of forces applied by fingers, we have

$$\sum_{i=1}^{n} F_i = \sum_{i=1}^{n} F_i \cos\theta_i = \sum_{i=1}^{n} F_i \sin\theta_i = 0 \tag{7.3}$$

Here,

$F_i \cos\theta_i, F_i \sin\theta_i$: The magnitudes of the finger force

d_i : The position vector of ith finger

Considering the equilibrium of moments due to the forces applied by the fingers on the object, the equation is:

$$\sum_{i=1}^{n} d_i \times F_i = \sum_{i=1}^{n} d_{iy} \times (F_i \cos\theta_i) + d_{ix} \times (F_i \sin\theta_i) = 0 \tag{7.4}$$

d_{ix} = perpendicular distance of Y component force

d_{ix} = perpendicular distance of X component force

7.4 Grasp Synthesis of Different Objects

Five different shaped objects i.e. cubical, cylindrical, conical, trapezoidal and parallelepiped are considered for the purpose of grasp synthesis. The dimensions of the different objects taken as base 5cm and height 5cm, same for all shapes and weight of cubical object taken as 3N. Accordingly the weight of all others shapes calculated as per proportionate with volume of different shapes. Co-efficient of friction, μ =0.25 is considered in case all objects.

Let the angles of the thumb and fingers of the hand with the normal to object plane are:

θ_T = angle between thumb and normal to contact plane of object.

θ_I = angle between index finger and normal to contact plane of object.

θ_M = angle between middle finger and normal to contact plane of object.

θ_R = angle between ring finger and normal to contact plane of object.

θ_L = angle between little finger and normal to contact plane of object.

W=weight of the object.

Assumptions for grasping and arbitrary selection of grasping points of an object:

- All the fingers are in contact with object during grasping even the object is very small.
- The points for grasping lie on the plane of Centre of gravity (CG), wherever possible or nearer to CG so that Z-coordinate remains same for all points.
- All the contacts are point contact with friction for a force closure grasp.
- The objects for grasping are located well within the workspace of the hand and no portion of the hand lies outside the workspace.
- Angle of inclination of the finger should be in the range of zero to angle of friction to the normal to the plane containing the contact point.

Let the coordinates of the fingertip contact points with respect to the coordinate axis having origin O at Centre of gravity of the object are (x_T, y_T, z_T), (x_I, y_I, z_I), (x_M, y_M, z_M), (x_R, y_T, z_R) and (x_L, y_L, z_L) for thumb, index finger, middle finger, ring finger and little finger respectively

According to Coulomb's law

$$F_t \leq \mu F_n \tag{7.5}$$

Here,

F_t is the total tangential force of the object and

F_n is the total normal force on the object.

The forces applied by the fingertips at the contact points of the object to grasp the object in stable condition. The fingers considered as hard finger with friction, so the weight of the object is resisted by the frictional forces at fingertip contact to provide the stable grasping of the object.

So, the total tangential force,

$$F_t = W$$

The total normal forces are the sum of normal component of all the fingertip forces at the contact points on the surface of the object.

7.4.1 Force closure condition for cubical object:

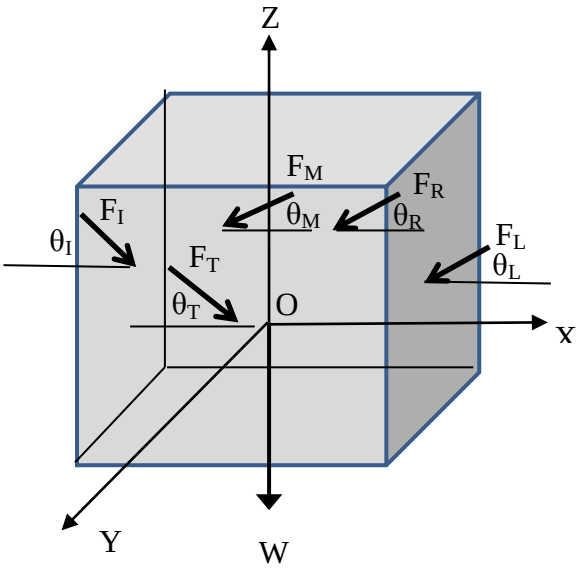

Figure 7.5: Forces applied on Cubical object.

The dimension of the cubical object is length is 5cm, breadth is 5 cm and height is also 5cm. The forces are applied at the contact points of the tips of thumb and fingers as shown in Figure 7.5.

The volume of the object is *V*, so V=5x5x5=125cm^3

Weight of the object assumed to be 3N, so W=3N.

Force Equilibrium:

The total tangential force is, F_t=W=3N

The total normal forces due to all the fingertip forces of the hand at grasping points is,

$$F_n = F_T \cos\theta_T + F_I \cos\theta_I + F_M \cos\theta_M + F_R \cos\theta_R + F_L cos\theta_L \quad (7.6)$$

From the relation 6.5, in limiting case considering the equality,

$$F_t = \mu F_n$$

$$W = \mu(F_T \cos\theta_T + F_I \cos\theta_I + F_M \cos\theta_M + F_R \cos\theta_R + F_L cos\theta_L)$$

$$0.25(F_T \cos\theta_T + F_I \cos\theta_I + F_M \cos\theta_M + F_R \cos\theta_R + F_L cos\theta_L) = 3 \quad (7.7)$$

The solution of the Eq. 7.7 will give the values of the forces exerted on the fingertips and angle of inclination of fingers. But it is observed that the equation having 10 unknowns and only one known variable *W*, which cannot be solved by

normal equation solving methods. It can either solved by hit and trial method or any new artificial intelligence techniques. Here, Adaptive Neuro-Fuzzy Inference System (ANFIS) technique is used to solve this equation and the solution for the unknown variables is predicted. The optimal solutions are obtained by using those FIS structures for each individual variable. The FIS structures are finalize using large data sets for training, testing and checking purpose. The details about the ANFIS have already been discussed in Section 5.6.4. The values of the forces and angles of inclinations are:

F_T=4.5659N, F_I=2.4546N, F_M=2.1740N, F_R=2.5274N, F_L=1.6424N,

θ_T=7.4636^0, θ_I= 6.9949^0, θ_M=6.9212^0, θ_R= 7.0788^0, θ_L=8.1463^0,

Moment Equilibrium:

Considering the point of contact of the thump tip at distance of 1 cm from the Centre of the face of the object, the coordinate of thumb contact pint is (-1cm, 2.5cm, 0).

The moment due to normal components of all the forces at contact points about Z axis is M_1.

$$M_1 = -F_T cos\theta_T . x_T - F_I cos\theta_I . y_I + F_M cos\theta_M . x_M - F_R cos\theta_R . x_R + F_L cos\theta_L . y_L \quad (7.8)$$

For moment equilibrium net moment acting on the object must be zero. So, equating Eq. 7.8 to zero the equation reduced to

$$-F_I cos\theta_I . y_I + F_M cos\theta_M . x_M - F_R cos\theta_R . x_R + F_L cos\theta_L . y_L = F_T cos\theta_T . x_T \quad (7.9)$$

Now, substituting the value of forces, angles calculated from the Eq. 7.7 and x-coordinate of the thumb tip position x_T, which assumed initially, the Eq. 7.9 reduced an equation having 4 unknown variables i.e. y_I, x_M, x_R and y_L. Similarly, by using ANFIS technique the Eq. 6.9 solved and the values of unknowns predicted as y_I=0.9538cm, x_m=1.7344cm, x_R=1.0659cm and y_L=1.3985cm.

7.4.2 Cylindrical Object

The dimension of the cylinder is considered as diameter of the base is 5cm diameter and height is 5cm.The thumb and fingers tip positions are shown in Figure 7.6.

The volume of cylindrical object=$\pi r^2 h$ = π(2.5)^{2}x5 =98.175cm^3

The proportionate weight of cylindrical object= W= 98.175x3/125=2.36N

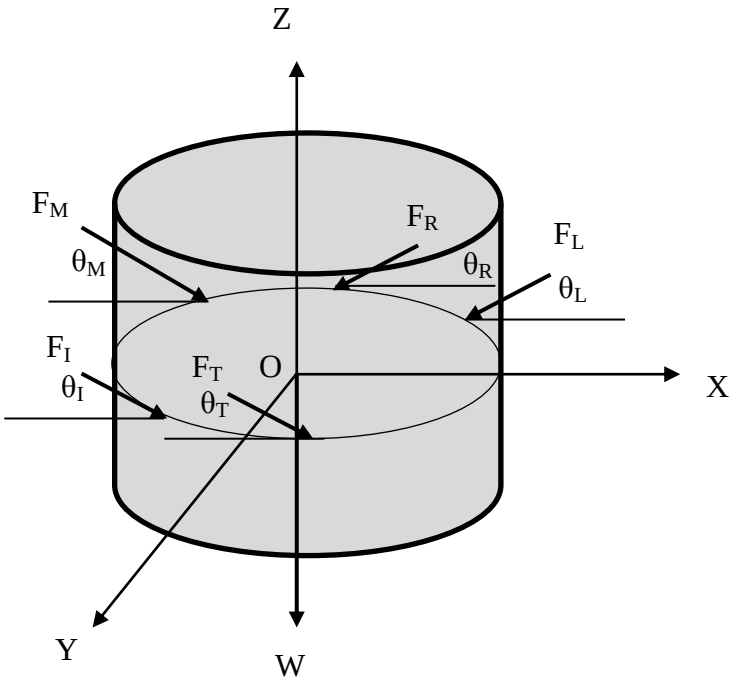

Figure 7.6: Forces applied on cylindrical object.

Force equilibrium:

The total tangential force,

$F_t = W$=2.36N

The total normal forces due to all the fingertip forces of the hand at grasping points is,

$$F_n = F_T \cos\theta_T + F_I \cos\theta_I + F_M \cos\theta_M + F_R \cos\theta_R + F_L cos\theta_L$$

From the relation 7.5, in limiting case considering the equality,

$F_t = \mu F_n$

$W = \mu (F_T \cos\theta_T + F_I \cos\theta_I + F_M \cos\theta_M + F_R \cos\theta_R + F_L cos\theta_L)$

$$0.25(F_T \cos\theta_T + F_I \cos\theta_I + F_M \cos\theta_M + F_R \cos\theta_R + F_L cos\theta_L)=2.36 \qquad (7.10)$$

By solving the Eq. 7.10 using the ANFIS technique, the values of the forces exerted on the fingertips and angle of inclination of fingers are calculated for the given weight of the object. The forces and angles are given as:

F_T=3.0491N, F_I=2.2416N, F_M=1.9497N, F_R=2.0557N, F_L= 3.2340N.

θ_T=6.6580^0, θ_I=6.9012^0, θ_M=6.4075^0, θ_R=8.1584^0, θ_L=8.0747^0.

Moment Equilibrium:

Considering the point of contact of the thump tip at the Centre of the face of the object, the coordinate of thumb contact pint is (0, -2.5cm, 0).

The moment due to normal components of all the forces at contact points about Z axis is M_1, which is equal to zero as all normal forces are passing through the Centre point O.

The moment due to tangential components of the forces at contact points of thumb, middle finger and index finger about X-axis is M_2.

$$M_2 = F_T sin\theta_T . y_T + F_I sin\theta_I . y_I - F_M sin\theta_M . y_M - F_R sin\theta_R . y_R - F_L sin\theta_L . y_L \quad (7.11)$$

For moment equilibrium net moment acting on the object must be zero. So, equating Eq. 7.11 to zero, the equation reduced to

$$F_T sin\theta_T . y_T + F_I sin\theta_I . y_I - F_M sin\theta_M . y_M - F_R sin\theta_R . y_R - F_L sin\theta_L . y_L = 0$$

$$F_I sin\theta_I . y_I - F_M sin\theta_M . y_M - F_R sin\theta_R . y_R - F_L sin\theta_L . y_L = -F_T sin\theta_T . y_T \quad (7.12)$$

Now, substituting the value of forces and angles, calculated from Eq. 7.10 and y-coordinate of the thumb tip position y_T, the equation reduced to an equation having 4 unknowns. The Eq. 7.12 solved using ANFIS and values of unknown coordinates calculated as y_I=0.8587cm, y_M=1.6664cm, y_R= 1.4039cm and y_L=0.5475cm.

7.4.3 Conical Object

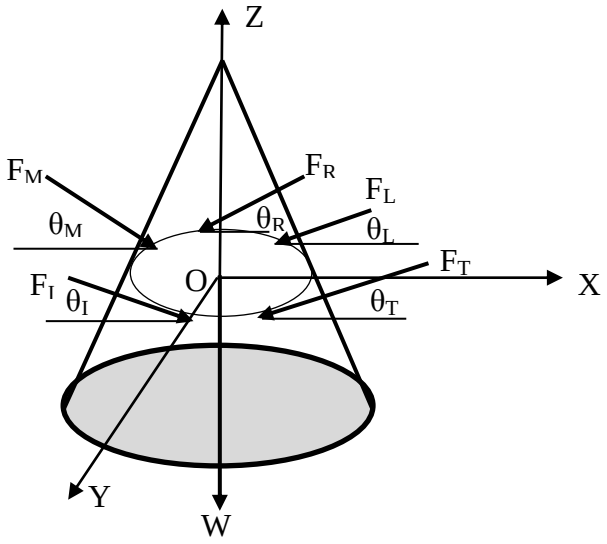

Figure 7.7: Forces applied on conical object.

The grasping of a conical object by the hand is shown in Figure 7.7. The dimension of the object is considered as, diameter of base is equal to 5cm and height is equal to 5cm.

Volume of the object is, $V = \pi r^2 h/3 = \pi(2.5)^2 x5 /3 = 32.725 cm^3$

The proportionate weight of the conical object is, W =32.725x3/125=0.785N.

The angle made by the surface of the cone with horizontal base of the conical object is, $\alpha = \tan^{-1}(5/2.5) = 63.43^0$

Force Equilibrium:

The total tangential force,

$F_t = W$=0.785N

The total normal forces due to all the fingertip forces of the hand at grasping points is,

$$F_n = F_T \cos\theta_T + F_I \cos\theta_I + F_M \cos\theta_M + F_R \cos\theta_R + F_L cos\theta_L$$

From the relation 7.5, in limiting case considering the equality,

$F_t = \mu F_n$

$$W = \mu (F_T \cos\theta_T + F_I \cos\theta_I + F_M \cos\theta_M + F_R \cos\theta_R + F_L cos\theta_L) \sin \propto$$

$$0.25(F_T \cos\theta_T + F_I \cos\theta_I + F_M \cos\theta_M + F_R \cos\theta_R + F_L cos\theta_L) = 0.878 \qquad (7.13)$$

The Eq. 7.13 solved using ANFIS and the values of the fingertip forces and angle of inclination are calculated as:

F_T =0.7109N, F_I =0.5796N, F_M =0.6519N, F_R =0.5824N, F_L =0.6666N.

$\theta_T = 8.1873^0$, $\theta_I = 6.4157^0$, $\theta_M = 6.2148^0$, $\theta_R = 7.0284^0$, $\theta_L = 7.8347^0$.

Moment Equilibrium:

Considering the point of contact of the thump tip at the Centre of the face of the object, the coordinate of thumb contact pint is (0, -0.0167m, 0).

The moment due to normal components of all the forces at contact points about Z axis is M_1.

$$M_1 = 0$$

The moment due to tangential components of the forces at contact points of thumb, middle finger and index finger about X-axis is M_2.

$$M_2 = F_T \sin(\theta_T + 26.57)\,.\,y_T - F_I sin(\theta_I + 26.57).\,y_I - F_M sin(\theta_M + 26.57).\,y_M - F_R \sin(\theta_R + 26.57).\,y_R + F_L \sin(\theta_L + 26.57).\,y_L \quad (7.14)$$

For moment equilibrium net moment acting on the object must be zero. So, equating Eq. 7.14 to zero, the equation reduced to

$$F_T \sin(\theta_T + 26.57)\,.\,y_T - F_I sin(\theta_I + 26.57).\,y_I - F_M sin(\theta_M + 26.57).\,y_M - F_R \sin(\theta_R + 26.57).\,y_R + F_L \sin(\theta_L + 26.57).\,y_L = 0$$

$$F_I sin(\theta_I + 26.57).\,y_I - F_M sin(\theta_M + 26.57).\,y_M - F_R \sin(\theta_R + 26.57).\,y_R - F_L sin(\theta_L + 26.57).\,y_L = -F_T sin(\theta_T + 26.57).\,y_T \quad (7.15)$$

Substituting the values of forces and angles calculated earlier and the value of y_T which is assumed, the equation reduced to a 4 unknown equation which is solved by ANFIS and the values of unknown y-coordinates calculated as: y_I=1.0210cm, y_M=0.7459cm, y_R= 0.7691cm and y_L=0.1984cm.

7.4.4 Trapezoidal Object

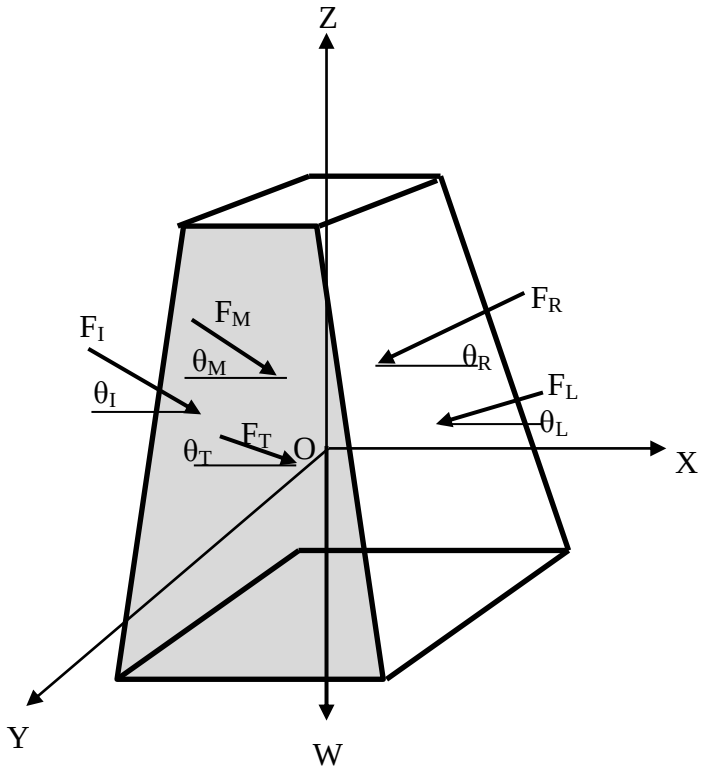

Figure 7.8: Forces applied on trapezoidal object.

The dimension of the object considerd as side of the base square is 5cm, side of top square is 2cm and keight is 5cm. The grasping forces applied on the obejct by the thumb and fingers of the hand is shown in Figure 7.8.

Volume of the object is, V=64cm^3

The proportionate weight of trapizoidal object is, W=3x64/125=1.54N

The angle of inclination surfaces with horizontal is, $\alpha = \tan^{-1}(5/1.5)=73.3^0$

Force Equilibrium:

So, the total tangential force,

$$F_t = W$$

The total normal forces due to all the fingertip forces of the hand at grasping points is,

$$F_n = F_T \cos\theta_T + F_I \cos\theta_I + F_M \cos\theta_M + F_R \cos\theta_R + F_L cos\theta_L$$

From the relation 7.5, in limiting case considering the equality,

$$F_t = \mu F_n$$

$$W = \mu (F_T \cos\theta_T + F_I \cos\theta_I + F_M \cos\theta_M + F_R \cos\theta_R + F_L cos\theta_L) \sin(\propto)$$

$$0.25(F_T \cos\theta_T + F_I \cos\theta_I + F_M \cos\theta_M + F_R \cos\theta_R + F_L cos\theta_L) = 1.61 \quad (7.16)$$

The Eq. 7.16 solved for fingertip forces and inclined angles using ANFIS and the values are given as:

F_T=1.2118N, F_I=1.1546N, F_M=1.4931N, F_R=1.4308N, F_L=1.1615N.

θ_T=6.8430^0, θ_I=6.0827^0, θ_M=6.7140^0, θ_R=6.8392^0, θ_L=7.0604^0.

Moment Equilibrium:

Considering the point of contact of the thump tip at the Centre of the face of the object, the coordinate of thumb contact pint is (0.3cm, -0.018m, 0).

The moment due to normal components of all the forces at contact points about Z axis is M_1.

$$M_1 = F_I cos(\theta_I + 16.7).y_I + F_I \cos(\theta_I + 16.7).y_I - F_M \cos(\theta_M + 16.7).x_M - F_R cos(\theta_R + 16.7).x_R + F_L cos(\theta_L + 16.7).y_L \quad (7.17)$$

For moment equilibrium net moment acting on the object must be zero. So, equating Eq. 7.17 to zero, the equation reduced to

$$-F_I \cos(\theta_I + 16.7) \,.\, y_I + F_M cos(\theta_M + 16.7).\, x_M + F_R \cos(\theta_R + 16.7) \,.\, x_R - F_L cos(\theta_L + 16.7).\, y_L = F_T cos(\theta_T + 16.7).\, x_T \quad (7.18)$$

Eq.7.18 solved using ANFIS and considering the calculated valuses of forcces and angles and assumed value of x_T, the values of unknown coordinates given as: y_I=1.4990cm, y_M=0.8518cm, x_R= 0.7379cm and x_L=1.4310cm.

7.4.5 Parallelepiped Object

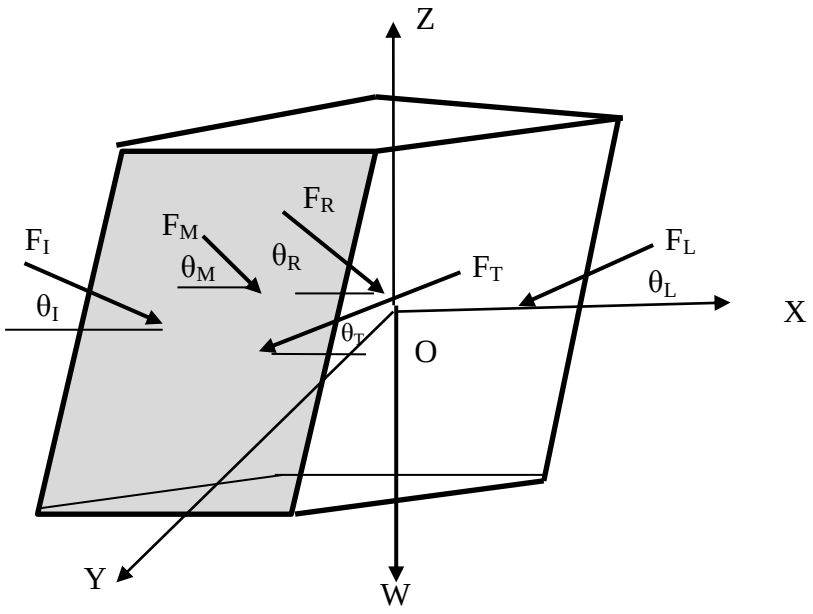

Figure 7.9: Forces applied on parallelepiped object.

Each side of the object is taken as 5cm.

Volume of the object is same as cubical object, so the weight of the object is '*W*' also taken as 3N. The angle of inclination of the inclined face is 60^0 with the horizonta. The point od contacts and applied forces are shown in Figure 6.9.

Force Equilibrium:

The total vertical component of the tangential forces,

$F_t = W$

The total normal forces due to the fingertip forces of the hand at grasping points of the two vertical faces of the object is,

$F_{n1} = F_I \cos\theta_I + F_M \cos\theta_M$

The total normal forces due to the fingertip forces of the hand at grasping points of the two inclined faces of the object is,

$F_{n2} = F_T \cos\theta_T + F_R cos\theta_R + F_L cos\theta_L$

From the relation 7.5, in limiting case considering the equality,

$F_t = \mu(F_{n1} + F_{n2} \cos \propto)$

W= μ ($F_T \cos\theta_T \cos \propto + F_I \cos\theta_I + F_M \cos\theta_M + F_R \cos\theta_R \cos \propto + F_L cos\theta_L \cos \propto$)

$0.25(F_T \cos\theta_T \cos \propto + F_I \cos\theta_I + F_M \cos\theta_M + F_R \cos\theta_R \cos \propto +$
$F_L cos\theta_L \cos \propto)$ =W=3 (7.19)

Using ANFIS, the Eq. 7.19 solved for the fingertip forces and inclined angles with the given weight of the object, W =3N. The values are given as:

F_T=4.5659N, F_I=2.4546N, F_M=2.1740N, F_R=2.5274N, F_L= 1.6424N.

θ_T=7.4636^0, θ_I=6.9949^0, θ_M=6.9212^0, θ_R= 7.0788^0, θ_L= 8.1403^0.

Moment Equilibrium:

Considering the point of contact of the thump tip at a distance of 1 cm from the Centre of the face of the object, the coordinate of thumb contact pint is (1cm, -2.5cm, 0).

The moment due to normal components of all the forces at contact points about Z axis is M_1.

$M_1 = F_T cos(\theta_T + \propto).x_T + F_I cos\theta_I.y_I - F_M cos\theta_M.y_M + F_R cos(\theta_R + \propto).x_R -$
$F_L \cos(\theta_L + \propto).y_L$ (7.20)

For moment equilibrium net moment acting on the object must be zero. So, equating Eq. 7.20 to zero, the equation reduced to

$-F_I cos\theta_I.y_I + F_M cos\theta_M.y_M - F_R cos(\theta_R + \propto).x_R + F_L cos(\theta_L + \propto).x_L =$
$F_T \cos(\theta_T + \propto).x_T$ (7.21)

Using ANFIS, Eq. 7.21 solved for the unknown coordinates considering the fingertip forces and inclined angles calculated earlier and the assumed value of the x_T. the values of coordinates are: y_I=1.0263cm, y_M=1.5549cm, x_R=1.1106cm and x_L=1.5785cm.

7.5 Stress Analysis of the Thumb and the Fingers using ANSYS

During grasping an object of any shape the fingers of the hand are applying forces on the objet at the point of contacts particularly in case of force closure grasp. As discussed in section 6.4, the tangential component of these forces must be equal to the weight of the object in limiting case so that the hand can perform an equilibrium grasp. Whenever fingers are applying forces on the object and equal amount of reaction forces are also exerted on the fingers. These forces are transmitted to the thumb and fingers which distributed over it. The analysis of the stress concentration over the thumb and fingers of the hand due to the reaction forces exerted on the fingertips at point of contacts are made. Since the point of interest is to check the stress concentration at the critical points of the finger-links, plane stress is the consideration for analysis. Therefore, equivalent von Mises stress is determined using ANSYS-13. The following sub-sections describe the underlying principles and theories of von Mises criterion used in the present work.

7.5.1 Von Mises Yield Criterion

The von Mises yield criterion suggests that the yielding of materials begins when the second deviatoric stress invariant J_2 reaches a critical value. For this reason, it is sometimes called the J_2-plasticity or J_2 flow theory. It is part of a plasticity theory that applies best to ductile materials, such as metals. Prior to yield, material response is assumed to be elastic.

The von Mises yield criterion can be also formulated in terms of the von Mises stress or equivalent tensile stress, σ_x, a scalar stress value. In this case, a material is said to start yielding when its von Mises stress reaches a critical value known as the yield strength, σ_y. The von Mises stress is used to predict yielding of materials under any loading condition from results of simple uniaxial tensile tests. The von Mises stress satisfies the property that two stress states with equal distortion energy have equal von Mises stress.

Because the von Mises yield criterion is independent of the first stress invariant, I_1, it is applicable for the analysis of plastic deformation for ductile materials such as metals, as the onset of yield for these materials does not depend on the hydrostatic component of the stress tensor.

Mathematical Formulation

Mathematically the von Mises yield criterion is expressed as:

$$J_2 = k^2 \tag{7.22}$$

Where k is the yield stress of the material in pure shear. As shown later, at the onset of yielding, the magnitude of the shear yield stress in pure shear is √3 times lower than the tensile yield stress in the case of simple tension. Thus we have:

$$k = \frac{\sigma_y}{\sqrt{3}} \tag{7.23}$$

where σ_y is the yield strength of the material. If the von Mises stress is set equal to the yield strength and Eq. 7.22 and Eq. 7.23 are combined, the von Mises yield criterion can be expressed as:

$$\sigma_v = \sigma_y = \sqrt{3J_2} \qquad \text{or} \qquad \sigma_v^2 = 3J_2 = 3k^2 \tag{7.24}$$

Substituting J_2 with terms of the Cauchy stress tensor components

$$\sigma_v^2 = \frac{1}{2}[(\sigma_{11} - \sigma_{22})^2 + (\sigma_{22} - \sigma_{33})^2 + (\sigma_{11} - \sigma_{33})^2 + 6(\sigma_{23}^2 + \sigma_{31}^2 + \sigma_{12}^2)] \tag{7.25}$$

This equation defines the yield surface as a circular cylinder whose yield curve, or intersection with the deviatoric plane, is a circle with radius$\sqrt{k}$, or$\sqrt{\frac{2}{3}\sigma_y}$. This implies that the yield condition is independent of hydrostatic stresses.

7.5.2 Reduced von Mises Equation for Different Stress Conditions

Eq. 6.25 can be reduced and reorganized for practical use in different loading scenarios. In the case of uniaxial stress or simple tension, $\sigma_1 \neq 0, \sigma_3 = \sigma_2 = 0,$ the von Mises criterion simply reduces to $\sigma_1 = \sigma_y$, which means the material starts to yield when σ_1 reaches the yield strength of the material σ_y, and is in agreement with the definition of tensile (or compressive) yield strength.

It is also convenient to define an equivalent tensile stress or von Mises stress,σ_v, which is used to predict yielding of materials under multi-axial loading conditions using results from simple uniaxial tensile tests. Thus,

$$\sigma_v = \sqrt{3J_2}$$

$$= \sqrt{\frac{(\sigma_{11} - \sigma_{22})^2 + (\sigma_{22} - \sigma_{33})^2 + (\sigma_{11} - \sigma_{33})^2 + 6(\sigma_{23}^2 + \sigma_{31}^2 + \sigma_{12}^2)}{2}}$$

$$= \sqrt{\frac{(\sigma_1 - \sigma_2)^2 + (\sigma_2 - \sigma_3)^2 + (\sigma_1 - \sigma_3)^2}{2}} = \sqrt{\frac{3}{2}s_{ij}s_{ij}}$$

Where $s_{ij}$are the components of the stress deviator tensor σ^{dev} :

$$\sigma^{dev} = \sigma - \frac{1}{3}(tr\sigma)\mathrm{I}$$

By means of the von Mises yield criterion, which depends solely on the value of the scalar von Mises stress, i.e., one degree of freedom, this comparison is straightforward: A larger von Mises value implies that the material is closer to the yield point.

The Table 7.1 summarizes von Mises yield criterion for the different stress conditions.

Table 7.1: Von Mises yield criteria for different stress conditions.

Load scenario	**Restrictions**	**Simplified von Mises equation**
General	No restrictions	$\sigma_v = \sqrt{\frac{1}{2}[(\sigma_{11}-\sigma_{22})^2 + (\sigma_{22}-\sigma_{33})^2 + (\sigma_{11}-\sigma_{33})^2 + 6(\sigma_{12}^2+\sigma_{23}^2+\sigma_{31}^2)]}$
Principal stresses	$\sigma_{12} = \sigma_{13} = \sigma_{23} = 0$	$\sigma_v = \sqrt{\frac{1}{2}[(\sigma_1-\sigma_2)^2 + (\sigma_1-\sigma_3)^2 + (\sigma_2-\sigma_3)^2]}$
Plane stress	$\sigma_3 = 0$ $\sigma_{31} = \sigma_{23} = 0$	$\sigma_v = \sqrt{\sigma_1^2 + \sigma_1\sigma_2 + \sigma_2^2 + 3\sigma_{12}^2}$
Pure shear	$\sigma_1 = \sigma_2 = \sigma_3 = 0$ $\sigma_{31} = \sigma_{23} = 0$	$\sigma_v = \sqrt{3\sigma_{12}}$
Uniaxial	$\sigma_2 = \sigma_3 = 0$ $\sigma_{12} = \sigma_{31} = \sigma_{23} = 0$	$\sigma_v = \sigma_1$

Notes: Subscripts 1, 2, 3 can be replaced with x, y, z, or other orthogonal coordinate system

7.5.3 Physical Interpretation of the von Mises Yield Criterion

A physical interpretation of von Mises criterion suggests that yielding begins when the elastic energy of distortion reaches a critical value. For this, the von Mises criterion is also known as the maximum distortion strain energy criterion.

7.5.4 Parameters Considered for Present Analysis

For analysing the stress concentration on the fingers due to forces exerted during grasping of an object, the different parameters taken into consideration are:

i) dimension of finger segments,

ii) material of the hand and

iii) forces exerted on the fingers.

In the present analysis the length of thumb and finger segments are taken as given in chapter 3. The analysis is made under following assumption and considerations:

- The cross-section of thumb and all finger segments assumed to be square cross-section for convenience of building and putting points even though the real human hand cross-section is elliptical. In the present work the cross-section considered as of 1cmx1cm dimension.
- The joints between the links of the thumb and fingers are considered as revolute joints providing rotational motions only.
- Only plain stress condition is considered in the present work.
- Static structural analysis is made for thumb and all fingers.
- Type of element considered is tetrahedral.
- Type of loading: Uniaxial force.
- The boundary conditions: Joints are fixed.

The 3-D modelling of the proposed five-fingered anthropomorphic hand is done using CATIA which shown in Figure 6.17 and that 3-D model used here for analysis. The CATIA model imported to ANSYS environment and divided into numbers of small tetrahedron elements having 8 nodes, the meshed view of the hand model is shown in Figure 7.10 and the total number of nodes on the thumb and fingers are given in Table 7.2.

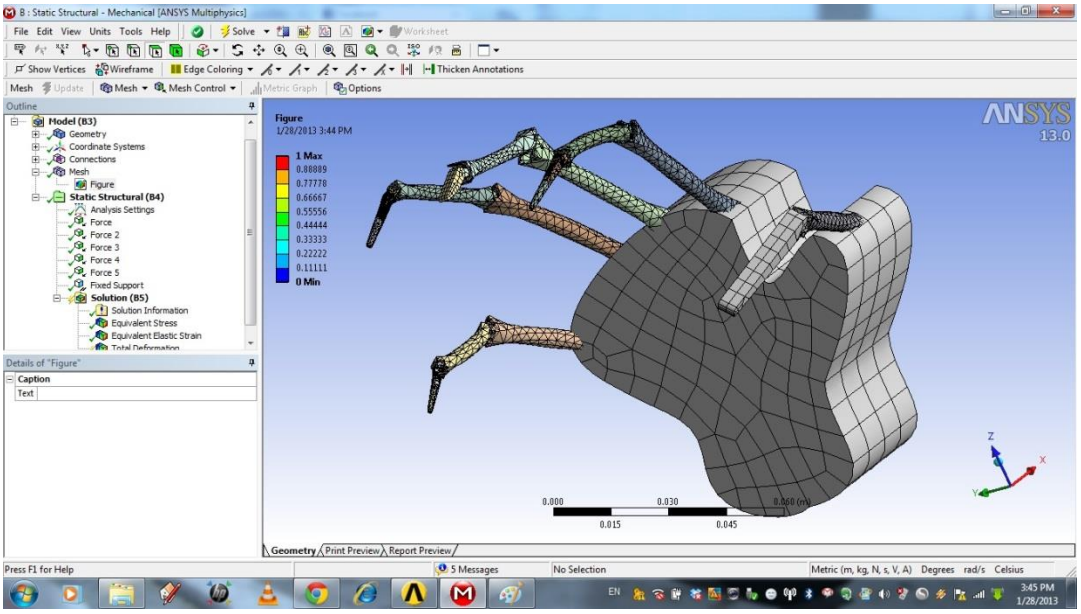

Figure 7.10: Meshed view of proposed hand model.

Table 7.2: Number of nodes on thumb and fingers.

Fingers	Total Number of nodes
Thumb	1792
Index finger	1223
Middle finger	2566
Ring finger	1947
Little finger	1692

Material: In the present analysis two different materials are considered one is Aluminium and other one is structural steel. The properties of material like Young's modulus and Poisson's ratio are taken the standard values as given in Table 7.3:

Table 7.3: Properties of used material.

Material	Young's modulus in N/m^2	Poisson's ratio
Aluminium alloy	$70x10^9$	0.33
Structural steel	$200x10^9$	0.3

The forces are assumed to be applied axially. Then taking into consideration the magnitude of the forces and values of incident angles (determined in section 7.4), the stresses at different points on the surface of the fingers are found out and also the point of stress concentration is marked. The results of the present analysis are given in chapter 8.

7.6 Summary

The detail calculation of forces and incident angles for grasping different shaped objects by five-fingered anthropomorphic hand is presented in this chapter. A simplest case of grasping is considered first with two fingers, from that the effect of co-efficient of friction between object surface and fingertip and angle of inclination on the force exerted in fingertip on grasping are analysed. Then the analysis extended to grasping of different shaped objects i.e. cubical, cylindrical, conical, trapezoidal and parallelepiped by five-fingered anthropomorphic hand. The forces on fingertips and point of contacts determined for a stable and equilibrium force closure grasp. Finally the analysis made for stress concentration on fingers due to grasping of objects using ANSYS-13. For the stress analysis two different type of material considered one is aluminium alloy and other is structural steel. All the results are presented in chapter 8.

Chapter 8

RESULTS AND ANALYSIS

8.1 Overview

The previous chapters have been primarily devoted to elaborately deal with the back ground of the research, developing model of the anthropomorphic robot hand, carrying out the kinematic analysis of the models as well as the grasp analysis including the stress analysis of the hand. The results so obtained in different analysis are summarized and presented in this chapter under following subsection as:

- Results of forward kinematic analysis and resulting work space of the hand.
- Results of inverse kinematic analysis of the hand
- Results of the forces exerted and position of fingertip while grasping different shaped objects for manipulation.
- Results of stress analysis on the thumb and fingers of the hand due to the grasping forces.

In order to have an integrated view of the exercise done and carry out proper analysis, all the results have been collated and are presented in this chapter.

8.2 Forward Kinematics Analysis

Typically, a robotic manipulator is designed to perform the task in 3-D space. The tool or end effector is required to follow a planned trajectory to grasp and/or manipulate the object in workspace. The control of the position of each link and joint of manipulator is required to control the position and orientation of the end-effector of the manipulator. The kinematical model describes the position of link

and joint of manipulator and the position of the end-effector. In forward kinematics a mathematical relationship is derived to know the position of end-effector for a particular configuration of the manipulator. Since thumb and each individual finger of the hand are considered as independent manipulator, the fingertips of the thumb and fingers are considered as the tool centre point. The positions of the fingertips are calculated using the mathematical formula for forward kinematics derived in Chapter-4. The variables used for calculating the fingertip positions are length of thumb and fingers segments which are considered as links of the manipulator and joint angles. A code is written in MATLAB-8 to determine the position of fingertips considering the segmental lengths and joint angles given in Chapter-3 for the proposed hand model and the results are presented in following sections.

8.2.1 Results of Position of tip of the Thumb

In the proposed hand model the thumb is considered as a 5-DOFs manipulator. Each segment of the thumb is taken as link of the manipulator. The proportionate length of segments of the thumb determined using formula given in Table 5.1 and Table 5.2. Considering these values and the angles within the respective range (as per Table 4.4), the position of the tip of the thumb is determined through a programme written in MATLAB using the forward kinematics equation developed in Chapter 4 (with respect to local coordinate system having origin at CMC joint).

Table 8.1: Position of the tip of the thumb with respect to CMC joint.

CMC joint		MCP joint		IP joint	Coordinates of the tip position w.r.t. local coordinate system.		
Abduction /adduction angle (q_1) in degree	Flexion/ extension angle (q_2) in degree	Abduction /adduction angle (q_3) in degree	Flexion/ extension angle (q_4) in degree	Flexion/ extension angle (q_5) in degree	X-coordinate in cm.	Y-coordinate in cm.	Z-coordinate in cm.
0	-25	0	-10	-15	9.0576	0	6.2814

The position of thumb's tip in terms of X, Y, and Z coordinates with respect to local coordinate system is presented in Table 8.1. The trajectory of the tip of the thumb with respect to the local coordinate system having origin at CMC joint is shown in Figure 8.1.

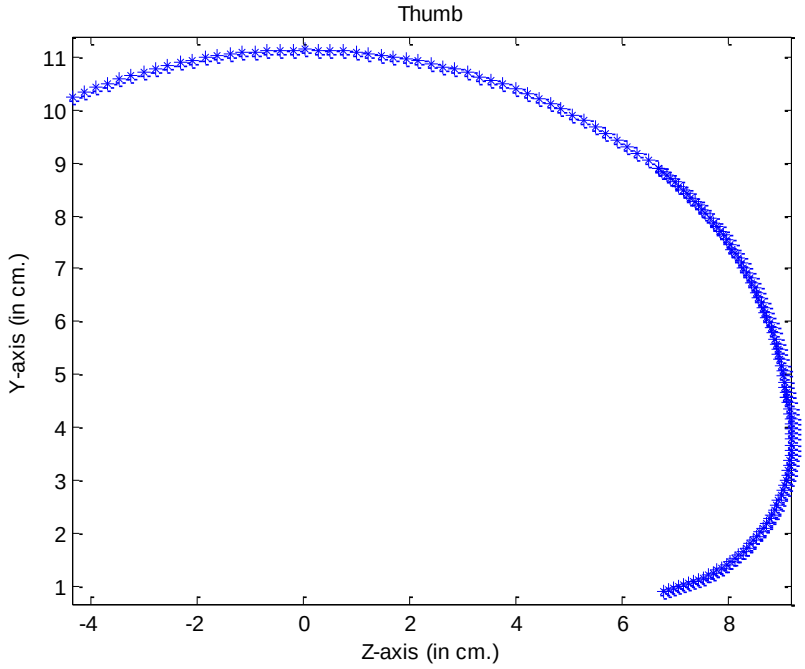

Figure 8.1: Trajectory of the tip of the thumb.

In the proposed hand model the wrist is considered as the origin of the global coordinate system. Introducing the transfer matrix for transferring the origin from CMC joint to wrist as discussed in Chapter 5, the position of the tip of the thumb is determined with respect to global coordinate system and the values are given in Table 8.2.

Table 8.2: Position of the tip of the thumb w.r.t. wrist.

CMC joint		MCP joint		IP joint	Coordinates of the tip position w.r.t. global coordinate system.		
Abduction /adduction angle (q_1) in degree	Flexion/ extension angle (q_2) in degree	Abduction /adduction angle (q_3) in degree	Flexion/ extension angle (q_4) in degree	Flexion/ extension angle (q_5) in degree	X-coordinate in cm.	Y-coordinate in cm.	Z-coordinate in cm.
0	-25	0	-10	-15	5.5353	7.4944	6.2815

8.2.2 Results of Fingertip position of Index Finger

The index finger is also considered as an individual manipulator with three joints and four links having 4-DOFs. The segments are considered as individual link and the proportionate lengths are calculated using formula given in Table 5.1 and Table 5.2. For a set of specific values of the all the four angles of the finger from the range given in Table 4.5, the position of fingertip is determined using the code

developed in MATLAB-8. The results are presented in Table 8.3 in terms of X, Y and Z coordinates of the tip position with respect to MCP joint which is considered as the origin of local coordinate system.

Table 8.3: Position of the tip of the index finger w.r.t. MCP joint.

MCP joint		PIP joint	DIP joint	Coordinates of the tip position w.r.t. local coordinate system.		
Abduction/ adduction angle (q_6) in degree	Flexion/ extension angle (q_7) in degree	Flexion/ extension angle (q_8) in degree	Flexion/ extension angle (q_9) in degree	X-coordinate in cm.	Y- coordinate in cm.	Z- coordinate in cm.
-12	42	36	53	2.9501	-0.6271	-7.2224

Figure 8.2 shows the positions of the fingertip of the index finger with respect to local coordinate system at MCP joint by varying the joint angles in their respective ranges. The trajectory of the index fingertip is drawn in Y-Z plane. By transferring the coordinate systems from local to global, having origin at MCP joint and wrist respectively with multiplication of the corresponding transfer matrix as given in Chapter 5 the coordinates of the index fingertip are calculated. The values of the fingertip position in terms of X, Y and Z coordinates with respect to wrist is presented in Table 8.4.

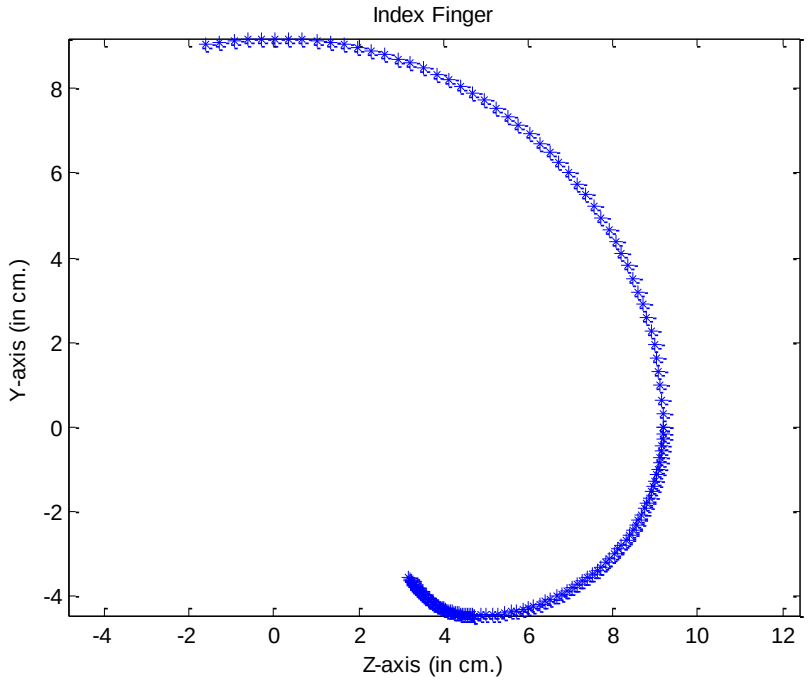

Figure 8.2: Trajectory of index fingertip.

Table 8.4: Position of the tip of the index finger w.r.t. wrist.

MCP joint		PIP joint	DIP joint	Coordinates of the tip position w.r.t. global coordinate system.		
Abduction/ adduction angle (q_6) in degree	Flexion/ extension angle (q_7) in degree	Flexion/ extension angle (q_8) in degree	Flexion/ extension angle (q_9) in degree	X-coordinate in cm.	Y- coordinate in cm.	Z- coordinate in cm.
-12	42	36	53	2.1509	6.6962	-7.2224

8.2.3 Results of Fingertip Position of Middle Finger

A manipulator with three joints and four links is in resemblance with the middle finger of the proposed hand model. The segments of the finger are considered as links whose lengths are calculated for an adult male human being. The position of the middle finger tip is determined for a set of particular values of the all four angles from the permissible range using the developed computer program in MATLAB-8 platform. The values of the coordinates of the tip position with respect to the local coordinate system at MCP joint of the finger are given in Table 8.5.

Table 8.5: Position of the tip of the middle finger w.r.t. MCP joint.

MCP joint		PIP joint	DIP joint	Coordinates of the tip position w.r.t. local coordinate system.		
Abduction/ adduction angle (q_{10}) in degree	Flexion/ extension angle (q_{11}) in degree	Flexion/ extension angle (q_{12}) in degree	Flexion/ extension angle (q_{13}) in degree	X-coordinate in cm.	Y- coordinate in cm.	Z- coordinate in cm.
21	52	76	63	-0.6933	-0.2661	-6.1352

Varying the values of the joint angles of the middle finger in their respective ranges the fingertip positions are determined and plotted in Y-Z plane as shown in Figure 8.3.

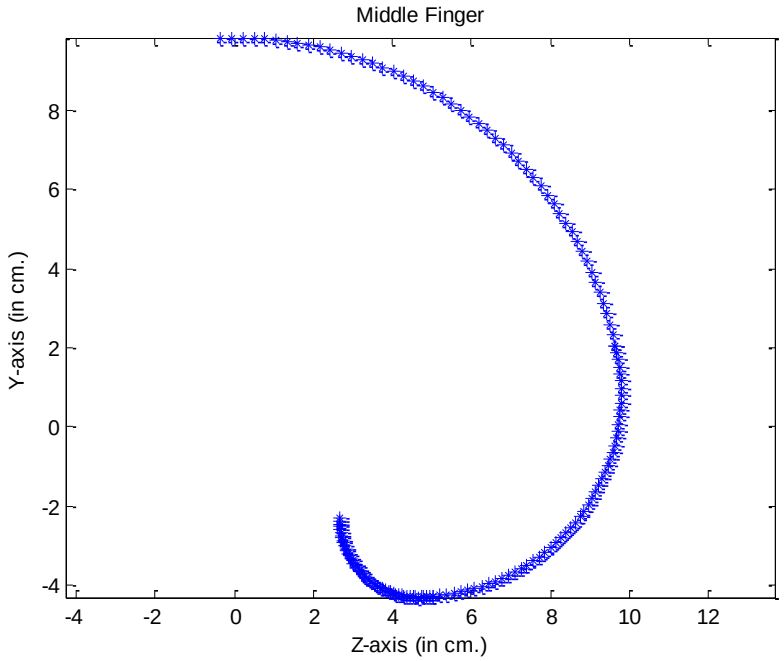

Figure 8.3: Trajectory of middle fingertip.

The position of the middle finger tip is calculated with respect to global coordinate system having origin at wrist of the hand by transferring local to global coordinate system. The values of the coordinates of the middle finger tip are given in Table 8.6.

Table 8.6: Position of the tip of the middle finger w.r.t. wrist.

MCP joint		PIP joint	DIP joint	Coordinates of the tip position w.r.t. global coordinate system.		
Abduction/ adduction angle (q_{10}) in degree	Flexion/ extension angle (q_{11}) in degree	Flexion/ extension angle (q_{12}) in degree	Flexion/ extension angle (q_{13}) in degree	X-coordinate in cm.	Y- coordinate in cm.	Z- coordinate in cm.
21	52	76	63	-2.1679	6.3084	-6.1352

8.2.4 Results of Fingertip Position of Ring Finger

The ring finger has four joints and five links. Unlike middle and index finger this has two more DOFs at CMC joint, as whole it has 6 DOFs. The link lengths are determined considering the finger segments are links using the formula given in Table 5.1 and Table 5.2. A set of values for all six angles of the finger are chosen from the range given in Table 4.7. With the help of a MATLAB program, the positions of the ring fingertip are calculated (using these values of the angles). The

results are presented in Table 8.7 in the form of X, Y, and Z coordinates with respect to CMC joint of the finger as origin of the coordinate system.

Table 8.7: Position of the tip of the ring finger w.r.t. CMC joint.

CMC joint		MCP joint		PIP joint	DIP joint	Coordinates of the tip position w.r.t. local coordinate system.		
Abduction /adduction angle (q_{14}) in degree	Flexion/ extension angle (q_{15}) in degree	Abduction /adduction angle (q_{16}) in degree	Flexion/ extension angle (q_{17}) in degree	Flexion/ extension angle (q_{18}) in degree	Flexion/ extension angle (q_{19}) in degree	X-coordinate in cm.	Y-coordinate in cm.	Z-coordinate in cm.
2	6	11	46	74	81	5.6100	0.1872	6.005

The fingertip positions are calculated with respect to local coordinate system having origin at CMC using MATLAB for the full range of the joint angles and the same are plotted as shown in Figure 8.4 as the trajectory of the ring fingertip in Y-Z plane.

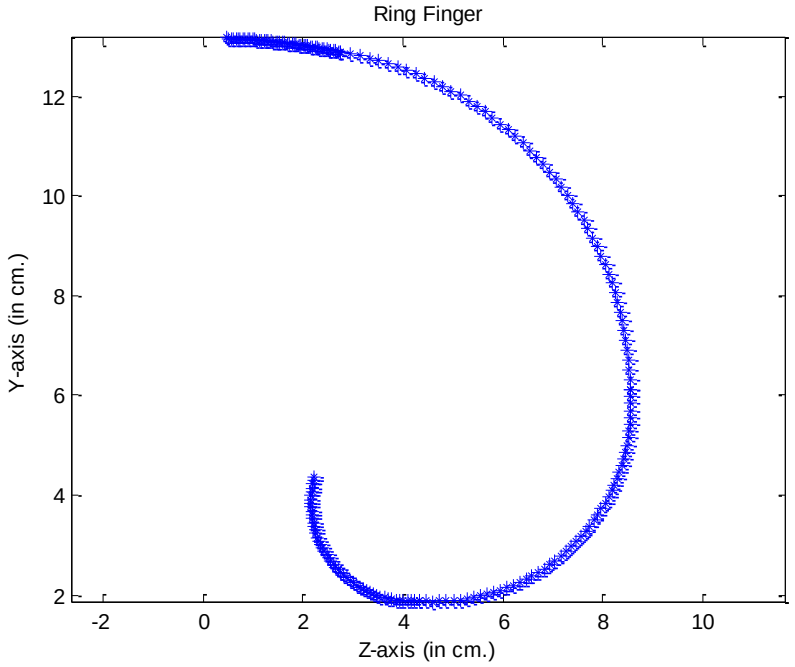

Figure 8.4: Trajectory of ring fingertip.

The fingertip positions are then calculated with respect to wrist which is considered as the origin of global coordinate system. This global coordinate system is for the thumb and all the fingers. The position of ring fingertip is presented in Table 8.8 in terms of X, Y and Z coordinates.

Table 8.8: Position of the tip of the ring finger w.r.t. wrist.

CMC joint		MCP joint		PIP joint	DIP joint	Coordinates of the tip position w.r.t. global coordinate system.		
Abduction /adduction angle (q_{14}) in degree	Flexion/ extension angle (q_{15}) in degree	Abduction /adduction angle (q_{16}) in degree	Flexion/ extension angle (q_{17}) in degree	Flexion/ extension angle (q_{18}) in degree	Flexion/ extension angle (q_{19}) in degree	X-coordinate in cm.	Y-coordinate in cm.	Z-coordinate in cm.
2	6	11	46	74	81	4.8699	3.6569	-6.005

8.2.5 Results of the Tip position of Little Finger

Like all other finger the little finger is modelled as a five link manipulator with four joints and six DOFs. Similarly, as done in the case of thumb and other fingers, the lengths of the finger segments are determined using formulas given in Table 5.1 and Table 5.2, which are considered as link lengths. Using the developed code in MATLAB-8 the position of the little finger tip is determined with respect to local coordinate system for a particular set of joint angles within the range (as given in Table 4.8). The results are presented in Table 8.9 in terms of X, Y, and Z coordinates with respect to local coordinate system, located at the CMC joint of the finger.

Table 8.9: Position of the tip of the little finger w.r.t CMC joint.

CMC joint		MCP joint		PIP joint	DIP joint	Coordinates of the tip position w.r.t. local coordinate system.		
Abduction /adduction angle (q_{20}) in degree	Flexion/ extension angle (q_{21}) in degree	Abduction /adduction angle (q_{22}) in degree	Flexion/ extension angle (q_{23}) in degree	Flexion/ extension angle (q_{24}) in degree	Flexion/ extension angle (q_{25}) in degree	X-coordinate in cm.	Y-coordinate in cm.	Z-coordinate in cm.
6	13	-9	62	74	32	2.9326	0.5364	6.0500

The joint angles are varied fully in their respective ranges and the positions of fingertip are determined and plotted in Y-Z plane as the trajectory of the little finger tip which is shown in Figure 8.5. The position of the little fingertip with respect to wrist, the global coordinate system, is calculated using a computer program in MATLAB-8 platform for set of joint angles and is presented in Table 8.10.

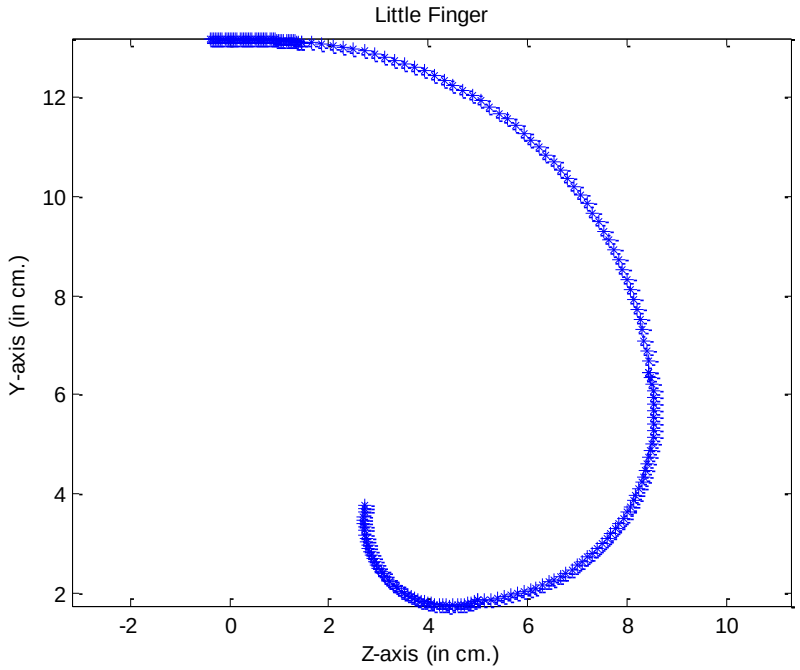

Figure 8.5: Trajectory of little fingertip.

Table 8.10: Position of the tip of the little finger w.r.t wrist.

CMC joint		MCP joint		PIP joint	DIP joint	Coordinates of the tip position w.r.t. global coordinate system.		
Abduction /adduction angle (q_{20}) in degree	Flexion/ extension angle (q_{21}) in degree	Abduction /adduction angle (q_{22}) in degree	Flexion/ extension angle (q_{23}) in degree	Flexion/ extension angle (q_{24}) in degree	Flexion/ extension angle (q_{25}) in degree	X-coordinate in cm.	Y-coordinate in cm.	Z-coordinate in cm.
6	13	-9	62	74	32	1.5086	3.7040	-6.0500

A computer code is developed in MATLAB- 8 platform to solve the forward kinematics problem of the hand model. The code is prepared in a generalized way for thumb and each finger such that by entering the values of hand length and hand breadth of the hand and a set of joint angles it will give the position of the tip in terms of X, Y and Z coordinates with respect to the local coordinate system. The results are shown in tabular form for thumb and fingers individually (Table 8.1, Table 8.3, Table 8.5, Table 8.7 and Table 8.9). It is observed that the flexion/extension motion of the joints are responsible for opening and closing of the human hand as a result for grasping the object, whereas the abduction/adduction motion contributes towards manipulation of grasped object. Therefore, the trajectory of the tips of the thumb and fingers are calculated using

MATLAB program with respect to the local coordinate frame and are plotted on a plane. These trajectories of tips give an idea about the reachable workspace of the proposed hand model. In the present work it is considered that wrist is a fixed point and act as the origin of a global coordinate system which is common for the thumb and all the fingers. By introducing the transfer matrix for transferring the coordinate system from local to global coordinate frame, the tip positions are determined and presented in tabular form (Table 8.2, Table 8.4, Table 8.6, Table 8.8 and Table 8.10).

8.3 Workspace Analysis

The workspace of a manipulator is the total volume of space the end effector can reach. The multi-fingered hand is considered as an ensemble of end effectors which consists five manipulating members. The workspace of the hand is the combination of workspace of all the fingers of the hand. Section 8.2 deals with the positions of the tip of the thumb and those of the fingers for a particular set of values of all the angles of thumb and fingers. The hand model consists of total 25-DOFs. All the 25-joint angles have a range of motion which is given in Table 4.4 through Table 4.8 in Chapter 5. The possible workspace of the proposed hand model can be visualized by plotting the tip positions of the thumb and fingers simultaneously, with all possible values of the joint angles within their respective ranges. A code is written in MATLAB-8 to determine the positions of the tip of the thumb and fingers and plotting them in 2D plane as well as 3D space. For the purpose of calculating the tip position of the thumb and fingers, the forward kinematic formula as stated in Eq. 5.11 is used. The different parameters required to evaluate the fingertip positions such as lengths of thumb and finger segments and the range of joint angles, are considered from Table 5.1, Table 5.2 and Table 4.4 through Table 4.8 respectively.

Figure 8.6 shows the all possible positions of the tip of the thumb and fingers in X-Y plane with variation of all joint angles in their respective ranges. This also shows the workspace of the proposed hand model in X-Y plane as the projection of the 3D workspace of the hand in X-Y plane.

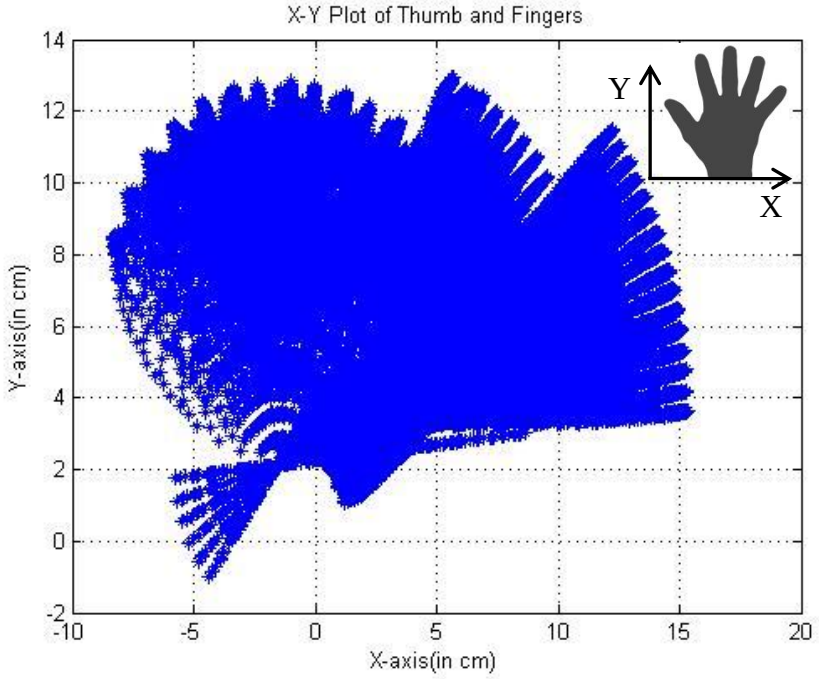

Figure 8.6: The positions of the tip of the thumb and finger in X-Y plane.

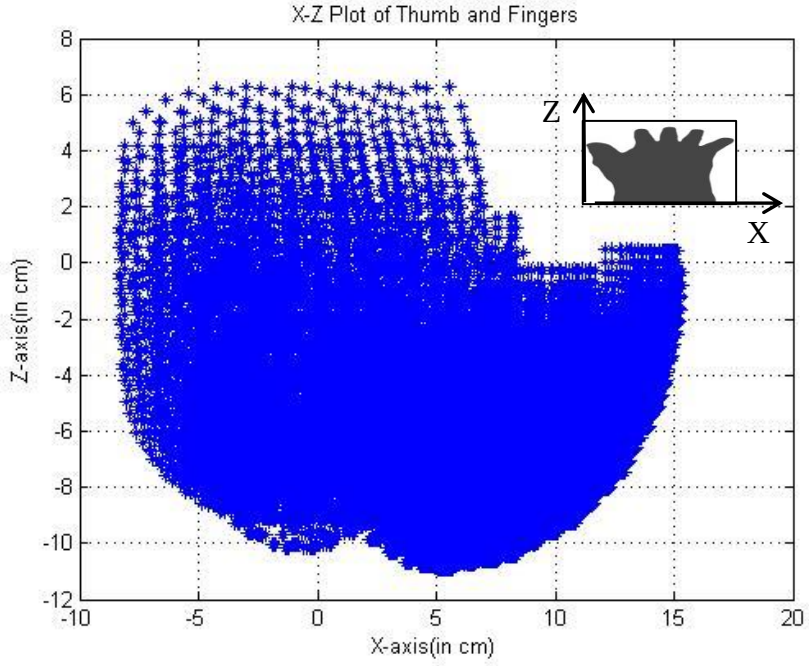

Figure 8.7: The positions of the tip of the thumb and finger in X-Z plane.

All the fingertip positions of the hand in the X-Z plane are plotted by varying the joint angles in their respective ranges and the same is shown in Figure 8.7. This shows the workspace of the hand in the X-Z plane.

The workspace of the proposed hand model is depicted in Figure 8.8 by plotting the tip positions of the thumb and the fingers simultaneously for the full range of joint angles. This also shows the projection of the 3D workspace of the hand in Y-Z plane.

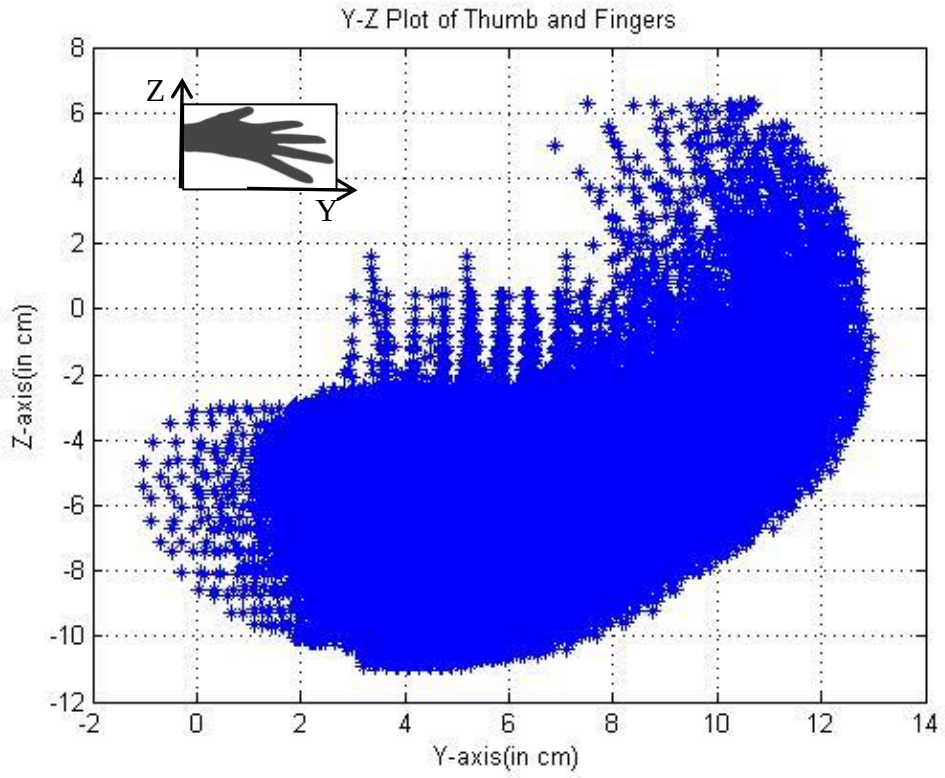

Figure 8.8: The positions of the tip of the thumb and fingers in Y-Z plane.

Figure 8.9 shows the position of the tips of the thumb and fingers by varying all the 25 joint angles in their respective ranges as per data mentioned in Table 4.4 through Table 4.8 in Chapter 4.

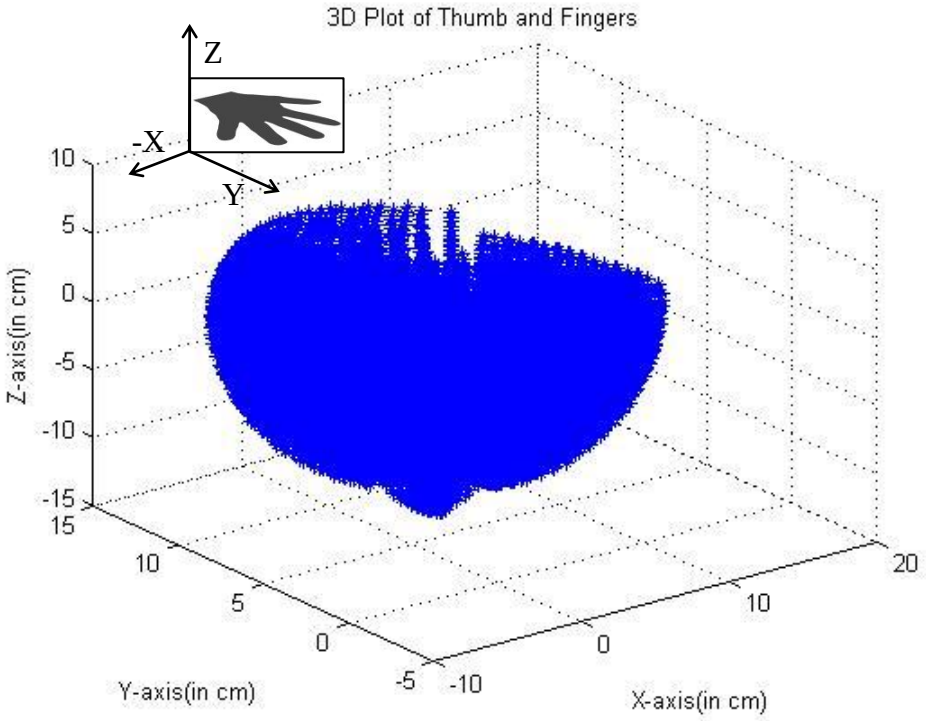

Figure 8.9: The workspace of the proposed hand in 3D space.

The workspace of the hand is obtained by combining the fingertip positions of thumb and fingers simultaneously in a common coordinate frame. The results are shown in form of four different graphs (Figure 8.6 through Figure 8.9) out of which three (Figure 8.6, Figure 8.7 and Figure 8.8) are projection of the workspace on three reference planes and one is 3D view(Figure 8.9). These figures show the reachable workspace of the hand model in all possible manners.

8.4 Inverse Kinematics Analysis

The inverse kinematics evaluates the configuration of a manipulator mainly the value of the joint angles with respect to a desired point. The solution of inverse kinematic problem is not as simple as that of forward kinematic problem due to the non-linear nature of the resulting equation that yields multiple solutions. Thus iterative or artificial intelligence methods are more suitable for solving the same. The details about the inverse kinematic problem have been already discussed in Section 5.6.2. The Adaptive Neuro-Fuzzy Inference System (ANFIS) is used for solving the inverse kinematic problem in the present work. The details of ANFIS are also discussed under the same section. The results obtained by solving the

inverse kinematic problem for each finger of the proposed hand using ANFIS in MATLAB platform is presented in following sections.

8.4.1 Solution of Inverse Kinematic Problem of Thumb

Considering the thumb of the hand as an individual manipulator with origin at wrist, the inverse kinematic problem is solved using ANFIS. In order to obtain the solution, numbers of points are chosen within the convex hull of the proposed hand model, the points are expressed in terms of their X, Y, Z coordinates with respect to the wrist frame. The values of the all five joint angles of the thumb are obtained for a particular position of tip of thumb. By repeating this process, the solutions of the inverse kinematic problem of thumb for all possible positions are obtained. Table 8.11 presents the values of the joint angles for various possible configurations of the thumb.

Table 8.11: Values of the joint angles of the thumb.

Coordinates of the tip position w.r.t. global coordinate system.			CMC joint		MCP joint		IP joint
X-coordinate in cm.	Y-coordinate in cm.	Z-coordinate in cm.	Predicted values of joint angles				
			Abduction /adduction angle (q_1) in degree	Flexion/ extension angle (q_2) in degree	Abduction /adduction angle (q_3) in degree	Flexion/ extension angle (q_4) in degree	Flexion/ extension angle (q_5) in degree
5.27	9.87	1.63	0.10	-12.71	31.44	-3.57	39.16
4.04	8.75	-2.27	4.26	-16.31	26.74	34.14	76.81
1.22	10.80	1.33	2.23	3.22	51.52	-9.28	-6.65
5.14	9.78	-0.29	1.04	-23.65	43.74	36.78	-1.85
5.39	10.26	0.37	0.62	7.29	35.00	-4.56	-2.78
5.33	10.05	-1.21	4.96	-6.82	56.47	13.54	25.48
5.22	9.82	-2.02	6.47	-21.53	56.82	37.80	48.11
1.21	10.79	-1.44	2.74	-8.71	49.84	30.58	-3.82
1.48	9.76	-2.63	15.96	-6.51	45.88	19.13	56.68
6.88	8.62	-2.60	0.21	2.46	5.57	21.19	-2.58
5.36	10.12	-0.91	4.64	-1.85	52.61	3.38	25.01
2.84	7.97	-7.70	19.47	28.92	52.26	39.87	19.20
0.89	7.43	-6.41	28.61	7.53	16.43	49.06	39.15
1.70	9.70	-5.97	28.03	33.50	29.06	9.71	1.27
0.82	10.57	-2.92	0.00	35.00	60.00	-10.00	-15.00
-0.53	7.57	-5.71	0.00	35.00	59.99	-10.00	80.00
3.57	10.29	4.96	3.87	-20.21	6.47	0.72	2.74
3.61	10.35	3.37	3.99	-18.09	32.29	-5.37	3.37

1.11	10.29	6.12	30.79	-24.81	1.79	-9.42	-14.79
2.23	11.33	0.08	37.04	-17.83	1.79	24.30	18.81
-0.54	11.49	3.55	23.02	-24.66	27.48	-1.01	27.21
-0.13	11.74	2.02	21.74	-18.37	43.60	-6.44	-10.62
1.01	10.29	-1.35	17.51	-12.84	57.78	22.77	19.06
0.82	11.08	-1.03	11.19	-5.92	58.05	-1.43	32.93
1.90	11.64	2.77	24.78	-17.21	18.59	6.51	-4.36
-0.24	12.02	1.13	25.38	-18.84	30.48	14.84	-6.34
0.02	11.60	-2.11	23.04	-0.91	31.83	39.25	34.49
-1.98	10.84	-0.52	38.04	1.58	50.38	12.20	13.09
-1.04	9.78	-4.24	54.74	-11.44	44.93	22.86	28.30
3.27	9.76	-5.52	10.51	30.43	57.52	5.20	10.22
0.75	7.77	-6.76	14.18	25.11	8.86	14.63	48.42
-0.44	7.78	-6.60	16.71	19.68	37.40	29.94	39.78
-2.95	10.21	-4.28	43.14	13.20	49.75	15.02	35.17
-1.69	11.58	3.22	39.77	-20.04	3.75	-6.74	30.43
-2.08	10.60	-1.35	29.99	-21.06	57.06	47.75	-10.62
-3.66	10.41	-1.52	45.37	-1.93	28.38	17.31	41.64
-1.72	12.62	0.37	47.81	-0.94	8.52	1.93	-8.25
-1.15	9.94	-2.95	58.24	-24.76	49.72	25.10	78.17
-1.13	10.04	-4.18	57.09	-24.05	3.67	26.22	75.25
-0.76	8.11	-5.27	26.45	32.86	26.92	19.15	78.86
-3.52	11.39	-0.38	43.43	-1.47	49.44	-8.11	24.40
-3.46	11.49	-2.11	40.06	-21.76	53.78	19.08	54.00
-2.10	6.21	-8.96	43.98	34.90	20.90	54.78	-13.50
-5.01	9.89	6.12	39.32	-19.33	22.25	-5.99	-5.83
-6.68	8.60	5.67	35.89	-21.14	23.54	-1.38	-6.27
-2.81	9.66	-5.06	44.91	11.67	16.71	37.56	35.53
-8.28	8.41	0.98	57.80	-16.85	56.59	13.54	-11.89
-3.28	12.32	-2.60	56.27	3.25	19.57	-7.84	30.48
-4.59	6.98	-6.60	59.65	33.39	19.27	-5.31	75.19
-4.00	7.42	-6.86	50.46	28.62	34.92	6.02	70.52

8.4.2 Solution of Inverse Kinematic Problem of Index Finger

The inverse kinematic solution of the index finger involves the determination of values of the four joint angles for a particular position of the fingertip. By using ANFIS the problem is solved for some of the positions of the index fingertips within the convex hull of the proposed hand. The solutions are presented in Table 8.12 in which all the joint angle values are within the range specified for those as presented (Table 4.5) in Chapter 4.

Table 8.12: Values of the joint angles of the index finger.

Coordinates of the tip position w.r.t. global coordinate system.			MCP joint		PIP joint	DIP joint
X-coordinate in cm.	Y-coordinate in cm.	Z-coordinate in cm.	Predicted values of joint angles			
			Abduction/ adduction angle (q_6) in degree	Flexion/ extension angle (q_7) in degree	Flexion/ extension angle (q_8) in degree	Flexion/ extension angle (q_9) in degree
5.16	4.41	-2.97	-30.00	-10.00	60.00	40.00
4.59	4.65	-2.86	-30.00	-10.00	60.00	59.99
6.73	3.74	-4.22	-30.00	23.33	0.00	20.00
3.76	5.00	-6.35	-30.00	23.33	60.00	0.00
2.66	5.47	-6.07	-29.99	23.33	60.00	40.00
0.85	6.24	-5.18	-29.99	23.34	89.99	40.01
3.34	5.18	-8.05	-30.00	56.67	0.00	20.00
0.78	6.27	-8.18	-30.00	56.67	29.99	40.01
-0.21	6.69	-8.06	-29.93	56.69	59.97	0.02
-1.12	7.07	-6.56	-29.92	56.65	60.01	59.98
7.82	6.50	-1.21	-10.00	-10.00	30.00	20.00
6.28	6.59	-2.86	-10.00	-10.00	60.00	20.00
5.67	6.62	-2.97	-10.00	-10.00	60.00	40.00
4.11	6.70	-3.52	-10.00	-10.00	90.00	20.00
3.53	6.73	-3.31	-10.00	-10.00	90.00	40.00
7.37	6.53	-4.22	-10.00	23.33	0.00	20.00
6.29	6.58	-5.50	-10.00	23.33	30.00	0.00
5.11	6.65	-5.86	-10.00	23.33	30.00	40.00
4.51	6.68	-5.71	-10.00	23.33	30.00	60.00
2.96	6.76	-6.07	-10.00	23.33	60.00	40.01
1.36	6.84	-5.68	-9.99	23.34	90.00	20.01
3.08	6.75	-8.09	-10.01	56.67	0.00	39.99
0.92	6.87	-8.18	-10.00	56.66	30.01	39.99
-1.47	6.99	-9.23	-10.04	89.99	0.02	19.96
7.74	9.59	0.41	10.00	-10.00	0.00	40.00
6.49	9.21	-2.55	10.00	-10.00	60.00	0.01
5.39	8.87	-2.97	10.00	-10.00	60.00	40.00
4.50	8.60	-3.52	10.00	-10.00	90.00	0.00
3.90	8.41	-3.52	10.00	-10.00	90.00	20.00
6.54	9.22	-4.59	10.00	23.33	0.00	40.00
5.97	9.05	-4.77	10.00	23.33	0.00	60.00
4.28	8.53	-5.71	10.00	23.33	30.00	60.00
3.35	8.24	-6.32	10.00	23.33	60.00	20.00
1.77	7.76	-6.02	10.00	23.33	89.99	0.01
0.91	7.50	-5.18	10.01	23.34	89.99	40.01

1.97	7.82	-8.53	10.00	56.67	30.00	0.01
0.84	7.48	-8.18	10.01	56.67	30.00	40.00
-0.18	7.16	-8.06	10.07	56.68	59.94	0.02
-1.13	6.88	-6.56	10.25	56.67	60.00	59.99
6.49	12.50	1.00	30.00	-10.00	0.00	20.00
4.85	11.26	-2.86	30.00	-10.00	60.00	20.00
5.32	11.61	-4.59	30.00	23.33	0.00	40.00
4.85	11.26	-4.77	30.00	23.33	0.00	60.00
3.92	10.56	-5.86	30.00	23.33	30.00	40.00
3.15	9.98	-6.35	30.00	23.33	60.00	0.00
2.29	9.33	-8.09	29.99	56.67	0.00	40.00
1.01	8.36	-8.46	29.99	56.66	30.00	20.00
0.56	8.03	-8.18	29.99	56.67	30.00	40.00
-0.97	6.87	-7.17	29.73	56.66	59.93	40.07
-1.08	6.79	-6.56	29.93	56.66	60.01	59.99

8.4.3 Solution of Inverse Kinematic Problem of Middle finger

The inverse kinematic problem of middle finger, which is considered as a 4-link mechanism having three joints with 4-DOFs, is done using ANFIS for some of the positions of its tip within the convex hull. The results so obtained are tabulated in the Table 8.13 and it is observed that all joint angle values are within the respective range.

Table 8.13: Values of the joint angles of the middle finger.

Coordinates of the tip position w.r.t. global coordinate system.			MCP joint		PIP joint	DIP joint
X-coordinate in cm.	Y-coordinate in cm.	Z-coordinate in cm.	Predicted values of joint angles			
			Abduction/ adduction angle (q_{10}) in degree	Flexion/ extension angle(q_{11}) in degree	Flexion/ extension angle(q_{12}) in degree	Flexion/ extension angle(q_{13}) in degree
6.39	7.42	-3.33	24.59	13.84	56.27	-7.14
5.55	7.35	-3.14	25.45	13.42	61.72	11.03
3.01	7.12	-5.10	34.46	27.78	47.80	76.84
4.78	7.28	-5.85	2.86	23.13	85.68	9.86
3.15	7.13	-6.88	33.10	29.99	27.87	2.60
-2.94	6.60	-7.66	11.27	1.14	58.68	3.05
-3.20	6.58	-6.84	5.29	0.99	47.37	1.56
-1.75	6.71	-9.29	32.63	15.78	42.13	23.50
-3.11	6.59	-9.23	0.25	0.12	9.59	0.28
-4.20	6.49	-6.17	6.07	0.03	2.14	0.06
-5.14	6.41	-7.52	-4.40	0.01	0.55	0.01

6.41	8.97	-2.00	29.06	11.93	12.81	60.71
5.31	8.66	-3.14	33.61	35.46	69.54	74.12
-0.46	7.03	-9.36	7.06	12.74	49.24	7.97
-2.89	6.35	-7.66	14.55	1.59	70.93	4.14
-3.03	6.31	-5.98	6.19	1.17	89.51	1.86
-1.75	6.67	-9.29	33.93	16.25	43.29	24.11
-3.37	6.21	-8.43	-2.00	0.47	28.51	1.16
-3.34	6.22	-7.57	12.61	0.57	26.43	1.20
-4.22	5.97	-8.60	-6.38	1.62	21.12	3.05
2.67	8.83	-6.88	25.85	9.74	81.48	30.83
5.14	10.06	-6.95	20.39	6.31	95.20	7.35
2.97	8.98	-6.85	30.99	12.67	98.86	15.90
4.18	9.58	-7.78	24.60	2.35	1.65	1.83
2.61	8.80	-9.09	-6.38	20.71	28.90	-8.36
-0.53	7.23	-9.36	3.10	5.41	40.05	3.74
-2.80	6.10	-7.66	19.51	2.96	86.73	7.38
-3.21	5.90	-7.57	23.47	2.98	33.95	6.30
1.96	9.39	-4.32	31.31	5.79	29.10	9.27
2.20	9.58	-6.88	11.65	1.41	69.42	3.69
1.52	9.06	-6.76	6.51	0.60	54.24	22.13
2.47	9.78	-6.85	17.30	3.60	95.76	6.79
3.54	10.60	-7.78	13.33	1.89	26.65	2.18
2.22	9.59	-8.07	-6.44	0.62	22.09	-0.17
1.19	8.81	-6.99	5.51	1.54	97.97	58.13
-0.21	7.75	-9.21	-7.08	1.70	74.78	-0.09
-0.65	7.41	-9.36	0.88	1.94	30.42	1.45
1.40	10.00	-4.32	8.91	0.69	9.78	1.04
0.95	9.50	-4.91	20.71	4.18	32.55	8.82
0.19	8.66	-2.75	25.33	9.13	12.66	25.16
1.44	10.05	-6.12	4.23	0.38	24.22	1.00
0.54	9.05	-6.30	8.19	3.53	26.69	25.66
0.16	8.63	-6.35	9.06	3.73	42.23	34.23
-0.54	7.85	-3.48	24.49	0.37	38.83	0.47
2.34	11.05	-7.25	13.84	2.29	72.30	4.39
1.83	10.48	-6.85	5.61	0.30	47.23	0.64
2.73	11.48	-7.78	8.70	0.95	19.24	1.23
1.31	9.90	-8.41	-7.14	0.09	13.79	-0.03
-0.26	8.16	-6.44	0.11	0.69	64.22	5.27
1.56	10.18	-9.09	-1.45	0.01	2.77	0.00

8.4.4 Solution of Inverse Kinematic Problem of Ring Finger

Ring finger is modelled as a 6-DOFs mechanism having 4 joints and 5-links including 2-DOFs at CMC joint. The values of the all six joint angles are presented in Table 8.14 by solving the inverse kinematics problem of the ring finger using ANFIS for the tip positions within the workspace of hand model.

Table 8.14: Values of the joint angles of the ring finger.

Coordinates of the tip position w.r.t. global coordinate system.			CMC joint		MCP joint		PIP joint	DIP joint
X-coordinate in cm.	Y-coordinate in cm.	Z-coordinate in cm.	Predicted values of joint angles					
			Abduction/adduction angle(q_{14}) in degree	Flexion/ extension angle(q_{15}) in degree	Abduction/ adduction angle (q_{16}) in degree	Flexion/ extension angle (q_{17}) in degree	Flexion/ extension angle(q_{18}) in degree	Flexion/ extension angle(q_{19}) in degree
2.70	3.58	-5.91	4.98	2.41	18.28	79.39	54.07	88.53
3.23	3.61	-2.88	0.27	2.03	-13.86	80.00	99.98	89.92
8.24	4.47	-4.84	1.89	2.15	2.95	0.01	99.86	30.29
7.83	4.35	-8.15	2.79	2.06	3.04	40.01	49.97	29.96
9.24	6.22	-6.93	1.11	2.45	14.43	26.42	47.68	-6.62
7.38	3.42	-8.73	0.05	6.09	-13.98	40.00	49.99	30.01
4.10	3.42	-8.62	1.99	6.11	3.23	79.65	1.95	89.15
4.37	3.31	-5.95	1.31	6.00	2.96	40.00	99.78	30.37
8.55	6.02	-8.92	0.53	6.56	18.09	46.59	43.70	-5.94
6.92	4.92	-8.72	2.36	7.29	19.90	39.99	50.09	29.73
6.28	4.41	-6.92	3.46	5.31	19.21	39.86	55.73	75.73
6.65	4.05	-9.28	3.02	9.73	2.93	39.98	50.07	29.87
3.96	3.20	-6.28	1.60	9.77	-5.95	40.97	95.55	39.19
1.12	2.32	-4.08	0.25	9.98	3.12	80.00	99.99	30.05
8.20	5.97	-8.32	2.51	9.61	-5.25	45.46	4.12	56.83
5.79	4.29	-7.40	4.24	9.35	19.86	40.06	53.41	83.29
7.79	4.30	-8.15	1.76	2.06	5.00	39.95	45.21	35.28
4.59	4.04	-5.58	8.00	2.16	-13.87	39.88	99.81	30.62
7.61	5.07	-8.15	6.62	2.02	3.01	40.00	49.93	30.03
6.75	4.72	-6.41	6.27	2.69	-6.19	40.10	44.71	89.05
5.32	4.14	-3.74	4.77	2.03	2.96	40.01	99.99	89.94
5.70	4.30	-9.82	5.42	2.28	2.94	80.00	0.19	29.79
10.75	8.57	-4.74	4.91	2.01	19.99	0.00	50.00	30.00
2.80	2.18	-7.85	6.65	2.25	19.90	79.93	50.21	29.80
3.57	2.73	-2.88	5.50	2.17	19.78	79.99	99.99	89.86
9.40	4.32	-7.66	5.06	6.25	-13.98	40.00	0.02	89.94
7.23	4.11	-8.73	2.15	6.41	-13.91	40.00	50.00	30.02

6.42	4.08	-6.92	2.17	5.69	-13.47	39.71	54.08	89.73
10.84	6.40	-8.22	5.01	5.98	3.00	40.00	0.00	30.04
7.05	4.88	-8.74	6.28	5.25	-13.01	44.95	38.84	28.19
6.31	4.57	-6.93	4.69	6.20	3.04	40.05	50.18	89.66
11.22	9.00	-3.39	5.00	6.00	19.99	0.00	0.02	89.94
6.05	5.00	-6.92	7.95	5.16	19.18	40.05	50.95	86.87
11.07	6.50	-6.54	5.11	9.95	3.00	0.00	49.99	30.01
8.54	5.50	-8.37	3.14	9.89	2.92	47.71	2.69	20.67
5.58	4.83	-7.40	8.45	9.19	-5.29	39.74	60.84	67.62
7.70	5.95	-4.84	8.14	2.24	2.79	0.00	99.98	29.98
7.32	5.77	-8.15	7.44	2.46	3.10	40.01	49.95	30.06
6.49	5.34	-6.41	9.18	2.21	7.10	40.57	62.27	25.06
2.23	1.88	-3.82	9.39	2.39	-2.68	78.90	99.93	29.56
7.03	4.77	-8.73	5.61	6.05	-13.97	40.01	49.93	30.26
6.23	4.68	-6.92	5.66	5.78	-4.63	40.11	51.01	88.06
4.09	4.14	-5.95	9.30	6.26	2.95	40.01	99.98	30.02
1.77	2.97	-8.03	7.93	6.05	3.07	80.00	49.96	30.13
6.32	6.17	-8.72	9.77	5.90	19.93	40.00	50.01	29.98
8.66	4.95	-8.34	9.75	9.82	9.67	43.58	7.29	79.90
9.12	6.71	-5.55	9.89	9.84	3.01	0.02	50.80	88.78
6.21	5.27	-9.28	6.24	9.91	2.96	40.00	49.92	29.95
5.32	5.36	-7.40	9.83	9.84	19.94	40.01	50.05	89.81

8.4.5 Solution of Inverse Kinematics Problem of Little Finger

The little finger is also considered as an open loop kinematic chain having four joints and five fingers with 6-DOFs. In order to determine the finger configuration for a particular position of the fingertip, the inverse kinematic problem is solved using ANFIS in MATLAB platform. A good number of points are chosen in the workspace of the hand and the corresponding joint angle values are calculated and are presented in Table 8.15. All these calculated angles lie well within the respective ranges of the joint angles as specified earlier (Table 4.8).

Table 8.15: Values of the joint angles of the little finger.

Coordinates of the tip position w.r.t. global coordinate system.			CMC joint		MCP joint		PIP joint	DIP joint
X-coordinate in cm.	Y-coordinate in cm.	Z-coordinate in cm.	Predicted values of joint angles					
			Abduction/adduction angle (q_{20}) in degree	Flexion / extension angle (q_{21}) in degree	Abduction /adduction angle(q_{22}) in degree	Flexion/ extension angle (q_{23}) in degree	Flexion/ extension angle(q_{24}) in degree	Flexion/ extension angle(q_{25}) in degree
1.85	4.00	-4.62	8.58	8.58	8.58	79.69	8.58	89.37

2.03	3.72	-7.82	6.15	6.15	6.15	79.98	6.15	-29.33
1.20	2.57	-3.32	8.34	8.34	8.34	79.84	8.34	7.36
5.15	7.08	-7.55	11.89	11.89	11.89	45.75	11.89	37.16
6.97	9.76	-5.12	9.51	9.51	9.51	32.85	9.51	-1.81
3.12	4.27	-6.89	7.04	7.04	7.04	46.91	7.04	-9.04
7.42	5.79	-3.57	7.49	7.49	7.49	0.00	7.49	89.94
5.41	5.22	-6.75	7.13	7.13	7.13	39.86	7.13	24.48
4.11	4.92	-5.99	8.09	8.09	8.09	40.09	8.09	-28.42
7.43	8.04	-6.38	7.51	7.51	7.51	40.00	7.51	29.99
3.97	5.20	-5.99	9.46	9.46	9.46	41.47	9.46	-20.47
4.98	6.05	-7.86	9.50	9.50	9.50	79.88	9.50	-28.57
1.22	2.91	-4.83	7.38	7.38	7.38	79.87	7.38	-27.48
7.97	5.65	-7.21	7.48	7.48	7.48	40.00	7.48	30.03
4.28	4.83	-5.73	6.59	6.59	6.59	39.96	6.59	88.18
2.78	4.51	-4.99	7.64	7.64	7.64	40.05	7.64	26.52
3.58	4.79	-3.50	6.50	6.50	6.50	39.27	6.50	89.98
8.65	9.06	-4.38	7.50	7.50	7.50	0.00	7.50	-29.98
6.35	7.17	-4.38	7.47	7.47	7.47	0.01	7.47	89.82
3.55	4.85	-3.50	7.50	7.50	7.50	39.99	7.50	89.70
4.88	8.27	-5.27	7.50	7.50	7.50	0.01	7.50	-29.99
5.09	9.15	-7.12	7.48	7.48	7.48	39.99	7.48	29.92
3.02	4.21	-5.00	7.36	7.36	7.36	39.95	7.36	34.82
4.33	4.53	-7.87	7.24	7.24	7.24	39.96	7.24	30.86
0.25	3.88	-3.53	7.50	7.50	7.50	80.00	7.50	30.12
7.07	7.86	-6.12	7.50	7.50	7.50	0.00	7.50	29.99
2.49	4.09	-5.36	7.56	7.56	7.56	40.26	7.56	32.57
3.28	4.68	-3.95	6.67	6.67	6.67	40.69	6.67	88.88
2.41	4.17	-8.83	12.92	12.92	12.92	79.77	12.92	26.74
0.86	2.68	-3.50	8.96	8.96	8.96	79.84	8.96	23.07
5.89	10.72	-5.12	7.45	7.45	7.45	0.01	7.45	-30.00
3.22	4.72	-3.94	7.70	7.70	7.70	39.95	7.70	89.78
1.97	2.50	-5.19	7.55	7.55	7.55	79.87	7.55	89.49
7.86	7.16	-6.36	14.99	14.99	14.99	39.97	14.99	30.09
6.53	6.63	-6.89	14.99	14.99	14.99	40.01	14.99	-29.82
5.43	7.86	-5.94	14.89	14.89	14.89	39.98	14.89	89.94
3.22	5.53	-8.01	14.83	14.83	14.83	79.99	14.83	29.98
1.19	3.28	-3.12	15.00	15.00	15.00	79.98	15.00	30.09
4.79	10.68	-4.24	14.99	14.99	14.99	0.01	14.99	30.01
2.53	4.81	-4.99	14.92	14.92	14.92	39.99	14.92	31.40
1.00	3.22	-6.49	14.87	14.87	14.87	79.98	14.87	30.27
3.14	6.85	-7.30	14.99	14.99	14.99	40.00	14.99	30.03
2.14	2.42	-3.40	14.99	14.99	14.99	79.99	14.99	30.18
8.38	7.24	-4.60	14.98	14.98	14.98	0.02	14.98	89.96

6.20	6.25	-6.08	14.88	14.88	14.88	0.01	14.88	-29.60
2.07	4.68	-5.37	14.91	14.91	14.91	40.04	14.91	29.56
6.58	9.27	-7.08	14.99	14.99	14.99	40.00	14.99	-29.99
4.54	7.12	-7.35	14.97	14.97	14.97	40.01	14.97	89.32
2.10	4.58	-8.83	14.95	14.95	14.95	80.00	14.95	30.53
1.88	3.87	-7.30	14.81	14.81	14.81	79.99	14.81	88.42

The inverse kinematics results are presented in tabular form in Table 8.11 through Table 8.15. These results show the predicted values of corresponding joint angles for particular positions of the tips of the thumb and fingers in 3D space. It is observed that in all cases the joint angles are within the prescribed range.

8.5 Multi-fingered Grasping

Grasping and manipulation are the basic functions of the multi-fingered hands. The details about the grasp theories and force-closure grasps are discussed in Chapter 5. The proposed multi-fingered hand is supposed to grasp different shaped objects under the assumption that the grasp is force-closure and it is under equilibrium condition. The detail calculations for grasping different shaped objects are presented in Chapter 6. The equations for grasping force and moment thereof have been derived for various conditions of grasping with friction. However, the number of equations and the number of unknown parameters are such that the relationship becomes indeterminate. ANFIS technique is used to determine the values of the forces, angle of inclination and position of finger tips. The results are presented in the following sections.

8.5.1 Cubical Objects

The dimension of the cubical object is taken as 5cmx5cmx5cm as given in Section 7.4.1 and the weight of the object considered is 3N for the present analysis.

Table 8.16: Results for cubical object.

	Thumb	Index finger	Middle finger	Ring finger	Little finger
Applied forces in Newton	4.5659	2.4546	2.1740	2.5274	1.6424
Incident angles in degrees.	7.4636	6.9949	6.9212	7.0788	8.1463
Position of the thumb and finger tips with respect to center of gravity of object.					
X-coordinate in cm	-1	2.5	-1.7344	1.0659	2.5
Y-coordinate in cm	-2.5	0.9538	2.5	2.5	1.3985
Z-coordinate in cm	0	0	0	0	0

The values of the force applied at the points of contact, the angles of inclination and the positions of contact points of thumb and fingers in the form of X, Y, and Z coordinate with respect to centre of gravity of the cubical object is presented in Table 8.16.

8.5.2 Cylindrical Object

The dimension of the cylinder is taken as; base diameter=5cm and height=5cm. Accordingly, proportionate weight of the cylindrical object with respect to cubical object is calculated as 2.36N. All equilibrium equations are derived in Section 7.4.2. The equations are solved using ANFIS in MATLAB platform. The values of forces by the thumb and other fingers and angle of inclination to normal of the face at point of contact are determined and are presented in Table 8.17. The positions of contact points are also determined by solving the moment equilibrium equation and the same are also presented in the Table 8.17.

Table 8.17: Results for cylindrical object.

	Thumb	Index finger	Middle finger	Ring finger	Little finger
Applied forces in Newton	3.0491	2.2416	1.9497	2.0557	3.2340
Incident angles in degrees.	6.6580	6.9012	6.4075	8.1584	8.0747
Position of the thumb and finger tips with respect to center of gravity of object.					
X-coordinate in cm	0	-2.3478	1.8623	2.0617	2.4393
Y-coordinate in cm	-2.5	-0.8587	1.6664	1.4039	0.5475
Z-coordinate in cm	0	0	0	0	0

8.5.3 Conical Object

The proportionate weight of the conical object having base diameter 5cm and height 5cm is calculated with respect to cubical object and it is found to be 0.785N. The equilibrium equations are derived in Section 7.4.3 for equilibrium force-closure grasp. The force equilibrium equations are solved using ANFIS. The applied forces and incident angles of thumb and all fingers are determined and are presented in Table 8.18. Similarly, solving the moment equilibrium equation using ANFIS, the positions of contact points are predicted and are given in Table 8.18.

Table 8.18: Results for conical object.

	Thumb	Index finger	Middle finger	Ring finger	Little finger
Applied forces in Newton	0.7109	0.5796	0.6519	0.5824	0.6666
Incident angles in degrees.	8.1873	6.4157	6.2148	7.0284	7.8397
Position of the thumb and finger tips with respect to center of gravity of object.					
X-coordinate in cm	0	-1.3215	1.4942	1.4824	1.6582
Y-coordinate in cm	-1.67	-1.0210	0.7459	0.7691	0.1984
Z-coordinate in cm	0	0	0	0	0

8.5.4 Trapezoidal Object

The force and moment equilibrium equations are derived for trapezoidal object in Section 7.4.4. The proportionate weight of the object is found to be 1.54N. The equations are solved using ANFIS and the values of the fingertip forces, incident angles and position of the contact points in terms of X, Y and Z coordinates with respect to centroid axis of the objects are predicted and tabulated in Table 8.19.

Table 8.19: Results for trapezoidal object.

	Thumb	Index finger	Middle finger	Ring finger	Little finger
Applied forces in Newton	1.2118	1.1546	1.4931	1.4308	1.1615
Incident angles in degrees.	6.8430	6.0827	6.7140	6.8392	7.0604
Position of the thumb and finger tips with respect to center of gravity of object.					
X-coordinate in cm	0.2	-1.8	-1.8	0.7379	1.4310
Y-coordinate in cm	-1.8	1.4990	0.8518	1.8	1.8
Z-coordinate in cm	0	0	0	0	0

8.5.5 Parallelopiped Object

Considering the dimensions and proportionate weight of the parallelopiped object, the weight of the object is same as that of cubical object i.e. 3N. The force and moment equilibrium equations are developed in Section 7.4.5. These equations are solved using ANFIS for thumb and fingertip forces and angle of inclinations with normal to the face of object at the contact points. The X, Y and Z coordinates of the contact points are predicted with respect to centroid of the object. All the values of forces, incident angles and contact point coordinates are presented in Table 7.20.

Table 8.20: Results for parallelepiped object.

	Thumb	Index finger	Middle finger	Ring finger	Little finger
Applied forces in Newton	4.5659	2.4546	2.1740	2.5274	1.6424
Incident angles in degrees.	7.4636	6.9949	6.9212	7.0788	8.1403
Position of the thumb and finger tips with respect to center of gravity of object.					
X-coordinate in cm	1	-2.5	2.5	-1.1106	1.5785
Y-coordinate in cm	-2.5	-1.0263	1.5549	2.5	2.5
Z-coordinate in cm	0	0	0	0	0

During the determination of forces on the thumb and finger tips for force-closure equilibrium grasp, it is assumed that the height, the dimension of the base and the density of the material of the object are same for all shapes of object considered in this work. These assumptions are made in a view to accommodate them well within the workspace of the hand and compare them with a common characteristic of material properties. Therefore, the co-efficient of friction has been taken to be same for all the objects. Accordingly the proportionate weights are calculated for each object and corresponding forces are calculated. It is observed that that the angle of inclination of the thumb and that of the fingers are within the range of approximately 6 to 8 degrees. This implies that less amount of force is required to be applied at the contact points as the force are minimum when the angle of inclination is zero i.e. when the forces applied are normal to the object surface.

8.6 Stress Analysis using ANSYS

During grasping of an object of any shape by the hand, forces are actually applied by the fingers of the hand at the point of contact to firmly grasp the object and also to neutralize the weight of the object when it is lifted. When forces are applied by the fingers, equal amount of reactive resistance forces are also exerted on the fingers, these forces are distributed along the fingers and internal stresses are developed. In the present work the proposed 5-fingered hand model has been virtually tried for grasping different shaped objects. The amount of forces exerted on the tips of the thumb and the fingers for achieving force-closure grasps are calculated using ANFIS and the results are given in Section 8.5. Considering these forces on the thumb and fingers of the hand, the analysis is made to find out the point of maximum stress concentration. ANSYS-13 is used in the present work for the said analysis purpose. The concept and the theories of such analysis are

discussed in Section 7.5. The parameters considered for the analysis of present hand model and the materials used are given in Section 7.5.4. Based on the analysis the following results are presented.

Figure 8.10 shows the stress concentration on the thumb made up of aluminium due to force exerted during grasping the object. Two views of the finger are shown Figure 8.10 (a) as top view and Figure 8.10 (b) as bottom view.

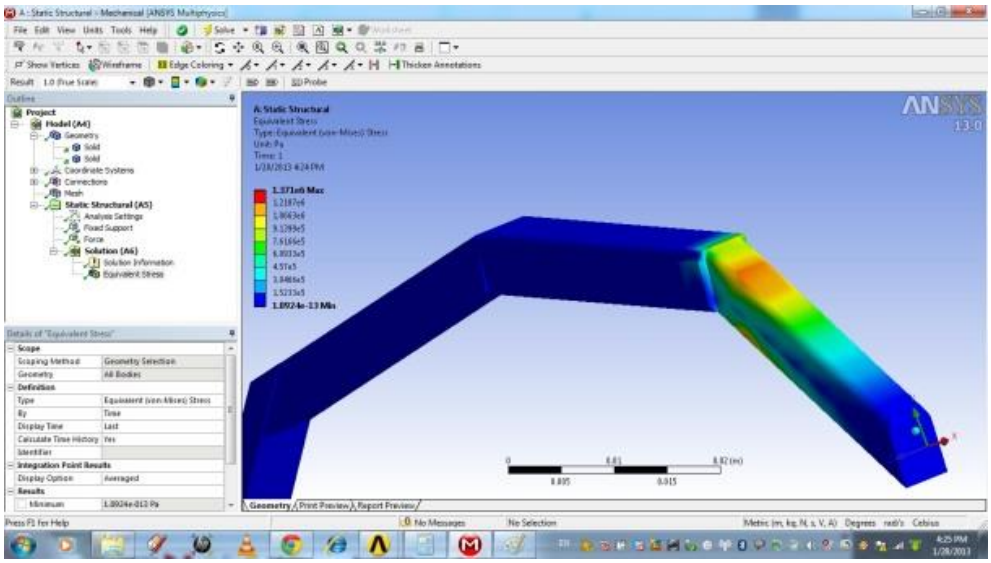

(a)

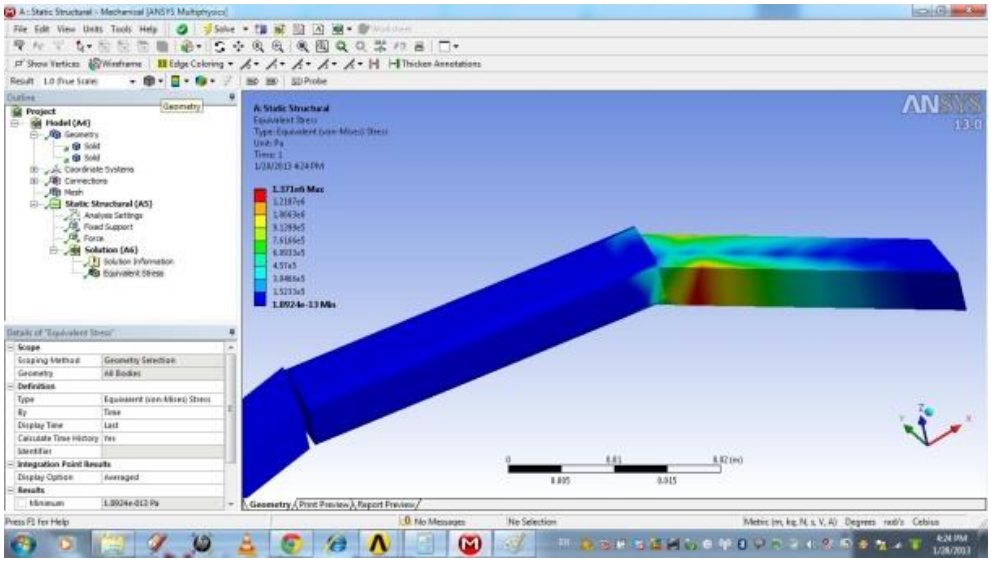

(b)

Figure 8.10: Stress concentration on thumb made of Aluminium (a) Top view (b) Bottom view

Similarly, the top and bottom view of the thumb made up of steel is shown in Figure 8.11 (a) and Figure 8.11 (b) respectively.

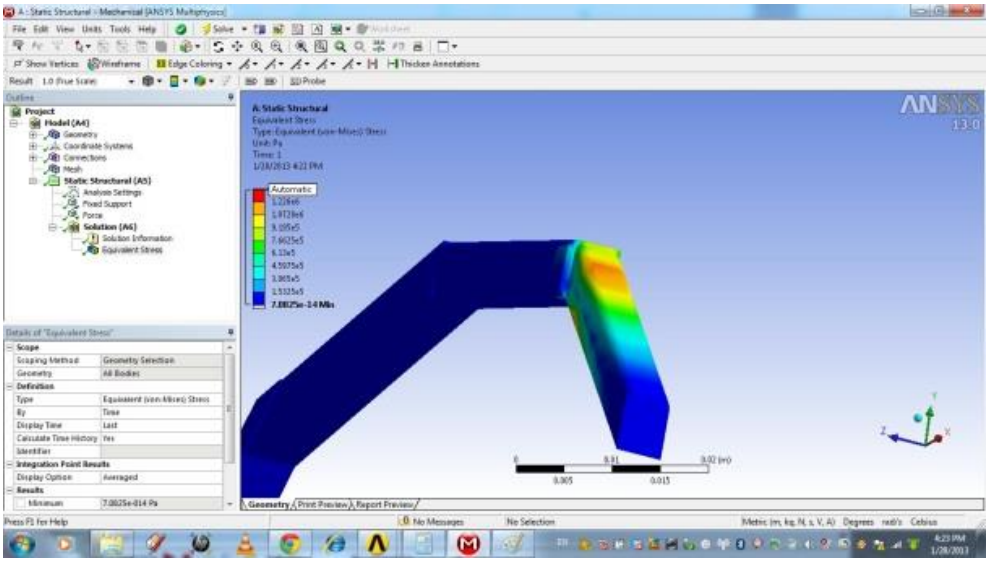

(a)

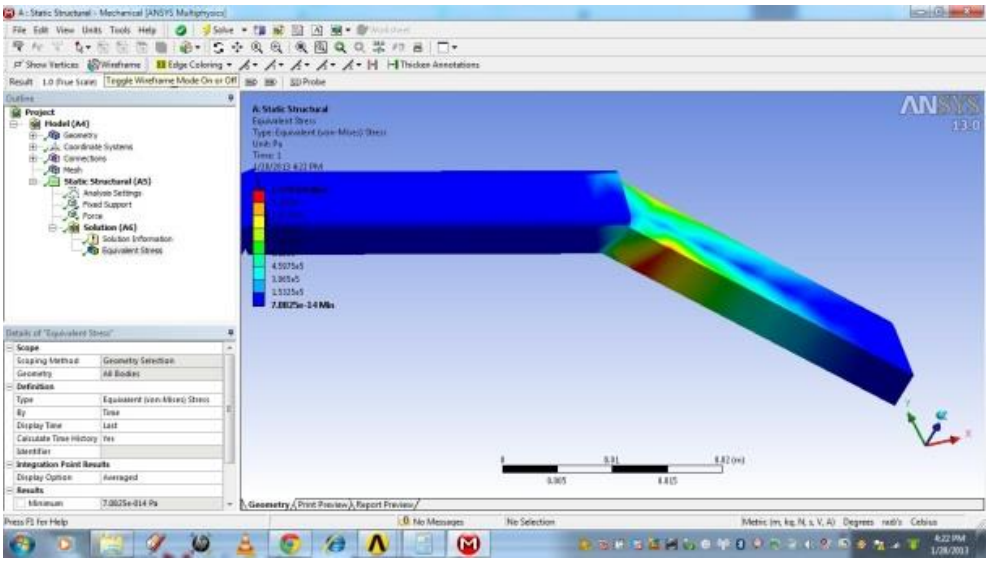

(b)

Figure 8.11: Stress concentration on thumb made of steel (a) Top view (b) Bottom view

The top and bottom view of the stress analysis result of the index finger made of aluminium is shown in Figure 8.12 (a) and Figure 8.12 (b) respectively. Figure 8.13 (a) and Figure 8.13 (b) show the top and bottom view of stress concentration in index finger made of steel.

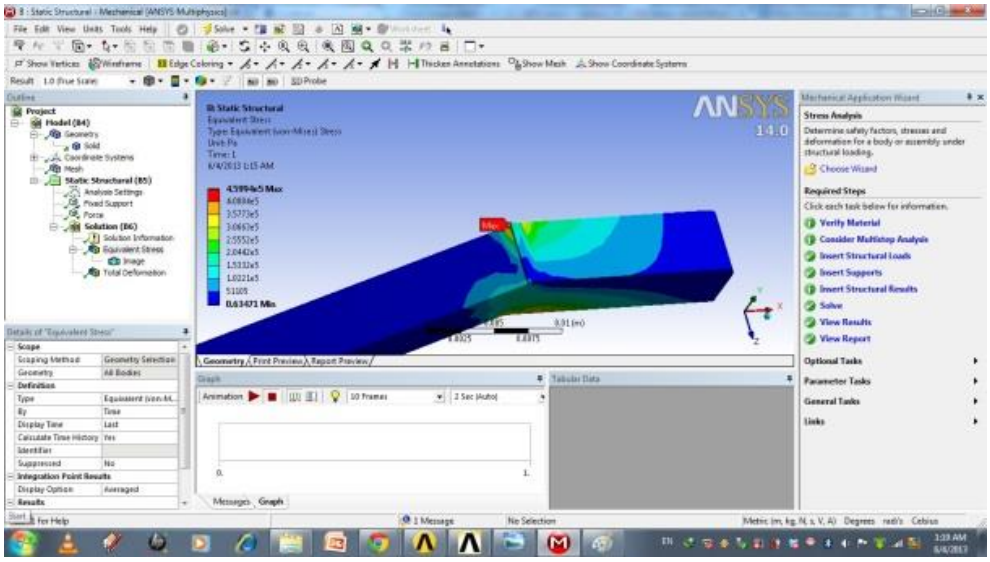

(a)

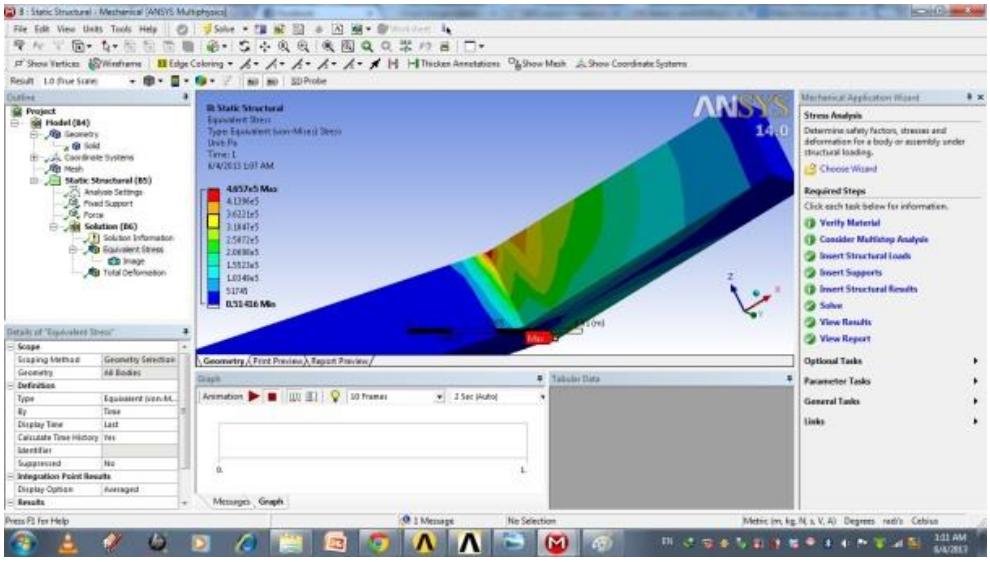

(b)

Figure 8.12: Stress concentration on index finger made of aluminium (a) Top view (b) Bottom view

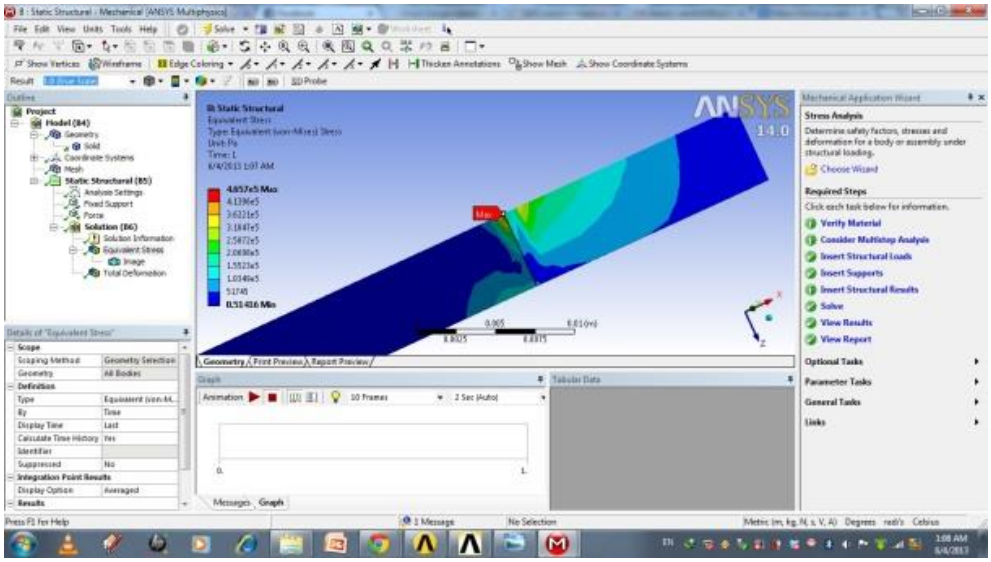

(a)

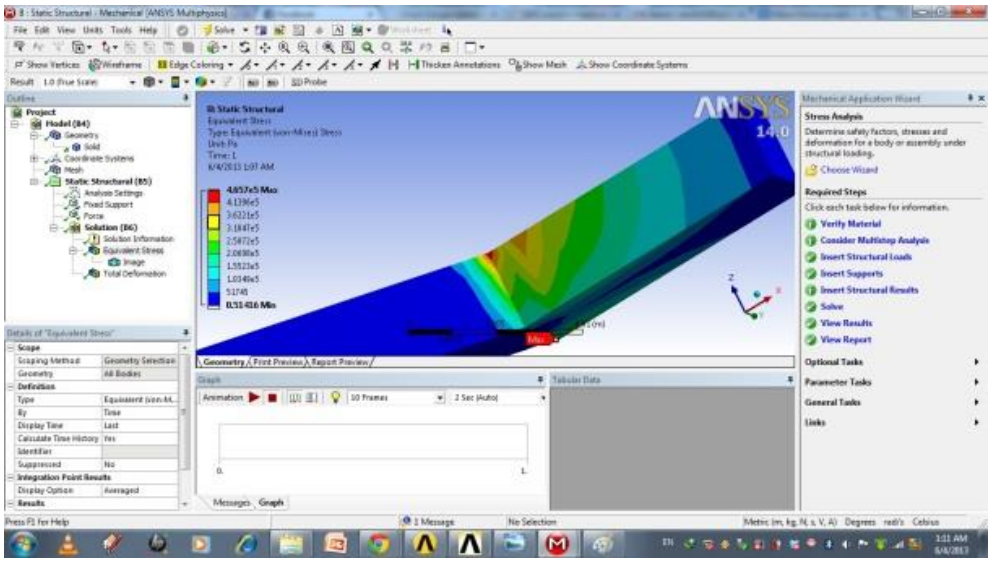

(b)

Figure 8.13: Stress concentration on index finger made of steel (a) Top view (b) Bottom view

The results of the distribution of stresses over the middle finger made of aluminium are presented in Figure 8.14 (a) and Figure 8.14 (b). The same results for the middle finger made of steel are presented in Figure 8.15 (a) and Figure 8.15 (b).

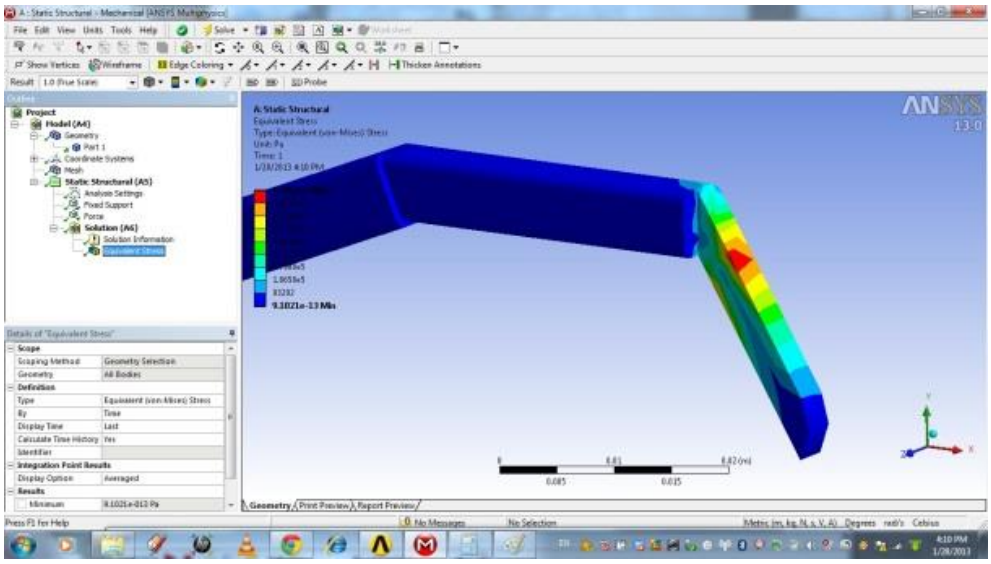

(a)

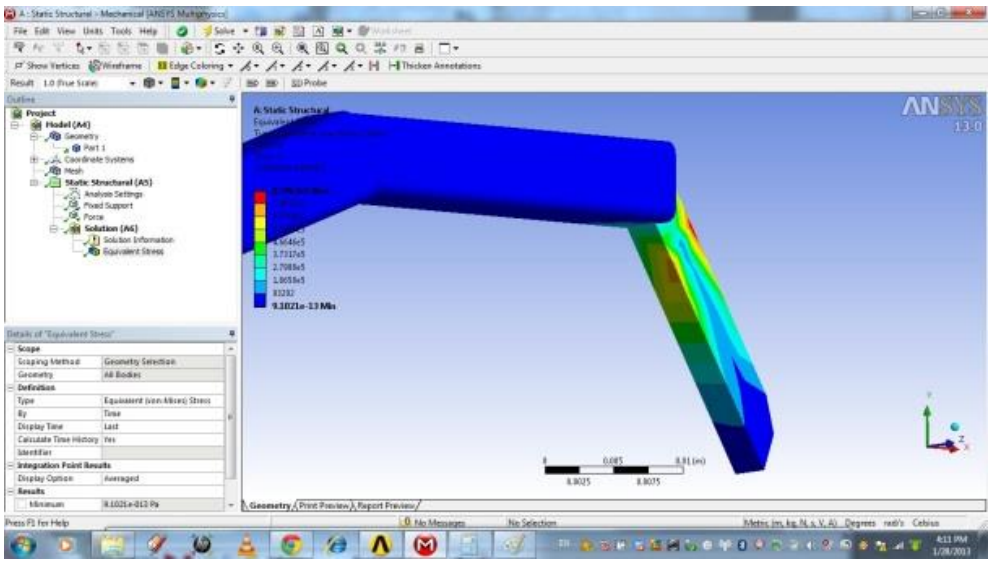

(b)

Figure 8.14: Stress concentration on middle finger made of aluminium
(a) Top view (b) Bottom view

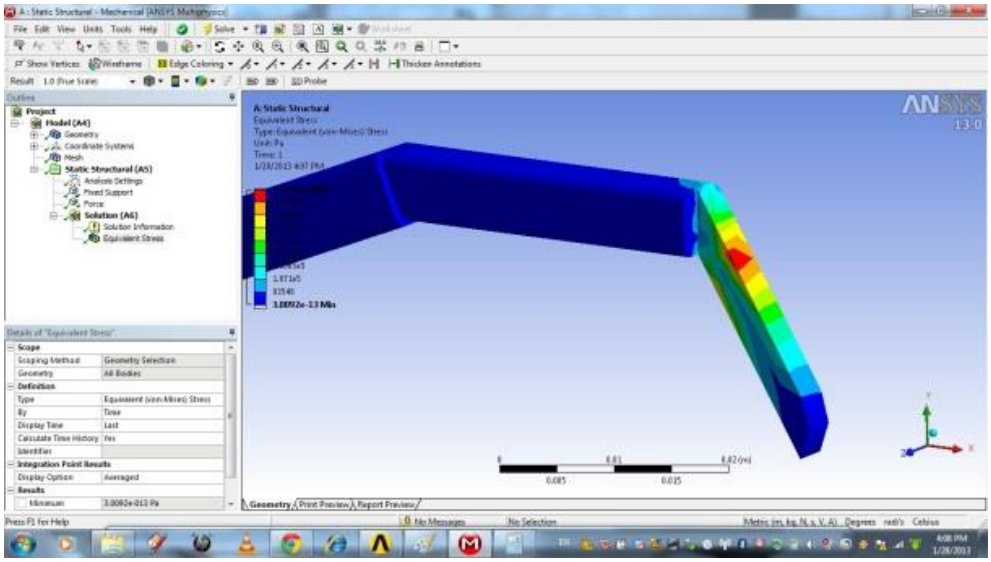

(a)

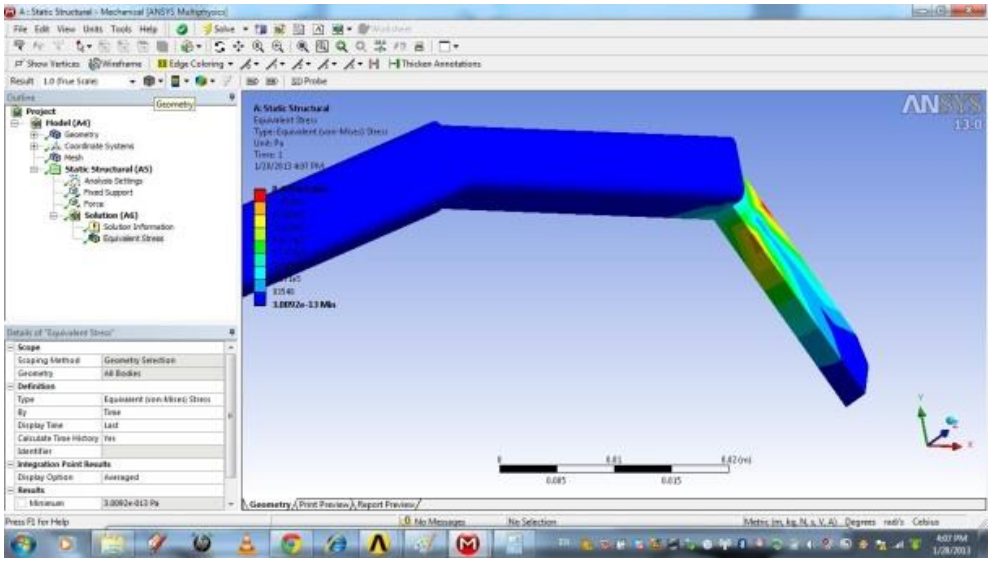

(b)

Figure 8.15: Stress concentration on middle finger made of steel (a) Top view (b) Bottom view

Considering the proportionate lengths of the ring finger and uniform square cross section of each segment of the finger, the stresses developed throughout the finger are found out for the force exerted on the fingertip during grasping an object. The stress concentration results as output of ANSYS analysis are shown in Figure 8.16 (a) and Figure 8.16 (b) for ring finger made of aluminium. The same results are shown for ring finger made of steel in Figure 8.17 (a) and Figure 8.17 (b).

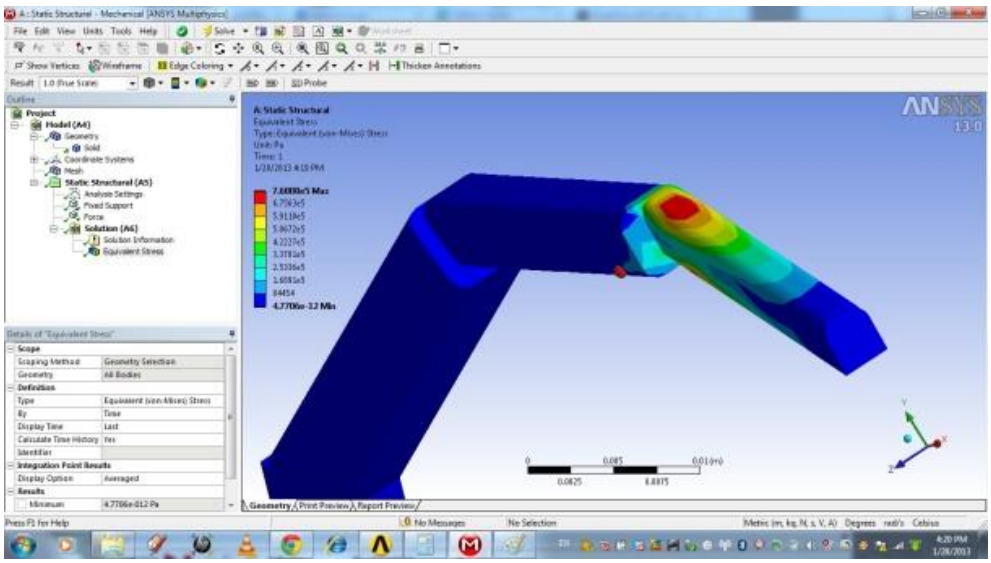

(a)

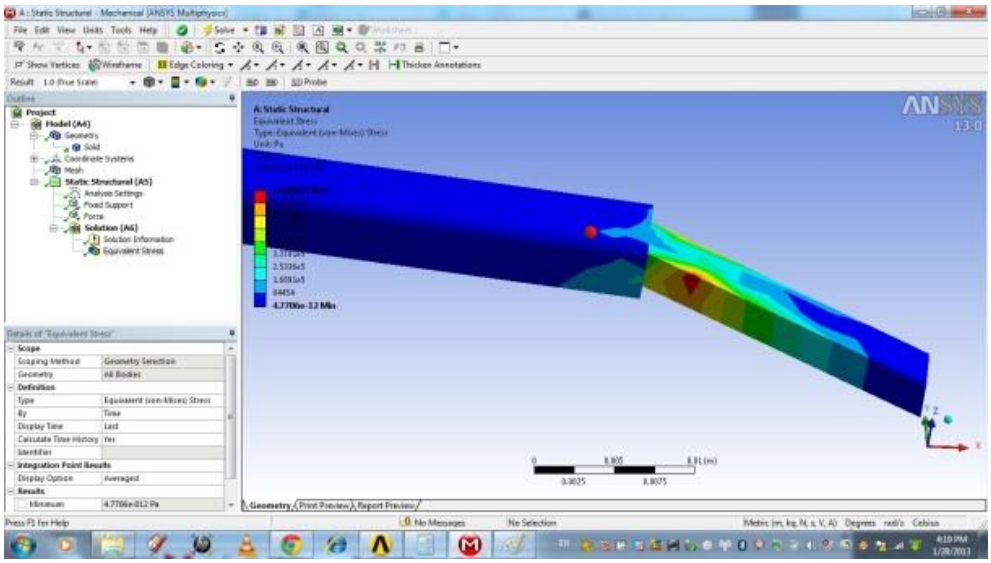

(b)

Figure 8.16: Stress concentration on ring finger made of aluminium (a) Top view (b) Bottom view

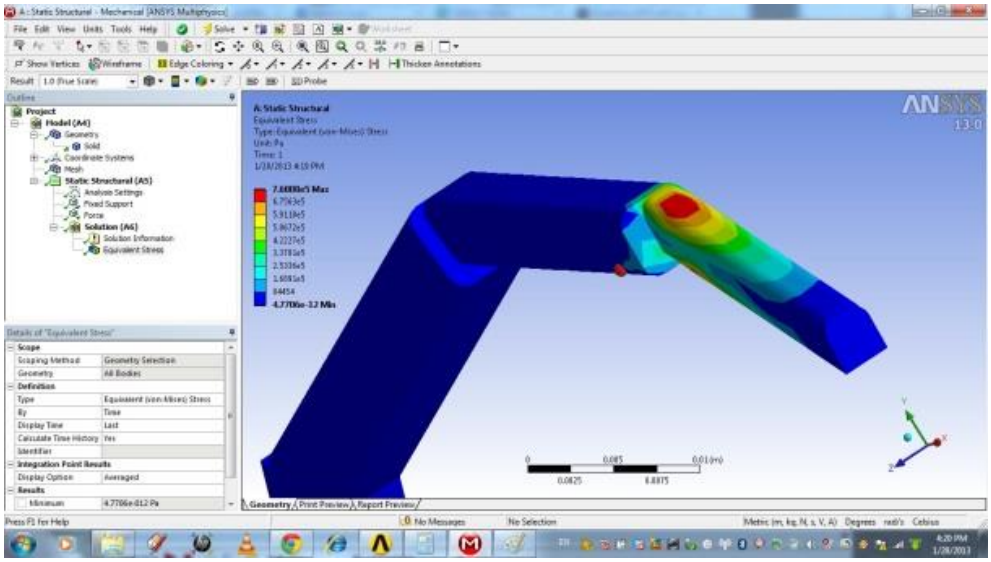

(a)

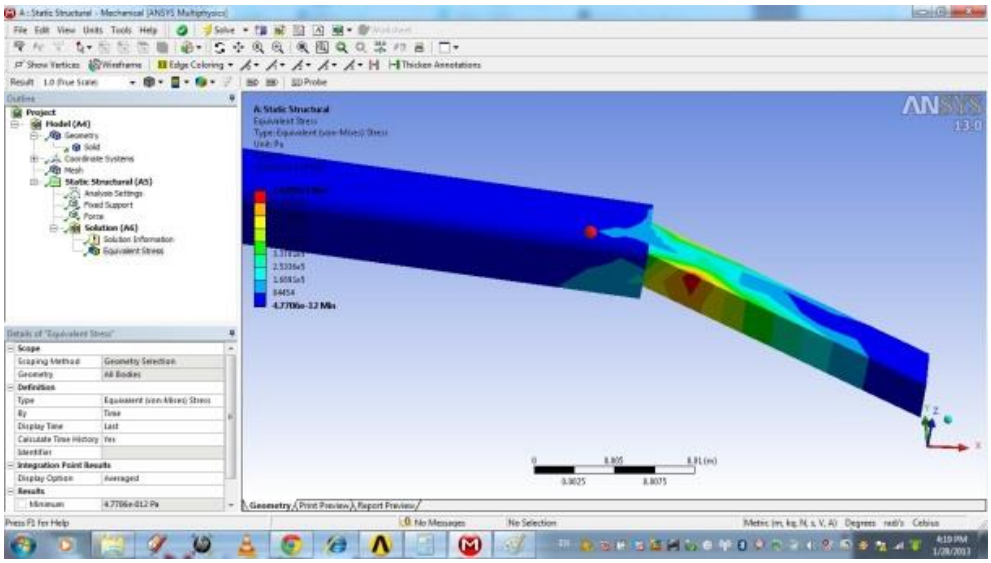

(b)

Figure 8.17: Stress concentration on ring finger made of steel (a) Top view (b) Bottom view

Figure 8.18 (a) and Figure 8.18 (b) show the stress distribution pattern and maximum stress concentration point on the little finger made of aluminium. These figures are obtained from ANSYS analysis of the little finger under the load due to grasping of the object. Similar graphs are shown in Figure 8.19 (a) and Figure 8.19 (b) for little finger made of steel.

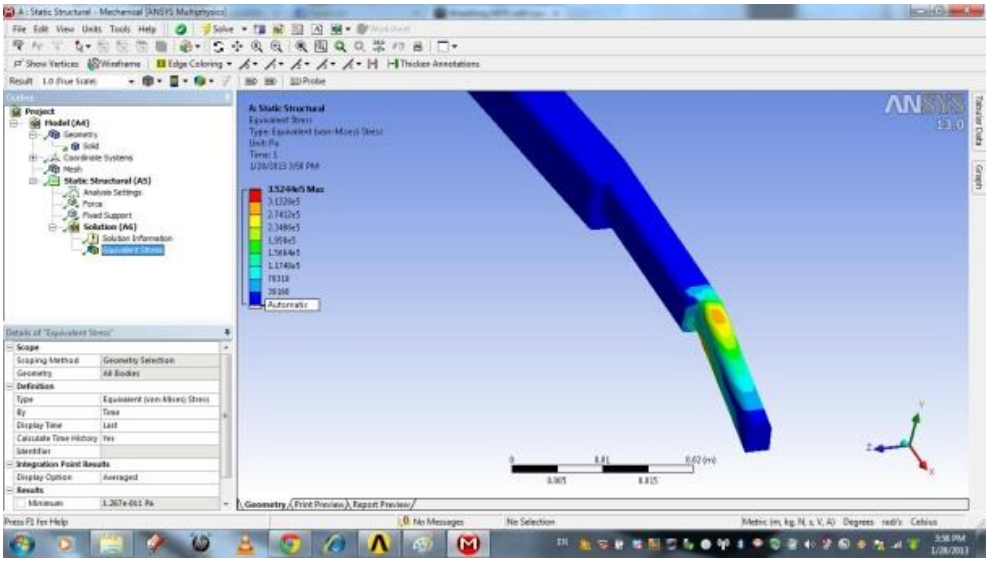

(a)

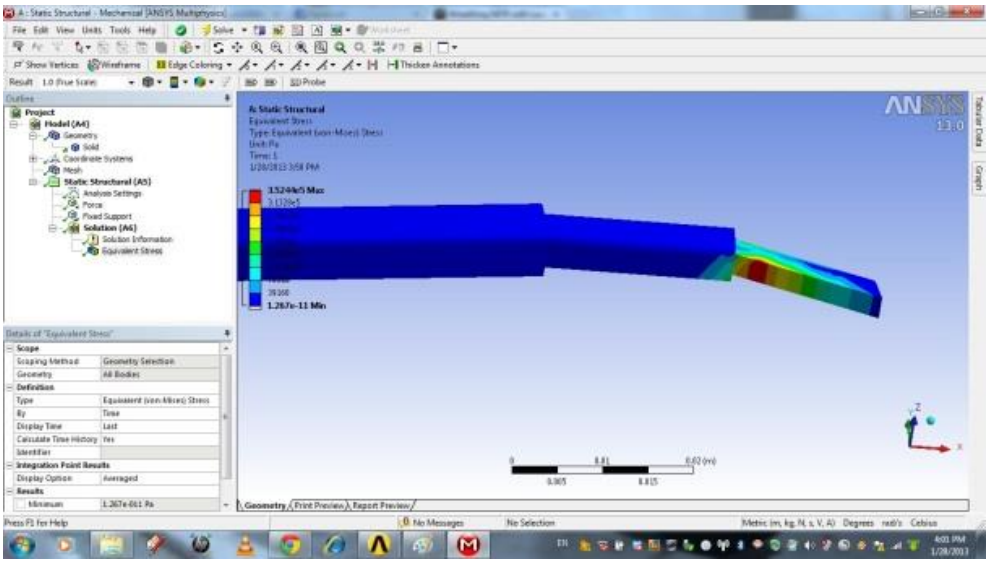

(b)

Figure 8.18: Stress concentration on little finger made of aluminium (a) Top view (b) Bottom view

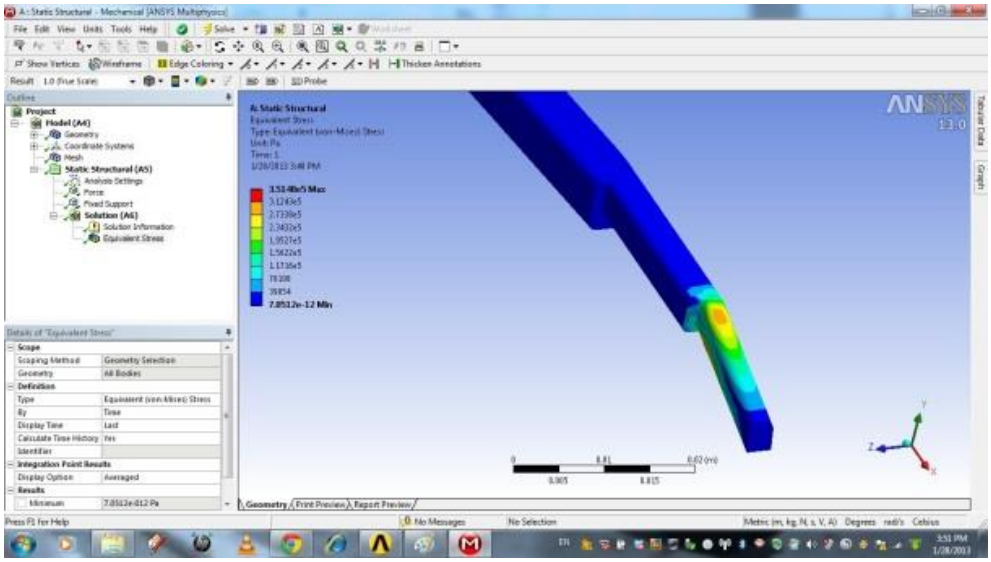

(a)

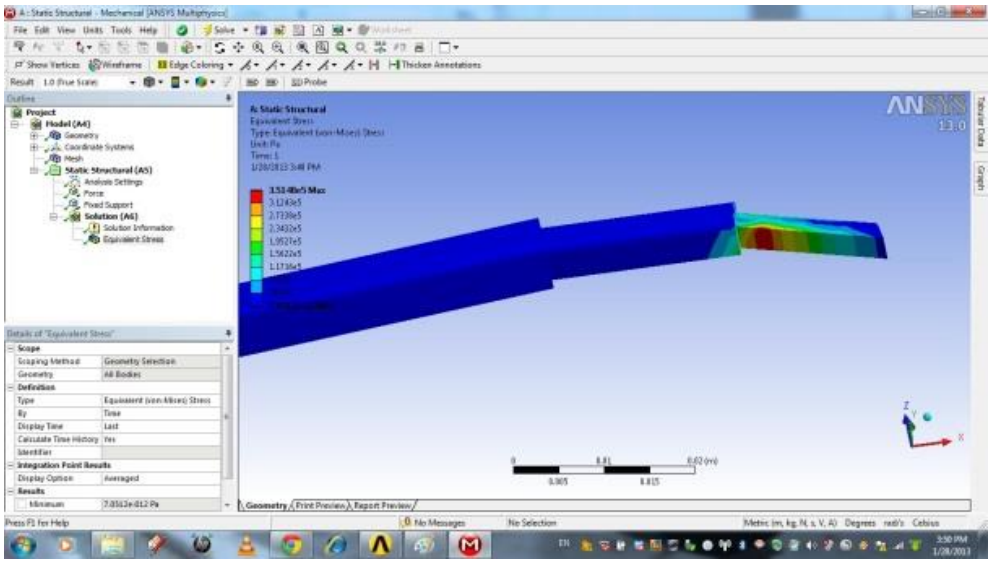

(b)

Figure 8.19: Stress concentration on little finger made of steel (a) Top view (b) Bottom view

The analysis for stress concentration on the thumb and fingers are done thoroughly for thumb and fingers using ANSYS and the results are presented. The stress developed at different points is displayed in different colour as safe load to critical point. For clarity of the stress distribution two views are shown for two different materials. From figure it is observed for all the fingers that the maximum stress concentration happens on the distal phalangeal of the thumb and fingers. Hence,

during the design process this must be taken care so that the segment is equally strong enough at each point against the grasping load.

8.7 Results Analyses

The results obtained through various analysis i.e. forward kinematics, inverse kinematics, grasping analysis and stress analysis of the proposed 5-fingered and 25- DoFs hand model are presented in the previous sections 8.2 through 8.6. The workspace of the hand is indicated in Figures 8.6 through 8.9 in X-Y plane, X-Z plane, Y-Z plane and 3D space respectively.

- The analyses of these figures indicate that the loci of the finger tips are distributed thickly across the work envelope. In other words, there are an increased number of loci due to increased DoFs. This is indicative of feasibility of complicated motion by the fingers. (Hypothesis-1)
- The workspace figures also indicate that the area covered under the trajectories is dependent on the number of DoFs. This shows that as the number of DoFs increases the apace covered in the work envelope also increases. (Hypothesis -2)
- The density of the loci of the finger tips with same number of angular increments in the joints is directly proportional to the number of DoFs in the hand and this increased density means less void space within the work envelope. Therefore, the total area under the work envelope in any given plane is more in present case than it would have been in case of a hand having less number of DoFs. This indicates that the reach is better with large number of DoFs. (Hypothesis -3)
- While formulating the forward kinematic problem it is assumed that every individual finger is considered to be an independent manipulator. Since each finger is connected to the palm having palm arch effect, the flexibility of these fingers gets increased while considering their motion from the wrist coordinate system. Hence the overall motion flexibility of each finger gets enhanced. This helps the hand in dealing with irregular shaped objects. (Hypothesis -4)

8.8 Summary

A detail analysis of a five fingered and 25-DOFs anthropomorphic robotic hand is done in the present work. The related results are presented in tabular forms and graphs in this chapter. A MATLAB code is developed for solving the forward kinematic problem of the hand. Using that code with input of joint angle values the thumb and fingertip positions are determined and shown in tables. Varying all 25 joint angles in their respective ranges simultaneously for thumb and all fingers, all possible tip positions are plotted which gives the workspace of the proposed hand model. The workspace is shown in three 2D plots as well as in 3D plots. The results of inverse kinematic problem of thumb and fingers are presented in separate tables. These results are obtained using ANFIS and are verified with those obtained through forward kinematic analysis. It is observed that the results are reasonable accurate and hence acceptable. The forces applied at contact points by thumb and fingers, their incident angles and position of contact points on the surface of the different shaped objects are determined using ANFIS and tabulated for individual objects separately. The stress concentration analysis results are presented in form of ANSYS graphs for thumb and fingers individually due to the reaction forces exerted on the fingers during grasping the object.

Chapter 9

CONCLUSIONS AND FURTHER WORK

9.1 Overview

Multi-fingered anthropomorphic robot hands are becoming more popular day by day due to its multi-functional and flexible activities like grasping and manipulating the object. The anthropomorphic appearance of the hand is also equally important when it is used for rehabilitation of human hand and be the part of the humanoid robots that perform different operations in human environment. The present work proposed a hand model with anthropomorphic appearance. The concepts and back ground theories are thoroughly discussed, based on which the modeling and subsequently the analysis have been done. The grasping theory and conditions of equilibrium for force-closure grasps are also discussed at length. The grasp synthesis of different shaped object with the proposed hand model and the stress analyses on the fingers due to grasping are also made. The work is summarized and concluded along with the statements on contributions of the present research work. The scope of future work to extend or to modify or to add some other new concept to the work is suggested in the present chapter.

9.2 Conclusions

Multi-fingered hands developed over the years have proved their distinct capabilities of flexibility and usefulness in handling precise tasks and manipulating objects of various shapes and characteristics. Inspired by the anatomy of human hand, many multi-fingered hands have been designed and developed to carry out a specific set of tasks. The human hand, as described earlier, is characterized by large number of joints, various joint types closely located within a limited space. It is

also true that as the number of joints increase and the distance between joints decrease, the modes of actuating the joints and controlling them become cumbersome. Therefore, the past researchers and designers of the robot hands having multi-finger configuration have chosen to limit the number of fingers to the minimum possible for the desired tasks and thereby making the control architecture simpler. Whenever there is increased number of joints, most of them are kept under actuated wilfully. So far as the developments of the multi-fingered hands are concerned, it is also convenient to use less number of fingers and joints. The actuation of all the fingers of the multi-fingered hand simultaneously either through common actuators or through the use of multiple actuators in synchronization also requires a great deal of control logics and mechanisms. Possibly all of these or some of these reasons have constrained the design of multi-fingered hands to think otherwise.

Under this backdrop of history and development it was a challenge to take up a task of designing multi0fingered anthropomorphic hand having 25 degrees-of-freedom. The present research work has been satisfactorily abetted through a well-thought and systematic approach. The various steps in designing this hand are as follows:

- A conceptual design of the anthropomorphic hand on the basis of a thorough study of the anatomy of human hand.
- Graphical and mathematical modelling of the hand for the forward kinematics as well as inverse kinematics analysis.
- Generation of workspace of the hand through graphical simulation to ensure the capability of the hand and to estimate the maximum size of the object that can be handled.
- Grasp analysis of the hand to estimate the grasping force/moments to handle the securing and manipulating tasks under desired grasping condition.

The summary of the research activities for completing this piece of work is be described in the following paragraphs:

- The present work proposes a novel 5-fingered, 25- DOFs anthropomorphic hand model. Unlike most of the earlier robotic hand models, the proposed hand model includes the palm arch effect of the human hand in its design. This effect of the palm is considered in the present model by introducing two DOFs each at the CMC joint of the ring and little fingers. The multi-fingered hands may be used for rehabilitation of the lost human hands and also may be used in humanoid robots which work in human environments

along with human beings. The increase in DOFs enhances the dexterity of the hand but simultaneously it also increases the control complexity. This problem can be minimized either by using some smart actuation systems at the joint itself or coupling some of the joints as in case of under-actuation system so that the numbers of actuation units are decreased. The detail kinematic and grasping analyses of the proposed hand are made based on the exhaustive study of human hand anatomy and past research work.

- The analysis of the forward and inverse kinematics is made on robotic principle, considering each finger as an open kinematic chain from the wrist of the hand. The wrist of the human hand is movable which mostly helps the positioning of the hand with respect to object before grasping the same. In the present work the wrist is assumed to be fixed and is considered to be the origin of the coordinate frame for the purpose of analysis. The kinematic model of the thumb and the fingers have been done individually considering them as individual manipulator with base at origin of local coordinate systems considered at CMC joints of thumb, ring finger and little finger and at MCP joints of index and middle finger for the respective fingers. The D-H parameters are determined from these kinematic models which are the basis for the further analysis of forward and inverse kinematics of the hand. The wrist is considered as the origin of global coordinate system. Using suitable transfer matrices, the origins are transferred from local to global coordinate system. Similarly the tip positions of the thumb and the fingers are calculated with respect to the origin of global coordinate system. The entire loci of tip positions are determined by the help of a computer programme, developed and operated in MATLAB-8 platform. The joint angles are varied in their respective ranges to determine the entire set of tip positions on 2D planes and 3D space. These tip positions of the thumb and the fingers give the reachable workspace of the proposed hand model. The analysis of workspace and grasping capability of the proposed hand model is made considering all anthropomorphic characteristics of human hand.

- Since the solution of inverse kinematic problem yields more number of alternate solutions, a suitable iterative or artificial intelligence method, ANFIS is used as the tool for inverse kinematic solution in the present work. Considering the tip positions of the thumb and fingers within the

workspace of the hand as the input data, the ANFIS structure was trained. Using ANFIS tool box of MATLAB the joint angles are determined and it is observed that the predicted values are within the permitted range of the angles. This technique gives a single output for any number of inputs. In all 25 FIS structures are developed and are used for predicting the joint angles of the 25 joints. The structures can be used for many inputs for predicting the joint angles with minimal and acceptable error.

- The detail grasp analysis including force analysis with various locations for points of contact and varying incident angles are made to ensure that force-closure grasp is achieved. The trajectories of the tips of the thumb and the fingers are plotted on the tip movement plane with variation of joint angles in their range. It is observed that the motion of the fingers and that of the thumb should oppose each other in directions and move closer to each other in order to grasp an object. Since the flexion/extension motion of the joints are mostly responsible for grasping of object, the DIP joint of the thumb and the fingers is kept at maximum angle position and other joints angles are kept at minimum position to obtained the maximum distance between the tips of thumb and that of the other fingers. This also determines the maximum size of the object the hand can grasp. A solid graphical model of the proposed hand is made in CATIA. The motion simulation is carried out by using the data over the entire range of the angles.

- It is assumed that the hand grasps the objects by contacts at the tips of the fingers only. The hand under design is expected to manipulate the object while grasping (force-closure grasping). It is also assumed that the tips are in contact with the objects on one plane parallel to base. The fingers are considered as hard fingers with friction at contact points. Considering the force equilibrium conditions, mathematical equations are derived in terms of fingertip forces and incident angles. However, while deriving the mathematical relationship for a possible solution, it was observed that the number of parameters to be determined and the number of equations obtained did not match for solving. Therefore, ANFIS is used to solve the equations and determine the values of forces and incident angles.

- The thumb and the fingers apply forces at the contact points to grasp the object firmly. These forces generate equal amount of reaction forces on the

thumb and the fingers. The stress analyses are made using ANSYS for fingers to check the strength and stability of the structure of the hand for handling the desired objects. The cross-section of the thumb and fingers are considered to be uniform square cross-section unlike human hand which is tapered towards the tip and has elliptical cross-section. In the present work two different finger materials are considered viz. structural steel and aluminium as examples. But the analysis is open to use other alternative materials.

9.3 Contributions

The prime contribution of the present work towards the design and development of multi-fingered robot hands are:

i. The designed hand is more flexible and is having better anthropomorphic features due to the fact that it has 25-degrees of freedom. The presence of 4-DOFs in the CMC joints of ring and little fingers is a special character added to the hand that makes the palm flexible. This characteristic is not available in the hands developed earlier.

ii. In order to make sure about the actual functioning of the hand within its workspace, the motion simulation and analysis of the thumb and all the fingers have been done simultaneously with reference to a single coordinate frame at the wrist. Such an analysis is indicative of the capability of the hand and is necessary for validating the claim that the hand is very close to that of a human being not only in appearance but also in its functions.

iii. While designing any mechanism, it is important to carry out analysis for both forward kinematics as well as the inverse kinematics. It is a challenge for the purpose of inverse kinematics of a mechanism having multiple degrees of freedom in a spatial coordinate space. Through the present work an appropriate method could be established to carry out the inverse kinematic analysis using ANFIS through systematic training a selected structure. This has been checked to meet the tolerance level.

iv. The hand under design during the present work had a specific set of tasks to do. The tasks primarily included grasping and manipulating the objects under grasped conditions. Therefore the research work, under its scope included the analysis of force-closure grasping by the hand for various differently shaped objects. The analysis considers all its fingers, their

parameters and the grasping conditions together to make it composite and complete. Such an approach will encourage researchers and designers to carry out such analysis before any product is developed.

The developments of the kinematic model and the associated algorithm have made it possible to virtually investigate the potential for a robotic hand with 25 DoFs and an associated enhanced, palm arch effect that will improve grip and performance.

9.4 Scope for Future Work

The present work proposed a novel multi-fingered hand model. The kinematical analysis and grasping analysis along with analysis of stress due to grasping forces are also made. The research work is a holistic approach for designing and developing a multi-fingered anthropomorphic robot hand for the already stated purpose. However, there also exists a scope for fine tuning this work with consideration to additional parameters and operating conditions. Some of the scopes for further work on this research may be as follows:

- The wrist of the hand is considered as fixed point in the present work. Some degrees of freedom may be considered to make it more dexterous.
- Fingers are considered as hard fingers with friction at contact points. The use of soft finger which is more realistic may be considered and accordingly the grasp analysis method can be modified.
- The hand under the present design is having as many as 25 DOFs. The kinematic modeling, especially for handling the inverse kinematic issues, may be done using other mathematical approaches such as Lie groups or Quaternions for convenience.
- Fingertip positions are assumed to be on the same plane for grasping the object. This has been done so for computational convenience. However, if the tip positions are distributed that may give more stable grasp. The work can be extended in that aspect.
- The stress analysis of the hand structure has been made without considering proper joints. The joint types and their characteristics may be considered to obtain more pragmatic results.
- The type of actuation and control aspects may be incorporated in the purview of the design to aid the development of hand in complete form.

REFERENCES

[1] A. Bichhi, "Hands for Dexterous Manipulation and Robust Grasping: A Difficult Road towards Simplicity", IEEE Transaction, Robotics and Automation. vol.16, no. 6, pp. 652-662, 2000.

[2] M. Santello, M. Flanders, and J. F. Soechting, "Poatural Hand Synerhies for Tool Use", The Journal of Neuroscience, vol. 18, No. 23, pp. 10105-10115, 1998.

[3] Official Roboethics website, http://www.roboethics.org.

[4] Scuola di Robotica home page, http://www.scuoladirobotica.it.

[5] Schmalz gripper web page, http://www.schmalz.com

[6] Shunk grippers web page, http:// www.shunk.com

[7] Adhesive grippers web page, http://news.thomasnet.com/fullstory/Custom-Vacuum-Grippers-provide-consistent-adhesion-591591.

[8] http://www.eu-nited.net/robotics/index.php?idcat=81&idart=108

[9] http://www.intelligentactuator.com/robo-cylinder-electric-gripper-and-rotary-type-actuators/

[10] http://blog.robotiq.com/bid/33127/How-To-Choose-The-Right-Robotic-Gripper-For-Your-Application

[11] T. Okada, "Computer Control of Multi Jointed Finger System for Precise Object Handling", Mechatronic Design of a Transradial Cybernetic Hand IEEE Transactions on System, Man and Cybernetics, vol. SMC-12, n0. 3, pp. 289-299, 1982.

[12] K.S. Salisbury and B. Roth, "Kinematics and Force Analysis of Articulated Mechanical Hands", ASME Journal of Mechanisms, Transmissions and Actuation in Design, vol. 105, no. 1, pp. 35-41,1983.

[13] S.C. Jacobsen, E.K. Iversen, D.F. Knutti, R.T. Johnson and K.B. Biggers, "Design of the UTAH/MIT Dexterous Hand", Proceedings of the IEEE International Conference on Robotics and Automation, 1986.

[14] W. T. Townsend, "MCB- Industrial Robot Feature Article- Barrett Hand Grasper", Industrial Robot: An International Journal, vol. 27, no. 3, pp. 181-188, 2000.

[15] Barret Hand webpage, http://www.barretttechnology.com

[16] J.P. Gazeau, S. Zeghloul, M. Arsicualt, and J.P. Lallemand, “The LMS Hand: Force and Position Controls in the Aim of Fine Manipulation of Objects”, Proceedings of the IEEE International Conference on Robotics and Automation, 1998.

[17] A. Caffaz and G. Cannata, “The Design and Development of the Dist-Hand Dextrous Gripper”, Proceedings of the IEEE International Conference on Robotics and Automation, 1998.

[18] Dist Hand webpage, http://www.graal.dist.unige.it/research.

[19] Robonaut Hand webpage, http://vesuvius.jsc.nasa.gov.

[20] C.S. Lovchik and M.A. Diftler, “The Robonaut Hand: A Dexterous Robot Hand for Space”, Proceedings of the IEEE International Conference on Robotics and Automation, 1999.

[21] J. Butterfass, M. Grebenstein, H. Liu, and G. Hirzinger, “DLR-hand II: Next Generation of a Dextrous Robot Hand”, Proceedings of the IEEE International Conference on Robotics and Automation, Seoul, Korea, May21-26, 2001.

[22] N. Fukaya, S. Toyama, T. Asfour, and R. Dillmann, “Design of the Tuat/Karlsruhe Humanoid Hand”, Proceedings of the IEEE/RSJ International Conference on Intelligent Robots and Systems, 2000.

[23] S. Schulz, C. Pylatiuk, and G. Bretthauer, “A New Ultra-light Anthropomorphic Hand”, Proceedings of the IEEE International Conference on Robotics and Automation, 2001.

[24] H. Kawasaki, H. Shimomura, and Y. Shimizu, “Educational-Industrial Complex Development of an Anthropomorphic Robot Hand 'Gifu Hand'”, Advanced Robotics, vol. 15, no. 3, pp. 357-363, 2001.

[25] Shadow Hand webpage, http://www.shadow.org.uk/.

[26] A. Namiki, Y. Imai, M. Ishikawa, and M. Kaneko, “Development of a High-Speed Multi-Fingered Hand System and its Application to Catching”, Proceedings of the IEEE/RSJ International Conference on Intelligent Robots and Systems, pp.2666-2671, 2003.

[27] K. Hoshino and I. Kawabuchi, “Pinching at Finger tips for Humanoid Robot Hand”, Journal of Robotics and Mechatronics, vol. 17, no. 6, pp.655-663, 2005.

[28] K. Kaneko, K. Harada, and F. Kanehiro, “Development of Multi-fingered Hand for Life-size Humanoid Robots”, Proceedings of IEEE International Conference on Robotics and Automation, pp. 913-920, 2007.

[29] T. Takaki and T. Omata, “High Performance Anthropomorphic Robot Hand with Grasp Force Magnification Mechanism”, Proceedings of IEEE International Conference on Robotics and Automation, pp.1697-1703, 2009.

[30] G. Berselli, G. Borghesan, M. Brandi, C. Melchiorri, C. Natale, G. Palli, S. Pirozzi, and G. Vassura, “Integrated Mechatronic Design for a New Generation of Robotic Hands”, Proceedings of the IFAC International Symposium on Robot Control, 2009.

[31] L. Biagiotti, F. Lotti, G. Palli, P. Tiezzi, G. Vassura and C. Melchiorri, “Development of UB Hand III: Early Results”, Proceedings of IEEE International Conference on Robotics and Automation, ICRA’05, Barcelona, Spain, April 18-20, 2005.

[32] M.C. Carrozza, C. Suppo, F. Sebastiani, B. Massa, F. Vecchi, R. Lazzarini, M.R. Cutkosky and P. Dario, “The SPRING Hand: Development of a Self-Adaptive Prosthesis for Restoring Natural Grasping”, Autonomous Robots, vol.16, no. 2, pp. 125–141, 2004.

[33] J. L. Pons, E. Rocon, R. Ceres, D. Reynaerts, B. Saro, S. Levin, W. Van Moorleghem, “ The MANUS-hand dextrous robotics upper limb prosthesis: mechanical and manipulation aspects”, Autonomous Robots**,** vol. 16, no. 2, pp. 143-165, 2004.

[34] http://www.mobilemag.com/2013/05/02/irobot-hand-darpa/

[35] http://robotiq.com/en/applications/robot-gripper-jig-less-welding.php

[36] http://www.barrett.com/robot/index.htm

[37] http://www.liberatingtech.com/

[38] http://www.living-with-michelangelo.com/gb/home/

[39] http://world.honda.com/ASIMO/

[40] http://www.designboom.com/technology/kobian-emotional-robot/

[41] http://en.wikipedia.org/wiki/Toyota_Partner_Robot

[42] http://www.bostondynamics.com/robot_Atlas.html

[43] http://www.roboy.org/

[44] R. Murray, Z. Li and S, Sastry, “A mathematical Introduction to Robotic Manipulator”, CRC press, Boca Raton, Florida, 1994.

[45] The Hand Embodied Research Project Home Page, http:// www.the handembodied.eu/project.

[46] Z. Li and S.S. Sastry, "Grasping and Coordinated Manipulation by a Multi-Fingered Robot Hand", International Journal of Robotic Research, vol. 8, no. 4, pp. 33-50, 1989.

[47] K.B. Shimoga, "Robot Grasp Synthesis Algorithms: A Survey", International Journal of Robotic Research, vol. 15, no. 3, pp. 230-266, 1996.

[48] R. Su´arez, M. Roa, and J. Cornell`a, "Grasp Quality Measures", Institute of Industrial and Control Engineering, Technical University of Catalonia, Tech, Report., 2006

[49] B. Sciliano and O. Khatib (rds.), "Springer Handbook of Robotics", chapter 15, Robot Hands, 2008.

[50] L.R. Lin and H.P. Huang, "Mechanism and Computer Simulation of a New Robot Hand for Potential Use as an Artificial Hand", Artificial Organs, vol. 21, pp. 59-69, Jan. 1997.

[51] J. Ponce, S. Sullivan, A. Sudsang, J. Boissonnat and J. Merlet, "On Computing Four-Finger Equilibrium and Force-Closure Grasps of Polyhedral Objects", The International Journal of Robotics Research, vol. 16, no. 1. pp. 11-35, February, 1997.

[52] K. Nagai, Y. Eto, D. Asai, and M. Yazaki, "Development of a Three-Fingered Robotic Hand-Wrist for Compliant Motion", Proceedings of 1998 IEEE/RSJ International Conference on Intelligent Robots and Systems. Innovations in Theory, Practice and Applications (Cat. No.98CH36190) , pp. 476-481, 1998.

[53] Ann. M. Ramos, I. a Gravagne, and I.D. Walker, "Goldfinger: a Non-Anthropomorphic, Dexterous Robot Hand", Proceedings of 1999 IEEE International Conference on Robotics and Automation (Cat. No.99CH36288C), pp. 913-919, 1999.

[54] Ch. Borst, M. Fischer and G. Hirzinger, "A Fast and Robust Grasp Planner for Arbitrary 3D Objects", Proceedings of the EEE International Conference on Robotics & Automation, Detroit, Michigan, May 1999.

[55] J. Butterfa, M. Grebenstein, H. Liu and G. Hirzinger "DLR-Hand II: Next Generation of a Dexterous Robot Hand", International Conference on Robotics and Automation, pp. 109-114, 2001.

[56] B. Massa, S. Roccella, M.C. Carrozza, and P. Dario, “Design and Development of an Under Actuated Prosthetic Hand”, Proceedings of IEEE International Conference on Robotics and Automation (Cat. No.02CH37292), pp. 3374-3379,2002.

[57] E. Ngale Haulin and R. Vinet, “Multi Objective Optimization Of Hand Prosthesis Mechanisms”, Mechanism and Machine Theory, vol. 38, pp. 3-26, Jan. 2003.

[58] X. Zhu and J. Wang, “Synthesis of Force-Closure Grasps on 3D Objects Based on the Q Distance”, IEEE Transactions on Robotics and Automation, vol. 19, no. 4, 2003.

[59] J. Li, M. Jin and H. Liu, “A New Algorithm for Three-finger Force-closure Grasp of Polygonal Objects”, Proceedings of the IEEE International Conference on Robotics & Automation Taipei, Taiwan, September 14-19, 2003.

[60] H. Huang, Li Jang,Y. Liu, L. Hou, H. Cai, and H. Liu, “The Mechanical Design and Experiments of HIT/DLR Prosthetic Hand,” IEEE International Conference on Robotics and Biomimetics, pp. 896-901, 2006.

[61] L. Zollo, S. Roccella, E. Guglielmelli, M.C. Carrozza, and P. Dario, “Bio-mechatronic Design and Control of an Anthropomorphic Artificial Hand for Prosthetic and Robotic Applications,” Hand, The, vol. 12, pp. 418-429, 2007.

[62] D. Dragulescu and L. Ungureanu, “The Modeling Process of a Human Hand Prosthesis”, 4th International Symposium on Applied Computational Intelligence and Informatics, pp. 263-268, May. 2007.

[63] A. Kargov, C. Pylatiuk, R. Oberle, H. Klosek, T. Werner, W. Roessler, and S. Schulz, “Development of a Multifunctional Cosmetic Prosthetic Hand”, IEEE 10th International Conference on Rehabilitation Robotics, June 12-15, Noordwijk, The Netherlands, pp. 550-553, 2007.

[64] D. Dragulescu, V. Perdereau, M. Drouin, L. Ungureanu, and K. Menyhardt, “3D Active Workspace of Human Hand Anatomical Model”, Biomedical Engineering Online, vol. 6, p. 15, Jan. 2007.

[65] Y. Kamikawa and T. Maeno, “Under Actuated Five-Finger Prosthetic Hand Inspired by Grasping Force Distribution of Humans”, IEEE/RSJ

International Conference on Intelligent Robots and Systems Acropolis, France, Sept, 22-26, pp. 717-722, 2008.

[66] M. Controzzi, C. Cipriani, and M. C. Carrozza, "Mechatronic Design of a Transradial Cybernetic Hand", IEEE/RSJ International Conference on Intelligent Robots and Systems Acropolis, France, Sept, 22-26, pp. 576-581, 2008.

[67] S. yoon Jung and I. Moon, "Grip Force Modeling of a Tendon-driven Prosthetic Hand," International Conference on Control, Automation and Systems, Oct. 14-17, COEX, Seoul, Korea, pp. 2006-2009, 2008.

[68] A. Peer, S. Einenkel, and M. Buss, "Multi-fingered Tele-manipulation Mapping of a Human Hand to a Three Finger Gripper", IEEE International Symposium on Robot and Human Interactive Communication, Technische, University of Munchen, Munich, Germany, Aug. 1-3, pp. 465-470,2008.

[69] B. Bounab, D. Sidbore and A. Zaatri, "Central Axis Approach for Computing n-Finger Force-closure Grasps", IEEE International Conference on Robotics and Automation (ICRA), pp. 1169 – 1174, Pasadena, CA, USA, May 19-23, 2008.

[70] N. Niparnan, A. Sudsang and P. Chongstitvatana, "Positive Span of Force and Torque Components in Three Dimensional Four Finger Force Closure Grasps", Advanced Robotics, Vol. 22, No. 13-14, pp. 1497-1520, 2008.

[71] S. Lee, S. Noh, Y. Lee, and J.H. Park, "Development of Bio-Mimetic Robot Hand Using Parallel Mechanisms", IEEE International Conference on Robotics and Bio-mimetic (ROBIO) , pp. 550-555, Dec. 2009.

[72] S.A. Dalley, T.E. Wiste, T.J.W. Member, and M. Goldfarb, "Design of a Multifunctional Anthropomorphic Prosthetic Hand with Extrinsic Actuation", IEEE/ASME Transactions on Mechatronics, vol. 14, no. 6, pp. 699-706, 2009.

[73] S. Parasuraman and C. Zhen, "Development of Robot Assisted Hand Stroke Rehabilitation System", International Conference on Computer and Automation Engineering, pp. 70-74, Mar. 2009.

[74] Wan Faizura Binit Wan Tarmizi, I. Elamvazuthi, and M. Begam, "Kinematic and Dynamic Modeling of a Multi- Fingered robot Hand,"

International Journal of Basic &Applied Sciences (IJBAS), vol.9, no. 10, pp. 89-96, Dec. 2009.

[75] M. Controzzi, C. Cipriani, B. Jehenne, M. Donati and M.C. Carrozza, "Bio-Inspired Mechanical Design of a Tendon-Driven Dexterous Prosthetic Hand", International Conference of the IEEE EMBS, Buenos Aires, Argentina, Aug. 31 – Sept. 4, pp. 499-502, 2010.

[76] X. Wang, J. Zhao, D. Yang, N. Li, C. Sun, and H. Liu, "Bio-mechatronic Approach to a Multi-Fingered Hand Prosthesis" , International Conference on Biomedical Robotics and Bio-mechatronics, The University of Tokyo, Tokyo, Japan, Sept. 26-29, pp. 209-214, 2010.

[77] M. Suhaib, R. A. Khan and S. Mukharjee, "Contact Force Optimization for Stable Grasp of Multi-fingered Robotic Grippers", Proceedings of the World Congress on Engineering, vol. 2192, no. 1, pp. 2194-2197, 2011.

[78] A. M. Zaid and M. A. Yaqub, "UTHM HAND: Performance of Complete System of Dexterous Anthropomorphic Robotic Hand" International Symposium on Robotics and Intelligent Sensors (IRIS), Procedia of Engineering, Elsevier, vol. 41, pp. 777-783, 2012.

[79] V. Lippiello, B. Siciliano and L. Villani, "Multi-fingered Grasp Synthesis based on the Object Dynamic Properties", Robotics and Autonomous Systems, Elsevier, vol. 61, pp. 626–636, 2013.

[80] R. Mosher, "Force Reflection Electrohydraulic Servo Manipulator", Electro-Technology, pp. 138, December 1960.

[81] F.Y. Chen, "Gripping Mechanisms for Industrial Robots". Mechanism and Machine Theory, vol. 17, no.5, pp.299–311, 1982.

[82] D. Kriegman, D. Siegel, S. Narasimhan, J. Hollerbach, and G. Gerpheide, "Computational Architecture for the Utah/MIT Hand," Proceedings of IEEE International Conference on Robotics and Automation, pp. 918–924, 1985.

[83] M. Bergamasco and S. Scattareggia Marchese, "The Mechanical Design of the MARCUS Prosthetic Hand," Proceedings of 4th IEEE International Workshop on Robot and Human Communication, pp. 95–100, 1995.

[84] Robert Vinet, Yves Lozac'h, Nicolas Beaudry and Gilbert Drouin, "Design Methodology for a Multifunctional Hand Prosthesis", Journal of Rehabilitation Research and Development, vol. 32, no . 4, pp. 316-324, November 1995.

[85] Y. Yasumuro, Qian Chen and K. Chihara, “3D Modeling of Human Hand with Motion Constraints, “Proceedings of International Conference on Recent Advances in 3-D Digital Imaging and Modelling” (Cat. No.97TB100134), pp. 275–282, 1997.

[86] T. Laliberte and Clement M. Gosselin, “Simulation and Design of Under-Actuated Mechanical Hands”, Mechanism and Machine Theory, vol. 33, no. 1/2, pp. 39-57, 1998.

[87] D. M. Lane, J. B. C. Davies, G. Robinson, D. J. O’Brien, J. Sneddon, E. Seaton, and a. Elfstrom, “The AMADEUS Dexterous Subsea Hand: Design, Modeling and Sensor Processing,” IEEE Journal of Oceanic Engineering, vol. 24, no. 1, pp. 96–111, 1999.

[88] H. d. Visser and J. L. Herder, “Force Directed Design of a Voluntary Closing Hand Prosthesis”, Journal of Rehabilitation Research and Development, vol. 37, no. 3, pp. 261–271, 2000.

[89] W. B. Griffin, R. P. Findley, M. L. Turner, and M. R. Cutkosky, “Calibration and Mapping of a Human Hand for Dexterous Tele-manipulation”, ASME IMECE Symposium on Haptic Interfaces for Virtual Environments and Teleoperator Systems, pp. 1-8, 2000.

[90] S. Schulz, C. Pylatiuk, and G. Bretthauer, “A New Ultra-light Anthropomorphic Hand”, Proceedings of IEEE International Conference on Robotics and Automation (Cat. No.01CH37164), pp. 2437–2441, May 2001.

[91] N. Dechev, “Multiple Finger Passive Adaptive Grasp Prosthetic Hand”, Mechanism and Machine Theory, vol. 36, no. 10, pp. 1157–1173, Oct. 2001.

[92] P. Chappell, M.M. Fateh and R.M. Crowder “Kinematic Control of a Three-Fingered and Fully Adaptive End-Effector Using a Jacobian Matrix”, Mechatronics, vol. 11, no. 3, pp. 355–368, Apr. 2001.

[93] M. Renault and F. B. Ouezdou, “Dynamic Simulation of Hand-Forearm System”, IEEE International Workshop on Robot and Human Interactive Communication Technology, pp. 20–25.

[94] M. C. Carrozza, B. Massa, S. Micera, R. Lazzarini, M. Zecca, and P. Dario, “The Development of a Novel Prosthetic Hand-Ongoing Research and Preliminary Results”, IEEE/ASME Transactions on Mechatronics, vol. 7, no. 2, pp. 108–114, Jun. 2002.

[95] D. D. Wilkinson, M. V. Weghe, and Y. Matsuoka, “An Extensor Mechanism for an Anatomical Robotic Hand”, 2003 IEEE International Conference on Robotics and Automation (Cat. No.03CH37422), pp. 238–243, 2003.

[96] I. Yamano, K. Takemura, and T. Maeno, “Development of a Robot Finger for Five-Fingered Hand Using Ultrasonic Motors”, Proceedings of IEEE/RSJ International Conference on Intelligent Robots and Systems (IROS 2003) (Cat. No.03CH37453), pp. 2648–2653, October, 2003.

[97] C. Borst, M. Fischer, S. Haidacher, H. Liu, and G. Hirzinger, “DLR Hand II: Experiments and Experience with an Anthropomorphic Hand”, Proceedings of IEEE International Conference on Robotics and Automation (Cat. No.03CH37422), pp. 702–707, 2003.

[98] S. Haidacher, J. Butterfass, M. Fischer, M. Grebenstein, K. Joehl, K. Kunze, M. Nickl, N. Seitz, and G. Hirzinger, “DLR Hand II : Hard and Software Architecture for Information Processing”, Proceedings of the 2003 IEEE International Conference on Robotics & Automation, Taipei, Taiwan, September 14-19, 2003.

[99] J. Yang, “A Multi-Fingered Hand Prosthesis”, Mechanism and Machine Theory, vol. 39, no. 6, pp. 555–581, Jun. 2004.

[100] A. Kargov, T. Asfour, C. Pylatiuk, R. Oberle, H. Klosek, S. Schulz, K. Regenstein, G. Bretthauer, and R. Dillmann, “Development of an Anthropomorphic Hand for a Mobile Assistive Robot”, 9th International Conference on Rehabilitation Robotics, (ICORR) 2005. June 28 - July 1, 2005, Chicago, IL, USA, pp. 182–186, 2005.

[101] D.W. Zhao, L. Jiang, H. Huang, M.H. Jin, H.G. Cai and H. Liu, “Development of a Multi-DOF Anthropomorphic Prosthetic Hand”, Proceedings of the 2006 IEEE International Conference on Robotics and Bio-mimetic, December 17 - 20, Kunming, China, 2006.

[102] Y. Moon, “Bio-Mimetic Design of Finger Mechanism with Contact Aided Compliant Mechanism”, Mechanism and Machine Theory, vol. 42, no. 5, pp. 600–611, May 2007.

[103] Onno A. van Nierop, Aadjan van der Helm, Kees J. Overbeeke and Tom J.P. Djajadiningrat, “A Natural Human Hand Model”, Visual Computation, Springer-Verlag, vol. 24, pp. 31–44, 2008.

[104] G. Carbone and M. Ceccarelli, “Design of LARM Hand: Problems and Solutions”, Proceedings of IEEE International Conference on Automation, Quality and Testing, Robotics, pp. 298–303, 2008.

[105] J. Shi, Y. Zheng, X. Chen, and H. Xie, “Modeling the Relationship Between Wrist Angle and Muscle Thickness During Wrist Flexion-Extension Based on the Bone-Muscle Lever System: A Comparison Study”, Medical Engineering & Physics, vol. 31, no. 10, pp. 1255–60, Dec. 2009.

[106] D. J. Montana, “The Kinematics of Multi-Fingered Manipulation”, IEEE Transaction on Robotics and Automation, vol. 11, no. 4, Aug 1995.

[107] Y. Kurita, Y. Ono, A. Ikeda and T. Ogasawara, “Human-sized Anthropomorphic Robot Hand with Detachable Mechanism at the Wrist”, Mechanism and Machine Theory, ELSEVIER, vol. 46, pp.53–66, 2011.

[108] J. L. Sancho-Bru, A. Pérez-González, M. Vergara, and D. J. Giurintano, “A 3D Biomechanical Model of the Hand for Power Grip”, Journal of Biomechanical Engineering, vol. 125, no. 1, p. 78, 2003.

[109] M. Natsuki, K. Makiko. K. Tsuneya , and M. Masaaki, “Modeling of Human Hand Link Structure from Optical Motion Capture Data” , Proceedings of IEEE/ RSJ International Conference on Intelligent Robots and Systems, Sendai, Japan, September 28 -October 2,2004.

[110] D. S. Barker, D. J. Netherway, J. Krishnan, and T. C. Hearn, “Validation of a Finite Element Model of the Human Metacarpal”, Medical engineering & physics, vol. 27, no. 2, pp. 103–113, Mar. 2005.

[111] W. Tsang, K. Singh, and E. Fiume, “Helping Hand : An Anatomically Accurate Inverse Dynamics Solution for Unconstrained Hand Motion”, Computer, pp. 1–10, 2005.

[112] A. R. Ahmed, A. Tatsuo, T. Tomohito, and I. Kenji, “Optimization of a Hybrid Two-Fingered Micro Hand Using Genetic Algorithms”, Proceedings of the IEEE International Symposium on Micro-Nano Mechatronics and Human Science, MHS2008, Nagoya, Japan, pp. 103-107, 2008.

[113] J. Lin, Y. Wu and T. S. Huang, “Modeling the Constraints of Human Hand Motion”, www.ifp.illinois.edu/~yingwu/papers/Humo00.pdf

[114] C. Walha, H. Bezine and A. M. Alimi, “An Adaptive Particle Swarm Optimization Method for Solving the Grasp Planning Problem”, International Symposium on Robotics and Intelligent Sensors (IRIS), Procedia Engineering, Elsevier, vol. 41, pp. 426 – 435, 2012.

[115] R. Tomovic, G. Bekey, and W. Karplus, “A Strategy for Grasp Synthesis with Multi-Fingered Robot Hands”, Proceedings of the IEEE International Conference on Robotics and Automation, pp. 83–89, 1987.

[116] P. J. Kyberd, O. E. Holland, P. H. Chappell, S. Smith, R. Tregidgo, P. J. Bagwell, and M. Snaith, “MARCUS: a Two Degree of Freedom Hand Prosthesis with Hierarchical Grip Control”, IEEE Transactions on Rehabilitation Engineering, vol. 3, no. 1, pp. 70–76, Mar. 1995.

[117] B. L. Shields, J. A Main, S. W. Peterson, and A. M. Strauss, “An Anthropomorphic Hand Exoskeleton to Prevent Astronaut Hand Fatigue during Extravehicular Activities”, IEEE Transactions on Systems, Man, and Cybernetics, vol. 27, no. 5, pp. 668–73, 1997.

[118] S. E. Baek, S. H. Lee and J. H. Chang, “Design and Control of a Robotic Finger for Prosthetic Hands”, IEEE/IRS International Conference on Intelligent Robots and Systems, 1999.

[119] M. Zecca, S. Micera, M. C. Carrozza, and P. Dario, “Control of Multifunctional Prosthetic Hands by Processing the Electromyographic Signal”, Critical Reviews in Biomedical Engineering, vol. 30, no. 4–6, pp. 459–85, 2002.

[120] E. L. Secco and G. Magenes, “A Feed Forward Neural Network Controlling the Movement of a 3-DOF Finger”, IEEE Transactions on Systems, Man, and Cybernetics - Part A: Systems and Humans, vol. 32, no. 3, pp. 437–445, May 2002.

[121] S. Ferguson and G. R. Dunlop, “Grasp Recognition from Myoelectric Signals”, Proceeding of 2002 Australasian conference on Robotics and Automation, Auckland, November, 27–29, 2002.

[122] G. Elkoura and K. Singh, “Handrix : Animating the Human Hand”, Euro graphics /SIGGRAPH Symposium on Computer Animation, 2003.

[123] Jun Ueda, Y. Ishida, M. Kondo, and T. Ogasawara, “Development of the NAIST-Hand with Vision-based Tactile Fingertip Sensor,” Proceedings of the IEEE International Conference on Robotics and Automation, Barcelona, Spain, April 2005.

[124] M. C. Carrozza, G. Cappiello, S. Micera, B. B. Edin, L. Beccai, and C. Cipriani, “Design of a Cybernetic Hand for Perception and Action”, Biological cybernetics, vol. 95, no. 6, pp. 629–44, Dec. 2006.

[125] D. Yang, J. Zhao, Y. Gu, X. Wang, N. Li, and L. Jiang, “An Anthropomorphic Robot Hand Developed Based on Under actuated

Mechanism and Controlled by EMG Signals", Journal of Bionic Engineering, vol. 6, no. 3, pp. 255–263, 2009.

[126] P. Wojtczak, T. G. Amaral, O. P. Dias, A. Wolczowski, and M. Kurzynski, "Hand Movement Recognition Based on Bio-signal Analysis", Engineering Applications of Artificial Intelligence, vol. 22, no. 4–5, pp. 608–615, Jun. 2009.

[127] P. Dario, M. C. Carrozza, A. Menciassi, S. Micera, M. Zecca, V. R. Piaggio, and P. Pi, "On the Development of a Cybernetic Hand Prosthesis", www.researchgate.net/.

[128] M. C. Carrozza, B. Massa, P. Dario, R. Lazzarini, M. Zecca, S. Micera, and P. Pastacaldi, "A Two DOF Finger for a Bio-mechatronic Artificial Hand", pp. 1–37, http://www.ncbi.nlm.nih.gov/pubmed/12082213.

[129] A. Peer, S. Einenkel, and M. Buss, "Multi-fingered Tele-manipulation - Mapping of a Human Hand to a Three Finger Gripper", Proceedings of the 17th IEEE International Symposium on Robot and Human Interactive Communication, Technische University München, Munich, Germany, August 1-3, 2008.

[130] A. Jaffar, M.S. Bahari, C. Y. Low and R. Jaafar, "Design and Control of a Multi-fingered Anthropomorphic Robotic Hand", International Journal of Mechanical & Mechatronics Engineering (IJMME-IJENS), vol. 11, no. 04, pp. 26-33,2011.

[131] R. Boughdiri , H. Nasser , H. Bezine , N. K. M'Sird, A. M. Alimi and A. Naamane, "Dynamic Modeling and Control of a Multi-Fingered Robot Hand for Grasping Task" , International Symposium on Robotics and Intelligent Sensors (IRIS), Procedia Engineering, Elsevier, vol. 41, pp. 923 – 931, 2012.

[132] C. H. Chen and D. S. Naidu, "Hybrid Control Strategies for a Five-finger Robotic Hand", Biomedical Signal Processing and Control, Elsevier, vol. 8, pp. 382– 390, 2013.

[133] J. J. Kuch and T. S. Huang, "Human computer interaction via the human hand: a hand model", Proceedings of 28th Asilomar Conference on Signals, Systems and Computers, pp. 1252–1256, 1995.

[134] R. Doshi, C. Yeh, and M. LeBlanc, "The Design and Development of a Gloveless Endoskeletal Prosthetic Hand", Journal of Rehabilitation Research and Development, vol. 35, no. 4, pp. 388–95, 1998.

[135] C. S. Lovchik and M. A. Diftler, “The Robonaut Hand: A Dexterous Robot Hand for Space,” Proceedings 1999 IEEE International Conference on Robotics and Automation, Detroit, Michigan May, 1999.

[136] F. J. Valero-Cuevas, “Applying Principles of Robotics to Understand the Biomechanics, Neuromuscular Control and Clinical Rehabilitation of Human Digits”, Proceedings of IEEE International Conference on Robotics and Automation. San Francisco, CA, April, 2000.

[137] J. Eriksson, M. J. Mataric and C. J. Winstein, “Hands-Off Assistive Robotics for Post-Stroke Arm Rehabilitation”, Proceedings of IEEE 9th International Conference on Rehabilitation Robotics, (ICORR), Chicago, IL, USA) June 28 - July 1, 2005.

[138] K. Nagata, F. Saito and T. Suehiro, “ Development of the Master Hand for Grasping Information Capturing”, Proceedings of the 2001 IEEE/RSJ International conference on Intelligent Robots and system, Mani, Hawali, USA, Oct. 29- Nov. 03, 2001.

[139] V. D. Nguyen, “The Synthesis of Stable Force Closure Grasp”, A Thesis, MIT Artificial Intelligence Laboratory, Massachusetts of Technology, 1986.

[140] V. D. Nguyen, “Constructing Stable Grasps in 3D”, Proceeding of IEEE International Conference on Robotics and Automation, vol.4, pp. 234–239, 1987.

[141] S. Haidacher and G. Hirzinger, “Contact Point Identification in Multi-Fingered Grasps Exploiting Kinematic Constraints”, proceeding of IEEE international conference on Robotics and Automation, pp. 1597-1603, Washington, DC, May 2002.

[142] B. Bounab, D. Sidbore and A. Zaatri, “Performance of Central Axis Approach in Grasp Analysis”, Proceedings of IEEE International Conference on Robotics and Automation (ICRA), pp. 1273 – 1278, Anchorage convention District, Anchorage, Alaska, USA, May 3-8, 2010.

[143] B. Mishra, J. T. Schwartz and M. Sharir, “On the Existence and Synthesis of Multi-Finger Positive Grips”, Algorithmica, vol. 2, no. 4, pp. 541–558, 1987.

[144] J. Trinkle, “A Quantitative Test for Form Closure Grasps”, Proceedings of IEEE /RSJ International Conference on Intelligent Robots and Systems, 1992.

[145] C. Ferrari and J. Canny, “Planning Optimal Grasps”, Proceedings of IEEE International Conference on Robotics and Automation, vol.3, pp. 2290 – 2295,1992.

[146] T. Omata, “Finger Position Computation for 3-Dimensional Equilibrium Grasps”, Proceedings of IEEE International Conference Robotics and Automation, vol.2, pp. 216 – 222, 1993.

[147] J. Ponce, S. Sullivan, J. D. Boissonnat and P. Merlet, “On Characterizing and Computing Three and Four-Finger Force-Closure Grasps of Polyhedral Objects”, Proceedings of IEEE International Conference on Robotics and Automation, pp. 821–827, 1993.

[148] B. Mirtich and J. Canny, “Easily Computable Optimum Grasps in 2-D and 3-D”, Proceedings of the IEEE International Conference on Robotics and Automation , pp. 739-747, DOI: 10.1109/ROBOT.1994.351399, 1994.

[149] V. Verma and U. Tasch, “Graphical Representation of Robot Grasping Quality Measures”, Proceedings of IEEE international conference on Robotics and Automation, vol.13, pp.287-295,1994.

[150] A. Bicchi, “On the Closure Properties of Robotic Grasping”, in The International Journal of Robotic Research, vol. 14, no.4, pp. 319-334, 1995.

[151] Y. Jia, “On Computing Optimal Planar Grasps”, Intelligent Robots and Systems 95. Proceedings 1995 IEEE/RSJ International Conference on Human Robot Interaction and Cooperative Robots, vol. 3, pp. 427 – 434, 1995

[152] M. Buss, H. Hashimoto and J. B. Moore, “Dextrous Hand Grasping Force Optimization”, IEEE Transactions on Robotics and Automation, Vol. 12, No. 3, PP. 406-418, 1996.

[153] W. S. Howard and V. Kumar, “On the Stability of Grasped Objects”, IEEE Transactions, Robotics and Automation, Vol. 12, No. 6, pp. 904 - 917 , 1996

[154] Y. H. Liu and M. Wang, “Qualitative Test and Force Optimization of 3D Frictional Force-Closure Grasps Using Linear Programming”, Proceedings

of 1998 IEEE International Conference Robotics and Automation, Vol. 4, pp. 3335 – 3340, 1998.

[155] R. Abu-Zitar and A. M. Al-Fahed Nuseirat, "A Neural Network Approach to the Frictionless Grasping Problem", Journal of Intelligent and Robotic Systems, vol. 29, No. 1 , pp. 27-45, 1999.

[156] A. T. Miller and P. K. Allen, "Examples of 3D Grasp Quality Computations", Proceedings of IEEE International Conference Robotics and Automation, Vol. 2, pp. 1240 – 1246, 1999.

[157] C. Xiong, Y. Li, Y. Xiong, H. Ding and Q. Huang, "Grasp Capability Analysis of Multi-fingered Robot Hands", Robotics and Autonomous Systems, vol. 27, no. 4, pp. 211-224, 1999.

[158] A. Bicchi and V. Kumar, "Robotic grasping and contact: a review", Proceedings of IEEE International Conference Robotics and Automation (ICRA), vol. 1, pp. 348 – 353, 2000.

[159] Dan Ding , Yun-Hui Liu, Jianwei Zhang and Alois Knoll, "Computation of Fingertip Positions for a Form-Closure Grasp", Proceedings of the IEEE International Conference on Robotics & Automation, Seoul, Korea, May 21-26, 2001.

[160] J. W. Li, H. Liu and H. G. Cai, "On Computing Three-Finger Force-Closure Grasps of 2D and 3D Objects", IEEE Transactions on Robotics and Automation, vol. 19, no. 1, 2003.

[161] Ch. Borst , M. Fischer and G. Hirzinger , "Grasp Planning: How to Choose a Suitable Task Wrench Space", Proceedings of IEEE International Conference on Robotics and Automation (ICRA), vol. 1, pp. 319-325, 2004.

[162] A. Sudsang, "Fast Computation of 4-Fingered Force-Closure Grasps from Surface Points", Proceedings of IEEE/RSJ International Conference Intelligent Robots and Systems, vol. 4, pp. 3692 – 3697, 2004.

[163] X. Zhu and H. Ding , "Planning Force-Closure Grasps on 3-D Objects", Proceedings of IEEE International Conference on Robotics and Automation, vol. 2, pp. 1258 – 1263, 2004.

[164] Y. Zheng and W. Qian, “Coping with the Grasping Uncertainties in Force-Closure Analysis”, The International Journal of Robotics Research, vol. 24, no. 4, pp. 311-327, 2005.

[165] J. Cornella, R. Suarez, R. Carloni and C. Melchiorri, “Grasping Force Optimization Using Dual Methods”, Proceeding of 8th International IFAC Symposium on Robot Control, vol. 8, no. 1, 2005.

[166] B. Wang, L. Jiang, J. W. Li, H. G. Cai and H. Liu, “Grasping Unknown Objects Based on 3D Model Reconstruction”, Proceedings of 2005 IEEE/ASME International Conference on Advanced Intelligent Mechatronics, pp.461 – 466, 2005.

[167] Y. Zheng and W. H. Qian, “An Enhanced Ray-Shooting Approach to Force-Closure Problems”, Journal of Manufacturing Science and Engineering, Transaction of the ASME, vol. 128, no. 4, pp. 960-968, 2006.

[168] M. A. Roa and R. Suarez, “Geometrical Approach for Grasp Synthesis on Discretized 3D Objects”, Proceedings of IEEE/RSJ International Conference on Intelligent Robots and Systems, pp. 3283 - 3288, 2007.

[169] S. S. Ohol and S. R. Kajale, “Simulation of Multi-finger Robotic Gripper for Dynamic Analysis of Dexterous Grasping”, Proceedings of the World Congress on Engineering and Computer Science, 2008.

[170] S. E. Khoury and A. Sahbani, “On Computing Robust n-Finger Force-Closure Grasps of 3D Objects”, Proceedings of IEEE International Conference on Robotics and Automation(ICRA) 2009, pp. 2480 – 2486, 2009.

[171] B. Bounab, A. Labed and D. Sidbore, “Stochastic Optimization Based Approach for Multifingered Grasps Synthesis”, Journal Robotica, vol. 28, no. 7, pp. 1021-1032, 2009.

[172] R. Krug, D. Dimitrov, K. Charusta and B. Iliev, “On the Efficient Computation of Independent Contact Regions for Force Closure Grasps”, Proceedings of IEEE/RSJ International Conference on Intelligent Robots and Systems (IROS), pp. 586 – 591, 2010.

[173] A. Sahbani, S. El-Khoury and P. Bidaud, “An Overview of 3D Object Grasp Synthesis Algorithms”, Robotics and Autonomous Systems, vol. 60, no. 3, pp. 326-336, 2012.

[174] J. P. Saut and D. Sidobre,"Efficient Models for Grasp Planning with a Multi-fingered Hand", Robotics and Autonomous Systems, Elsevier, vol. 60, pp. 347–357, 2012.

[175] T. Iberall, "The Nature of Human Prehension: Three dexterous hands in One", Proceedings of the IEEE International Conference on Robotics and Automation, pp. 396-401, 1987.

[176] T. Iberall, "Grasp planning for Human Prehension", Proceedings of the International Joint Conference on Artificial Intelligence, Milan, Italy, Aug. 22-28, pp. 1153-1156, 1987.

[177] L. Cohen, L. manion and K. Morrison, "Research Mrthods in Education", 5th edition, Routledge/ falmer, Taylor & Francis Group, Londan and New York, 2000.

[178] L. Balxter, C' Hughes and M. Tight, "How to Research", McGraw Hill International, pp.8, 2006.

[179] D. Johnson, "Research Methods in Educational Management", Prentice Hall, pp. 172-175, 1998.

[180] N. Ulrich, R. Paul and R. Bajcsy, "A Medium Complexity Compliant End Effector", in the proceedings of IEEE International Conference of Robotics and Automation, Philadelphia, PA, pp. 434-439, April, 1988.

[181] A. Miller, P. Allen, V. Santos and F. Valero-Cuevas, "From Robotic Hands to Human hands: a Visualization and Simulation Engine for Grasping Research", Industrial Robot: An International Journal, vol. 32, no. 1, pp. 55-63, 2005.

[182] K. J. DeLaurentis, C. Pfeiffer, and C. Mavroidis, "Development of a Shape Memory Alloy Actuated Hand" Proceedings of the 7th International Conference on New Actuators, pp. 281-284, Bremen, Germany, June 2000, Messe Bremen GMBH.

[183] I.A. kapandij, "The Physiology of the Joints, Volume 1, Upper limbs", Churchill Livingstone, 1982.

[184] B. Buchcholz, T. Armstrong, and S. Goldstein. "Anthropometric Data For Describing the Kinematics of the Human Hand", Ergonomics, vol.35, no.3, pp.261–273, 1992.

[185] X. Sancho-Bru, "Model biomecanic de la ma orientat al disseny d'eines manuals". PhD Thesis, University of Jaume I, 2000.

[186] J. Yang and E. P. Pitarch, "Digital Human Modeling and Virtual Reality for FCS: Kinematic Human Modeling", The Universoty of Iowa, Iowa, Technical Report, 2004.

[187] P. W. Brand and A. M. Hollister, "Clinical Mechanics of the Hand", Mosby, Inc. Third edition, 1990.

[188] J. S. R. Jang, "ANFIS: Adaptive-Network-based Fuzzy Inference Systems", IEEE Transactions on Systems, Man, and Cybernetics, vol. 23, no.3, pp. 665-685, 1993.

[189] Kapandji, "Fisiologia Articular. Miembro Superior", Medica Panamericana, Madrid. 5th Edition, 1996.

[190] R. Tubiana, "The Hand. Volume I", W.B. Saunders Company. 2nd Edition, 1981.

[191] R. Tubiana, J. Thomine, and E. Mackin, "Examination of the hand and wrist", Martin Dunitz. 2nd Edition, 1996.

[192] C. P. Neu, J. J. Crisco, and S. W. Wolfe, "In Vivo Kinematic Behaviour of the Radio-Capitate Joint during Wrist Flexion-Extension and Radio-Ulnar Deviation", Journal of Biomechanics, vol. 34, no. 11, pp.1429–1438, 2001.

[193] S. E. Sonenblum, J. J. Crisco, L. Kang, and E. Akelman, "In Vivo Motion of the Scaphotrapezio-Trapezoidal (STT) Joint", Journal of Biomechanics, vol. 37, no. 5, pp.645–652, 2004.

[194] J. Denavit and R. Hartenberg, " A Kinematic Notation for Lower-Pair Mechanisms Based on Matrices" , Journal of Applied Mechanic, vol. 22, pp. 215-221, 1955.

[195] J. J. Craig, "Introduction to Robotics: Mechanics and Control", International Student Edition, AWL, 2nd edition, 1999.

[196] R. K. Mittal and I. J. Nagrath, "Robotics and Control", Tata McGraw- Hill Publishing Company Limited, New Delhi, 2003.

[197] J. Angeles. "Fundamentals of Robotic Mechanical Systems: Theory, Methods, and Algorithms", Mechanical Engineering Series. 2nd edition, 2002.

[198] Dr. Bob John, "Adaptive Network Based Fuzzy Inference Systems (ANFIS)", www.cse.dmu.ac.uk/~hseker/ANFISnotes.doc, 2002.

[199] P. R. Kraus, V. I. Kumar, and P. Dupont, "Analysis of Frictional Contact Models for Dynamic Simulation", Proceedings of IEEE International Conference on Robotics and Automation, 1997.

[200] M. A. R. Garzon, “Grasp Planning Methodology for 3D Arbitrary Shaped Objects”, Ph.D. Thesis, Universidad Politécnica de Cataluña, March 2009.

[201] X. Markenscoff, L. Ni and C. Papadimitriou, “The Geometry of Grasping”, International Journal of Robotic Research, vol.9, no. 1, pp. 61-74, 1990.

[202] V.D. Nguyen, “Constructing Force-closure Grasps”, The International Journal of Robotic Research, vol. 7, no. 3, pp. 3-16,1988.

CURRICULUM VITAE

National Institute of Technology
Rourkela, Odisha, India

Personal Details:

Name **: PRAMOD KUMAR PARIDA**

Father's Name **: NATABARA PARIDA**

Date of Birth **: 25th**, April 1971

Fields of Interest **:** Robotics, FMS, CAD/CAM/CIM & Soft Computing

Phone : +91 9437131705**, E-mail :** pramodparida71@yahoo.com

Academic Qualification:

2013	Ph.D. Dissertation submitted at NIT, Rourkela.
1998	M.E. (Mech. Engg.) from BESU (former BE college), Howrah
1994	B.Tech (Mech. Engg.), CET, OUAT, Bhubaneswar, Odisha
1989	+2 Science, CHSE, Odisha
1987	Matriculation, BSE, Odisha

Work Experience:

Work as Lecturer in Mechanical Engineering Department of College of Engineering and Technology, BPUT, Bhubaneswar, Odisha from July 2000 to till date.

Pramod Kumar Parida

List of Publications

International Journals:

1. **P.K. Parida** and B. B. Biswal, "Design and Analysis of a Multi-fingered Robot Hand", International Journal of Robotics and Automation (IJRA), Vol. 1, no. 2, pp. 69-77 (2012).
2. **P.K. Parida**, B.B.Biswal and M.R. Khan, "Kinematic modeling and Analysis of a multi-fingered Robotic Hand", International Journal of Advanced Materials Research Vols. 383-390, pp. 6684-6688 (2012).
3. B. B. Biswal, **P. K. Parida** and K. C. Pati, "Kinematic analysis of a dexterous hand", International Journal of Advanced Materials Research Vol. 433-440, pp. 754-762 (2012).
4. **P.K. Parida**, B.B.Biswal and D.N. Thatoi, "Kinematic Analysis of an Anthropomorphic Robot Hand", International Journal of Applied Mechanics and Materials, Vols. 187, pp. 293-297 (2012).
5. **P.K. Parida** and B.B.Biswal, "Inverse Kinematics of an Anthropomorphic Robotic Hand", Accepted for publication in International Journal of Robotics and Automation (IJRA), Vol. 2, no. 3,(2013).
6. **P.K. Parida** and B.B.Biswal, "Analysis of the Forward Kinematics of a Multi-fingered Robotic Hand", Accepted for publication in International Journal of Computer Science and Management Studies (IJCSMS), Vol. 5, no. 2, (2013).

Book Chapters:

1. **P. K. Parida**, B. B. Biswal and R. N. Mahapatra,"Conceptual Design and Kinematic Analysis of a Five-Fingered Anthropomorphic Robotic Hand" , J. S. Dai et al. (eds.), Advances in Reconfigurable Mechanisms and Robots I, DOI: 10.1007/978-1-4471-4141-9_55, _ Springer-Verlag London, 2012

International conferences:

1. **P. K. Parida**, B. B. Biswal and S. Kumar, "Kinematic Design and Compliant Grasp Analysis of a 5- Fingered Robotic hand" Proceeding of the 4th International and 25th All India Manufacturing Technology, Design

and Research conference (AIMTDR 2012), held at Jadavpur University, Kolkata, India during December 14-16, 2012

2. **P.K. Parida**, B.B.Biswal and M.R.Khan, "Kinematic modeling of a multi-fingered Robotic Hand", Proceedings of the International Conference on Manufacturing Science and Technology (ICMST 2011), held at Singapore during September 16-18, 2011.
3. **P.K. Parida**, B.B.Biswal and S. Saragi, "Kinematic modeling of a multi-fingered Robotic Hand", Proceedings of the 5th International Conference on Advances in Mechanical Engineering (ICAME-2011), June 06-08, 2011, hold at SVNIT, Surat, June 06-08, 2011, pp. 169-174.
4. B. B. Biswal, **P. K. Parida** and K. C. Pati, "Kinematic analysis of a dexterous hand", Proceedings of the 2nd International Conference on Mechanical, Industrial and Manufacturing Technologies (MIMT 2011) by IEEE at Singapore, Feb. 26-28,2011.
5. S. K. Pattanayak, B. B. Biswal, **P.K. Parida** and R. N.Mohapatra, "Robot Kinematics using Quaternion Theory" Proceedings of the 12th International Conference on Towards Autonomous Robotic Systems 2010 (TAROS 2010), Sheffield, UK, 31st Oct. -2nd Nov., 2010.

National Conferences:

1. **P.K. Parida** and B.B.Biswal, "Analysis of the Forward Kinematics of a Multi Fingered Robotic Hand", Proceedings of the National Conference on Emerging Trend and its Appliction in Engineering (NCETAE-2011), December 26-28, 2011, Indira Gandhi Institute of Technology (IGIT), Saranga, Odisha , India.
2. **P.K.Parida** and B. B. Biswal, "Inverse Kinematics Solution for a 5-DOF Manipulator using ANFIS" Proceedings of All India conference on Recent Advances in mechanical Engineering, March 16-17, Bhubaneswar, Mechanical Division of Institute of Engineers India, 2013.